THE ROLE OF BRAIN-DERIVED NEUROTROPHIC FACTOR IN THE REGULATION OF DENDRITIC ARBOR MORPHOLOGY, NEURONAL NETWORK ACTIVITY, AND NEUROPROTECTION

By

KATE M. O'NEILL

A dissertation submitted to the

Graduate School-New Brunswick

And

The Graduate School of Biomedical Sciences

Rutgers, The State University of New Jersey

In partial fulfillment of the requirements

For the degree of

Doctor of Philosophy

Graduate Program in Biomedical Engineering

Written under the direction of

Bonnie L. Firestein

And approved by

_____

_____

_____

_____

_____

New Brunswick, New Jersey

May 2017

ABSTRACT OF THE DISSERTATION

THE ROLE OF BRAIN-DERIVED NEUROTROPHIC FACTOR IN THE REGULATION OF DENDRITIC ARBOR MORPHOLOGY, NEURONAL NETWORK ACTIVITY, AND NEUROPROTECTION

By KATE M. O'NEILL

Dissertation Director:

Bonnie L. Firestein

The dendritic architecture of a neuron determines how it receives inputs, and thus, changes in dendrite morphology will affect connectivity among neurons. Aberrant changes in the development of the arbor, or after the arbor has formed, can disrupt the functioning of neural circuits, causing severe brain dysfunction and leading to pathologies seen in cognitive disorders, neurological diseases, and trauma. Brain-derived neurotrophic factor (BDNF) is one of the most well-studied regulators of dendritic and synaptic plasticity. It is also known to be a pro-survival factor and is overexpressed in neurons that survive injuries, such as ischemia. This dissertation explores how BDNF shapes the dendritic arbor of single hippocampal neurons and the dynamics of *in vitro* hippocampal networks. Previous work in our laboratory has shown that BDNF significantly increases proximal dendrite branching in hippocampal neurons after 72 hours of bath application. Building on this work, we show that local application of

BDNF via microbeads increases both proximal and distal dendrite branching in a shorter time than does bath application. We also show that overexpression of BDNF shapes the dendritic arbor differently depending on the intracellular targeting of BDNF transcripts. To understand how BDNF affects the development of hippocampal neuronal networks, we use microelectrode arrays (MEAs) to record the spontaneous activity of these networks before and after bath application of BDNF. Our results suggest a role for BDNF in the long-term development of neuronal network dynamics, as changes in network parameters were only observed at one week after treatment. Finally, we explore whether BDNF exerts neuroprotective effects following excitotoxic injury. Global activity parameters decrease following injury with excess glutamate with no benefit from BDNF treatment, but BDNF does protect connections with distinct baseline synchronizations from injury-induced decreases. Taken together, our results indicate that BDNF is involved in the development of the dendritic arbor, the maturation of neuronal networks, and the protection of distinct connections after excitotoxic injury.

ACKNOWLEDGEMENTS

I am eternally grateful for the many people that made this work possible. First and foremost, I would like to acknowledge my advisor, Dr. Bonnie Firestein, for everything she has done for me during my graduate career. Her enthusiasm for scientific research is contagious, and I am so grateful to have had the opportunity to work in her laboratory for my PhD. I am definitely an engineer in how I approach my work, and I thank Dr. Firestein for teaching me to think like a biologist. I would also like to thank her for being a role model. It has meant so much to have a mentor who loves science but also fashion, fitness, and puppies. I appreciate so much how she has supported me in everything from this work to conferences to the outreach. Her support and guidance have been invaluable to my development as a scientist and have made the completion of this work possible.

My committee members have also all been indispensable to this work. Thank you to Dr. Troy Shinbrot, Dr. Smita Thakker-Varia, Dr. Ken Paradiso, and Dr. Barclay Morrison for everything. Their expertise, support, kindness, and the time they took to provide feedback on my work has been so appreciated. The work is better and I am a better scientist because of them. I would especially like to thank Dr. Shinbrot, whose mentorship early in my graduate career made much of the programming work in this dissertation possible.

I have been lucky to have many unofficial mentors. Dr. David Shreiber, Dr. Martin Yarmush, and Dr. Ann Stock have been thoughtful mentors over the past several years. I thank them for their time, energy, and support in my times of need. I would also be remiss if I did not acknowledge my original mentors at Princeton,

Dr. Stanislav Shvartsman and Dr. Yoosik Kim. They originally taught me how to be a scientist and conduct research in a laboratory, and I am very grateful to both of them. My goal for my PhD has been to be as kind, hardworking, and knowledgeable as Yoosik. I am not sure if I achieved that, but it is the standard to which I have held myself.

The rest of the Firestein lab has made my days (and nights) in the lab as enjoyable as possible. Thank you to all past and present members that have taught me, supported me, and become my friends over the years. The help of Dr. Ana Rodriguez was essential to the MEA work presented in this dissertation. Ana taught me how to dissect and culture neurons on MEAs. She also worked tirelessly to find new ways to improve our analysis system. I am so grateful for her mentorship and friendship over the years. I would also like to acknowledge Katherine Donohue, whose help has been crucial to the completion of the bead and UTR work. Her enthusiasm and positive attitude have made working on these projects so much more fun than they would have been otherwise.

The work in this dissertation was made possible by several funding sources. The Biotechnology Training Program, New Jersey Commission on Brain Injury Research, and the GAANN Program in Precision and Personalized Medicine have provided the funding for my PhD and allowed me to conduct my research without other demands on my time.

I was lucky to enter graduate school with my best friends from high school and college close by, and their support of me during my PhD has been so important. What I did not expect was to meet and become close friends with four other amazing women who inspire me on a daily basis: Dr. Laura Higgins, Dr. Kathryn Drzewiecki, (soon to be Dr.) Maria Qadri, and (soon to be Dr.) Grace Bundens. Thank you for being there for me from problem sets to proposals to dissertations and everything in between. Thank you

also to the other friends I have made in Rutgers BME. You have all made classes, conferences, and everything in between a lot of fun.

My family has been a constant source of support and encouragement during graduate school. To my parents and brother, thank you. I love you more than words can say and appreciate your endless love and belief in my abilities. Special thanks go to my incredible mother: I wonder if you realized that you created a scientist when you bought me the “How Come?” book all those years ago. To all the other family that has supported me in this journey (especially Pop-pop, Eileen, Eddie, Sarah, and Aunty Ann), thank you. Grandma and Nanny, I wish you could be here to see this. Nanny’s Alzheimer’s Disease is the reason I became interested in neuroscience in the first place, and I hope Grandma is proud to know that I am not just using my brain but am studying brains, too.

Last but not least, my husband Trevor has been my hero and deserves an honorary Ph.D. (in addition to his M.Eng. and nearly completed J.D.). He gave up his dreams and moved back to New Jersey so that I could pursue mine. His commute has always been longer, and yet he has been the one to get up earlier, cook dinner, and keep our lives together. Thank you for everything you (and our puppies!) do for me on a daily basis. The past several months have been particular trying for me, but you, Archie, and Raisin have kept me sane. Thank you. I love you.

DEDICATION

To my parents, who have not only given me the world but have taken me to see it, too.

Thank you, thank you, thank you.

TABLE OF CONTENTS

ABSTRACT OF THE DISSERTATION ii

ACKNOWLEDGEMENTS iv

DEDICATION vii

TABLE OF FIGURES xi

TABLE OF TABLES xiv

CHAPTER 1: INTRODUCTION 1

1.1 PHYSIOLOGICAL IMPORTANCE OF DENDRITE MORPHOLOGY 1
1.2 BRAIN-DERIVED NEUROTROPHIC FACTOR 2
1.3 TRAUMATIC BRAIN INJURY 4
1.4 RECEPTORS IMPLICATED IN GLUTAMATE-INDUCED EXCITOTOXICITY 6
1.5 MICROELECTRODE ARRAY ANALYSIS OF NEURONAL NETWORK ACTIVITY 8
1.6 THESIS OVERVIEW 9

CHAPTER 2: DISTINCT WAYS OF LABELING THE DENDRITIC ARBOR REVEAL UNIQUE CHANGES CAUSED BY CYPIN OVEREXPRESSION 10

2.1 INTRODUCTION 10
2.2 MATERIALS AND METHODS 13
2.2.1 Primary culture of hippocampal neurons 13
2.2.2 Transfection of cultured cells 14
2.2.3 Immunostaining and imaging 14
2.2.4 Assessment of dendrite number using semi-automated Sholl analysis and statistics 15
2.3 RESULTS 16
2.3.1 Sholl analysis for neurons overexpressing cypin from DIV 6-10 16
2.3.2 Dendrite number for neurons overexpressing cypin from DIV 6-10 21
2.3.3 Dendrite length for neurons overexpressing cypin from DIV 6-10 24
2.3.4 Sholl analysis for neurons overexpressing cypin from DIV 10-12 27
2.3.5 Dendrite number for neurons overexpressing cypin from DIV 10-12 32
2.3.6 Dendrite length for neurons overexpressing cypin from DIV 10-12 35
2.4 DISCUSSION 37

CHAPTER 3: MICROBEAD APPLICATION OF BRAIN-DERIVED NEUROTROPHIC FACTOR REGULATES THE DENDRITIC ARBOR DIFFERENTLY THAN DOES GLOBAL ADMINISTRATION OF BRAIN-DERIVED NEUROTROPHIC FACTOR 44

3.1 INTRODUCTION 44
3.2 MATERIALS AND METHODS 46
3.2.1 Primary culture of hippocampal neurons 46
3.2.2 Transfection of cultured cells 47

3.2.3 Preparation of BSA- and BDNF-coated microbeads *47*
3.2.4 Treatment with BSA- and BDNF-coated beads *48*
3.2.5 Live imaging *49*
3.2.6 Assessment of dendrite number using semi-automated Sholl analysis and statistics *49*
3.3 RESULTS 50
3.3.1 Treatment with BDNF-coated beads increases overall dendrite branching in a location and time-dependent manner *50*
3.3.2 Treatment with BDNF-coated beads affects dendrite number and length *58*
3.3.3 Knockdown of cytosolic PSD-95 interactor (cypin) blocks a subset of effects resulting from treatment with BDNF-coated beads *64*
3.4 DISCUSSION 71

CHAPTER 4: THE ROLE OF INTRACELLULAR TARGETING OF BRAIN-DERIVED NEUROTROPHIC FACTOR TRANSCRIPTS IN REGULATING THE DENDRITIC ARBOR 77

4.1 INTRODUCTION 77
4.2 MATERIALS AND METHODS 79
4.2.1 Primary culture of hippocampal neurons *79*
4.2.2 Optimization of transfection procedure *79*
4.2.3 Primary neuronal transfection *80*
4.2.4 Immunostaining *81*
4.2.5 Imaging and fluorescence quantification *82*
4.2.6 Assessment of dendrite number using semi-automated Sholl analysis *83*
4.3 RESULTS 84
4.3.1 Intracellular targeting of BDNF transcripts affects the spatial distribution, number, and length of the overall dendritic arbor *84*
4.3.2 Intracellular targeting of BDNF transcripts affects the spatial distribution of specific orders of dendrites *91*
4.3.3 Intracellular targeting of BDNF transcripts affects the number and length of specific orders of dendrites *104*
4.4 DISCUSSION 106
4.5 ACKNOWLEDGEMENTS 110

CHAPTER 5: THE ROLE OF BRAIN-DERIVED NEUROTROPHIC FACTOR IN REGULATING NEURONAL NETWORK DEVELOPMENT AND DYNAMICS 111

5.1 INTRODUCTION 111
5.2 MATERIALS AND METHODS 113
5.2.1 Preparation of microelectrode arrays (MEAs) and cell culture *113*
5.2.2 Microelectrode array recordings *115*
5.2.3 Experimental setup: BDNF treatment and recording schedule *115*
5.2.4 Signal processing *117*
5.2.5 Spike detection and related parameters *117*
5.2.6 Burstlet detection and related parameters *120*
5.2.7 Global burst detection and related parameters *121*
5.2.8 Synchronization calculation *122*
5.2.9 Data representation and statistics *123*

5.3 RESULTS 123
5.3.1 BDNF treatment affects spike rate and variability 124
5.3.2 BDNF treatment modulates certain aspects of bursting activity 128
5.3.3 BDNF modulates the synchronization of hippocampal networks over time 133
5.4 DISCUSSION 139
5.5 ACKNOWLEDGEMENTS 144

CHAPTER 6: THE ROLE OF BRAIN-DERIVED NEUROTROPHIC FACTOR IN NEUROPROTECTION FROM GLUTAMATE-INDUCED EXCITOTOXICITY 145

6.1 INTRODUCTION 145
6.2 MATERIALS AND METHODS 147
6.2.1 Preparation of microelectrode arrays (MEAs) and cell culture 147
6.2.2 Microelectrode array recordings 148
6.2.3 Determination of glutamate concentrations that result in mild and moderate injury of hippocampal neurons 149
6.2.4 Experimental setup: Injury with glutamate, BDNF recovery treatment, and recording schedule 151
6.2.5 Signal processing and parameter calculation 152
6.2.6 Data representation and statistics 152
6.3 RESULTS 153
6.3.1 Hippocampal neuron networks are more sensitive to glutamate-induced injury than are cortical neuron networks 153
6.3.2 Spiking dynamics are affected by mild and moderate injury with glutamate and BDNF treatment 157
6.3.3 Bursting dynamics are affected by mild and moderate injury with glutamate and BDNF treatment 162
6.3.4 Synchronization of specific categories of connections is affected by mild and moderate injury with glutamate and BDNF treatment 167
6.4 DISCUSSION 173
6.5 ACKNOWLEDGEMENTS 178

CHAPTER 7: SUMMARY AND FUTURE DIRECTIONS 179

REFERENCES 186

TABLE OF FIGURES

FIGURE 2-1: THREE DIFFERENT SHOLL ANALYSES USED TO ASSESS THE EFFECTS OF CYPIN OVEREXPRESSION ON THE DENDRITIC ARBOR. 12
FIGURE 2-2: OVEREXPRESSION OF CYPIN FROM DIV 6-10 INCREASES PROXIMAL BRANCHING AND TOTAL DENDRITE NUMBER BUT DECREASES AVERAGE DENDRITE LENGTH. 17
FIGURE 2-3: SHOLL ANALYSIS USING THREE DIFFERENT LABELING METHODS FOR NEURONS OVEREXPRESSING CYPIN FROM DIV 6-10. 20
FIGURE 2-4: CYPIN INCREASES THE NUMBER OF DENDRITES BY SPECIFICALLY TARGETING CERTAIN CATEGORIES OF DENDRITES WHEN OVEREXPRESSED IN NEURONS FROM DIV 6-10. 23
FIGURE 2-5: CYPIN DECREASES THE LENGTH OF DENDRITES BY SPECIFICALLY TARGETING CERTAIN CATEGORIES OF DENDRITES WHEN OVEREXPRESSED IN NEURONS FROM DIV 6-10. 26
FIGURE 2-6: CYPIN OVEREXPRESSION FROM DIV 10-12 INCREASES PROXIMAL BRANCHING WITH NO SIGNIFICANT EFFECT ON TOTAL DENDRITE NUMBER OR AVERAGE DENDRITE LENGTH. 28
FIGURE 2-7: SHOLL ANALYSIS USING THREE DIFFERENT LABELING METHODS FOR NEURONS OVEREXPRESSING CYPIN FROM DIV 10-12. 31
FIGURE 2-8: CYPIN INCREASES OUTERMOST DENDRITES WHEN OVEREXPRESSED IN NEURONS FROM DIV 10-12. 34
FIGURE 2-9: CYPIN DECREASES THE LENGTH OF INNERMOST DENDRITES WHEN OVEREXPRESSED IN NEURONS FROM DIV 10-12. 36
FIGURE 2-10: SCHEMATIC OF RESULTS WHEN COMBINING ANALYSIS USING ALL THREE LABELING SCHEMES 42
FIGURE 3-1: AVERAGE NUMBER OF BEADS PER DENDRITE CALCULATED FOR EACH GROUP OF EXPERIMENTS. 48
FIGURE 3-2: LOCAL STIMULATION OF DENDRITES USING MICROBEADS. 51
FIGURE 3-3: SHOLL ANALYSIS OF HIPPOCAMPAL NEURONS SHOWS THAT BDNF-COATED BEADS INCREASE BRANCHING. 53
FIGURE 3-4: ORDER-SPECIFIC SHOLL ANALYSIS REVEALS THAT BDNF EXERTS EFFECTS ON DIFFERENT TYPES OF DENDRITES. 55
FIGURE 3-5: GROUPING ORDER-SPECIFIC SHOLL ANALYSIS BY CONDITION REVEALS HOW BDNF MODULATES PRUNING OF HIGHER ORDER DENDRITES. 57
FIGURE 3-6: AVERAGE NUMBER OF DENDRITES PER NEURON IS SIGNIFICANTLY INCREASED AFTER TREATMENT WITH BDNF-COATED BEADS. 59
FIGURE 3-7: ORDER-SPECIFIC ANALYSIS OF DENDRITE NUMBERS REVEALS THAT TREATMENT WITH BDNF-COATED BEADS SIGNIFICANTLY AFFECTS CERTAIN TYPES OF DENDRITES IN A TIME-DEPENDENT MANNER. 60
FIGURE 3-8: AVERAGE DENDRITE LENGTH PER NEURON IS NOT ALTERED BY TREATMENT WITH BDNF-COATED BEADS. 62
FIGURE 3-9: ORDER-SPECIFIC ANALYSIS OF DENDRITE LENGTHS REVEALS THAT TREATMENT WITH BDNF-COATED BEADS SIGNIFICANTLY INCREASES THE LENGTH OF TERTIARY AND HIGHER ORDER DENDRITES AFTER 72 HOURS. 63

FIGURE 3-10: SHOLL ANALYSIS REVEALS A ROLE FOR CYPIN IN REGULATING HOW TREATMENT WITH BDNF-COATED BEADS ALTERS THE DENDRITIC ARBOR. 66
FIGURE 3-11: ORDER-SPECIFIC SHOLL ANALYSIS ILLUSTRATES HOW KNOCKING DOWN CYPIN AFFECTS MODULATION OF DENDRITE BRANCHING BY BDNF-COATED BEADS 69
FIGURE 3-12: SCHEMATIC ILLUSTRATING THE CHANGES THAT OCCUR AS A RESULT OF TREATMENT WITH BDNF-COATED BEADS. 71
FIGURE 4-1: SCHEMATIC DEPICTING DIFFERENT PLASMIDS CONTAINING THE BDNF CODING SEQUENCE WITH OR WITHOUT 3' UTRS. 81
FIGURE 4-2: REPRESENTATIVE PLOT OF CORRECTED TOTAL CELL FLUORESCENCE DATA FOR GFP. 83
FIGURE 4-3: OVEREXPRESSION OF BDNF WITH AND WITHOUT THE TARGETING UTRS RESULTS IN CHANGES TO SHOLL CURVES, TOTAL DENDRITE NUMBER, AND AVERAGE DENDRITE LENGTH 86
FIGURE 4-4: TOTAL SHOLL ANALYSIS SHOWING COMPARISONS BETWEEN ALL CONDITIONS. 90
FIGURE 4-5: ORDER-SPECIFIC SHOLL ANALYSIS REVEALS HOW OVEREXPRESSION OF BDNF AFFECTS THE SPATIAL ORGANIZATION OF DIFFERENT ORDERS OF DENDRITES. 92
FIGURE 4-6: SHOLL ANALYSIS OF PRIMARY DENDRITES SHOWING COMPARISONS BETWEEN ALL CONDITIONS. 95
FIGURE 4-7: SHOLL ANALYSIS OF SECONDARY DENDRITES SHOWING COMPARISONS BETWEEN ALL CONDITIONS. 99
FIGURE 4-8: SHOLL ANALYSIS OF TERTIARY AND HIGHER ORDER DENDRITES SHOWING COMPARISONS BETWEEN ALL CONDITIONS. 103
FIGURE 4-9: TARGETING BDNF MRNA TO DIFFERENT PARTS OF THE CELL HAS DISTINCT EFFECTS ON SPECIFIC ORDERS OF DENDRITES. 105
FIGURE 4-10: TARGETING BDNF MRNA WITH THE LONG 3' UTR AFFECTS TERTIARY AND HIGHER ORDER DENDRITE LENGTH 105
FIGURE 4-11: SCHEMATIC DEPICTING CHANGES CAUSED BY OVEREXPRESSION OF BDNF WITH AND WITHOUT 3' UTRS. 107
FIGURE 5-1: DENSE CULTURES OF HIPPOCAMPAL NEURONS ON MEAS EXHIBIT SPONTANEOUS SPIKING AND BURSTING ACTIVITY 114
FIGURE 5-2: RECORDING AND TREATMENT SCHEDULE FOR BDNF DOSE RESPONSE EXPERIMENTS. 116
FIGURE 5-3: DIAGRAM DEMONSTRATING SPIKE AND BURSTLET DETECTION. 118
FIGURE 5-4: ADAPTIVE THRESHOLDING IMPROVES THE NUMBER OF SPIKES AND BURSTLETS DETECTED DURING RECORDING COMPARED WITH MANUAL THRESHOLDING. 121
FIGURE 5-5: SPIKE RATE AND VARIABILITY ARE AFFECTED BY BDNF TREATMENT. 125
FIGURE 5-6: BDNF TREATMENT DOES NOT AFFECT THE ISI LENGTH OR VARIABILITY. 127
FIGURE 5-7: BDNF TREATMENT ALTERS THE NUMBER OF SPIKES PER BURSTLET WITHOUT ALTERING BURSTLET RATE OR THE AVERAGE BURSTLET WIDTH. 129
FIGURE 5-8: BDNF TREATMENT ALTERS GLOBAL BURST NUMBER WITHOUT ALTERING OTHER PARAMETERS. 131
FIGURE 5-9: BDNF TREATMENT AFFECTS THE AVERAGE INTERBURST INTERVAL OF GLOBAL BURSTS AND INDIVIDUAL BURSTLETS, DEPENDING ON BDNF CONCENTRATION. 132

FIGURE 5-10: TREATMENT WITH 50 NG/ML BDNF SIGNIFICANTLY INCREASES LONG-TERM SYNCHRONIZATION. 133
FIGURE 5-11: BDNF MODULATES THE SYNCHRONIZATION OF ELECTRODES (AVERAGED PER MEA) WITH DIFFERENT INITIAL SYNCHRONIZATIONS. 135
FIGURE 5-12: BDNF MODULATES THE SYNCHRONIZATION OF ELECTRODES WITH DIFFERENT INITIAL SYNCHRONIZATIONS. 137
FIGURE 6-1: RECORDING AND TREATMENT SCHEDULE USED FOR DETERMINING THE APPROPRIATE CONCENTRATIONS OF GLUTAMATE FOR INJURING HIPPOCAMPAL CULTURES. 150
FIGURE 6-2: RECORDING AND TREATMENT SCHEDULE USED FOR GLUTAMATE INJURY AND BDNF RECOVERY EXPERIMENTS. 151
FIGURE 6-3: THE SPIKE RATE AND AVERAGE SPIKE MAGNITUDE DECREASE WITH INJURY. 154
FIGURE 6-4: BURSTING PARAMETERS ARE AFFECTED BY INJURY. 155
FIGURE 6-5: NUMBER OF GLOBAL BURSTS AND AVERAGE SYNCHRONIZATION DECREASE AS A RESULT OF INJURY. 156
FIGURE 6-6: GLUTAMATE-INDUCED INJURY AND BDNF TREATMENT AFFECT SPIKE RATE. 159
FIGURE 6-7: THE LENGTH AND VARIABILITY OF THE ISI ARE AFFECTED BY INJURY AND BDNF TREATMENT. 161
FIGURE 6-8: BURSTING ACTIVITY IS MODULATED BY INJURY AND BDNF TREATMENT. 163
FIGURE 6-9: GLOBAL BURST NUMBER AND COMPOSITION ARE ALTERED BY INJURY AND BDNF TREATMENT. 165
FIGURE 6-10: INTERBURST INTERVAL IS AFFECTED BY INJURY AND BDNF TREATMENT. 166
FIGURE 6-11: AVERAGE SYNCHRONIZATION OF NETWORKS IS AFFECTED BY INJURY AND BDNF TREATMENT. 168
FIGURE 6-12: NEITHER INJURY WITH EXCESS GLUTAMATE NOR BDNF TREATMENT MODULATES THE SYNCHRONIZATION OF CONNECTIONS (AVERAGED PER MEA) WITH DIFFERENT BASELINE VALUES. 169
FIGURE 6-13: BDNF AIDS IN THE RECOVERY OF MILDLY INJURED NETWORKS WITH SPECIFIC INITIAL SYNCHRONIZATIONS. 172

TABLE OF TABLES

TABLE 4-1: STATISTICAL DETAILS OF COMPARISONS BETWEEN CONDITIONS FOR TOTAL SHOLL ANALYSIS. 91
TABLE 4-2: STATISTICAL DETAILS OF COMPARISONS BETWEEN CONDITIONS FOR PRIMARY SHOLL ANALYSIS. 96
TABLE 4-3: STATISTICAL DETAILS OF COMPARISONS BETWEEN CONDITIONS FOR SECONDARY SHOLL ANALYSIS 100
TABLE 4-4: STATISTICAL DETAILS OF COMPARISONS BETWEEN CONDITIONS FOR TERTIARY+ SHOLL ANALYSIS. 104
TABLE 5-1: SUMMARY OF SIGNIFICANT CHANGES TO THE NETWORK DYNAMICS OF HIPPOCAMPAL NEURONS OVER TIME AND AS A RESULT OF BDNF TREATMENT. 140
TABLE 6-1: SUMMARY OF SIGNIFICANT CHANGES TO THE NETWORK DYNAMICS OF HIPPOCAMPAL NEURONS AFTER INJURY WITH GLUTAMATE AND RECOVERY WITH BDNF TREATMENT 177

CHAPTER 1: INTRODUCTION

1.1 Physiological importance of dendrite morphology

Proper patterning of dendrites is essential for the functioning of individual neurons and the neuronal network into which they are integrated. The overall shape of the dendritic arbor determines the inputs that a neuron receives and how information is interpreted, thus affecting synaptic output (Miller and Jacobs 1984). Modifications in the dendritic arbor of a neuron due to trauma or disease alter postsynaptic transmission, thus affecting the contribution of that neuron to overall network dynamics. For example, aberrant changes to the dendritic arbor are present in neurological disorders, ranging from Autism Spectrum Disorder to Alzheimer's Disease. Although these changes often occur in a relatively small percentage of neurons, the functional consequences of these changes are clear because the cognitive deficits present in individuals with these disorders are severe (Zoghbi 2003, Kulkarni and Firestein 2012). Disorders in which neuronal morphology is implicated highlight the importance of proper dendritic shape to the overall functioning of the network.

Moreover, recent work suggests that dendrites are not simply passive highways through which information travels from the synapse to the cell body (Torben-Nielsen and Stiefel 2009, Branco and Häusser 2010). Action potentials can back-propagate through the dendritic arbor, influencing the plasticity of dendrites and active synapses, and therefore, the generation of future action potentials (Vetter, Roth et al. 2001). Additionally, single dendrites may act as individual functional units (Branco and Häusser 2010) and perform computation, such as interpreting the spatiotemporal relationship of

excitatory and inhibitory inputs in pyramidal neurons (Liu 2004, Hao, Wang et al. 2009). These abilities, coupled with activity-dependent regulation of local protein translation, allow for constant refinement of neuronal network architecture and underscore the necessity of a properly formed arbor to overall network function (Larkum and Nevian 2008).

1.2 Brain-derived neurotrophic factor

The precise patterning of dendrites is crucial for proper neuronal communication. The process of dendritic arborization is tightly regulated, and this regulation often occurs locally, such as at small regions of the dendrite (reviewed in (Koleske 2013)). Brain-derived neurotrophic factor (BDNF) is one of most well-studied extrinsic regulators of dendrite development (McAllister, Lo et al. 1995, McAllister, Katz et al. 1996, Baker, Dijkhuizen et al. 1998, Horch, Kruttgen et al. 1999, Jin, Hu et al. 2003, Segal 2003, Dijkhuizen and Ghosh 2005). A member of the neurotrophin family, BDNF is essential for neuronal development and dendrite outgrowth. As a protein, it exists in two states: pro-BDNF, an unprocessed form that binds to the p75 neurotrophin receptor ($p75^{NTR}$) with high affinity, and mature BDNF, the proteolytically processed form that preferentially binds to the tropomyosin-related kinase B (TrkB) receptor. The two receptors activate distinct pathways. Activation of $p75^{NTR}$ leads to apoptosis while activation of the TrkB receptor promotes neuronal development and dendritic outgrowth (Barbacid 1994, Chao 2003, Lu, Nagappan et al. 2013).

BDNF plays many roles in neuronal development and in the regulation of dendritic outgrowth. In cortical neurons, BDNF enhances activity-dependent dendritic

outgrowth, such as in layer IV of the developing cortex (McAllister, Lo et al. 1995, McAllister, Katz et al. 1996), and makes dendrites and spines more dynamic (Horch, Kruttgen et al. 1999, Horch and Katz 2002). In cortical neurons, BDNF increases primary branching via the phosphatidylinositol 3-kinase (PI3K) and mitogen-activated protein kinase (MAPK) pathways in as little as 5 hours (Dijkhuizen and Ghosh 2005), and it is thought to act through an autocrine mechanism to increase dendritic outgrowth when overexpressed (Horch, Kruttgen et al. 1999). Our laboratory has shown that BDNF increases proximal branching in a different neuron type, hippocampal neurons, when applied exogenously to cultures for 72 hours. These increases are mediated via cAMP response element binding protein (CREB)-dependent transcriptional regulation of cytosolic PSD-95 interactor (cypin), an intrinsic regulator of dendritic outgrowth (Kwon, Fernandez et al. 2011).

BDNF is an important player in mediating synaptic plasticity, as local translation and posttranslational modifications of many synaptic proteins are induced by exogenous application of BDNF (Waterhouse and Xu 2009). BDNF exerts its actions specifically on active synapses through local translation of itself and TrkB as well as activity-dependent release and subsequent cleavage of proBDNF into BDNF (Waterhouse and Xu 2009). Intracellular targeting of mRNAs allows for the local protein synthesis that drives neuronal development and synaptic plasticity (Tongiorgi, Righi et al. 1997, Steward and Schuman 2001, Soulé, Messaoudi et al. 2006, Rodriguez, Czaplinski et al. 2008, Martin and Ephrussi 2009, Tongiorgi 2009, Baj, Pinhero et al. 2016). For example, BDNF is preferentially targeted to different parts of the cell, the soma or the dendrites, when encoded by transcripts with different length 3' untranslated regions (UTRs), and these

unique transcripts regulate distinct aspects of neuronal physiology (Timmusk, Palm et al. 1993, Ghosh, Carnahan et al. 1994, An, Gharami et al. 2008).

In addition to modulating both dendritic and synaptic plasticity, BDNF is a pro-survival factor (Sendtner, Holtmann et al. 1992, Lindholm, Dechant et al. 1993, Mattson, Lovell et al. 1995, Giehl and Tetzlaff 1996, Hofer and Bardet 1998, Kiprianova, Freiman et al. 1999). BDNF preserves the levels of protein markers for axons (neurofilament-H) and dendrites (microtubule-associated protein 2) after glutamate-induced excitotoxicity through the phosphatidylinositol 3-kinase (PI3K) and phospholipase C (PLCγ) pathways. BDNF also partially prevents glutamate-induced decreases in excitatory synaptic markers vesicular glutamate transporter 1 (VGLUT1) and 2 (VGLUT2). Interestingly, BDNF does not protect against the loss of GABA(gamma-aminobutyric acid)-ergic synaptic markers glutamic acid decarboxylase 65 (GAD65) and 67 (GAD67), suggesting excitatory synapse-specific protection (Melo, Okumoto et al. 2013). Moreover, TrkB signaling is involved in BDNF-mediated neuroprotection because the expression of TrkB mRNAs increases after injury (Merlio, Ernfors et al. 1993, Mudó, Persson et al. 1993, Rostami, Krueger et al. 2014).

1.3 Traumatic brain injury

After a traumatic brain injury (TBI), decreased dendrite branching (Gao, Deng et al. 2011) and other morphological abnormalities (Ray, Dixon et al. 2002, Arundine and Tymianski 2004) observed in the affected areas cause functional deficits. TBI affects millions of people each year in the U.S., often with devastating results. A recent study by the Center for Disease Control suggests that as many as 6 million people (almost 2% of

the U.S. population) are currently living with long-term disabilities caused by TBI (Coronado, Xu et al. 2011). Despite improved knowledge of the mechanisms underlying damage caused by TBI, there is still no agreed-upon treatment for the secondary, excitotoxic effects of the trauma (Kazanis 2005). As promising drugs, such as N-methyl-D-aspartate receptor (NMDAR) antagonists, have failed in recent years, we will examine how the long-lasting effects of glutamate-induced excitotoxicity can be prevented and how injured neurons can be protected from long-term damage and death.

Damage caused by TBI is the result of two distinct insults: a primary mechanical injury and secondary chemical injury. Mechanical injury to brain tissue occurs at the time of trauma; it can act at a specific location, such as in focal injuries, or be more diffuse. Chemical injury, a secondary insult activated by the primary injury, wreaks havoc on brain tissue hours to days after the initial trauma (Ray, Dixon et al. 2002). Excitatory amino acids, particularly glutamate, are implicated in this secondary insult. Injured neurons release excess glutamate, which then damages neighboring neurons, stimulating them to release more glutamate and damage more neurons (Arundine and Tymianski 2004, Yi and Hazell 2006). The cascade is self-propagating, often leading to severe cognitive deficiencies in patients because the action of glutamate-induced excitotoxicity is not limited to the trauma site, but rather it causes widespread damage by injuring healthy tissue not directly affected by the primary injury (Patterson and Holahan 2012). Thus, finding a solution for this aspect of TBI is of utmost importance to improving treatment.

1.4 Receptors implicated in glutamate-induced excitotoxicity

Excess glutamate causes excitotoxicity in neurons through overstimulation of N-methyl-D-aspartate (NMDA) and alpha-amino-3-hydroxy-5-methyl-4-isoxazolepropionic acid (AMPA) glutamate receptors (Arundine and Tymianski 2004). Prolonged or increased activation of these receptors leads to ionic imbalance caused by longer or additional depolarization events. Excessive activation of glutamate receptors increases calcium influx, causing an increase in intracellular calcium (Ca^{2+}) levels and resulting in overactivation of normal cellular events. In a healthy individual, astrocytes express excitatory amino acid transporters (EAATs), such as the glutamate transporters EAAT1 and EAAT2. Normally, these transporters take up excess glutamate near the synapse, preventing it from spilling out of the synaptic cleft and activating extrasynaptic NMDARs. However, astrocytes damaged by TBI cannot function normally, and a decrease in EAAT1- and EAAT2-positive cells occurs, preventing normal function and contributing to the excess extracellular glutamate (Ross and Cleveland 2006, Van Landeghem, Weiss et al. 2006, Yi and Hazell 2006).

NMDARs are a type of ionotropic glutamate receptor and can be localized synaptically, perisynaptically, or extrasynaptically (Hardingham and Bading 2010). Early in development, extrasynaptic NMDARs dominate until synaptic NMDARs become more prevalent later in development (Gladding and Raymond 2011). After neuronal maturity, NMDAR localization determines the downstream pathways activated and whether the overall effect on neuronal survival is beneficial or detrimental (Leveille, El Gaamouch et al. 2008). Differentially located NMDARs play specific roles in regulating

CREB function and cell death pathways that are likely related to the location of calcium influx (Hardingham, Fukunaga et al. 2002).

Synaptically localized NMDARs are present at the postsynaptic density (PSD) of excitatory neurons (Leveille, El Gaamouch et al. 2008). Their activation results in calcium influx that releases more calcium from intracellular storage, which in turn activates nuclear calcium signaling and results in phosphorylation of CREB. CREB is a transcription factor that activates several genes responsible for enhancing neuronal survival, synaptic plasticity, and neurogenesis. One of the genes upregulated by CREB is the *BDNF* gene (Hardingham, Fukunaga et al. 2002). Extrasynaptic NMDARs are located outside the synapse – on the spine neck, dendritic shaft, or soma – and are activated by bath-applied glutamate (Gladding and Raymond 2011). Activation of extrasynaptic NMDARs by bath application of glutamate blocks CREB function through dephosphorylation. Additionally, although bath-applied glutamate also activates synaptic NMDARs, the CREB-promoting effects are overridden by activation of extrasynaptic NMDARs and subsequent dephosphorylation of CREB. Extrasynaptic NMDARs also trigger cell death pathways and breakdown of the mitochondrial membrane (Hardingham, Fukunaga et al. 2002, Leveille, El Gaamouch et al. 2008). Moreover, the extracellular signal-related kinase (ERK) signaling pathway, which mediates NMDAR-dependent plasticity and survival in neurons, also becomes inactivated (Ivanov, Pellegrino et al. 2006).

1.5 Microelectrode array analysis of neuronal network activity

It has long been recognized that complex cognitive functions are governed by strengths of synaptic connections in neuronal networks. Over the past few decades (Gross, Rieske et al. 1977, Pine 1980), the understanding of *in vitro* network development has advanced considerably due to the development of microelectrode arrays (MEAs). MEAs provide a non-invasive platform through which network activity of neurons can be observed, recorded, and subsequently analyzed. MEAs contain a grid of planar electrodes in the center of the culture well upon which cultured neurons can grow. A major advantage of MEAs over other electrophysiology techniques is that network activity can be recorded over longer periods of time. This permits monitoring of changes in network dynamics as the networks mature or after treatment (Hales, Rolston et al. 2010). While single-cell recordings of neurons, using techniques such as patch-clamping, provide unparalleled detail of individual neuron activity, these data are collected in isolation from the rest of the network. MEAs provide a way to non-invasively measure relevant network activity, as *in vitro* cultures have been shown by several groups to recapitulate many functional characteristics observed *in vivo*, such as connectivity, plasticity, and repeating activity motifs (Wagenaar, Pine et al. 2006, Chiappalone, Massobrio et al. 2008, Raichman and Ben-Jacob 2008). Our laboratory has shown that MEAs can be used to detect changes in the network activity of cortical neurons when damaged by glutamate (Kutzing, Luo et al. 2011) and when neuroprotective agents are applied (Kutzing, Luo et al. 2012). Additionally, we have used spike sorting techniques to determine how overexpression of cypin alters neuronal network dynamics over time (Rodriguez et al., 2017, unpublished data).

1.6 Thesis overview

The goal of this dissertation is to understand how BDNF changes the dendritic arbor of hippocampal neurons and the dynamics of hippocampal neuron networks. Chapter 2 explores how novel Sholl analyses reveal changes to the dendritic arbor after overexpression of cypin, an intrinsic regulator of branching, that would otherwise not be detected by conventional Sholl analysis. Chapter 3 examines how BDNF shapes the dendritic arbor when applied locally via microbeads. Chapter 4 reveals how overexpression of BDNF regulates dendritic arbor development and how these changes depend on BDNF mRNA targeting to specific intracellular locations. Chapter 5 employs MEA technology to understand how BDNF treatment affects the development of hippocampal neuron networks. Chapter 6 extends this work to more mature hippocampal networks and seeks to determine whether BDNF exerts neuroprotective effects on networks after glutamate-induced injury. Finally, Chapter 7 provides a summary and discussion of the data presented in the previous five chapters.

CHAPTER 2: DISTINCT WAYS OF LABELING THE DENDRITIC ARBOR REVEAL UNIQUE CHANGES CAUSED BY CYPIN OVEREXPRESSION

The work in this chapter has previously been published in the following article: O'Neill KM, Akum BF, Dhawan ST, Kwon M, Langhammer CG, Firestein BL (2015). "Assessing effects on dendritic arborization using novel Sholl analyses." *Frontiers in Cellular Neuroscience* 9:285.

2.1 Introduction

The development and patterning of dendrites is a tightly regulated process that is essential for proper functioning of the central nervous system. A number of metrics may be used to describe dendritic arbor morphology, such as number of dendrites, number of branch and terminal points, branching angles, and analysis of sub-trees within the overall dendritic arbor (Uylings and Van Pelt 2002). Sholl analysis (Sholl 1953) has been an instrumental tool in analyzing changes to the dendritic arbor as a whole. Sholl analysis includes counting the number of dendritic intersections that occur at fixed distances from the soma in concentric circles. This analysis reveals the number of dendrite branches, branch geometry, and overall branching patterns of neurons (Caserta, Eldred et al. 1995). Performing this process by hand is time-consuming and introduces inherent variability due to inconsistency and experimenter bias.

Previously, our laboratory developed a semi-automated Sholl analysis program, called Bonfire, that not only performs analysis on the entire arbor but also analyzes

subsets of dendrites within the arbor (Kutzing, Langhammer et al. 2010, Langhammer, Previtera et al. 2010). The most commonly used labeling scheme, the Inside-Out method, classifies dendrites as primary/secondary/tertiary and higher (Langhammer, Previtera et al. 2010). Primary dendrites extend from the soma, secondary dendrites extend from primary dendrites, and so on. We also developed a labeling scheme known as the Root-Intermediate-Terminal (RIT) method (Langhammer, Previtera et al. 2010). In the RIT labeling method, root dendrites emerge from the cell body, and terminal dendrites are those that do not branch any further. Intermediate dendrites are those that exist between root and terminal dendrites, and they can be a combination of secondary, tertiary, and higher order dendrites as labeled by the Inside-Out method. A comparison of these two labeling schemes is demonstrated in Figure 2-1.

To extend this work, we introduce an additional method for labeling the dendritic arbor, known as the Tips-In method (Rodriguez 2007, O'Neill, Akum et al. 2015). Tips-In analysis is the opposite of Inside-Out analysis. This scheme defines the outermost, terminal dendrites as primary dendrites. Secondary dendrites are dendrites that are one order in from the outermost dendrite; they can be the penultimate dendrite or a root dendrite with only one branch, as shown in the right panel of Figure 2-1. Tertiary and higher order dendrites are one order closer to the soma after the penultimate (secondary) dendrite. These dendrites correspond to primary dendrites in the Inside-Out labeling scheme that branch at least twice.

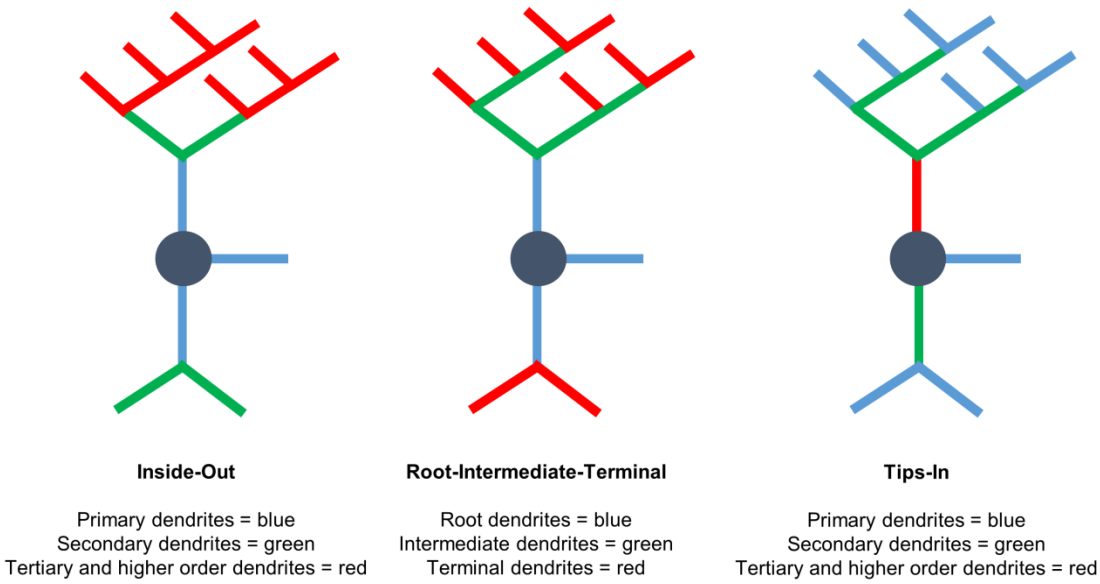

Figure 2-1: Three different Sholl analyses used to assess the effects of cypin overexpression on the dendritic arbor.
Left. Inside-Out Sholl analysis is conventional Sholl analysis. Primary dendrites extend from the cell body; secondary dendrites extend from primary dendrites; etc. Dendrites classified as tertiary and higher are grouped together. **Middle.** In the Root-Intermediate-Terminal (RIT) scheme, root dendrites emerge from the cell body, and terminal dendrites are those dendrites that do not branch further. All other dendrites are considered intermediate dendrites. **Right.** Tips-In analysis defines terminal dendrites as primary dendrites. Secondary dendrites are dendrites that are one order in from the outermost dendrite and can be the penultimate dendrite or a root dendrite with only one branch, as shown in the figure. Tertiary and higher order dendrites are one order closer to the soma after the penultimate (secondary) dendrite. These dendrites correspond to primary dendrites in the Inside-Out labeling scheme that branch at least twice.

To illustrate the utility of using all three labeling schemes, we probed the effects of overexpressing the dendrite-promoting protein cypin (cytosolic PSD-95 interactor) in cultured rat hippocampal neurons at two different developmental timepoints: from day *in vitro* (DIV) 6 to 10 and from DIV 10 to 12. Our laboratory previously identified cypin as a core regulator of dendritic arborization (Firestein, Brenman et al. 1999, Akum, Chen et al. 2004, Fernandez, Welsh et al. 2008). Cypin promotes local microtubule assembly in

the dendrite by binding tubulin heterodimers, resulting in increased primary and secondary dendrite numbers (Akum, Chen et al. 2004). Since our previous studies have only assessed the effects of overexpression and knockdown of cypin by either counting primary and secondary dendrites (Akum, Chen et al. 2004, Charych, Akum et al. 2006, Fernandez, Welsh et al. 2008) or by using conventional Sholl analysis (Chen and Firestein 2007, Kwon, Fernandez et al. 2011), it is not yet known whether changes to cypin expression result in region-specific effects on the dendritic arbor. In the work described in this chapter, we alter cypin protein levels and apply several types of Sholl analyses to reveal previously unknown effects of cypin on specific regions of the dendritic arbor. Additionally, we use different labeling schemes to examine changes in overall and order-specific dendrite numbers and dendrite lengths.

2.2 Materials and Methods

2.2.1 Primary culture of hippocampal neurons

Hippocampal neurons were isolated from embryonic rats at day 18 of gestation (E18) as previously described (Firestein, Brenman et al. 1999). After isolation, the hippocampi were dissociated via manual trituration and plated at a density of $2x10^5$/well on 12-mm glass coverslips (Fisher) in 24-well plates (Corning). Coverslips were coated with 0.5 mg/mL poly-D-lysine (PDL; Sigma) for at least 1 hr at 37 ˚C prior to plating cells. Cultures were maintained in Neurobasal medium supplemented with B27, GlutaMAX, and penicillin/streptomycin (all from Life Technologies) in a humidified 37 ˚C incubator with 5% CO_2. Cells were grown for 6 days *in vitro* (DIV) or

10 DIV prior to transfection. All animals used for dissection were cared for ethically in accordance with Institutional Animal Care and Use Committee (IACUC) standards.

2.2.2 Transfection of cultured cells

A subset of neurons were transfected at DIV 6 with pEGFP-C1 or pEGFP-C1-cypin and pmRFP using Lipofectamine LTX and Plus reagent according to the manufacturer's instructions (Kwon, Fernandez et al. 2011) and fixed with 4% paraformaldehyde in phosphate-buffered saline (PBS), pH 7.4, at DIV 10. Additional neurons were transfected at DIV 10 with pEGFP-C1 or pEGFP-C1-cypin using Lipofectamine 2000 according to the manufacturer's instructions and fixed at DIV 12 for imaging and analysis (O'Neill, Akum et al. 2015).

2.2.3 Immunostaining and imaging

At the appropriate DIV, neurons were fixed with 4% paraformaldehyde in PBS for 15 min and incubated in blocking buffer (PBS containing 0.1% Triton X-100, 2% normal goat serum, and 0.02% sodium azide) for 1 hr. All antibodies were diluted in blocking buffer. Cells were incubated with primary antibody for 2 hr at room temperature. Primary antibodies were used at a concentration of 1:500 and included mouse anti-MAP2 (BD Pharmigen), chicken anti-GFP (Rockland), and rabbit anti-cypin (Chen and Firestein 2007). After primary antibody incubation, coverslips were washed three times with PBS and incubated with secondary antibody for 1 hr at room temperature. Secondary antibodies were used at a concentration of 1:250 and included Alexa Fluor 488 donkey anti-chicken, Alexa Fluor 555 donkey anti-rabbit, and Alexa Fluor 647 donkey anti-mouse (all from Life Technologies). After secondary antibody incubation, coverslips were washed twice with PBS and incubated with Hoechst

dye for 5 min at room temperature to stain nuclei. Coverslips were washed one final time with PBS and mounted onto glass microscope slides with Fluoromount G (Southern Biotechnology). Transfected cells were visualized by immunofluorescence on an Olympus Optical IX 50 microscope (Tokyo, Japan) with a Cooke SensiCam charge-coupled device (CCD) cooled camera fluorescence imaging system and Image Pro software (Media Cybernetics).

2.2.4 Assessment of dendrite number using semi-automated Sholl analysis and statistics

Semi-automated Sholl analysis was used as previously described (Kutzing, Langhammer et al. 2010, Langhammer, Previtera et al. 2010). Briefly, 8-bit images of hippocampal neurons were traced using the NeuronJ plugin (Meijering, Jacob et al. 2004) for ImageJ (NIH, Bethesda, MD), and tracing files (*.ndf files) were generated. The data were organized and converted to SWC files (Cannon, Turner et al. 1998) using MATLAB (Mathworks), and the connectivity of the tracings was checked in NeuronStudio (Rodriguez, Ehlenberger et al. 2006). Once the tracings were finalized in NeuronStudio, the data were exported to Excel using MATLAB. Prism (Graphpad) was used for all statistical analyses. For analysis of Sholl curves, two-way ANOVA was used followed by Bonferroni's Multiple Comparisons test. For analysis of dendrite numbers, Student *t*-tests were used, and Welch's correction was included when appropriate. All tracings and analyses were performed with the experimenter blinded to the condition. A subset of neurons for this study was retraced from images analyzed previously (Kwon, Fernandez et al. 2011). All analyses of the retraced images presented here are new, and data generated from non-conventional Sholl analyses (RIT and Tips-In) are novel and

were not included in our previous work (Kwon, Fernandez et al. 2011). Neurons were counted only when at least two authors agreed that they were viable without access to condition information. All dendrites are defined as not branching or resulting in bifurcation (Van Pelt and Verwer 1985, Van Pelt and Verwer 1986, Verwer and Van Pelt 1990).

2.3 Results

2.3.1 Sholl analysis for neurons overexpressing cypin from DIV 6-10

Overexpression of cypin from DIV 6-10 promotes dendrite branching in hippocampal neurons, in agreement with our previous work (Akum, Chen et al. 2004, Charych, Akum et al. 2006, Chen and Firestein 2007, Fernandez, Welsh et al. 2008, Kwon, Fernandez et al. 2011). Sholl analysis performed with all branch orders grouped (Total Sholl, Figure 2-2B), as is standard in the field, is the same analysis regardless of whether we perform Inside-Out, Root-Intermediate-Terminal (RIT), or Tips-In analysis. Total Sholl analysis shows that cypin significantly increases proximal branches at 0-42 μm from the soma when overexpressed from DIV 6-10 (Figure 2-2B). The causes for this change can be parsed out when examining Sholl curves for different branch categories and comparing these differences among the three methods of analysis.

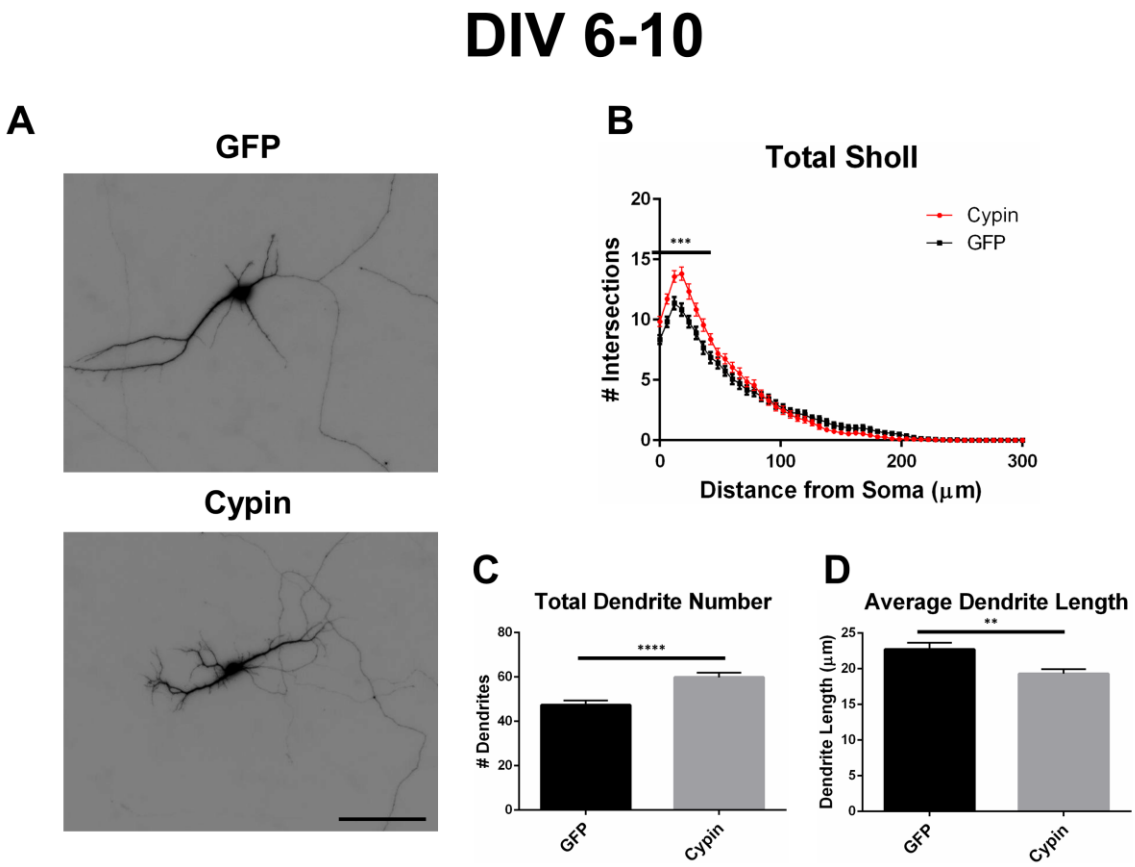

Figure 2-2: Overexpression of cypin from DIV 6-10 increases proximal branching and total dendrite number but decreases average dendrite length.
A. Representative images of hippocampal neurons overexpressing GFP or GFP-cypin (cypin) from DIV 6-10. Scale bar = 100 µm. **B.** Sholl analysis of all orders of branches (Total Sholl) shows that overexpression of cypin significantly increases dendrite branching at 0-42 µm from the cell body (***p<0.001). Statistics were calculated using two-way ANOVA followed by Bonferroni's multiple comparisons test. **C.** Overexpression of cypin results in a significant increase in the total number of dendrites (****p<0.0001). Statistics were calculated by unpaired, two-tailed Student's *t*-test. **D.** Overexpression of cypin results in a significant decrease in the average length of dendrites (**p<0.001). Statistics were calculated by unpaired, two-tailed Student's *t*-test with Welch's correction. Error bars indicate SEM. n=50 neurons for GFP, and n=55 neurons for cypin.

When analyzing the dendritic arbor using the Inside-Out method, cypin overexpression promotes the greatest increase in primary branches, branches that emerge from the soma, and higher order branches (tertiary and above). Primary branches significantly increase at 0-18 µm from the soma when cypin is

overexpressed (Figure 2-3A). Secondary branches, which emerge from primary dendrites, significantly increase at 6-12 μm from the soma (Figure 2-3B). Higher order dendrites significantly increase at 18-42 μm and at 54-60 μm from the soma in neurons overexpressing cypin (Figure 2-3C). These results indicate that, at DIV 6-10, when dendritic branches extend from primary and secondary branches and very little pruning has yet to occur (i.e. stage 4) (Dotti, Sullivan et al. 1988, Akum, Chen et al. 2004), cypin exerts the greatest effects on primary and higher order branches (tertiary and above) but not on secondary branches.

When analyzing the dendritic arbor using the RIT method, cypin overexpression significantly changes all categories of dendrites. Like the Inside-Out method, significant changes occur in proximal dendrites less than 100 μm from the soma. Because primary dendrites in the Inside-Out method and root dendrites in the RIT method are defined as the same, changes observed in root dendrites are the changes observed in primary dendrites: cypin overexpression significantly increases root dendrites at 0-42 μm from the soma (Figure 2-3D). This method of Sholl analysis shows a difference from that of Inside-Out Sholl analysis when comparing secondary dendrites and intermediate dendrites (Figure 2-3E). Intermediate dendrites include all dendrites that are not root dendrites or terminal dendrites. Significant increases in dendrites of neurons overexpressing cypin are observed at 6-12 μm from the soma, similar to changes seen in secondary dendrites analyzed by the Inside-Out method. Additionally, an increase in intermediate dendrites at 30 μm from the soma is also observed. These results indicate that the significant increases observed at 6 and 12 μm are due to increased secondary dendrites but that the increase at 30 μm is due to increased higher order, intermediate

branches. The Sholl curves for terminal dendrites show similar increases to those seen in tertiary and higher order dendrites: neurons overexpressing cypin have significantly increased dendrite branching at 18-42 μm from the soma (Figure 2-3F). Interestingly, the increases observed at 54 and 60 μm from the soma that are observed for tertiary and higher order dendrites are not observed for terminal dendrites, indicating that terminal dendrites closer to the cell body (within 50 μm) are most affected by cypin overexpression.

When analyzing the dendritic arbor using the Tips-In method, cypin overexpression from DIV 6-10 exerts the greatest effect on primary dendrites and on tertiary and higher order dendrites. In this labeling scheme, primary dendrites are the outermost (terminal) dendrites. The resulting curve from this analysis is distinct from the terminal Sholl curve resulting from the RIT method, likely because primary dendrites in this case are a combination of terminal dendrites as well as root dendrites that do not branch (see Figure 2-1, right panel). For primary dendrites in the Tips-In scheme, significant increases are observed at 0-42 μm from the soma (Figure 2-3G), which are the same distances observed for increased dendrites resulting from Total Sholl analysis (Figure 2-2B). Secondary dendrites in this scheme are dendrites that are one order in from the outermost dendrite, either the penultimate dendrite or a root dendrite with only one branch (Figure 2-1, right panel). This curve is distinct from the intermediate Sholl curve from the RIT method and the secondary Sholl curve from the Inside-Out method. Significant increases are only observed at 6 μm from the soma (Figure 2-3H), indicating that the penultimate dendrite is only affected by cypin overexpression at distances very close to the soma. Finally, dendrites labeled as tertiary

and higher order are one order closer to the soma after the penultimate (secondary) dendrite; they are the antepenultimate (third to last) dendrite. These dendrites correspond to primary dendrites in the Inside-Out labeling scheme that branch at least twice (Figure 2-1, right panel). For tertiary and higher order dendrites, significant increases are observed at 0-24 μm away from the soma (Figure 2-3I).

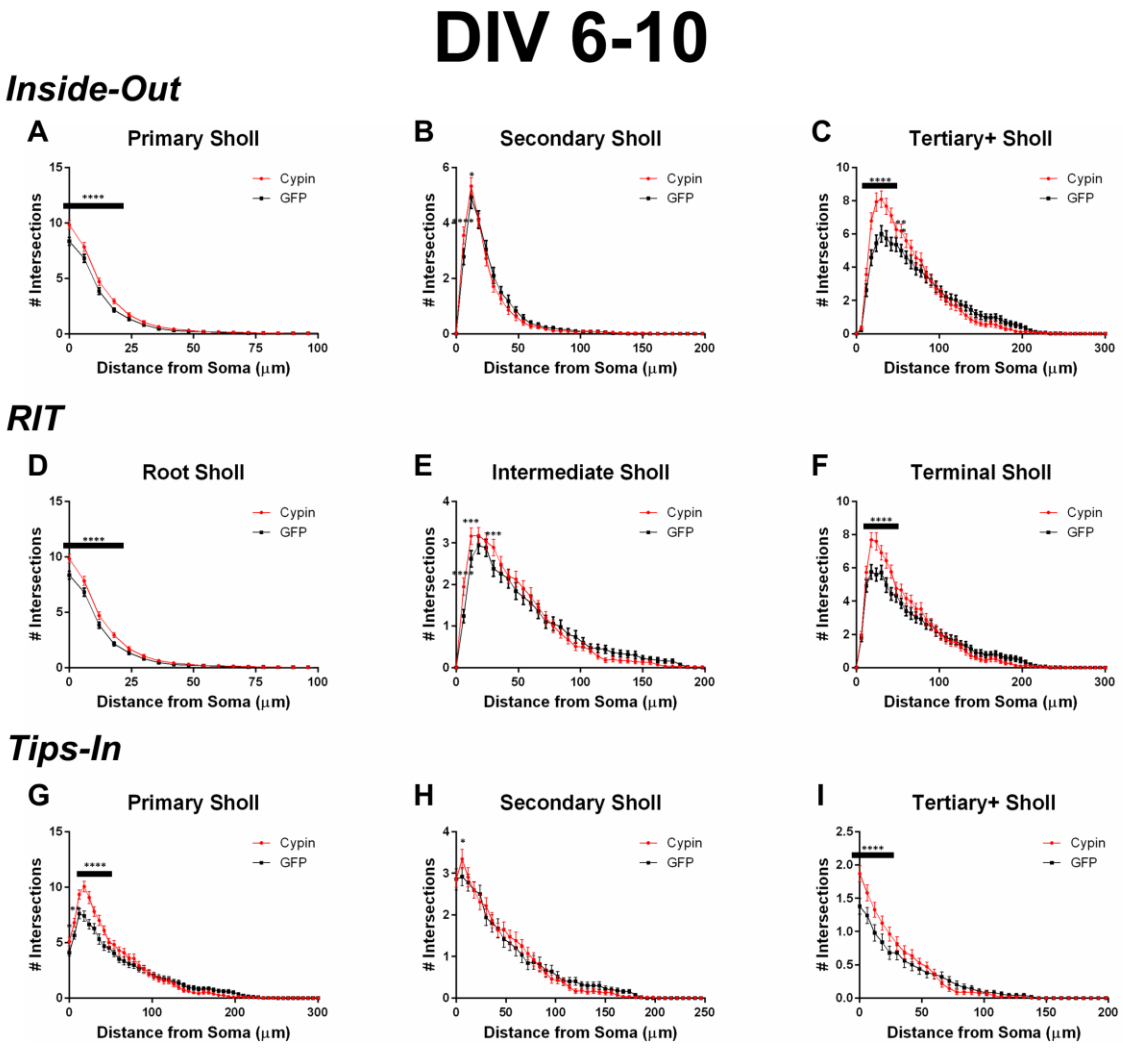

Figure 2-3: Sholl analysis using three different labeling methods for neurons overexpressing cypin from DIV 6-10.
A.-C. Sholl analysis using Inside-Out (conventional) labeling method. **A.** Sholl analysis of primary dendrites (Primary Sholl) shows that overexpression of cypin significantly increases branching at 0-18 μm (****p<0.0001). **B.** Sholl analysis of secondary

dendrites (Secondary Sholl) shows that overexpression of cypin significantly increases dendrites at 6 and 12 μm from the soma (****p<0.0001 and *p<0.05, respectively). **C.** Sholl analysis of tertiary and higher order dendrites (Tertiary+ Sholl) shows that overexpression of cypin significantly increases dendrites at 18-42 μm (****p<0.0001), at 54 μm (**p<0.01), and at 60 μm (*p<0.05) from the soma. **D.-F.** Sholl analysis using RIT labeling method. **D.** Sholl analysis of root dendrites (Root Sholl) shows that overexpression of cypin significantly increases branching at 0-18 μm from the cell body (****p<0.0001). **E.** Sholl analysis of intermediate dendrites (Intermediate Sholl) shows that overexpression of cypin significantly increases dendrites at 6 μm (****p<0.0001) from the soma and at 12 and 30 μm from the soma (both ***p<0.001). **F.** Sholl analysis of terminal dendrites (Terminal Sholl) shows that overexpression of cypin significantly increases dendrites at 18-42 μm from the soma (****p<0.0001). **G.-I.** Sholl analysis using Tips-In labeling method. **G.** Sholl analysis of primary dendrites shows that overexpression of cypin significantly increases branching at 0 μm (*p<0.05), 6 μm (**p<0.01), and 12-42 μm from the soma (****p<0.0001). **H.** Sholl analysis of secondary dendrites shows that overexpression of cypin significantly increases branching at 6 μm from the soma (*p<0.05). **I.** Sholl analysis of tertiary and higher order dendrites shows that overexpression of cypin significantly increases dendrite branching at 0-24 μm from the soma (****p<0.0001). Statistics were calculated using two-way ANOVA followed by Bonferroni multiple comparisons test. Error bars indicate SEM. n=50 neurons for GFP, and n=55 neurons for cypin.

2.3.2 Dendrite number for neurons overexpressing cypin from DIV 6-10

Cypin overexpression from DIV 6-10 affects the total number of dendrites and dendrites of specific orders, depending on the labeling scheme. For all labeling schemes, the total dendrite count is identical, and cypin overexpression from DIV 6-10 significantly increases dendrites (Figure 2-2C). The different labeling schemes indicate unique regulation of dendrite number by cypin.

For the Inside-Out labeling scheme, cypin overexpression significantly increases primary dendrites (Figure 2-4A) as well as tertiary and higher order dendrites (Figure 2-4C), with no significant effect on secondary dendrites (Figure 2-4B). This labeling scheme points to cypin-promoted increases in primary and higher order (> secondary) dendrite number.

For the RIT labeling scheme, overexpression of cypin significantly increases all dendrite types; root, intermediate, and terminal dendrite numbers are significantly increased (Figure 2-4D-F). When comparing these graphs to the Inside-Out graphs, it becomes clear that different labeling schemes demonstrate cypin-promoted effects on dendrite number differently. As with the Sholl curves, the difference in root dendrites is identical for that of primary dendrites because the two types of dendrites are identical (Figure 2-4D). While there is no significant difference observed for secondary dendrites for the Inside-Out method, there is a significant increase in intermediate dendrites when cypin is overexpressed (Figure 2-4E). This is also reflected in the Sholl curves, with an additional significant difference at 30 μm from the soma for intermediate dendrites (Figure 2-3E) when compared to secondary dendrites (Figure 2-3B). Additionally, terminal dendrites significantly increase due to cypin overexpression, indicating that increased branching is due to increased intermediate branches (Figure 2-4F).

Interestingly, unlike the Inside-Out method, the Tips-In method shows significantly increased numbers of dendrites for all categories (Figure 2-4G-I). As with Sholl analysis for this method, the primary dendrites are terminal dendrites or root dendrites that do not branch, and these types of dendrites are significantly increased for neurons overexpressing cypin from DIV 6-10 (Figure 2-4G). Secondary dendrites, defined under this labeling scheme, are either the penultimate dendrite or a root dendrite with only one branch. In this case, they significantly increase with cypin overexpression (Figure 2-4H). Finally, tertiary and higher order dendrites are primary

dendrites with two or more branches. We also observe a significant increase in these branches as a result of cypin overexpression (Figure 2-4I).

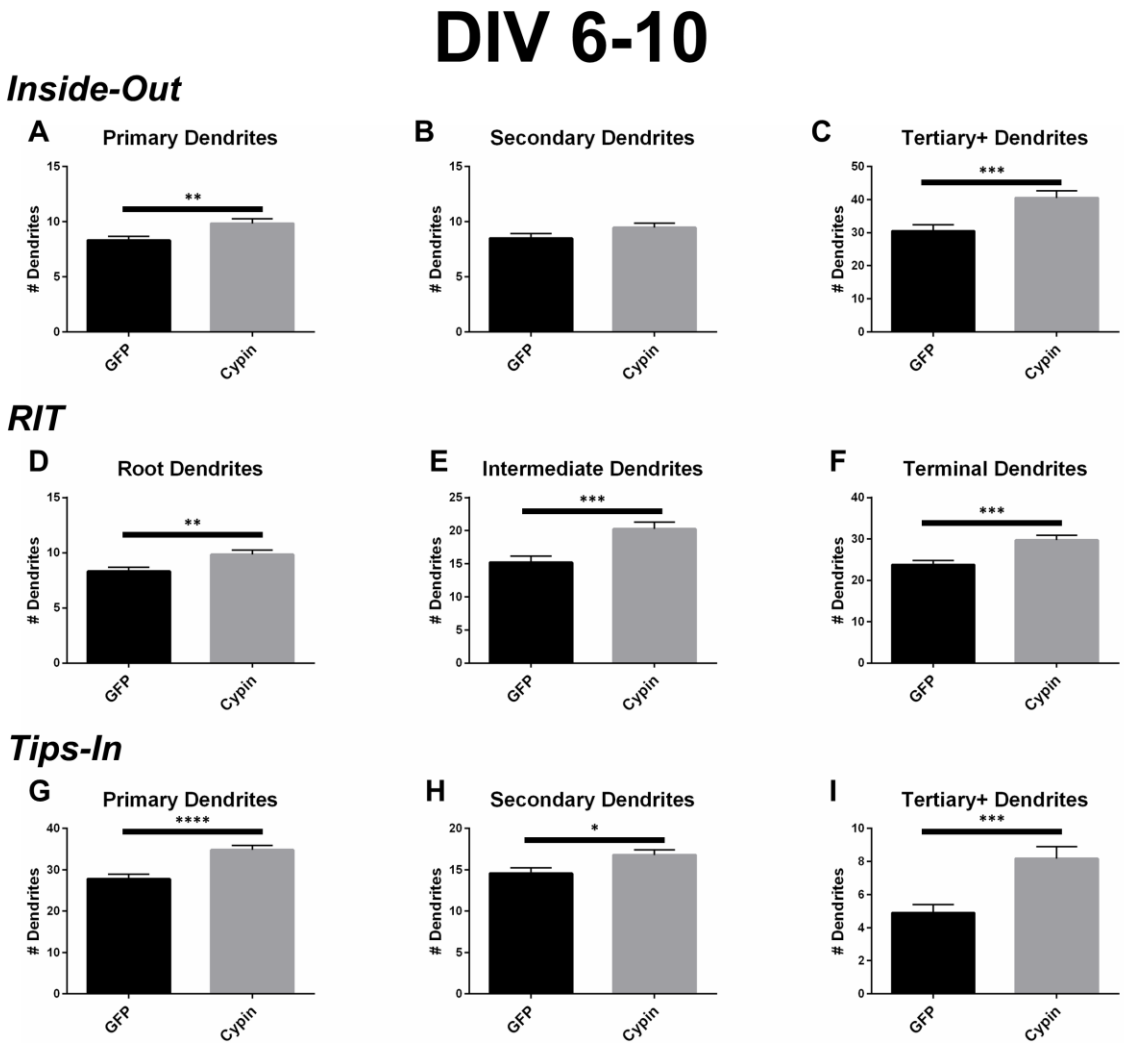

Figure 2-4: Cypin increases the number of dendrites by specifically targeting certain categories of dendrites when overexpressed in neurons from DIV 6-10.
A.-C. Dendrite numbers divided into categories using Inside-Out (conventional) labeling method. **A.** Overexpression of cypin significantly increases the number of primary dendrites (**p<0.01). **B.** Overexpression of cypin does not significantly increase the number of secondary dendrites. **C.** Overexpression of cypin significantly increases the number of tertiary and higher order dendrites (***p<0.001). **D.-F.** Dendrite numbers divided into categories using RIT labeling method. **D.** Overexpression of cypin significantly increases the number of root dendrites (**p<0.01). **E.** Overexpression of cypin significantly increases the number of intermediate dendrites (***p<0.001). **F.** Overexpression of cypin significantly increases the number of terminal

dendrites (***p<0.001). **G.-I.** Dendrite numbers divided into categories using Tips-In labeling method. **G.** Overexpression of cypin significantly increases the number of primary dendrites (****p<0.0001). **H.** Overexpression of cypin significantly increases the number of secondary dendrites (*p<0.05). **I.** Overexpression of cypin significantly increases the number of tertiary and higher order dendrites (***p<0.001). Statistics calculated by unpaired, two-tailed Student's *t*-test. Error bars indicate SEM. n=50 neurons for GFP, and n=55 neurons for cypin.

2.3.3 Dendrite length for neurons overexpressing cypin from DIV 6-10

In addition to the effects of cypin overexpression from DIV 6-10 on dendrite number and spatial arrangement, cypin overexpression affects the lengths of dendrites. As shown in Figure 2-2C, overexpression of cypin significantly increases the total number dendrites, but as shown in Figure 2-2D, it also significantly decreases the average dendritic length, perhaps due to the exhaustion of a limiting reagent required for dendrite growth (Charych, Akum et al. 2006).

When analyzed according to the Inside-Out labeling method, overexpression of cypin significantly decreases the length of tertiary and higher order dendrites (Figure 2-5C). Interestingly, the length of primary dendrites is not affected (Figure 2-5A) although their numbers are increased (as shown in Figure 2-4A). Secondary dendrite length is not affected by cypin overexpression (Figure 2-5B). These data indicate that overexpression of cypin specifically changes the length of higher order dendrites.

The dendrite length data from the RIT method complement the data gathered using the Inside-Out method. While cypin overexpression does not affect the length of root dendrites (Figure 2-5D), it significantly decreases the lengths of intermediate and terminal dendrites (Figure 2-5E and F, respectively). Only tertiary and higher order dendrite numbers significantly decrease with cypin overexpression when analyzed using

the Inside-Out method, indicating that analysis of two different classes (intermediate and terminal) are combined, thus eliminating information. Additionally, while no significant difference in length is observed for secondary dendrites (Figure 2-5B), a significant decrease in intermediate dendrite length results from cypin overexpression (Figure 2-5E). Based on these data, cypin overexpression affects the length of intermediate branches, most likely higher order (> secondary) dendrite branches, and terminal branches.

Finally, the data for the Tips-In method indicate that overexpression of cypin significantly decreases the length of primary and secondary dendrites (Figure 2-5G and H). Primary dendrites are terminal dendrites or root dendrites that have not branched, and secondary dendrites are the penultimate branch or a root dendrite that has branched once (Figure 2-1, right panel). While these are two very different categories of branches, cypin overexpression significantly decreases the lengths of both of these types of branches. Cypin overexpression does not result in a change in length of tertiary and higher order dendrites (Figure 2-5I).

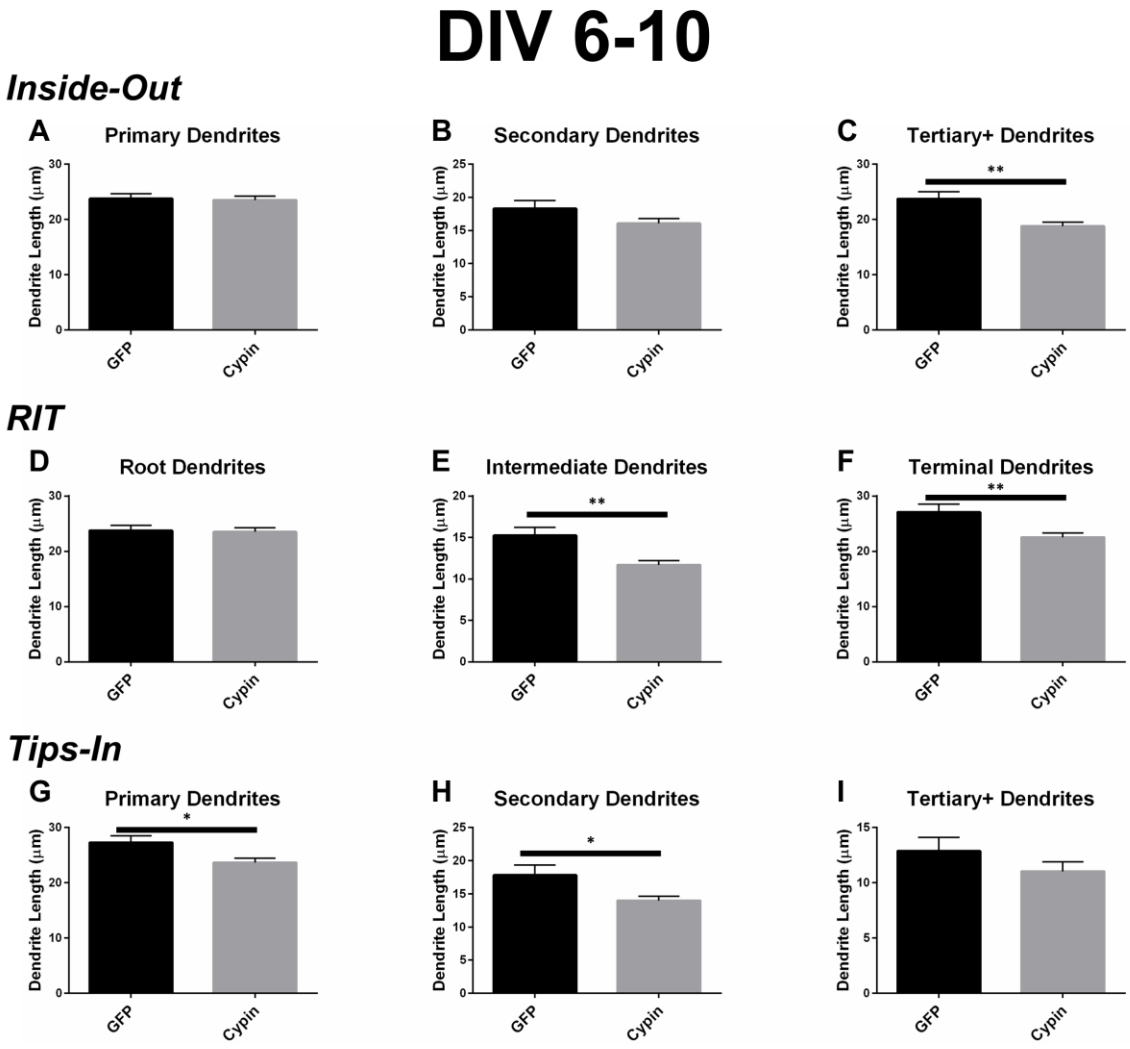

Figure 2-5: Cypin decreases the length of dendrites by specifically targeting certain categories of dendrites when overexpressed in neurons from DIV 6-10.
A.-C. Average dendrite length divided into categories using Inside-Out (conventional) labeling method. **A.** Cypin overexpression does not significantly change the length of primary dendrites. **B.** Cypin overexpression does not significantly decrease the length of secondary dendrites. **C.** Cypin overexpression significantly decreases the length of tertiary and higher order dendrites (**p<0.001). For **A.** and **B.**, statistics were calculated by unpaired, two-tailed Student's *t*-tests, and for **C.**, statistics were calculated by unpaired, two-tailed Student's *t*-tests with Welch's correction. **D.-F.** Average dendrite length divided into categories using RIT labeling method. **D.** Cypin overexpression does not significantly change the length of root dendrites. **E.** Cypin overexpression significantly decreases the length of intermediate dendrites (**p<0.001). **F.** Cypin overexpression significantly decreases the length of terminal dendrites (**p<0.001). For **D.**, statistics were calculated by unpaired, two-tailed Student's *t*-tests, and for **E.** and **F.**, statistics were calculated by unpaired, two-tailed Student's *t*-tests with Welch's correction. **G.-I.** Average dendrite length divided into categories using Tips-In labeling method. **G.** Cypin overexpression significantly

decreases the length of primary dendrites (*p<0.05). **H.** Cypin overexpression significantly decreases the length of secondary dendrites (*p<0.05). **I.** Cypin overexpression does not significantly decrease the length of tertiary and higher order dendrites. For **G.-I.**, statistics were calculated by unpaired, two-tailed Student's *t*-tests with Welch's correction. Error bars indicate SEM. n=50 neurons for GFP, and n=55 neurons for cypin.

2.3.4 Sholl analysis for neurons overexpressing cypin from DIV 10-12

As we previously reported (Akum, Chen et al. 2004, Chen and Firestein 2007, Fernandez, Welsh et al. 2008, Kwon, Fernandez et al. 2011), overexpression of cypin from DIV 10-12 also promotes dendrite branching in hippocampal neurons. Sholl analysis performed with all branch orders grouped (Total Sholl, Figure 2-6B) is the same analysis regardless of which labeling method is used. Total Sholl analysis shows that overexpression of cypin significantly increases proximal branches at 18-30 μm from the soma when it is overexpressed from DIV 10-12. As with our analysis of neurons overexpressing cypin from DIV 6-10, we can identify the mechanism by which this change occurs by examining Sholl curves for different branch categories and comparing these differences among the three analysis methods.

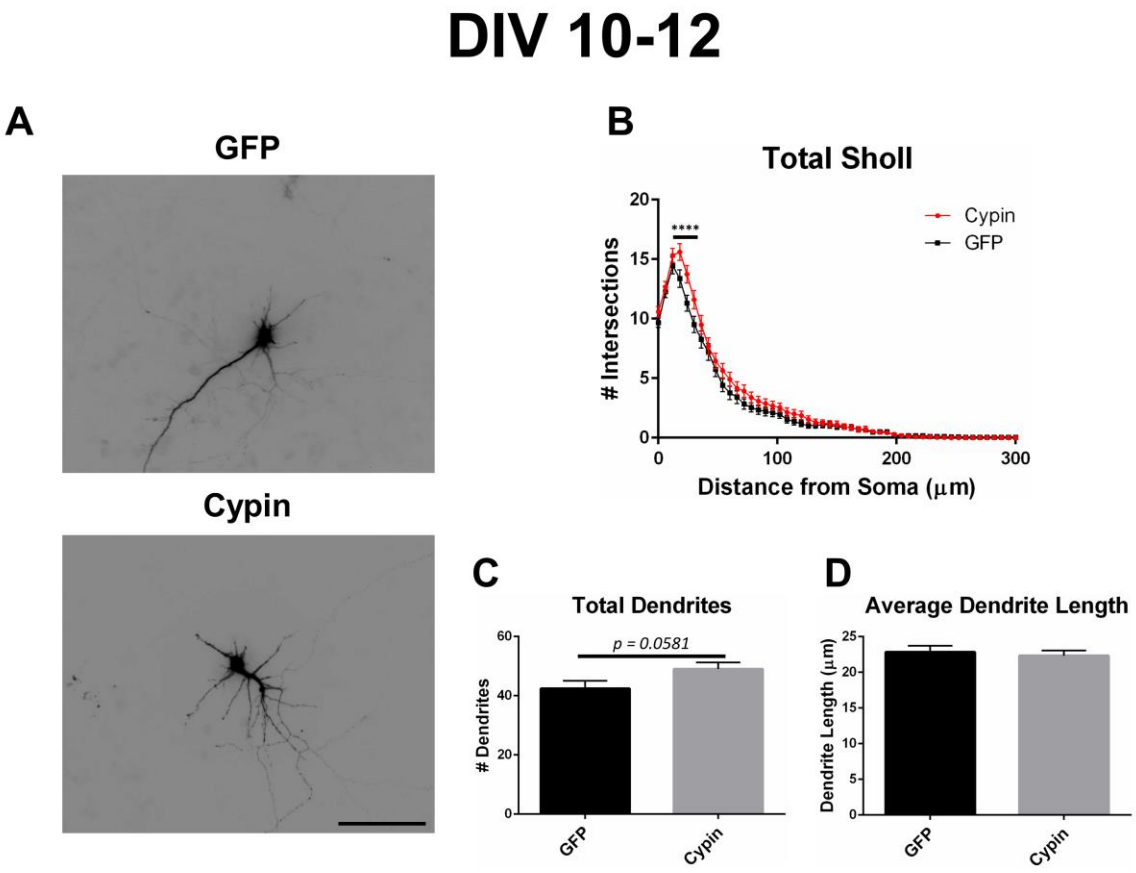

Figure 2-6: Cypin overexpression from DIV 10-12 increases proximal branching with no significant effect on total dendrite number or average dendrite length.
A. Representative images of hippocampal neurons overexpressing GFP or GFP-cypin (cypin) from DIV 10-12. Scale bar = 100 μm. **B.** Sholl analysis for all orders of branches (Total Sholl) shows that overexpression of cypin significantly increases dendrite branching at 18-30 μm from the soma (****$p<0.0001$). Statistics were calculated using two-way ANOVA followed by Bonferroni multiple comparisons test. **C.** Cypin overexpression results in a marginally significant increase in the number of total dendrites ($p=0.0581$). **D.** Cypin overexpression does not significantly change average dendrite length. For **C.** and **D.**, statistics were calculated by unpaired, two-tailed Student's *t*-test. Error bars indicate SEM. n=35 neurons for GFP, and n=51 neurons for cypin.

When analyzing the dendritic arbor using the Inside-Out method, cypin overexpression from DIV 10-12 promotes proximal branching in all branch types. Primary branches significantly increase at 0-6 μm from the soma when cypin is overexpressed (Figure 2-7A). Secondary dendrites, which emerge from primary

dendrites, significantly increase at 12 μm from the soma (Figure 2-7B). Higher order dendrites significantly increase at 18-36 μm from the soma in neurons overexpressing cypin (Figure 2-7C). These results indicate that during DIV 10-12, at the end of the active dendrite branching period in our cultured neurons (i.e. stage 4) (Dotti, Sullivan et al. 1988, Akum, Chen et al. 2004), cypin overexpression promotes increases in all branch types at specific distances from the soma.

Cypin overexpression also promotes increases in all categories of dendrites when analyzed by the RIT labeling method. As with the Inside-Out method, significant changes occur in proximal dendrites less than 50 μm from the soma. Primary dendrites identified by the Inside-Out method and root dendrites identified by the RIT method are identical, and thus, the changes observed in these dendrite categories are the same: a significant increase in root dendrites at 0-6 μm from the soma (Figure 2-7D). There is a difference, however, when comparing secondary dendrites from the Inside-Out method and intermediate dendrites from the RIT method because intermediate dendrites include all dendrites that are not root or terminal dendrites. For neurons overexpressing cypin, significant increases in intermediate dendrites are observed at 12-18 μm from the soma using the RIT method (Figure 2-7E), whereas there is a sole significant increase at 12 μm from the soma for secondary dendrites when using the Inside-Out method (Figure 2-7B). This difference indicates that the significant increase at 12 μm is due to increased secondary dendrites, whereas the increase at 18 μm is due to increases in higher order dendrites. The Sholl curves for terminal dendrites analyzed using the RIT method show similar increases to those identified as tertiary and higher order using the Inside-Out method. Neurons overexpressing cypin show significantly increased branching 18-36 μm

from the soma (Figure 2-7F). These results reveal that cypin-promoted increases in higher order dendrites at these distances are specifically due to increased terminal dendrite branching.

When analyzing the dendritic arbor using the Tips-In method, cypin overexpression results in increased dendrites of all categories. Primary branches are the outermost, or terminal, dendrites in this labeling scheme. The Sholl curve for these branches is similar to that of the terminal branches for RIT but has some important differences. For the Tips-In labeling scheme, primary dendrites include terminal dendrites and root dendrites that do not branch (Figure 2-1, right panel). Primary dendrites significantly increase in neurons overexpressing cypin at 18-30 μm from the soma (Figure 2-7G), which are the same distances observed for increased dendrites identified by Total Sholl analysis (Figure 2-6B). These data indicate that the outermost dendrites and root dendrites that do not branch are responsible for the overall increases observed. Secondary dendrites in this scheme are dendrites that are one order in from the outermost dendrite, either the penultimate dendrite or a root dendrite with only one branch (Figure 2-1, right panel). The Sholl curve resulting from analysis of secondary dendrites from the Tips-In method is distinct from the intermediate Sholl curve from the RIT method and the secondary Sholl curve from the Inside-Out method. For the Tips-In method, significant increases in branching occur at 6-18 μm from the soma for neurons overexpressing cypin (Figure 2-7H). In contrast, intermediate dendrites identified by the RIT method significantly increase at 12-18 μm from the soma (Figure 2-7E). These differences can be explained by how dendrites are grouped. Secondary dendrites, as defined by the Tips-In scheme, include intermediate dendrites and root dendrites with

only one branch. Thus, the additional significant increase at 6 μm could be due to an increase in root dendrites with only one branch. Finally, dendrites labeled as tertiary and higher order are the antepenultimate (third to last) dendrite. These dendrites correspond to root dendrites that branch twice or more. For tertiary and higher order dendrites of the Tips-In scheme, significant increases occur at 0-6 μm from the soma (Figure 2-7I). These increases correspond to those observed for primary dendrites identified by the Inside-Out scheme and root dendrites identified by the RIT scheme.

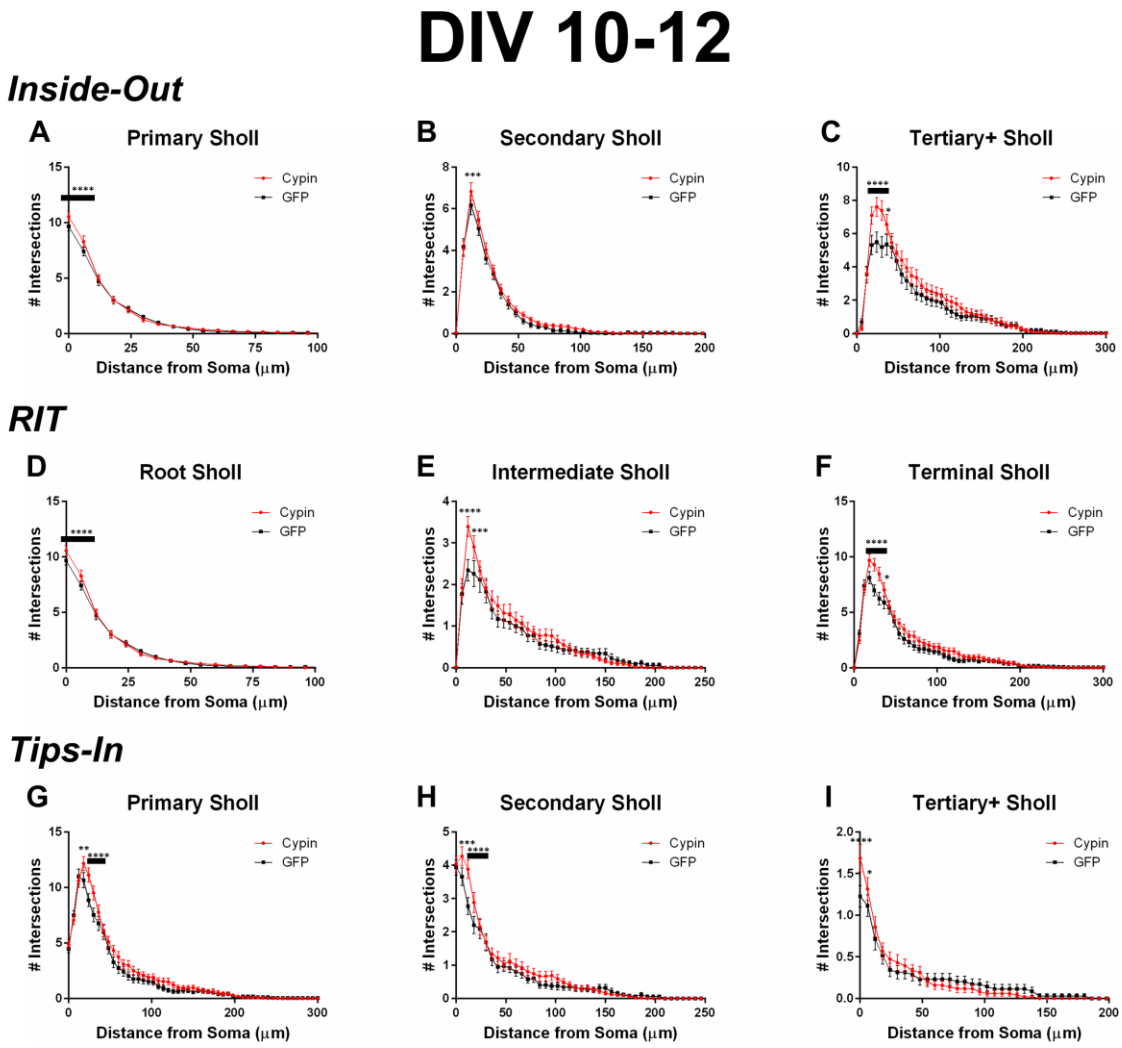

Figure 2-7: Sholl analysis using three different labeling methods for neurons overexpressing cypin from DIV 10-12.

A.-C. Sholl analysis using Inside-Out (conventional) labeling method. **A.** Sholl analysis of primary dendrites (Primary Sholl) shows that overexpression of cypin significantly increases branching at 0-6 μm from the soma (****p<0.0001). **B.** Sholl analysis of secondary dendrites (Secondary Sholl) shows that overexpression of cypin significantly increases branching at 12 μm from the soma (***p<0.01). **C.** Sholl analysis of tertiary and higher order dendrites (Tertiary+ Sholl) shows that overexpression of cypin significantly increases branching at 18-30 μm from the soma (****p<0.0001) and at 36 μm from the soma (*p<0.05). **D.-F.** Sholl analysis using RIT labeling method. **D.** Sholl analysis of root dendrites (Root Sholl) shows that overexpression of cypin significantly increases branching at 0-6 μm from the soma (****p<0.0001). **E.** Sholl analysis of intermediate dendrites (Intermediate Sholl) shows that overexpression of cypin significantly increases dendrite branching at 12 μm (****p<0.0001) and at 18 μm (***p<0.001) from the soma. **F.** Sholl analysis of terminal dendrites (Terminal Sholl) shows that overexpression of cypin significantly increases dendrite branching at 18-30 μm from the soma (****p<0.0001) and at 36 μm from the soma (*p<0.05). **G.-I.** Sholl analysis using Tips-In labeling method. **G.** Sholl analysis of primary dendrites shows that overexpression of cypin increases branching at 18 μm from the soma (**p<0.01) and at 24-30 μm from the soma (****p<0.0001). **H.** Sholl analysis of secondary dendrites shows that overexpression of cypin increases dendrite branching at 6 μm from the soma (***p<0.001) and at 12-18 μm from the soma (****p<0.0001). **I.** Sholl analysis of tertiary and higher order dendrites shows that overexpression of cypin significantly increases branching at the soma (0 μm, ****p<0.0001) and at 6 μm from the soma (*p<0.05). Statistics were calculated using two-way ANOVA followed by Bonferroni multiple comparisons test. Error bars indicate SEM. n=35 neurons for GFP, and n=51 neurons for cypin.

2.3.5 Dendrite number for neurons overexpressing cypin from DIV 10-12

Cypin overexpression from DIV 10-12 affects dendrites of specific orders, depending on the labeling scheme. For all labeling schemes, the total dendrite count is identical, and cypin overexpression from DIV 10-12 results in a marginally significant increase in dendrite number (p=0.0581; Figure 2-6C). The Inside-Out labeling scheme shows that cypin overexpression does not increase primary, secondary, or tertiary and higher order dendrite number (Figure 2-8A-C). Similarly, the RIT labeling scheme suggests that cypin overexpression does not increase root or intermediate dendrite number (Figure 2-8D and E, respectively). However, cypin overexpression does result in

a marginally significance increase in terminal dendrite number (p=0.0747; Figure 2-8F). Complementing these results, the Tips-In labeling scheme shows that cypin overexpression results in a significant increase in primary dendrites (Figure 2-8G), which are terminal dendrites or dendrites with no branches (Figure 2-1, right panel). This significant increase was masked in the previous labeling schemes due to how the dendrites are grouped. Additionally, cypin overexpression causes a marginally significant increase (p=0.0503) in secondary branches (Figure 2-8H), which are the penultimate intermediate branch or root dendrites that have branched once (Figure 2-1, right panel). Using this method, no increases in tertiary and higher order dendrites are detected (Figure 2-8I).

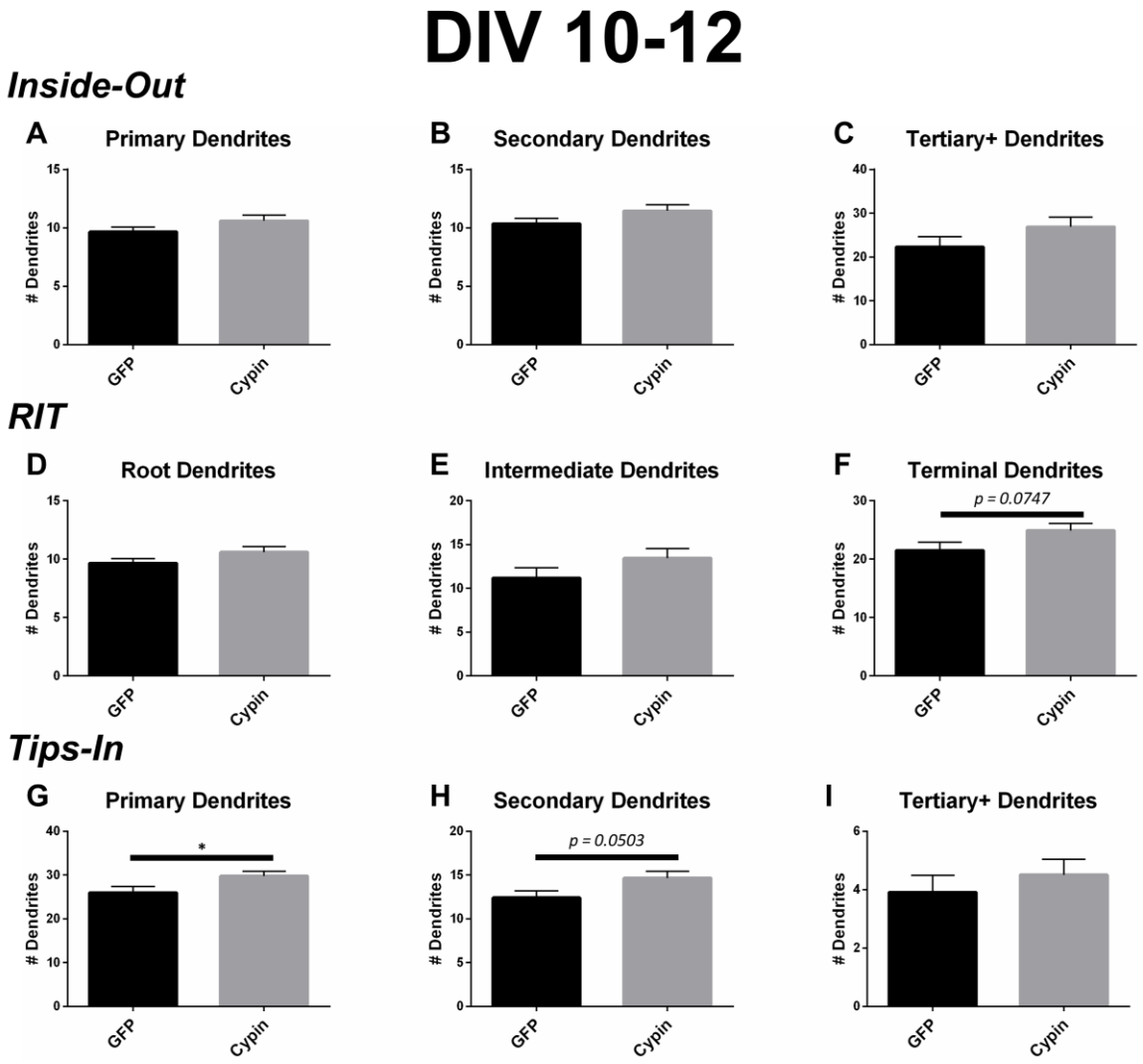

Figure 2-8: Cypin increases outermost dendrites when overexpressed in neurons from DIV 10-12.

A.-C. Dendrite numbers divided into categories using Inside-Out (conventional) labeling method. **A.** Cypin overexpression does not increase the number of primary dendrites. **B.** Cypin overexpression does not increase the number of secondary dendrites. **C.** Cypin overexpression does not increase the number of tertiary and higher order dendrites. For **A.** and **B.**, statistics were calculated by unpaired, two-tailed Student's *t*-tests with Welch's correction, and for **C.**, statistics were calculated by unpaired, two-tailed Student's *t*-tests. **D.-F.** Dendrite numbers divided into categories using RIT labeling method. **D.** Cypin overexpression does not increase the number of root dendrites. **E.** Cypin does not increase the number of intermediate dendrites. **F.** Cypin overexpression results in a marginally significant increase in the number of terminal dendrites (p=0.0747). For **D.** and **E.**, statistics were calculated by unpaired, two-tailed Student's *t*-tests with Welch's correction, and for **F.**, statistics were calculated by unpaired, two-tailed Student's *t*-tests. **G.-I.** Dendrite numbers divided into categories using Tips-In labeling method. **G.** Cypin overexpression significantly increases the

number of primary dendrites (*p<0.05). **H.** Cypin overexpression results in a marginally significant increase in the number of secondary dendrites (p=0.0503). **I.** Cypin overexpression does not significantly change the number of tertiary and high order dendrites. For **G.-I.**, statistics were calculated by unpaired, two-tailed Student's *t*-test. Error bars indicate SEM. n=35 neurons for GFP, and n=51 neurons for cypin.

2.3.6 Dendrite length for neurons overexpressing cypin from DIV 10-12

Cypin overexpression from DIV 10-12 results in changes to the lengths of specific orders of dendrites, depending on the labeling scheme. For all labeling schemes, the total dendrite count is identical, and cypin overexpression from DIV 10-12 does not affect overall dendrite length (Figure 2-6D). The Inside-Out labeling scheme suggests that cypin overexpression does not affect dendrite length according to this labeling method (Figure 2-9A-C). Similarly, the RIT labeling scheme suggests that cypin overexpression has no effect on dendrite length (Figure 2-9D-F). In contrast, the Tips-In labeling scheme suggests that cypin overexpression results in a significant decrease in the length of tertiary and higher order dendrites (Figure 2-9I) without any effect on primary or secondary dendrite length (Figure 2-9G and H, respectively). Taken together, these data suggest that overexpression of cypin specifically affects the lengths of root dendrites with two or more branches. Moreover, we would not have detected this subtle change without using the Tips-In labeling method.

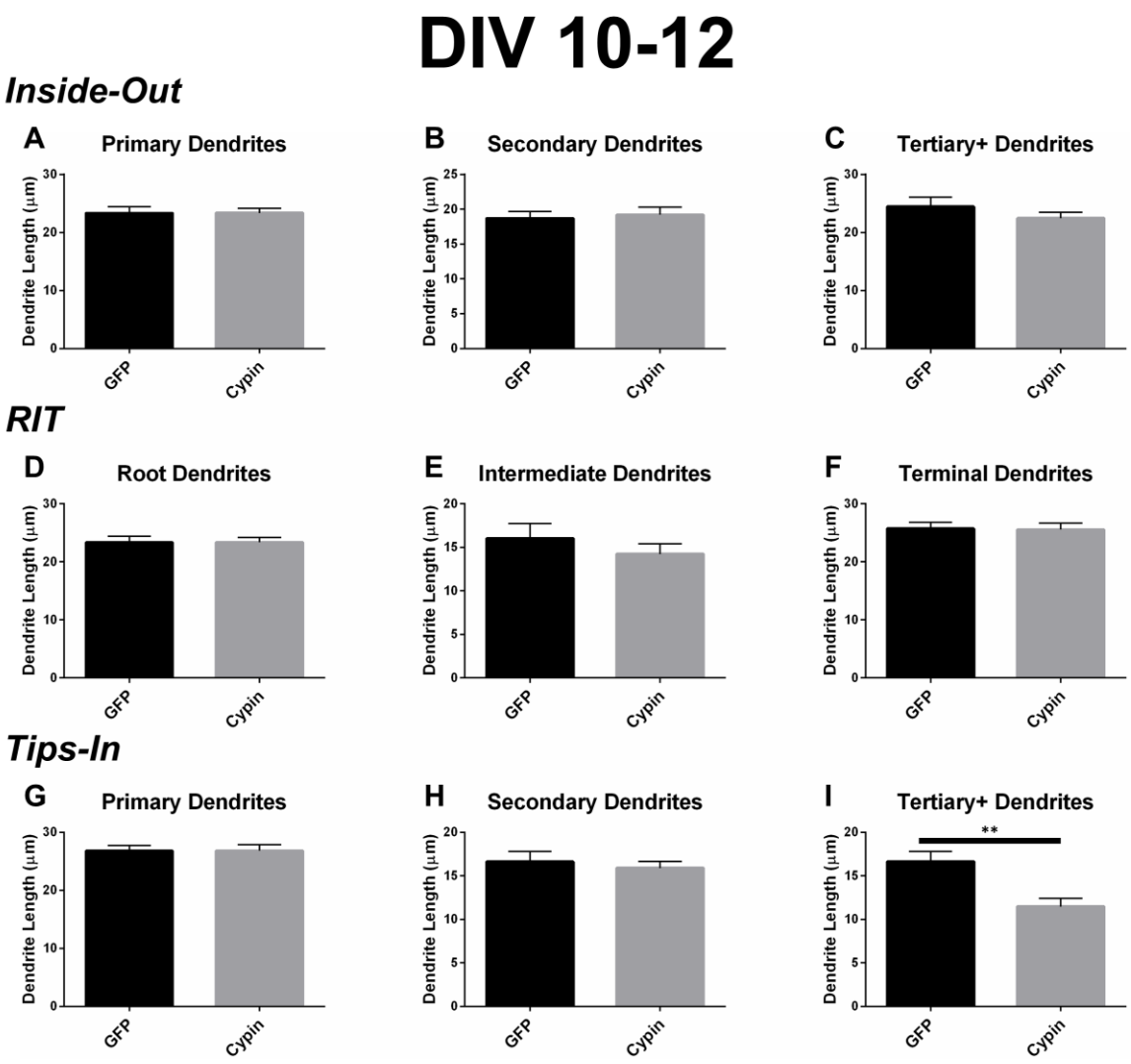

Figure 2-9: Cypin decreases the length of innermost dendrites when overexpressed in neurons from DIV 10-12.

A.-C. Average dendrite length divided into categories using Inside-Out (conventional) labeling method. **A.** Cypin overexpression does not significantly change the length of primary dendrites. **B.** Cypin overexpression does not significantly change the length of secondary dendrites. **C.** Cypin overexpression does not significantly change the length of tertiary and higher order dendrites. For **A.**, statistics were calculated by unpaired, two-tailed Student's *t*-tests, and for **B.** and **C.**, statistics were calculated by unpaired, two-tailed Student's *t*-tests with Welch's correction. **D.-F.** Average dendrite length divided into categories using RIT labeling method. **D.** Cypin overexpression does not significantly change the length of root dendrites. **E.** Cypin overexpression does not significantly change the length of intermediate dendrites. **F.** Cypin overexpression does not significantly change the length of terminal dendrites. For **D.**, statistics were calculated by unpaired, two-tailed Student's *t*-tests, and for **E.** and **F.**, statistics were calculated by unpaired, two-tailed Student's *t*-tests with Welch's correction. **G.-I.** Average dendrite length divided into categories using Tips-In labeling method. **G.** Cypin overexpression

does not significantly change the length of primary dendrites. **H.** Cypin overexpression does not significantly change the length of secondary dendrites. **I.** Cypin overexpression significantly decreases the length of tertiary and higher order dendrites (**p<0.01). For **G.** and **H.**, statistics were calculated by unpaired, two-tailed Student's *t*-tests with Welch's correction, and **I.**, statistics were calculated by unpaired, two-tailed Student's *t*-tests. Error bars indicate SEM. n=35 neurons for GFP, and n=51 neurons for cypin.

2.4 Discussion

Our laboratory has published a number of studies reporting an important role for the protein cypin in the regulation of dendrite branching and arborization (Akum, Chen et al. 2004, Charych, Akum et al. 2006, Chen and Firestein 2007, Fernandez, Welsh et al. 2008, Kwon, Fernandez et al. 2011). Until now, our data have been presented as changes in primary and secondary dendrite number and analyzed by conventional Sholl analysis. In this chapter, we asked whether the combination of different types of Sholl analysis can uncover local changes to the dendritic arbor promoted by cypin overexpression. This work employs our semi-automated Sholl analysis program ("Bonfire") (Langhammer, Previtera et al. 2010) and includes three different labeling schemes (Inside-Out, RIT, and Tips-In) to identify previously unreported changes to the dendritic arbor.

To elucidate whether cypin mediates distinct effects on the arbor at different developmental timepoints, we overexpressed cypin from DIV 6-10 and from DIV 10-12, corresponding to periods of active proximal and distal branching (Dotti, Sullivan et al. 1988). When overexpressed from DIV 6-10, cypin increases dendritic branching at 0-42 μm from the soma (Figure 2-2B), but when overexpressed from DIV 10-12, cypin increases dendritic branching at 18-30 μm from the soma (Figure 2-6B). Thus, the increase in dendrite branching caused by cypin occurs farther out from the soma at the later developmental time point, suggesting that cypin has specific effects. This may be

due to the fact that cypin promotes local microtubule assembly (Akum, Chen et al. 2004), and the location of this assembly during distinct times in development, possibly dependent on to where cypin is targeted, may affect specific regions of the arbor.

In terms of dendrite number, cypin significantly increases total dendrite number (Figure 2-2C) when overexpressed from DIV 6-10 with decreased overall dendrite length (Figure 2-2D). A marginally significant ($p=0.0581$) increase in total dendrite number is observed when cypin is overexpressed from DIV 10-12 (Figure 2-6C) with no change in average length (Figure 2-6D). Taken together, these data suggest that cypin alters the dendritic arbor uniquely depending on when in development it is overexpressed. The observed differences in the effect on total dendrite number and average dendrite length could be caused by overexpression of cypin for 96 h versus 48 h. While 48 h (DIV 10-12) was sufficiently long enough to change the dendritic arbor as seen in Total Sholl analysis (Figure 2-6B), it may not have been long enough to significantly change overall dendrite number in the experiments used for this study.

We have shown that when using these different labeling schemes – Inside-Out, RIT, and Tips-In – the Sholl curves produced can lead to different interpretations of the effects of cypin overexpression on the process of dendrite branching. Inclusion of all three of the labeling schemes in analysis provides the most complete picture of changes occurring to the arbor. Several tools (Sholl 1953, Van Pelt and Verwer 1985, Van Pelt and Verwer 1986, Verwer and Van Pelt 1990, Caserta, Eldred et al. 1995, Cannon, Turner et al. 1998, Uylings and Van Pelt 2002, Meijering, Jacob et al. 2004, Rodriguez, Ehlenberger et al. 2006) have been developed to assist in Sholl analysis, but to our

knowledge, Bonfire is the first to offer multiple labeling schemes and generate individual Sholl graphs of different dendrite categories.

While Inside-Out is the traditional method for labeling dendrites, information is lost by grouping tertiary and higher order dendrites together. Depending on how the neuron has developed, there may be many tertiary dendrites proximal to the cell body, and they may be several orders away from the terminal branch that is quite far from the cell body. These two types of dendrites would be grouped together in the Inside-Out labeling scheme. The Root-Intermediate-Terminal (RIT) labeling scheme is better suited for uncovering differences in intermediate and terminal dendrites, as they are in separate categories. The RIT scheme suggests that during DIV 6-10, cypin-promoted increases in intermediate dendrites (Figure 2-3E) are due to increased secondary dendrites at 6-12 μm from the soma (Figure 2-3B) and to increased tertiary and higher order dendrites at 30 μm (Figure 2-3C). Additionally, increased terminal branching (Figure 2-3F) appears to result in increased tertiary and higher order dendrites due to the corresponding distances at which significant increases occur. However, terminal branching is not responsible for the increases seen at 54-60 μm from the soma for tertiary and higher order dendrites (Figure 2-3C). For DIV 10-12, the differences in the RIT scheme compared with the Inside-Out scheme indicate that cypin-promoted increases in tertiary and higher order dendrites (Figure 2-7C) are due to an increase in terminal branches (Figure 2-7F) at the corresponding distances, which was the same trend observed for DIV 6-10 overexpression. For intermediate dendrites (Figure 2-7E), it is likely that increased secondary dendrites account for the increased dendrites at 12 μm (Figure 2-7B), whereas

tertiary and higher order dendrites are likely responsible for increased dendrites at 18 μm from the soma (Figure 2-7C).

The Tips-In labeling scheme reveals subtle differences that are not uncovered by the other two labeling schemes, even when used in combination. Sholl analysis of primary dendrites using the Tips-In method (Figure 2-3G) suggests that during DIV 6-10, increased proximal dendrites are root dendrites that do not branch, and increased dendrites further from the cell body are higher order terminal branches. For DIV 6-10 overexpression, significant increases are observed at 0-24 μm from the soma for tertiary and higher order dendrites (Figure 2-3I). The increases at 12 μm and closer to the soma are likely due to primary/root dendrites (Figure 2-3D), whereas increases further than 12 μm from the soma are likely due to a combination of intermediate dendrites (Figure 2-3E). For DIV 10-12, increases in Tips-In primary dendrites are observed at 18-30 μm (Figure 2-7G) due to increased terminal branching (Figure 2-7F). Unlike changes detected when cypin is overexpressed at DIV 6-10, there are no increases observed at distances that correspond to the root Sholl analysis using the RIT method, indicating that the increases observed in Figure 2-7G are due to increased terminal branching only and not due to root dendrites. For Tips-In secondary dendrites, increases are observed from 6-18 μm from the soma (Figure 2-7H). The increase at 6 μm is likely due to primary/root dendrites (Figure 2-7A), the increase at 12 μm due to secondary dendrites (Figure 2-7B), and the increase at 18 μm due to tertiary and higher order dendrites (Figure 2-7C). For tertiary and higher order dendrites (Figure 2-7I), increases seen within 6 μm from the soma are likely due to root/primary dendrites that have

branched twice since no corresponding increases are observed in other dendrite categories.

Regardless of the type of Sholl analysis used, our results strongly suggest that cypin promotes shorter dendrites that are of second order or above. Why would cypin promote increased branching but decreased length? One possibility is that cypin-promoted increases in total dendrites may exhaust a limiting reagent, possibly tubulin or membrane components. A second possibility is that cypin acts via the protein PSD-95. Cypin promotes decreased clustering of PSD-95 (Firestein, Brenman et al. 1999), which dramatically increases dendrite number but decreases dendrite length (Charych, Akum et al. 2006, Sweet, Previtera et al. 2011). The de-clustering of PSD-95 may allow correct polarity of microtubules, increasing branching closer to the cell body (Sweet, Previtera et al. 2011, Sweet, Tseng et al. 2011). It is interesting that all labeling schemes yield this result, although the particular orders of dendrites differ. Combining all three Sholl analyses allows us to detect changes to dendrite number and length at subdivisions of the dendritic arbor.

Overall, we find that cypin overexpression affects Sholl curves, dendrite numbers, and dendrite lengths differently depending on the developmental timepoint and length of time cypin is overexpressed. Combining our Bonfire program (Langhammer, Previtera et al. 2010) and these different labeling schemes allows us to better understand how factors, such as cypin, act to regulate neuronal morphology, and hence, function. A schematic summarizing the changes that cypin overexpression exerts on the dendritic arbor is included in Figure 2-10A for overexpression at DIV 6-10 and in Figure 2-10B for overexpression at DIV 10-12. Future studies will include collaborations with

mathematicians to construct ways to integrate the Inside-Out, RIT, and Tips-In schemes to describe arbors without having to perform the analyses separately. In addition, we would like to use these analyses to devise a system by which we can describe different arbor types (*i.e.* pyramidal, stellate). Ultimately, we hope that our analyses can be combined with data stored in other neuronal morphology databases (Ascoli, Donohue et al. 2007). Our future goal is to construct an analysis method that is easy to use, clearly understood, and can serve as a base for comparison between neuron types, different treatments, and experiments performed by different laboratories.

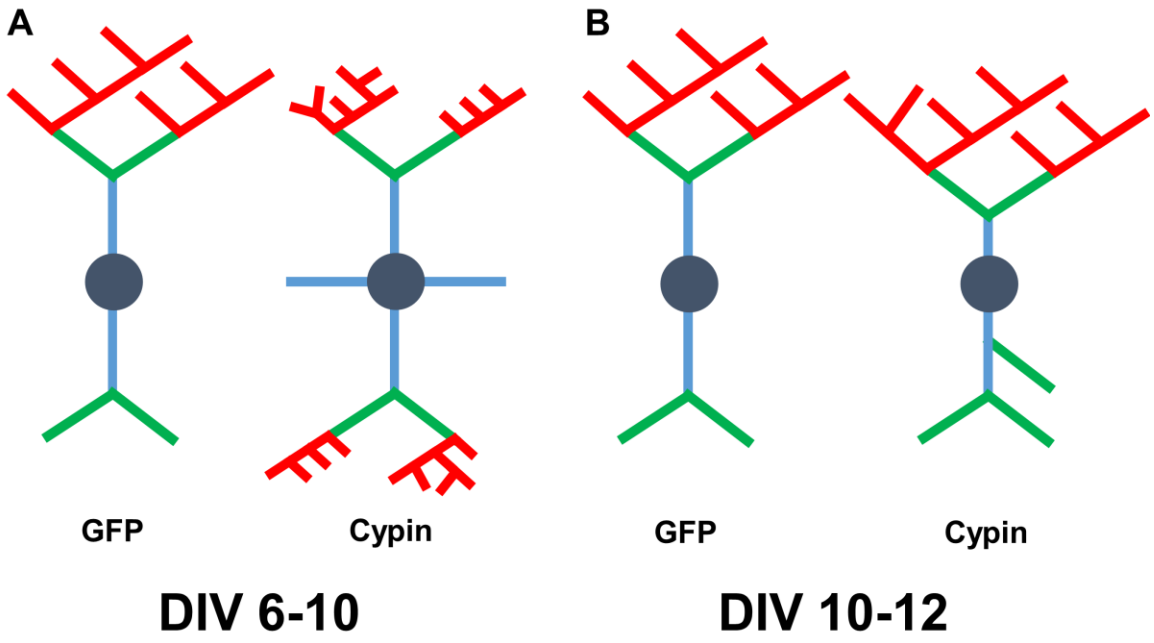

Figure 2-10: Schematic of results when combining analysis using all three labeling schemes.
A. Changes that occur to the arbor as a result of cypin overexpression from DIV 6-10. Overexpression of cypin increases primary dendrite numbers (blue) and tertiary and higher order dendrite numbers (red). Overexpression of cypin also increases intermediate dendrite numbers (green and red) and terminal dendrite numbers (green and red) but not secondary dendrite numbers (green). Overexpression of cypin decreases tertiary and higher order dendrite length, intermediate dendrite length, and terminal dendrite length but does not affect primary or secondary dendrite length. **B.** Changes that occur to the arbor as a result of cypin overexpression from DIV 10-12. Overexpression of cypin

increases primary dendrites as labeled by Tips-In (terminal dendrites, green and red) and secondary dendrites as labeled by Tips-In (intermediate or root dendrites, green and blue). Overexpression of cypin significantly decreases tertiary and higher order dendrite length as labeled by Tips-In (root dendrites that branch twice or more). Dendrites are labeled according to the Inside-Out (conventional) method.

CHAPTER 3: MICROBEAD APPLICATION OF BRAIN-DERIVED NEUROTROPHIC FACTOR REGULATES THE DENDRITIC ARBOR DIFFERENTLY THAN DOES GLOBAL ADMINISTRATION OF BRAIN-DERIVED NEUROTROPHIC FACTOR

The work in this chapter has been accepted with revisions for publication in *Cellular and Molecular Life Sciences* as the following: O'Neill KM*, Kwon M*, Donohue KE, Firestein BL (2017). "Distinct effects on the dendritic arbor occur by microbead versus bath administration of Brain-Derived Neurotrophic Factor."

**equal contribution*

3.1 Introduction

Recent studies have revealed much about how brain-derived neurotrophic factor (BDNF) regulates the dendritic arbor. Several studies have shown that BDNF is a mediator of activity-dependent dendrite branching (Ghosh, Carnahan et al. 1994, McAllister, Katz et al. 1996, Shooter 2001, Jin, Hu et al. 2003). Additionally, our laboratory and others have investigated how bath application of BDNF to neuronal cultures influences dendritic branching. Bath application of BDNF to cortical neuron cultures increases primary dendrite branching via the phosphatidylinositol 3-kinase (PI3K) and mitogen-activated protein kinase (MAPK) pathways in as little as 5 hours (Dijkhuizen and Ghosh 2005). Moreover, we have shown that bath application of BDNF to hippocampal neuron cultures increases proximal branching

via CRE-binding protein (CREB)-dependent transcriptional regulation of cytosolic PSD-95 interactor (cypin) when cultures are treated for at least 72 hours (Kwon, Fernandez et al. 2011).

Treatment with BDNF also causes dendrites to be more active; that is, dendrites are both gained and lost more quickly than when no treatment is present (Horch, Kruttgen et al. 1999). Importantly, release of BDNF from single cells elicits local dendritic growth in nearby neurons, but this occurs only if the source of BDNF is within 4.5 μm of the recipient neuron (Horch and Katz 2002), suggesting that local dendritic stimulation with BDNF may result in different effects on the arbor than bath BDNF application. For example, local puff application of BDNF to dendrites of hippocampal neurons in culture results in phosphorylation of S6, which is a mediator of mTOR-induced local protein synthesis (Takei, Inamura et al. 2004).

Outgrowth of proximal and distal dendrites from neuronal cell bodies is regulated by different mechanisms. For example, in cortical neurons, overexpression of the full length TrkB receptor increases proximal dendrite branching while overexpression of the truncated TrkB receptor T1 (TrkB.T1) results in elongation of distal dendrites (Yacoubian and Lo 2000). In addition, developmental expression patterns of these receptor isoforms differ (Muragaki, Timothy et al. 1995), suggesting the possibility of differential control of dendrite development mediated by distinct receptors or TrkB receptor subtypes. Local stimulation of dendrites can occur when BDNF is released synaptically, and global stimulation of neurons in culture simulates BDNF release by astrocytes, which would more broadly activate signals in the dendritic arbor.

In this chapter, we used our hippocampal neuron culture system to ask how local stimulation with BDNF affects both proximal and distal dendrites. Importantly, we consider these results in the context of our previous study (Kwon, Fernandez et al. 2011). We also investigated whether these changes to the arbor are mediated by cypin, which our laboratory has previously shown to be an intrinsic regulator of dendrite branching (Akum, Chen et al. 2004, Fernandez, Welsh et al. 2008) and of which expression is regulated by bath application of BDNF (Kwon, Fernandez et al. 2011).

3.2 Materials and Methods

3.2.1 Primary culture of hippocampal neurons

Neuronal cultures were prepared from the hippocampi of rat embryos at 18 days of gestation (E18) as described previously (Firestein, Brenman et al. 1999, Kwon, Fernandez et al. 2011). The hippocampi were dissociated using manual trituration, and cells were plated onto poly-D-lysine (PDL; Sigma)-coated 12 mm glass coverslips (Fisher) in 24 well plates (Corning) at a density of 1800 cells/mm^2. Cultures were maintained in Neurobasal medium (Life Technologies) supplemented with B27, GlutaMAX, and penicillin/streptomycin (all Life Technologies) and kept in a humidified 37 ºC incubator with 5% CO_2. Cells were grown for 7 days *in vitro* (DIV) prior to treatment and used for specific experiments as indicated below. All studies were performed in accordance with the Institutional Animal Care and Use Committee (IACUC) standards.

3.2.2 Transfection of cultured cells

To visualize dendritic arbors, cultured hippocampal neurons were transfected at DIV 6 with cDNA encoding GFP or at DIV 5 with shRNAs using Lipofectamine LTX and PLUS reagent following the manufacturer's protocol (Invitrogen). The pSuper GFP vector (Oligoengine) contained shRNAs against the cypin transcript or an unrelated sequence as a negative control (GST) as previously described (Chen and Firestein 2007, Kwon, Fernandez et al. 2011).

3.2.3 Preparation of BSA- and BDNF-coated microbeads

Fluorescent monodispersed polystyrene microspheres (641 nm for excitation wavelength; Polysciences, Inc. Warrington, PA) containing primary amine surface functional groups and a glutaraldehyde kit (Polyscience, Inc., Warrington, PA) were used for coupling BDNF (Promega) to beads by activating carboxylate groups. BDNF was coupled using Protein Coupling Kit (Polyscience, Inc. Warrington, PA) following the manufacturer's protocol. Briefly, microparticles were resuspended in coupling buffer (50 mM MES, pH 5.2, 0.05% Proclin-300) and activated by adding 1-ethyl-3-(3-dimethylaminopropyl) carbodiimide (EDAC) solution. BDNF (200 μg) was incubated with activated microparticles for 1 hour at room temperature with gentle end-to-end mixing. After washing with wash buffer (10 mM Tris, pH 8.0, 0.05% bovine serum albumin (BSA; Fisher), 0.05% Proclin-300), BDNF-coupled particles were resuspended in wash buffer and stored at 4°C. BSA was used as the control protein bound to beads since it should not alter dendrite branching.

3.2.4 Treatment with BSA- and BDNF-coated beads

To mimic local exposure to BDNF, neurons were treated with 1.75 µm fluorescent beads. Each well contained 0.7 ml of medium, and 10 µl of a 0.0625% aqueous suspension of beads (either coupled to BDNF or BSA) was added to each well of a 24 well plate (10^7 beads/well). Cultures were treated with BDNF- or BSA-coated beads for the indicated duration at DIV 7 prior to imaging. To obtain an estimate for the number of beads that contacted each dendrite, the number of beads within 4.5 µm of a dendrite was counted. The estimates were obtained by choosing 10 neurons randomly per condition and evaluating 3-5 dendrites per neuron. The number of beads per dendrite ranged from 1.36 to 2.21 for the first set of experiments and 1.58 to 2.47 for the second set of experiments (as shown in Figure 3-1), and the average number of beads per dendrite was not significantly different between any of the conditions (determined by one-way ANOVA followed by Bonferroni's Multiple Comparisons test).

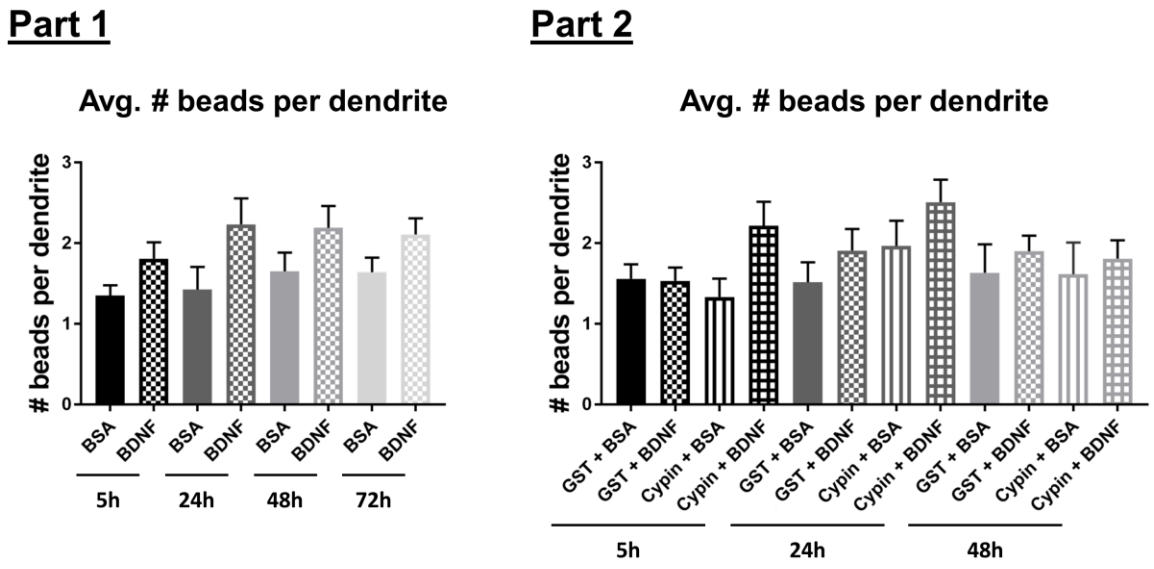

Figure 3-1: Average number of beads per dendrite calculated for each group of experiments.

Part 1. The first group of experiments analyzed neurons transfected with pEGFP-C1 and treated with either BSA- or BDNF-coated beads for 5, 24, 48, or 72 hours. The range in average number of beads per dendrite ranges from 1.36 to 2.21 across all of the conditions, but there are no significant differences observed among the different conditions. **Part 2**. The second group of experiments analyzed neurons transfected with the pSuper-GFP vector containing shRNAs against GST (as a negative control) or cypin and then, 48 hours later, treated with BSA- or BDNF-coated beads for 5, 24, or 48 hours. The range in average number of beads per dendrite ranges from 1.58 to 2.47, but there are no significant differences observed among the different conditions. n=10 neurons for all conditions in both Part 1 and Part 2. Statistics calculated by one-way ANOVA followed by Bonferroni's multiple comparisons test. Error bars indicate SEM.

3.2.5 Live imaging

Live images were taken using an Olympus Optical (Tokyo, Japan) IX50 microscope with a Cooke Sensicam charge-coupled device cooled camera fluorescence imaging system and Image Pro software (Media Cybernetics, Silver Spring, MD). The plate containing the cultures remained on a heated stage for the duration of imaging. Transfected neurons were identified under the GFP channel, and beads were identified under the far red channel. Fluorescent images of transfected neurons were taken live with no fixation since we observed bead movement when we attempted to fix the cultures.

3.2.6 Assessment of dendrite number using semi-automated Sholl analysis and statistics

Dendrites were assessed as previously described (Kutzing, Langhammer et al. 2010, Langhammer, Previtera et al. 2010, Kwon, Fernandez et al. 2011) using the most common Sholl analysis, also known as the Inside-Out labeling scheme (O'Neill, Akum et al. 2015). We used the "Bonfire" program developed by our laboratory to perform semi-automated Sholl analysis with a 6 µm ring interval starting at 9.3 µm from the soma. The experimenter was blinded to conditions during all data analyses. Dendrites less than 3 µm in length were not counted (Yu and Malenka 2004, Charych, Akum et al. 2006).

Prism (Graphpad) was used for statistical analyses. Two-way ANOVA followed by Bonferroni's multiple comparisons test was used to evaluate Sholl curves, and Student *t*-tests were used for analysis of dendrite numbers and lengths.

3.3 Results

3.3.1 Treatment with BDNF-coated beads increases overall dendrite branching in a location and time-dependent manner

To mimic a local source BDNF, we seeded microbeads coated with covalently-bound BDNF (or BSA, as the control) onto neuronal cultures. Microbeads were distributed across the entire neuron, from proximal to distal areas of the dendritic arbor, and made multiple contacts with dendrites (Figure 3-2).

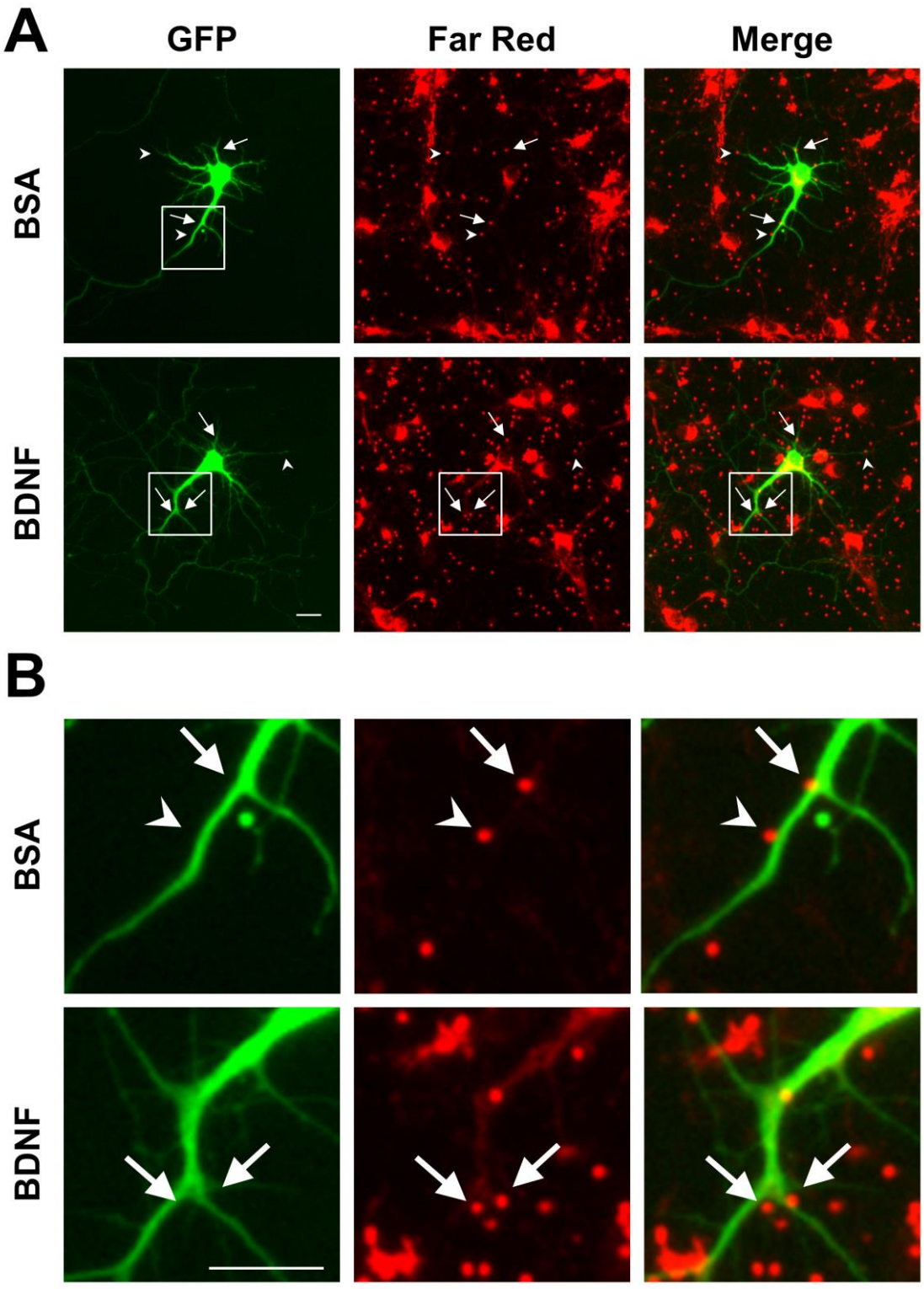

Figure 3-2: Local stimulation of dendrites using microbeads.
A. Representative images of neurons treated with BSA-coated beads (top) or BDNF-coated beads (bottom). Arrows indicate bead-dendrite contact close to a branching point, and arrowheads indicate bead-dendrite contact where no branching point was observed.

Four sites of dendrite bead-contact were indicated for each condition. **B.** Boxed regions from A at higher magnification showing BSA-coated (top) and BDNF-coated (bottom) beads in contact with dendrites. Scale bars indicate 20 μm.

To investigate how exposure to local sources of BDNF affects dendrite branching over time, hippocampal cultures were treated at DIV 7 with control (BSA-coated) or BDNF-coated beads for 5, 24, 48, and 72 hours. Representative images are shown in Figure 3-3A. We then performed Sholl analysis and found that treatment for 24 hours or less does not have a significant effect on the overall dendritic arbor (Figure 3-3B,F and Figure 3-3C,G). However, treatment with BDNF-coated beads significantly increases dendrites when neurons are treated for 48 hours and more. Interestingly, the location of increased branching differs when neurons are treated with BDNF-coated beads for 48 hours versus 72 hours. After 48 hours (Figure 3-3D,H), significant increases in branching occur distally (93.3 to 159.3 μm from the soma), whereas at 72 hours (Figure 3-3E,I), significant increases in branching occur both proximally (21.3 to 29.3 μm from the soma) and distally (123.3 to 153.3 μm from the soma). This change to the dendritic arbor over time indicates that local sources of BDNF affect the arbor as it develops. A subset of proximal and distal dendrites represented on Sholl curves decrease between 48 and 72 hours in the control condition whereas the decrease in these dendrites is attenuated when the neurons are treated with BDNF-coated beads (compare Figure 3-3D,H and Figure 3-3E,I). Moreover, the increases observed after exposure to local sources of BDNF differ when compared to those we previously observed after neurons were treated with bath application of BDNF (Kwon, Fernandez et al. 2011).

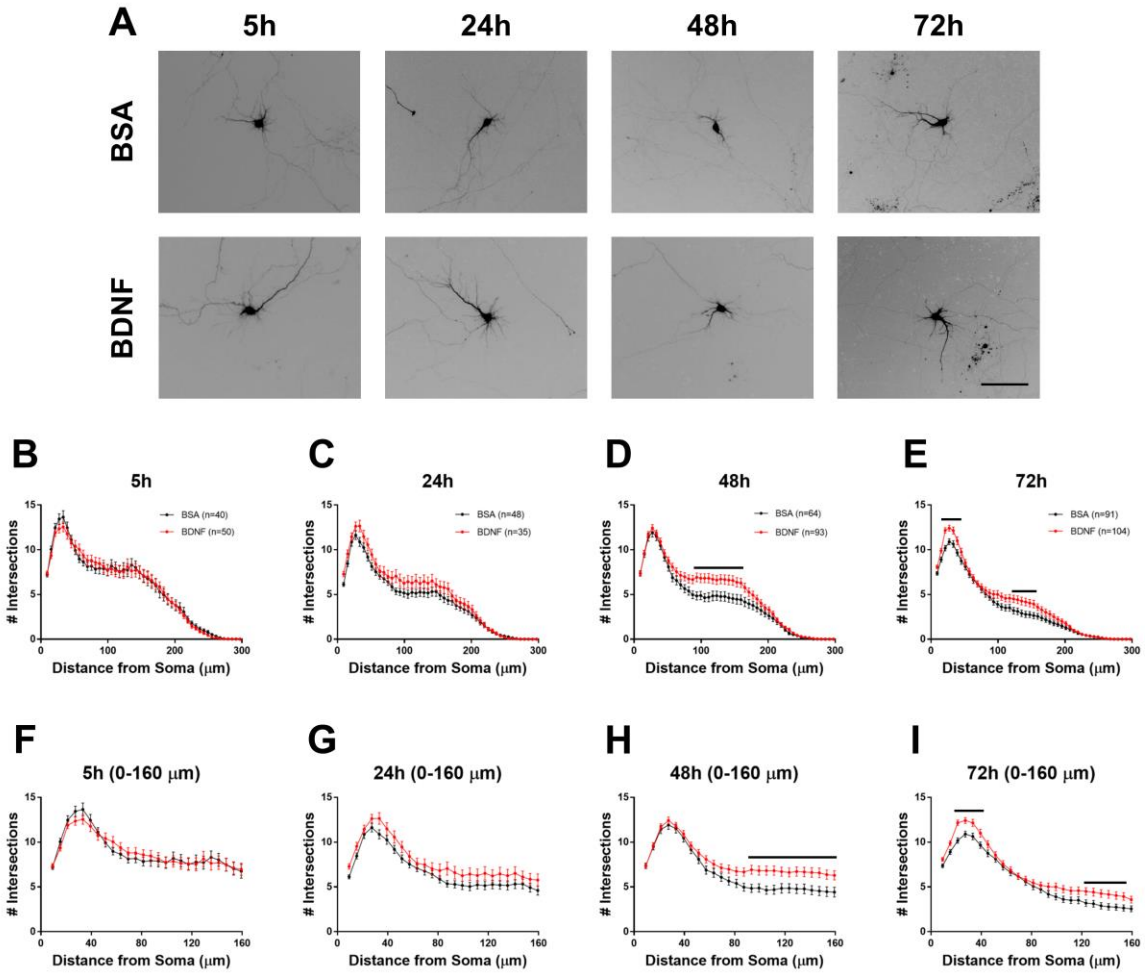

Figure 3-3: Sholl analysis of hippocampal neurons shows that BDNF-coated beads increase branching.

A. Representative images from each condition (BSA- or BDNF-coated bead treatment) at each of the time points (5, 24, 48, and 72 hours). Scale bar indicates 100 μm. **B.** No significant changes in the Sholl curves are observed after 5 hours of treatment with BDNF-coated beads compared with the control treatment (BSA-coated beads). **C.** No significant changes in the Sholl curves are observed after 24 hours of treatment with BDNF-coated beads compared with the control treatment. **D.** Treatment with BDNF-coated beads for 48 hours significantly increases distal branching (93.3-159.3 μm; *p<0.05). **E.** Treatment with BDNF-coated beads for 72 hours significantly increases both proximal (21.3-39.3 μm) and distal (123.3-153.3 μm) branching (both *p<0.05). **F**, **G**, **H**, and **I.** Plots showing the first 160 μm of the Sholl curve from **B**, **C**, **D**, and **E** (respectively). For 5 hour treatment: n(BSA)=40 and n(BDNF)=50. For 24 hour treatment: n(BSA)=48 and n(BDNF)=35. For 48 hour treatment: n(BSA)=64 and n(BDNF)=93. For 72 hour treatment: n(BSA)=91 and n(BDNF)=104. Statistics calculated by Two-Way ANOVA followed by Bonferroni's Multiple Comparisons test. Error bars indicate SEM.

We also performed order-specific Sholl analysis (Figure 3-4; (Langhammer, Previtera et al. 2010)), which sheds light on the mechanism behind the observed increases in certain regions of the overall dendritic arbor. Treatment with BDNF-coated beads for 5 hours, 24 hours, and 72 hours significantly increases primary dendrites (Figure 3-4A, D, and J, respectively). The most prominent increase was observed at 24 hours (Figure 3-4D), with significantly increased branching occurring at 9.3 to 57.3 μm from the soma. Secondary dendrites significantly increase at all time points of BDNF-coated bead treatment (Figure 3-4B, E, H, and K, respectively). After 5 hours of incubation (Figure 3-4B), neurons exposed to BDNF-coated beads show decreased secondary dendrites proximal to the soma (15.3 to 33.3 μm from the soma) and increased secondary dendrites distally (69.3 to 75.3 μm from the soma). After longer incubation periods with beads, exposure to BDNF results in increases in secondary dendrites at similar distances from the soma (between 21.3 and 45.3 μm from the soma). Furthermore, increases in tertiary and higher order dendrites are observed distally and only after 48 hours and 72 hours of exposure to BDNF-coated beads (Figure 3-4I and L, respectively).

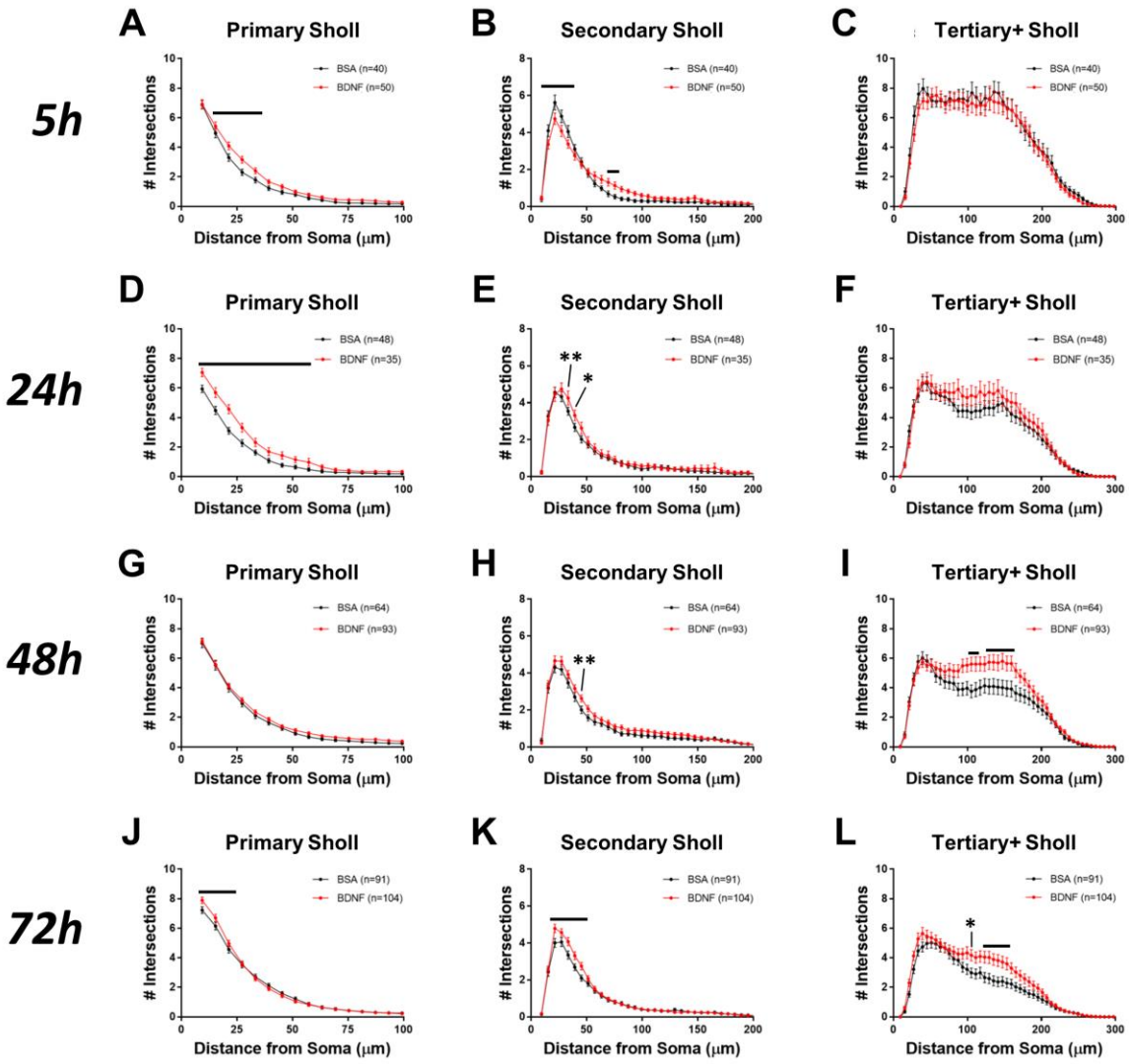

Figure 3-4: Order-specific Sholl analysis reveals that BDNF exerts effects on different types of dendrites.

Stars indicate exact levels of significance, and bars indicate significance of at least *p<0.05. **A-C.** Order-specific Sholl analysis of neurons treated for 5 hours with BSA- or BDNF-coated beads. **A.** Sholl analysis of primary dendrites shows that treatment with BDNF-coated beads significantly increases dendrites at 15.3 to 33.3 μm from the soma (*p<0.05). **B.** Sholl analysis of secondary dendrites shows that treatment with BDNF-coated beads significantly increases dendrites at 15.3 to 33.3 μm (**p<0.01) and at 69.3 to 75.3 μm (*p<0.05) from the soma. **C.** Sholl analysis of tertiary and higher order dendrites shows that treatment with BDNF-coated beads does not significantly alter branching of these dendrites. **D-F.** Order-specific Sholl analysis of neurons treated for 24 hours with BSA- or BDNF-coated beads. **D.** Treatment with BDNF-coated beads significantly increases primary dendrites at 9.3 to 57.3 μm from the soma (*p<0.05). **E.** Treatment with BDNF-coated beads significantly increases secondary dendrites at

33.3 μm (**p<0.01) and at 39.3 μm (*p<0.05) from the soma. **F.** Treatment with BDNF-coated beads does not significantly alter the Sholl curves of tertiary and higher order dendrites. **G-I.** Order-specific Sholl analysis of neurons treated for 48 hours with BSA- or BDNF-coated beads. **G.** Treatment with BDNF-coated beads does not significantly alter the Sholl curves of primary dendrites. **H.** Treatment with BDNF-coated beads significantly increases secondary dendrites at 45.3 μm from the soma (**p<0.01). **I.** Treatment with BDNF-coated beads significantly increases tertiary and higher order dendrites at 105.3 to 111.3 μm and at 129.3 to 159.3 μm from the soma (both *p<0.05). **J-L.** Order-specific Sholl analysis of neurons treated for 72 hours with BSA- or BDNF-coated beads. **J.** Treatment with BDNF-coated beads significantly increases primary dendrites at 9.3 to 21.3 μm from the soma (*p<0.05). **K.** Treatment with BDNF-coated beads significantly increases secondary dendrites at 21.3 to 45.3 μm from the soma (**p<0.01). **L.** Treatment with BDNF-coated beads significantly increases tertiary and higher order branching at 105.3 μm and at 123.3 to 153.3 μm from the soma (both *p<0.05). Statistics calculated by Two-Way ANOVA followed by Bonferroni's Multiple Comparisons test. Error bars indicate SEM.

To better understand how treatment with BDNF-coated beads affects dendritic arborization, we grouped the order-specific and total Sholl curves according to condition and re-graphed our data, as shown in in Figure 3-5. Interestingly, treatment with BDNF-coated beads changes development of the dendritic arbor for all orders of dendrites. For primary dendrites, decreases in Sholl distribution curves are observed between each successive time point in the control (Figure 3-5A) but not in cultures treated with BDNF-coated beads (Figure 3-5D). In addition, Sholl distributions for secondary dendrites significantly decrease in control cultures over time (Figure 3-5B). The natural pruning process that occurs between 5 and 24 hours is attenuated with exposure to BDNF-coated beads (Figure 3-5E). Pruning of tertiary and higher order dendrites occurs between 5 and 24 hours in control cultures (Figure 3-5C) and is blocked by treatment with BDNF-coated beads (Figure 3-5F).

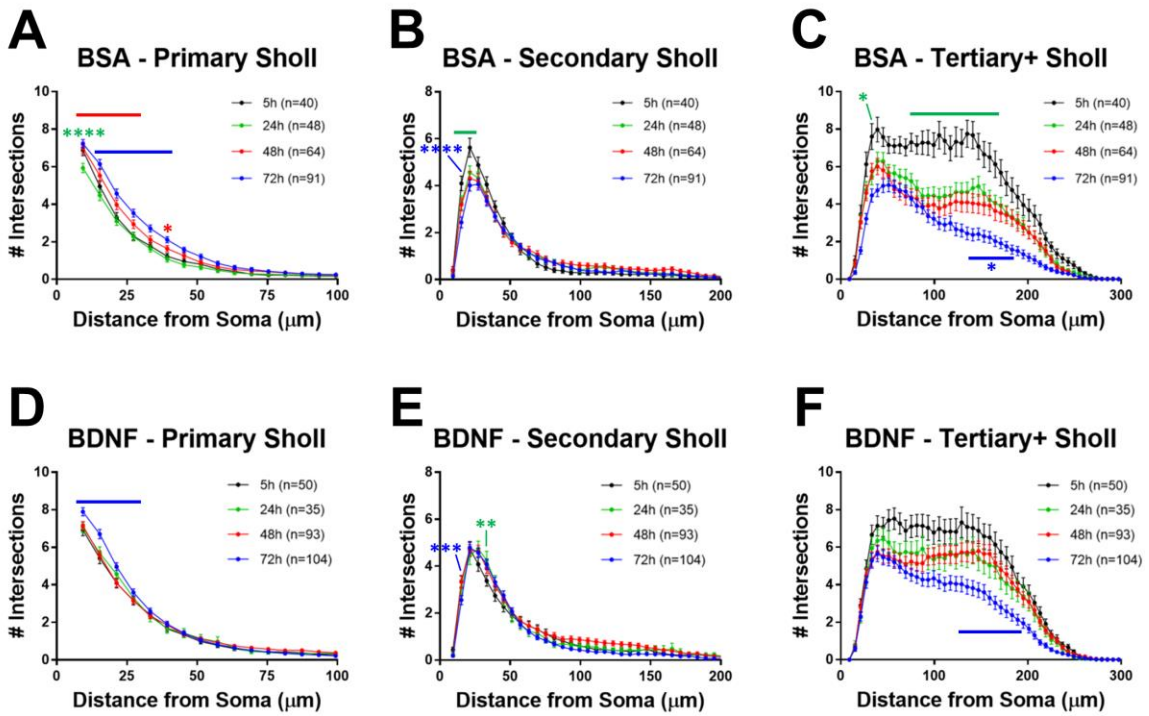

Figure 3-5: Grouping order-specific Sholl analysis by condition reveals how BDNF modulates pruning of higher order dendrites.

To indicate sites of significant differences in dendritic arborization, the following notation is used: 1) green stars/bars to compare the 5 hour and 24 hour time points (black vs. green lines); 2) red stars/bars to compare the 24 hour and 48 hour time points (green vs. red lines); and 3) blue stars/bars to compare the 48 hour and 72 hour time points (red vs. blue lines). Stars indicate exact levels of significance, and bars indicate significance of at least *p<0.05. **A-C.** Order-specific Sholl analysis of neurons treated with BSA-coated beads. **A.** Primary dendrites at 9.3 μm from the soma are significantly decreased between 5 and 24 hours (green stars, ****p<0.0001). Primary dendrites significantly increase between 24 and 48 hours (red bar/star, 9.3-27.3 and 39.3 μm; ***p<0.001). Primary dendrites significantly increase between 48 and 72 hours (blue bar, 15.3-39.3 μm; *p<0.05). **B.** Secondary dendrites at 15.3 to 21.3 μm from the soma are significantly decreased between 5 and 24 hours (green bar; **p<0.01). Secondary dendrites at 15.3 μm from the soma significantly decrease between 48 and 72 hours (blue stars, ****p<0.0001). **C.** Tertiary and higher order dendrites are significantly decreased at 33.3 μm and at 75.3-165.3 μm from the soma between 5 and 24 hours (green star/bar; both *p<0.05). Tertiary and higher order dendrites at 141.3 to 183.3 μm from the soma are also significantly decreased between 48 and 72 hours (blue bar; *p<0.05). **D-F.** Order-specific Sholl analysis of neurons treated with BDNF-coated beads. **D.** BDNF attenuates the changes that occurs between 5 and 24 hours and between 24 and 48 hours of treatment, and it significantly increases primary dendrites after 72 hours of

treatment (blue bar, 9.3-27.3 μm; **p<0.01). **E.** Treatment with BDNF-coated beads not only attenuates the pruning seen between 5 and 24 hours of treatment but also significantly increases secondary branching at 33.3 μm from the soma (green stars; **p<0.01). Secondary dendrites at 15.3 μm from the soma remain significantly decreased between 48 and 72 hours of treatment (blue stars; ***p<0.001). **F.** Treatment with BDNF-coated beads attenuates pruning seen between 5 and 24 hours, but the pruning that occurs between 48 and 72 hours is still observed: tertiary and higher order dendrites are significantly decreased between 48 and 72 hours at 129.3 to 189.3 μm from the soma (blue bar, *p<0.05). Statistics calculated by Two-Way ANOVA followed by Bonferroni's Multiple Comparisons test. Error bars indicate SEM.

3.3.2 Treatment with BDNF-coated beads affects dendrite number and length

In addition to performing multiple Sholl analyses, we quantified how exposure to local sources of BDNF changes the number and length of dendrites, both overall and in an order-specific manner, versus control treatment (BSA-coated beads). Treatment with BDNF-coated beads significantly increases the total number dendrites after at least 48 hours of treatment (Figure 3-6C and D).

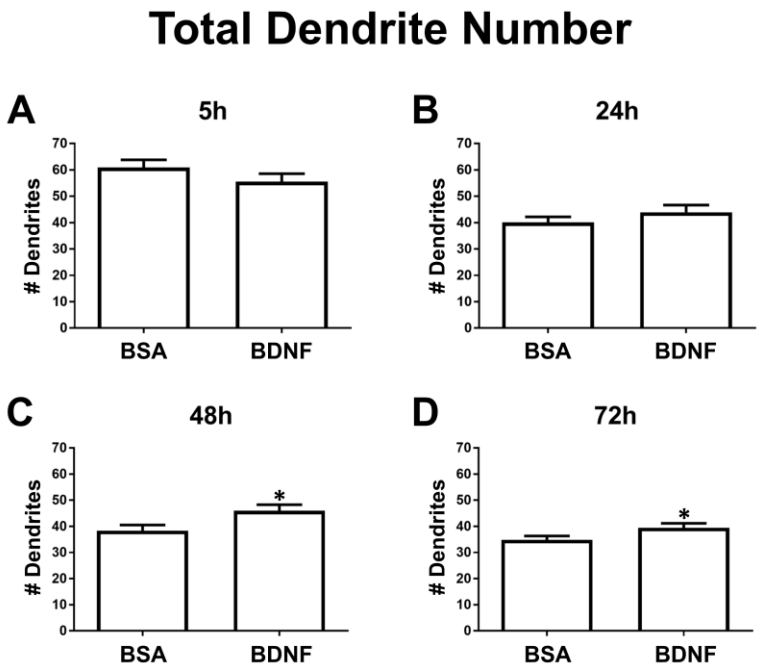

Figure 3-6: Average number of dendrites per neuron is significantly increased after treatment with BDNF-coated beads.
A. Treatment with BDNF-coated beads for 5 hours does not significantly change the average number of dendrites per neuron. **B.** Treatment with BDNF-coated beads for 24 hours does not significantly change the average number of dendrites per neuron. **C.** Treatment with BDNF-coated beads for 48 hours significantly increases the average number of dendrites per neuron (*$p<0.05$). **D.** Treatment with BDNF-coated beads for 72 hours significantly increases the average number of dendrites per neuron (*$p<0.05$). Statistics calculated by Student's *t*-test. Error bars indicate SEM.

Primary dendrite number is significantly increased after 24 hours and 72 hours of treatment (Figure 3-7D and J, respectively), consistent with primary dendrite-specific Sholl curves at these time points. Secondary dendrites significantly decrease after 5 hours of treatment with BDNF-coated beads (Figure 3-7B), do not change after 24 or 48 hours of treatment (Figure 3-7E and H, respectively), and then significantly increase after 72 hours of treatment (Figure 3-7K). Finally, tertiary and higher order dendrites significantly increase after 48 hours of treatment (Figure 3-7I). In particular, the data from tertiary and higher order dendrites (Figure 3-7C, F, I, and L) indicate that BDNF

does not promote addition of new dendrites to the neuron but instead blocks pruning of higher order dendrites that occurs after DIV 7.

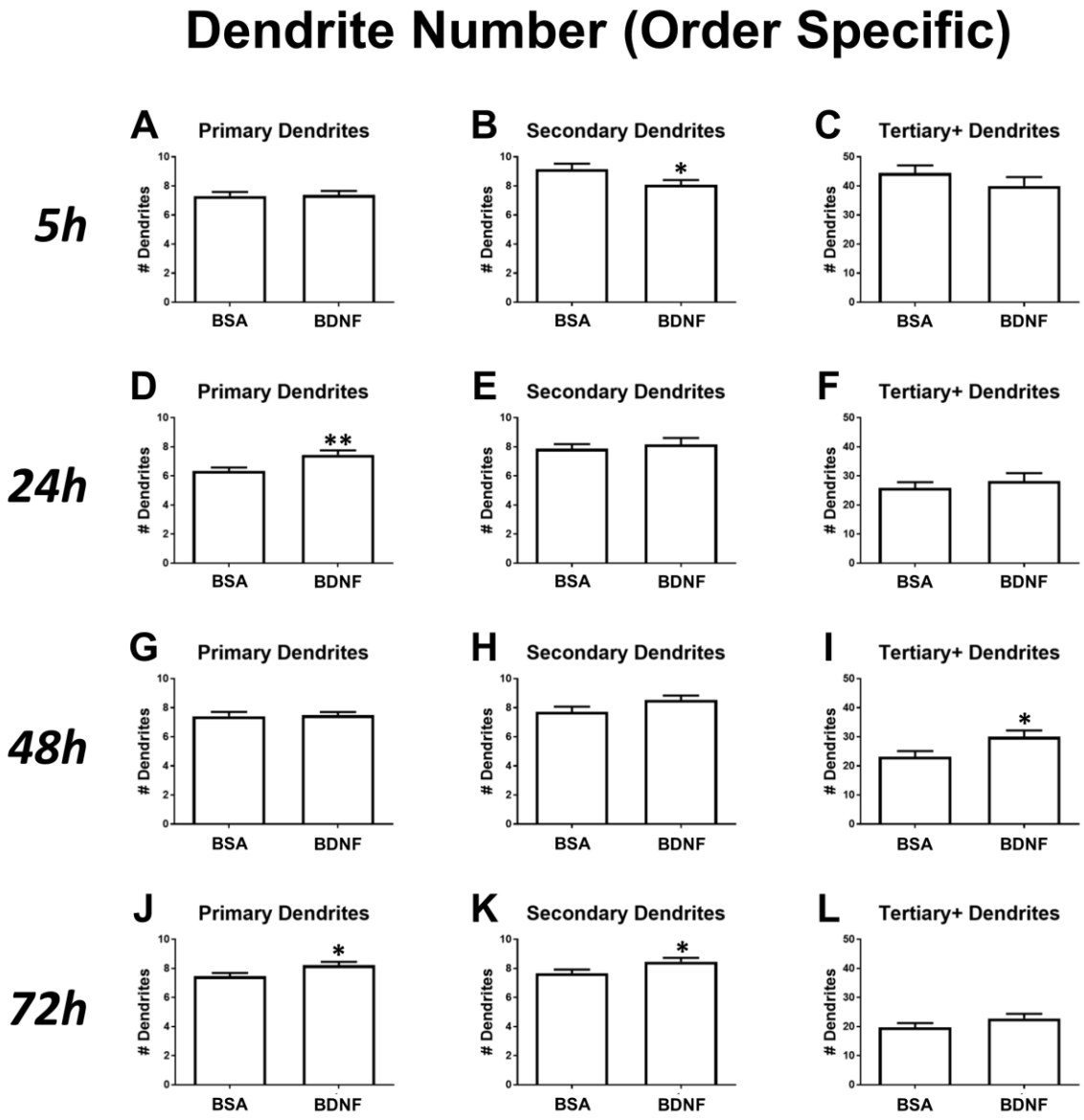

Figure 3-7: Order-specific analysis of dendrite numbers reveals that treatment with BDNF-coated beads significantly affects certain types of dendrites in a time-dependent manner.

A-C. Analysis of dendrites of neurons treated for 5 hours with BSA- or BDNF-coated beads. **A.** Treatment with BDNF-coated beads does not significantly change the number of primary dendrites. **B.** Treatment with BDNF-coated beads significantly decreases the number of secondary dendrites (*$p<0.05$). **C.** Treatment with BDNF-coated beads does

not significantly change the number of tertiary and higher order dendrites. **D-F.** Analysis of dendrites of neurons treated for 24 hours with BSA- or BDNF-coated beads. **D.** Treatment with BDNF-coated beads significantly increases the number of primary dendrites (**p<0.01). **E.** Treatment with BDNF-coated beads does not significantly change the number of secondary dendrites. **F.** Treatment with BDNF-coated beads does not significantly change the number of tertiary and higher order dendrites. **G-I.** Analysis of dendrites of neurons treated for 48 hours with BSA- or BDNF-coated beads. **G.** Treatment with BDNF-coated beads does not significantly change the number of primary dendrites. **H.** Treatment with BDNF-coated beads does not significantly change the number of secondary dendrites. **I.** Treatment with BDNF-coated beads significantly increases the number of tertiary and higher order dendrites (*p<0.05). **J-L.** Analysis of dendrites of neurons treated for 72 hours with BSA- or BDNF-coated beads. **J.** Treatment with BDNF-coated beads significantly increases the number of primary dendrites (*p<0.05). **K.** Treatment with BDNF-coated beads significantly increases the number of secondary dendrites (*p<0.05). **L.** Treatment with BDNF-coated beads does not significantly change the number of tertiary and higher order dendrites. Statistics calculated by Student's *t*-test. Error bars indicate SEM.

The average length of dendrites does not change when all dendrites are grouped together (Figure 3-8); however, order-specific analysis demonstrates that the length of tertiary and higher order dendrites increases only after 72 hours of treatment with BDNF-coated beads (Figure 3-9L). Treatment with BDNF-coated beads does not alter primary dendrite length (Figure 3-9A, D, G, J) or secondary dendrite length (Figure 3-9B, E, H, and K) after any length of treatment.

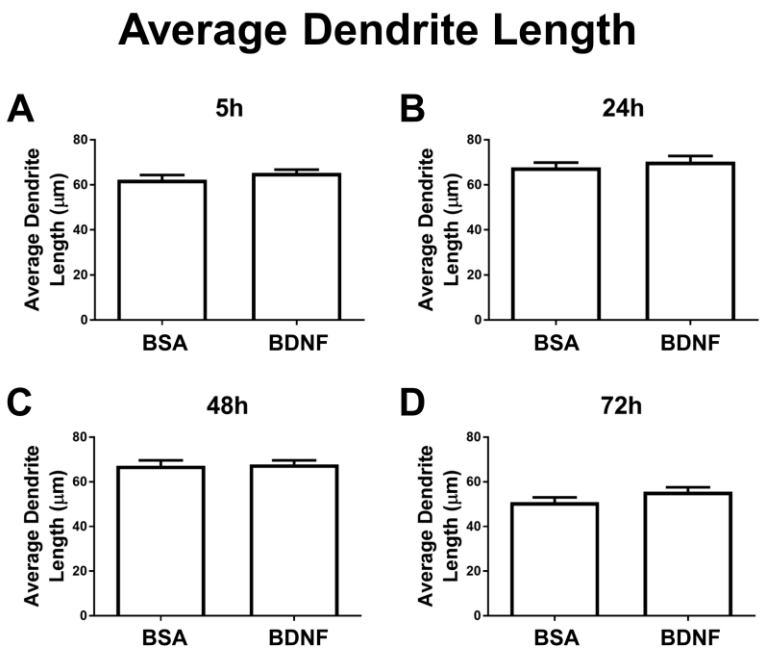

Figure 3-8: Average dendrite length per neuron is not altered by treatment with BDNF-coated beads.
A. Treatment with BDNF-coated beads for 5 hours does not significantly change the average length of dendrites per neuron. **B.** Treatment with BDNF-coated beads for 24 hours does not significantly change the average length of dendrites per neuron. **C.** Treatment with BDNF-coated beads for 48 hours does not significantly change the average length of dendrites per neuron. **D.** Treatment with BDNF-coated beads for 72 hours does not significantly change the average length of dendrites per neuron. Statistics calculated by Student's *t*-test. Error bars indicate SEM.

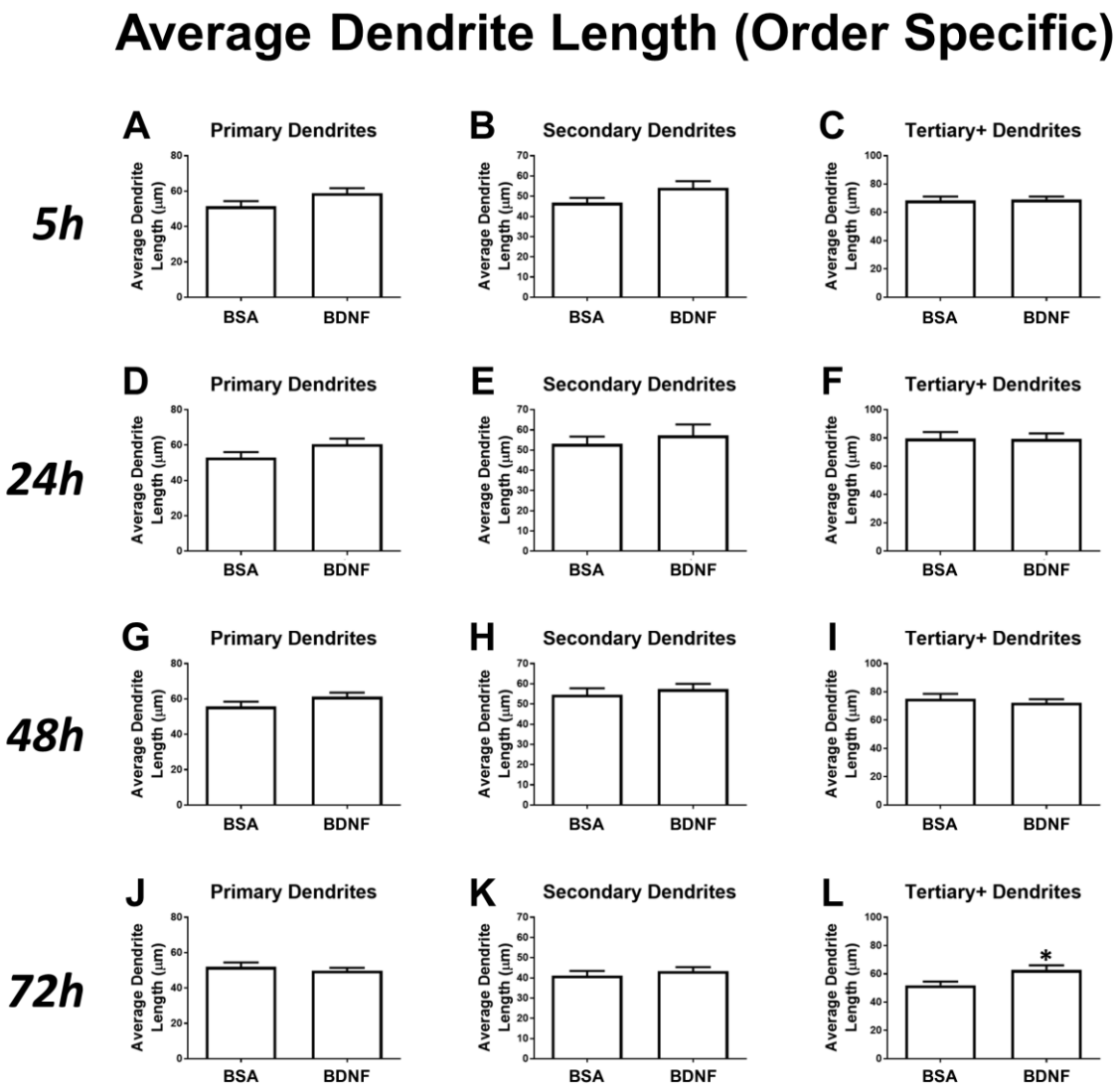

Figure 3-9: Order-specific analysis of dendrite lengths reveals that treatment with BDNF-coated beads significantly increases the length of tertiary and higher order dendrites after 72 hours.

A-C. Analysis of dendrites of neurons treated for 5 hours with BSA- or BDNF-coated beads. **A.** Treatment with BDNF-coated beads does not significantly change the average length of primary dendrites. **B.** Treatment with BDNF-coated beads does not significantly change the average length of secondary dendrites. **C.** Treatment with BDNF-coated beads does not significantly change the average length of tertiary and higher order dendrites. **D-F.** Analysis of dendrites of neurons treated for 24 hours with BSA- or BDNF-coated beads. **D.** Treatment with BDNF-coated beads does not significantly change the average length of primary dendrites. **E.** Treatment with BDNF-coated beads does not significantly change the average length of secondary dendrites. **F.** Treatment with BDNF-coated beads does not significantly change the average length of tertiary and higher order dendrites. **G-I.** Analysis of dendrites of neurons treated for 48 hours with BSA- or BDNF-coated beads. **G.** Treatment with BDNF-coated beads does not significantly change the average

length of primary dendrites. **H.** Treatment with BDNF-coated beads does not significantly change the average length of secondary dendrites. **I.** Treatment with BDNF-coated beads does not significantly change the average length of tertiary and higher order dendrites. **J-L.** Analysis of dendrites of neurons treated for 72 hours with BSA- or BDNF-coated beads. **J.** Treatment with BDNF-coated beads does not significantly change the average length of primary dendrites. **K.** Treatment with BDNF-coated beads does not significantly change the average length of secondary dendrites. **L.** Treatment with BDNF-coated beads significantly increases the average length of tertiary and higher order dendrites (*$p<0.05$). Statistics calculated by Student's *t*-test. Error bars indicate SEM.

3.3.3 Knockdown of cytosolic PSD-95 interactor (cypin) blocks a subset of effects resulting from treatment with BDNF-coated beads

Previously, our laboratory reported that cytosolic PSD-95 interactor (cypin) is an intrinsic regulator of dendrite branching (Akum, Chen et al. 2004, Charych, Akum et al. 2006, Chen and Firestein 2007, Fernandez, Welsh et al. 2008, O'Neill, Akum et al. 2015). Specifically, overexpression of cypin results in an increase in dendrite branching while knockdown of cypin results in a decrease in dendrite branching. Recently, we demonstrated that bath application of BDNF to hippocampal cultures increases dendrite branching and that this increase occurs through transcriptional regulation of cypin mRNA (Kwon, Fernandez et al. 2011). We wanted to extend these previous studies by investigating whether local exposure to BDNF via microbeads signals through cypin to alter the dendritic arbor. Therefore, we transfected neurons with shRNA against cypin, which decreases cypin by approximately 40% (Chen and Firestein 2007), or with control shRNA against GST, and then we treated each set of cultures with either BSA- or BDNF-coated beads at DIV 7 for a period of 5, 24, and 48 hours. We did not investigate the effects of a 72 hour treatment because neurons must be imaged live and GFP expressed from the pSUPER plasmid does not express at the high levels observed when GFP is

expressed from the pEGFP-C1 plasmid (as was done for experiments in Figure 3-3 through 9**)**. In this current set of experiments, control neurons are transfected with GST shRNA and treated with BSA-coated beads.

We performed Sholl analysis for all conditions and found that knockdown of cypin blocks some of the effects resulting from treatment with BDNF-coated beads (Figure 3-10). Representative images from each condition are shown in Figure 3-10A. Importantly, we observed significant decreases at all time points for neurons transfected with cypin shRNA and treated with BSA-coated beads compared with the control (neurons transfected with GST shRNA and treated with BSA-coated beads). As expected, the most prominent decreases occurred at the 48 hour time point (Figure 3-10D,G; green stars). Additionally, in neurons expressing the control GST shRNA, we also observed that treatment with BDNF-coated beads increased dendrite branching proximally at 24 hours and 48 hours, although only at two distances from the cell body (Figure 3-10C,F and 10D,G, respectively; blue stars). Similarly, at the 5 hour time point (Figure 3-10B,E), cultures transfected with cypin shRNA and treated with BDNF-coated beads resulted in restoration of dendritic arborization to control levels (red vs. black lines). After 24 hours of treatment with beads, not only does cypin knockdown decrease dendrites but also blocks increases in dendrites promoted by BDNF-coated beads (Figure 3-10C,F; purple stars). The difference in the effect of knockdown of cypin on changes to dendrites by exposure to BDNF-coated beads between 48 and 72 hours of knockdown (5 hours and 24 hours of bead exposure, respectively) is most likely due to the fact that maximal knockdown of cypin protein occurs after 48 hours (Chen and Firestein 2007, Kwon, Fernandez et al. 2011). After 48 hours of treatment with beads

(96 hours of cypin knockdown), cypin knockdown does not attenuate the increases in dendrite branching promoted by BDNF-coated beads (Figure 3-10D,G). Since BDNF may increase endogenous cypin levels between 24 and 72 hours of exposure (Kwon, Fernandez et al. 2011), this may account for the inability of cypin knockdown to block the effects of BDNF-coated beads after 48 hours of treatment.

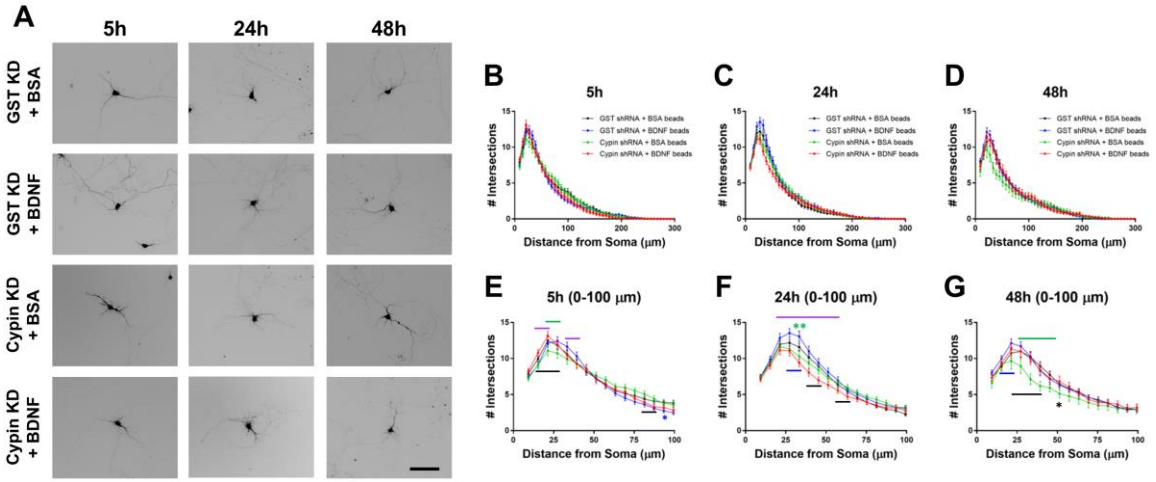

Figure 3-10: Sholl analysis reveals a role for cypin in regulating how treatment with BDNF-coated beads alters the dendritic arbor.
To indicate sites of significant differences in dendritic arborization, the following notation is used: 1) blue bars/stars compare control neurons (black line) to those transfected with GST shRNA and treated with BDNF-coated beads (blue line); 2) green stars/bars compare control neurons (black line) to those transfected with cypin shRNA and treated with BSA-coated beads (green line); 3) purple stars/bars compare neurons transfected with cypin shRNA and treated with BDNF-coated beads (red line) to neurons transfected with GST shRNA and treated with BDNF-coated beads (blue line); and 4) black stars/bars compare neurons transfected with cypin shRNA and treated with BDNF-coated beads (red line) to neurons transfected with cypin shRNA and treated with BSA-coated beads (green line). Stars indicate exact levels of significance, and bars indicate significance of at least *$p<0.05$. **A.** Representative images from each condition. Scale bar indicates 100 μm. **B.** Sholl analysis for 5 hour timepoint. **C.** Sholl analysis for 24 hour timepoint. **D.** Sholl analysis for 48 hour timepoint. **E.** The first 100 μm of the Sholl curve from panel B. BDNF treatment significantly increases branching at 93.3 μm from the soma (blue vs. black lines, blue stars; *$p<0.05$). Cypin knockdown significantly decreases branching at 21.3 to 27.3 μm from the soma (green vs. black lines, green bar;

p<0.01). The Sholl curve for cypin knockdown + BDNF-coated beads (red line) is significantly increased over cypin knockdown + BSA-coated beads (green line) at 15.3 to 27.3 μm and at 81.3 to 87.3 μm from the soma (black bars; both *p<0.05). Compared with the Sholl curve for the control neurons treated with BDNF-coated beads (blue line), the Sholl curve for cypin knockdown + BDNF-coated beads (red line) is significantly increased at 15.3 to 21.3 μm and significantly decreased at 33.3 to 39.3 μm from the soma (purple bars; both *p<0.05). **F. The first 100 μm of the Sholl curve from panel C. Treatment with BDNF-coated beads significantly increases branching at 27.3 to 33.3 μm from the soma (blue vs. black lines, blue bar; **p<0.01). Cypin knockdown significantly decreases branching at 33.3 μm from the soma (green vs. black lines; green stars; **p<0.01). The Sholl curve for cypin knockdown + BDNF-coated beads (red line) is significantly decreased versus cypin knockdown + BSA-coated beads (green line) at 39.3 to 45.3 μm from the soma (black bar; **p<0.01) and at 57.3 to 63.3 μm from the soma (black bar; *p<0.05). Compared with the Sholl curve for the control neurons treated with BDNF-coated beads (blue line), the Sholl curve for cypin knockdown + BDNF-coated beads (red line) is significantly decreased at 21.3 to 57.3 μm from the soma (purple bar; ****p<0.0001). **G.** The first 100 μm of the Sholl curve from panel D. Treatment with BDNF-coated beads significantly increases branching at 15.3 to 21.3 μm from the soma (blue vs. black lines, blue bar; *p<0.05). Cypin knockdown significantly decreases branching at 27.3 to 45.3 μm from the soma (green vs. black lines, bar stars; **p<0.01). The Sholl curve for cypin knockdown + BDNF-coated beads (red line) is significantly decreased versus cypin knockdown + BSA-coated beads (green line) at 21.3 to 39.3 μm and at 51.3 μm from the soma (black bar/star; both *p<0.05). GST KD indicates neurons that were transfected with GST shRNA, and Cypin KD indicates neurons that were transfected with Cypin shRNA. For 5 hour treatment: n(GST+BSA)=46, n(GST+BDNF)=50, n(Cypin+BSA)=40, n(Cypin+BDNF)=49. For 24 hour treatment: n(GST+BSA)=67, n(GST+BDNF)=43, n(Cypin+BSA)=48, n(Cypin+BDNF)=54. For 48 hour treatment: n(GST+BSA)=42, n(GST+BDNF)=53, n(Cypin+BSA)=17, n(Cypin+BDNF)=29. Statistics calculated by Two-Way ANOVA followed by Bonferroni's Multiple Comparisons test. Error bars indicate SEM.

We also utilized order-specific Sholl grouped by condition in this set of data to illuminate pruning patterns. Very little pruning of primary dendrites is observed in control cultures (Figure 3-11A). Interestingly, treatment with BDNF-coated beads increases primary dendrites proximal to the soma over time (Figure 3-11D). As expected,

cypin knockdown results in decreased primary dendrites proximal to the soma over time (Figure 3-11G), and this decrease is seen even with treatment with BDNF-coated beads (Figure 3-11J), though at an earlier time. In contrast, secondary dendrites are pruned over time in control cultures (Figure 3-11B), and treatment with BDNF-coated beads not only blocks this pruning but actually increases secondary dendrites after 48 hours (Figure 3-11E). Knockdown of cypin increases pruning after 48 hours of control bead treatment (Figure 3-11H), and treatment with BDNF-coated beads partially blocks the increased pruning seen with cypin knockdown (Figure 3-11K). Furthermore, tertiary and higher order dendrites appear to be subject to the greatest pruning over time in control cultures (Figure 3-11C). Exposure to BDNF-coated beads significantly attenuates this pruning and even increases higher order dendrites after 24 hours, but treatment exerts no effect on the pruning of these dendrites after 48 hours in culture (Figure 3-11F), suggesting a transient effect of local sources of BDNF on arbor pruning. Cypin knockdown increased higher order dendrite pruning at 48 hours (Figure 3-11I), and treatment with BDNF-coated beads attenuated pruning, resulting in a pattern similar to that of control cultures (compare Figure 3-11C and L). These results suggest that local sources of BDNF may act, in part, through cypin to regulate pruning of the dendritic arbor.

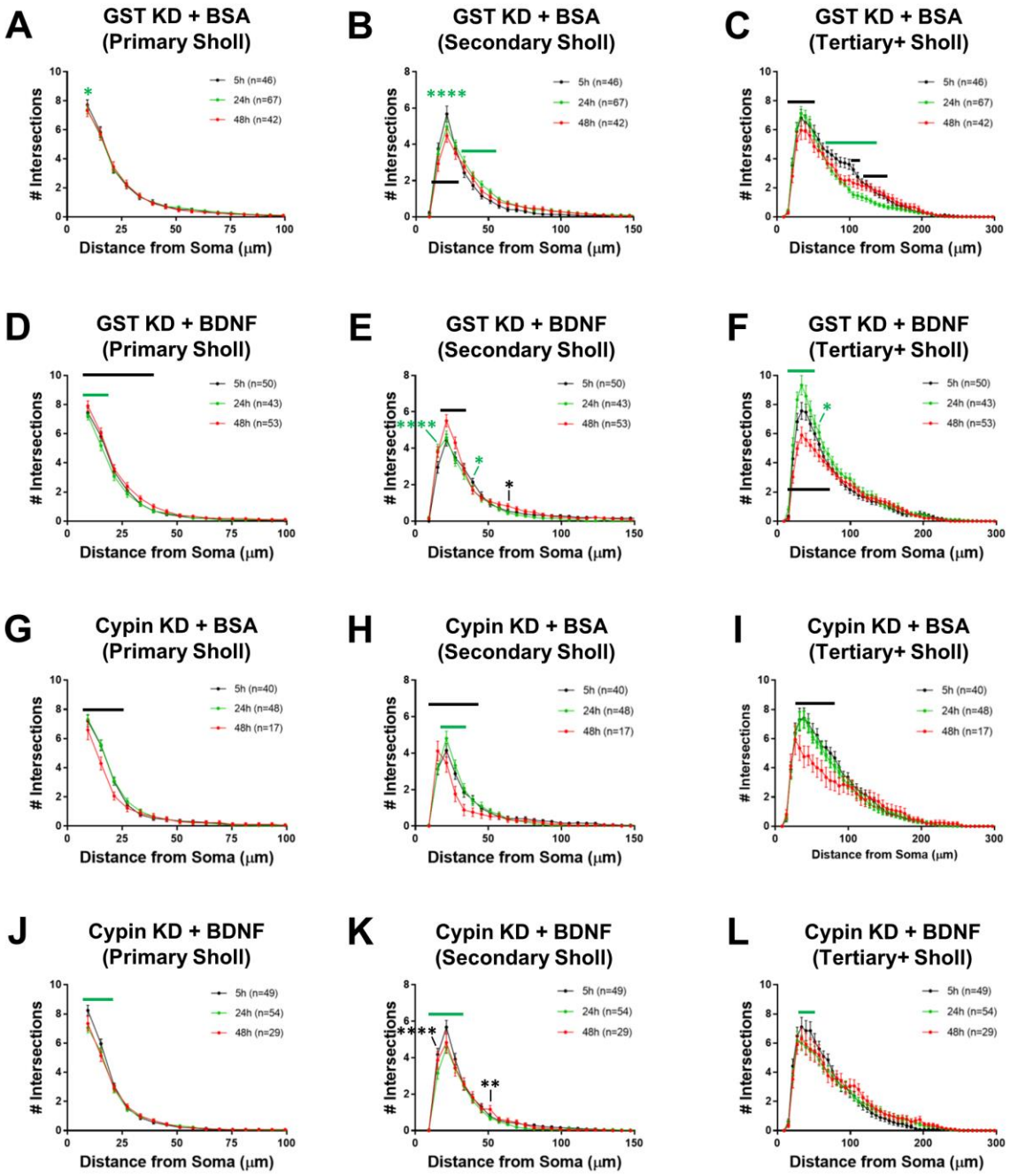

Figure 3-11: Order-specific Sholl analysis illustrates how knocking down cypin affects modulation of dendrite branching by BDNF-coated beads

To indicate significance, green stars/bars show significance between the 5 hour and 24 hour time points (black vs. green lines), and black stars/bars show significance between the 24 hour and 48 hour time points (green vs. red lines). Stars indicate exact levels of significance, and bars indicate significance of at least *p<0.05. **A-C.** Order-specific Sholl analysis of neurons transfected with cDNA encoding GST shRNA and treated with BSA-coated beads. **A.** Primary dendrites significantly decrease between 5 and 24 hours at 9.3 μm from the soma (green star; *p<0.05). **B.** Between 5 and

24 hours, secondary dendrites significantly decrease at 21.3 μm from the soma (green stars; ****p<0.0001) and significantly increase at 33.3 to 51.3 μm from the soma (green bar; **p<0.01). Secondary dendrites significantly decrease between 24 and 48 hours at 15.3 to 27.3 μm from the soma (black bar; *p<0.05). **C.** Tertiary and higher order dendrites significantly decrease between 5 and 24 hours at 69.3 to 135.3 μm from the soma (green bar; *p<0.05). Between 24 and 48 hours, tertiary and higher order dendrites significantly decrease at 21.3 to 45.3 μm from the soma (black bar; *p<0.05), and they significantly increase at 105.3 to 111.3 μm and at 123.3 to 147.3 μm from the soma (black bars; both *p<0.05). **D-F.** Order-specific Sholl analysis of neurons transfected with cDNA encoding GST shRNA and treated with BDNF-coated beads. **D.** Primary dendrites significantly decrease between 5 and 24 hours at 15.3 to 21.3 μm from the soma (green bar; *p<0.05), but they significantly increase between 24 and 48 hours at 9.3 to 33.3 μm from the soma (black bar; **p<0.01). **E.** Between 5 and 24 hours, secondary dendrites significantly increase at 15.3 μm from the soma (green stars; ****p<0.0001) and significantly decrease at 39.3 μm from the soma (green stars; *p<0.05). Between 24 and 48 hours, secondary dendrites significantly increase at 21.3 to 27.3 μm (black bar; ****p<0.0001) and at 63.3 μm from the soma (black star; *p<0.05). **F.** Tertiary and higher order dendrites significantly increase between 5 and 24 hours at 21.3 to 45.3 μm and at 57.3 μm from the soma (green bar/star; both *p<0.05). Between 24 and 48 hours, tertiary and higher order dendrites significantly decrease at 21.3 to 69.3 (black bar; *p<0.05). **G-I.** Order-specific Sholl analysis of neurons transfected with cDNA encoding cypin shRNA and treated with BSA-coated beads. **G.** Primary dendrites significantly decrease between 24 and 48 hours at 9.3 to 21.3 μm from the soma (black bar; ****p<0.0001). **H.** Secondary dendrites significantly increase between 5 and 24 hours at 21.3 to 27.3 μm from the soma (green bar; **p<0.01). The Sholl curve shifts at 48 hours, resulting in a significant increase at 15.3 μm and significant decreases at 21.3 to 39.3 μm from the soma (black bar; **p<0.01). **I.** Tertiary and higher order dendrites significantly decrease between 24 and 48 hours at 33.3 to 75.3 μm from the soma (black bar; *p<0.05). **J-L.** Order-specific Sholl analysis of neurons transfected with cDNA encoding cypin shRNA and treated with BDNF-coated beads. **J.** Primary dendrites significantly decrease between 5 and 24 hours at 9.3 to 15.3 μm from the soma (green bar; ****p<0.0001). **K.** Secondary dendrites significantly decrease between 5 and 24 hours at 15.3 to 27.3 μm from the soma (green bar; ***p<0.001). Between 24 and 48 hours, secondary dendrites significantly increase at 15.3 μm (black stars; ****p<0.0001) and at 51.3 μm (black stars; **p<0.01) from the soma. **L.** Tertiary and higher order dendrites significantly decrease at 33.3 to 45.3 μm from the soma (green bar; **p<0.01). GST KD indicates neurons that were transfected with GST shRNA, and Cypin KD indicates neurons that were transfected with Cypin shRNA. Statistics calculated by Two-Way ANOVA followed by Bonferroni's Multiple Comparisons test. Error bars indicate SEM.

3.4 Discussion

The major finding of the present study is that local stimulation of cultured hippocampal neurons with BDNF results in changes to dendritic arbor and that these changes are not evident until after 48 hours of stimulation. Furthermore, these changes are observed distal from the cell body after 48 hours and both proximally and distally after 72 hours, suggesting that localized stimulation with BDNF actively shapes neuronal morphology. Moreover, BDNF attenuates pruning of dendrites, specifically higher order dendrites, resulting in an increase in the overall Sholl curve representing the arbor. Our results strongly suggest that BDNF signals in part through a cypin-dependent mechanism. A model representing the effects of BDNF on the dendritic arbor is shown in Figure 3-12.

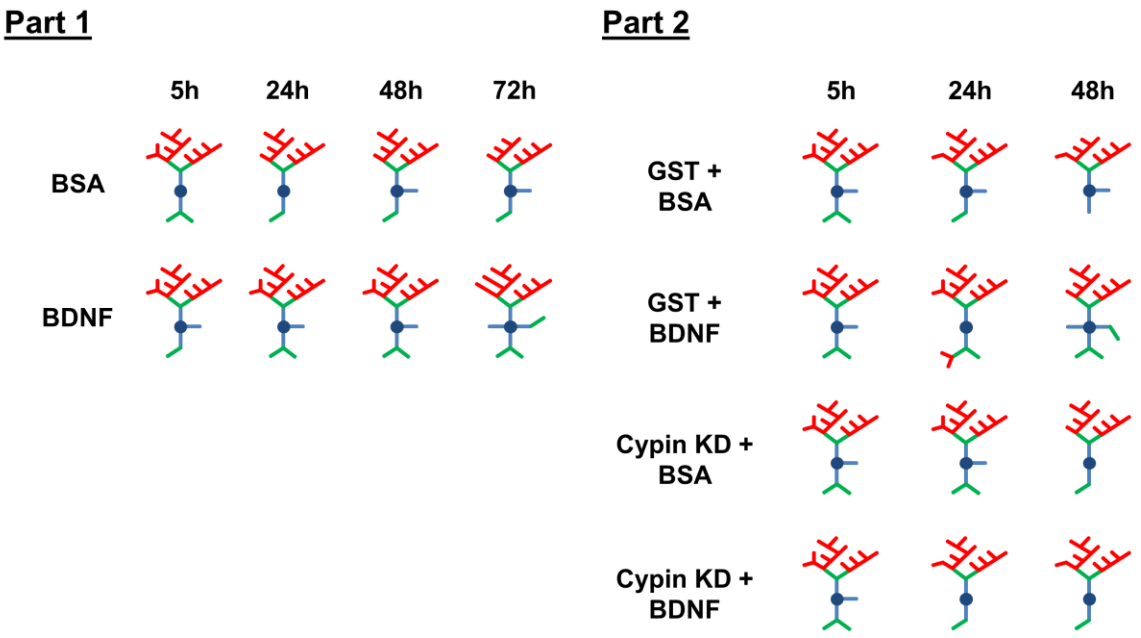

Figure 3-12: Schematic illustrating the changes that occur as a result of treatment with BDNF-coated beads.
Primary dendrites are shown in blue, secondary dendrites in green, and tertiary and higher order dendrites in red. **Part 1.** Treatment with BDNF-coated beads causes an increase in primary dendrites at 5 hours and then results in a transient decrease in secondary dendrites at 24 hours. At 48 hours, the increase in primary dendrites is no

longer present, but tertiary and higher order dendrites increase. After 72 hours of treatment, the overall number of primary and secondary dendrites increases, and distal tertiary and higher order dendrite numbers and length increase. Pruning over time for both conditions is also shown. **Part 2.** Treatment of control neurons (transfected with cDNA encoding GST shRNA) with BDNF results in increased tertiary dendrites after 24 hours and increased secondary dendrites after 48 hours. Neurons with cypin knockdown and BSA-coated bead treatment have fewer secondary dendrites after 5 hours, fewer tertiary and higher order dendrites after 24 hours, and even fewer primary, tertiary, and higher order dendrites after 48 hours. Neurons with cypin knockdown and BDNF-coated bead treatment did not show these decreases. There was no change in dendrites of any order at 5 hours, a loss of primary, tertiary, and higher order dendrites after 24 hours, and no further loss of dendrites at 48 hours. Pruning over time for all conditions is also shown. GST KD indicates neurons that were transfected with GST shRNA, and Cypin KD indicates neurons that were transfected with Cypin shRNA.

How do the effects of local stimulation of the dendritic arbor, as we have done in this study, differ from those observed when neurons are exposed to bath application of BDNF? To answer this question, we compare our current results with those from our previous work (Kwon, Fernandez et al. 2011), where all experimental conditions were the same except that cultures were treated with BDNF as a bath application. Similarities between the two studies include the following: 1) greater than 24 hours of treatment with either bath or bead application of BDNF is needed to result in overall changes to the dendritic arbor as observed by Sholl analysis; 2) increases in primary and secondary dendrite number are observed after 72 hours of treatment for both studies; and 3) both types of BDNF treatment depend on cypin to promote effects on the arbor. Differences include the following: 1) five hours of treatment with bead, but not bath, application of BDNF results in a transient decrease in secondary dendrites; 2) bath application of BDNF increases dendrites close to the soma while bead application increases dendrites both proximal and distal to the soma; and 3) cypin knockdown affects increases in dendrites

promoted after 24 hours of bead application of BDNF but only after 72 hours of bath application. Taken together, the two studies suggest that there is partial, but not complete, overlap of signaling mechanisms that mediate changes to the dendritic arbor by the two types of stimulation with BDNF.

Our previous data demonstrate a role for MAPK and CREB-mediated cypin transcription in how global BDNF stimulates the promotion of dendritogenesis (Kwon, Fernandez et al. 2011). Although we do not rule out a role for this signaling pathway in mediating the effects of local BDNF stimulation on the dendritic arbor, our data suggest additional pathways for local BDNF signaling since knockdown of cypin has no effect on BDNF-mediated increases at 48 hours for local application of BDNF via beads. One possibility is that, in this scenario, BDNF promotes the local translation of cypin, as it has been reported that local BDNF application in cultured hippocampal neurons phosphorylates the S6 protein, which is involved in mTOR-dependent local protein synthesis (Takei, Inamura et al. 2004). Furthermore, global BDNF treatment increases proximal dendrite branching, resulting from increased cypin transcription and protein levels (Kwon, Fernandez et al. 2011). However, localized treatment using BDNF-coated microbeads increases branching in both proximal and distal areas of the dendrite in a time-dependent manner, suggesting that there exists distinct regulation of proximal and distal dendrites.

The complex actions of BDNF on the dendritic arbor may be mediated, in part, by multiple receptors, resulting from alternative splicing of the full length TrkB receptor (TrkB.FL). Like other neurotrophins, BDNF exists in two states, proteolytically processed, which is the active form that can bind Trk receptors, or unprocessed, which

allows BDNF to bind with high affinity to $p75^{NTR}$. Three alternative splice variants of TrkB.FL have been identified. The full-length TrkB.FL contains a cytoplasmic tyrosine kinase domain, which is responsible for autophosphorylation and clustering of the receptor when activated by BDNF (Chao 2003, Segal 2003). Two truncated isoforms, termed TrkB.T1 and TrkB.T2, have also been identified, and both lack the cytoplasmic tyrosine-kinase domains (Barbacid 1994). TrkB.FL and TrkB.T2 are expressed exclusively in neurons, and TrkB.T1 is expressed in both neurons and nonneuronal cells (Frisen, Verge et al. 1993, Rudge, Li et al. 1994, Armanini, McMahon et al. 1995, Biffo, Offenhauser et al. 1995, Wetmore and Olson 1995). Importantly, stimulation of TrkB.FL increases proximal branching, and activation of TrkB.T1 increases distal dendrites (Yacoubian and Lo 2000). Bath treatment of neurons would result in synchronized activation of both TrkB receptors (Yacoubian and Lo 2000, Hartmann, Brigadski et al. 2004) while local stimulation with BDNF-coated beads could result in differential spatial stimulation of these two receptors, minimizing receptor cross-talk and regulating proximal and distal dendritogenesis separately. In addition, TrkB.T1 has been shown to regulate dendritic growth via $p75^{NTR}$ (Hartmann, Brigadski et al. 2004), again suggesting that global versus local stimulation of neurons by BDNF acts via different signaling cascades. Since there are variations in expression and localization of the different BDNF receptors between brain regions (Fryer, Kaplan et al. 1996, Ohira, Shimizu et al. 1999, Ohira and Hayashi 2003), different distributions of these receptors on the neuron most likely play a role in localized BDNF function.

As neurons develop, the dendritic arbor undergoes age-dependent changes (Dotti, Sullivan et al. 1988). Periods of active branching are followed by periods of pruning, and

neurons undergo pruning during development (Cline 2001, Wong and Ghosh 2002, Charych, Akum et al. 2006). Most studies have focused on the role of BDNF in axonal pruning (reviewed in (Deinhardt and Chao 2014)); the fact that our current study focuses on dendritic pruning provides a novel role for BDNF in shaping neuronal morphology. Importantly, acute versus chronic exposure of neurons to BDNF influences activation of different transcription factors (Ji, Lu et al. 2010), which may explain changes to dendrite pruning by BDNF over time. Our data suggest that local BDNF treatment reduces the pruning of all types of branches, with the most prominent attenuation of pruning occurring to tertiary and higher order branches. Stimulation of $p75^{NTR}$ by BDNF is important for developmental axonal pruning (Singh, Park et al. 2008), supporting the idea that binding of BDNF to this receptor, and potentially TrkB.T1, distally plays an important role in shaping the dendritic arbor by localized but not global BDNF exposure. In contrast, our previous studies suggest that global application of BDNF increases terminal dendrites with no effect on intermediate dendrites (Langhammer, Previtera et al. 2010). Thus, the mechanism by which the different modes of BDNF stimulation increase dendritic arbor complexity differ.

What is the significance of global stimulation versus local dendritic stimulation of neurons with BDNF? BDNF is secreted from both neurons and astrocytes (Rudge, Li et al. 1994). Astrocytes can release BDNF in an exocytotic manner (Takemoto, Ishihara et al. 2015, Stenovec, Lasič et al. 2016), resulting in exposure of neurons to BDNF similar to that seen with bath application. In addition, BDNF can act in a peri-synaptic, or more localized, manner. Recycling of synaptic BDNF by astrocytes stabilizes long-term potentiation and mediates memory retention (Vignoli, Battistini et al. 2016). Furthermore,

neurons release BDNF synaptically, where it can act in a localized manner at postsynaptic sites (reviewed in (Deinhardt and Chao 2014) and (Mitre, Mariga et al. 2017)). Thus, local stimulation with BDNF-coated beads can help us uncover mechanisms underlying changes to dendrites by synaptic or peri-synaptic BDNF.

CHAPTER 4: THE ROLE OF INTRACELLULAR TARGETING OF BRAIN-DERIVED NEUROTROPHIC FACTOR TRANSCRIPTS IN REGULATING THE DENDRITIC ARBOR

4.1 Introduction

The *BDNF* gene is transcribed from nine different promoters (Metsis, Timmusk et al. 1993, Timmusk, Palm et al. 1993) and can be processed at two different polyadenylation sites: one results in transcription of BDNF mRNA with a short 3' untranslated region (UTR), and one results in transcription of BDNF mRNA with a long 3' UTR (Liu, Walther et al. 2005, Liu, Lu et al. 2006, Aid, Kazantseva et al. 2007). The short and long transcripts are present in different relative amounts in various brain regions, and they are also preferentially localized to different parts of the cell. The short 3' UTR preferentially targets BDNF transcripts to the cell body while the long 3' UTR targets transcripts to both the cell body and dendrites (An, Gharami et al. 2008). Moreover, this targeting is regulated by several RNA-binding proteins and by exposure to NT-3 for the short 3' UTR or with BDNF treatment for the long 3' UTR (Oe and Yoneda 2010, Vicario, Colliva et al. 2015).

Expression of BDNF translated from mRNA containing the long 3' UTR results in changes to neuronal morphology. In a mutant mouse model that expresses a truncated version of BDNF mRNA containing the long 3' UTR (An, Gharami et al. 2008), targeting of BDNF transcripts to hippocampal dendrites is severely impaired although the total amount of BDNF mRNA is not affected. Moreover, the total amount of BDNF protein (pro-BDNF and mature BDNF) in hippocampal and cortical neurons is also

unaffected by the mutation, but when hippocampal neurons containing the mutant transcript are cultured *in vitro,* there is a higher ratio of BDNF protein in cell bodies than in dendrites compared with control neurons. Thus, while the total amounts of BDNF mRNA and protein are unaffected, the subcellular localization is altered when the long 3' UTR is truncated. This difference in localization does not affect hippocampal dendrite structure, but spines on distal dendrites are thinner and more numerous due to insufficient pruning and lack of maturation. Finally, the difference in spine morphology and number results in significant impairment in hippocampal long-term potentiation (An, Gharami et al. 2008).

Despite limiting the cellular localization of BDNF transcripts to the cell body, the short 3' UTR plays important roles in other aspects of neuronal physiology. In particular, specific regions within the short 3' UTR BDNF mRNA are necessary for the activity-dependent stabilization of the mRNA caused by calcium influx (Fukuchi and Tsuda 2010). The short 3' UTR also mediates translation when the neuron is at rest. On the other hand, the long 3' UTR acts as a translational suppressor when the neuron is at rest but an enhancer of translation during periods of neuronal activity. Thus, the opposing roles of the short and long 3' UTRs act in concert to maintain appropriate levels of BDNF protein (Lau, Irier et al. 2010). Furthermore, translation of transcripts containing the short 3' UTR increases phosphorylation of TrkB, CREB, and other proteins that lead to enhanced synaptic plasticity, and the *in vivo* consequences of this translation include improvement in both long- and short-term memory formation (Wang, Li et al. 2016).

This chapter will explore the effects of overexpression of BDNF transcripts containing the short and long 3' UTRs on the dendritic morphology of cultured

hippocampal neurons. Neurons are cultured for 7 days *in vitro* (DIV), at which time they are transfected with cDNAs encoding the BDNF coding sequence with and without 3' UTRs. Sholl analyses are then used to understand how overexpression and intracellular targeting of BDNF affects the spatial arrangement of dendrites as well as the number and length of dendrites.

4.2 Materials and Methods

4.2.1 Primary culture of hippocampal neurons

Hippocampal neurons were isolated from embryonic rats at day 18 of gestation (E18) as previously described (Firestein, Brenman et al. 1999). After isolation, the hippocampi were dissociated via manual trituration and plated at a density of $2x10^5$/well on 12-mm glass coverslips (Fisher) in 24-well plates (Corning). Coverslips were coated with 0.5 mg/mL poly-D-lysine (PDL; Sigma) for at least 1 hr at 37 ˚C prior to plating cells. Cultures were maintained in Neurobasal medium supplemented with B27, GlutaMAX, and penicillin/streptomycin (all from Life Technologies) in a humidified 37 ˚C incubator with 5% CO_2. Cells were grown for 7 days *in vitro* (DIV) prior to transfection. All animals used for dissection were cared for ethically in accordance with Institutional Animal Care and Use Committee (IACUC) standards.

4.2.2 Optimization of transfection procedure

Several optimization steps were performed to obtain transfection of neurons that were bright enough for the experimenter to trace the dendritic arbor with sufficient detail. The original plasmids contained the BDNF coding sequence with or without the 3' UTRs in the pEGFP-C1 vector. Increasing the ratio of DNA to the transfection agent

(Lipofectamine LTX, Lipofectamine 2000, or calcium phosphate) did not yield higher levels of GFP expression or higher transfection rates. Transfected neurons were not bright enough to be identified or traced. Additionally, co-transfection with pmRFP did not alleviate the brightness issue since GFP fluorescence was still not high enough to allow for confirmation of co-transfection. Therefore, the BDNF coding sequences with or without the 3' UTRs were subcloned into the pIRES2-EGFP vector, which contains an internal ribosomal entry site (IRES) that results in transcription of the BDNF and GFP mRNAs together but translation of the BDNF and GFP proteins separately. These constructs allow for higher GFP fluorescence because the GFP protein diffuses throughout the cell while BDNF protein acts locally where it has been targeted. While transfection using pIRES2-EGFP constructs allows for identification of transfected neurons due to improved GFP fluorescence, the fluorescence does not extend far enough into the dendrites to allow for sufficiently detailed tracing. Therefore, co-transfection with a plasmid encoding mOrange was attempted using mass ratios of 1:1, 1:2, 1:3, and 1:4 (pmOrange:pIRES). The ratio of pmOrange:pIRES that results in the brightest transfection and highest co-transfection rate is 1:4 and used for all experiments in this chapter.

4.2.3 Primary neuronal transfection

Hippocampal neurons were co-transfected at DIV 7 with pmOrange and one of the following plasmids as shown in Figure 4-1: pIRES2-EGFP (control), pIRES2-EGFP-BDNF cds (coding sequence), pIRES2-EGFP BDNF cds + short 3' UTR, pIRES2-EGFP-BDNF cds + long 3' UTR, pIRES2-EGFP-BDNF cds + short & long 3' UTR.

Effectene (Qiagen), the transfection reagent, was used according to the manufacturer's instructions.

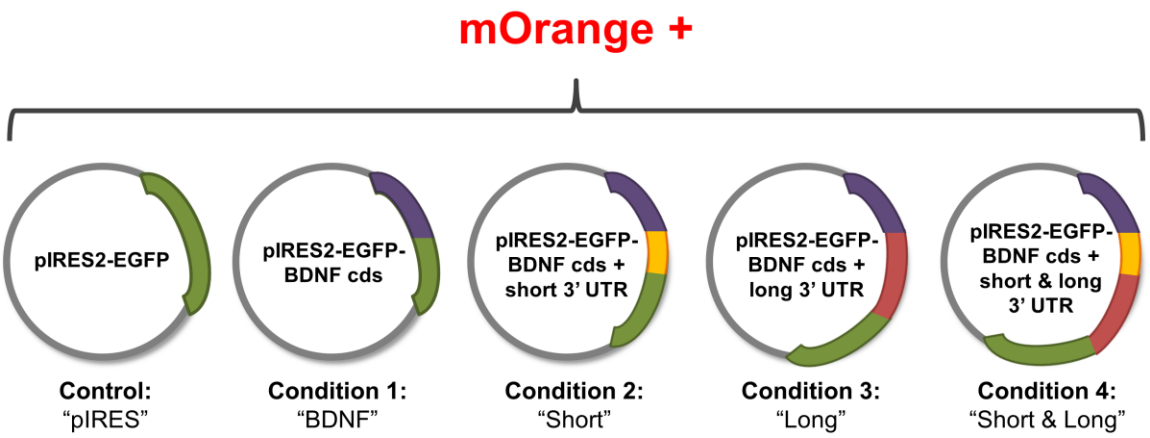

Figure 4-1: Schematic depicting different plasmids containing the BDNF coding sequence with or without 3' UTRs.
The schematic demonstrates the various transfection conditions used in experiments in this chapter and the abbreviations that will be used as shorthand in graphs. The control is transfection of neurons with pIRES2-EGFP, with the GFP sequence represented as a green arc, and is referred to as "pIRES". The first condition, referred to as "BDNF," is transfection of neurons with pIRES2-EGFP containing the BDNF coding sequence (cds) without targeting UTRs, represented as a purple arc. The second condition, referred to as "Short," is transfection of neurons with pIRES2-EGFP containing BDNF cds with the short 3' UTR, represented as purple and yellow arcs, respectively. The third condition, referred to as "Long," is transfection of neurons with pIRES2-EGFP containing the BDNF cds with the long 3' UTR, represented as purple and red arcs, respectively. The final condition, referred to as "Short & Long," is transfection of neurons with pIRES2-EGFP containing the BDNF cds (purple arc) with both short (yellow arc) and long (red arc) 3' UTRs. The IRES site occurs prior to the beginning of the GFP coding sequence.

4.2.4 Immunostaining

Neurons were fixed at DIV 10, approximately 72 hours after transfection, in 4% paraformaldehyde in phosphate buffered saline (PBS) for 15 min at room temperature (RT). After fixing, coverslips were washed 3 times in PBS and incubated in blocking buffer (0.1% Triton X-100, 1% sodium azide, 2% normal goat serum) for 1 hr at RT. Coverslips were incubated in primary antibodies (chicken anti-GFP (1:500;

Rockland) and mouse anti-MAP2 (1:1000; BD Pharmingen)) diluted in blocking buffer for 2 hours at RT or overnight at 4 ˚C. After primary antibody incubation, coverslips were washed three times with PBS, after which they were incubated with secondary antibodies (Alexa Fluor 488 donkey anti-chicken (1:250; Life Technologies) and Alexa Fluor 647 donkey anti-mouse (1:250; Life Technologies)) diluted in blocking buffer for 1 hr at RT. Staining for mOrange was not necessary due to inherently high fluorescence. After secondary antibody incubation, coverslips were washed twice with PBS and incubated with Hoechst dye for 5 min at RT to stain nuclei. Coverslips were washed one final time with PBS and mounted onto glass microscope slides with Fluoromount G (Southern Biotechnology).

4.2.5 Imaging and fluorescence quantification

Transfected cells were visualized by immunofluorescence on an EVOS FL microscope (Thermo Fisher Scientific) using a 20x objective. Neurons were initially identified by mOrange expression under the RFP channel, and then co-transfection was confirmed by GFP expression. Images of mOrange, GFP, and DAPI fluorescence were taken for each neuron.

After imaging and before tracing, GFP and mOrange fluorescence were quantified using the corrected total cell fluorescence (CTCF) method. A CTCF threshold for GFP fluorescence was set for neurons determined to co-express mOrange and GFP by eye, and all neurons falling below this threshold were excluded from further analysis. Since absolute GFP fluorescence varies between conditions and between experiments, the threshold was reset for each condition within an experiment. A representative plot is

shown in Figure 4-2. mOrange fluorescence (data not shown) was quantified but was not used for confirming co-transfection.

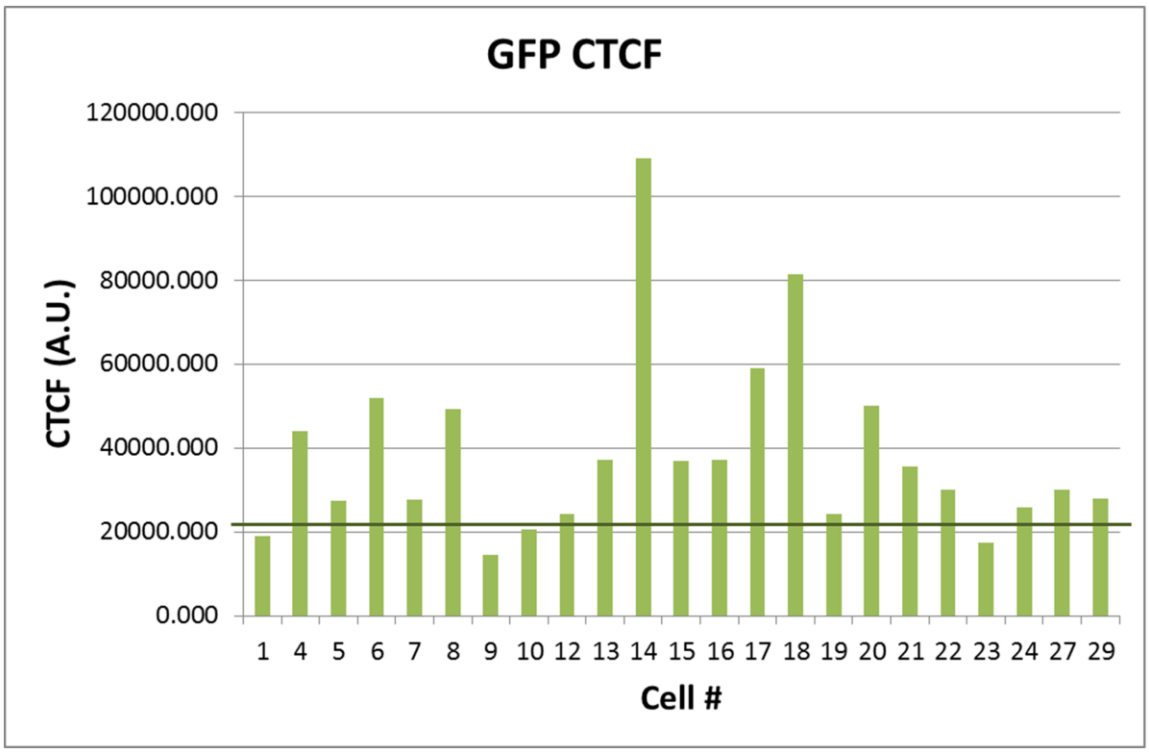

Figure 4-2: Representative plot of corrected total cell fluorescence data for GFP. In this plot of corrected total cell fluorescence (CTCF) data, the threshold was determined to be approximately 20,000 A.U. (shown as a dark green bar). All neurons falling below this level of fluorescence were not used for further analysis.

4.2.6 Assessment of dendrite number using semi-automated Sholl analysis

Dendrites were assessed as previously described (Kutzing, Langhammer et al. 2010, Langhammer, Previtera et al. 2010, Kwon, Fernandez et al. 2011) using the most common Sholl analysis, the Inside-Out labeling scheme (O'Neill, Akum et al. 2015). We used the "Bonfire" program developed by our laboratory to perform semi-automated Sholl analysis with a 6 µm ring interval starting at 0 µm from the soma. The

experimenter was blinded to conditions during all data analyses. Dendrites less than 3 μm in length were not counted (Yu and Malenka 2004, Charych, Akum et al. 2006).

Prism (Graphpad) was used for determining significance by two-way ANOVA followed by Bonferroni's multiple comparisons test for Sholl curves. InStat (GraphPad) was used for determining significance by one-way ANOVA or Kruskal-Wallis test (non-parametric ANOVA) for dendrite numbers and lengths.

4.3 Results

4.3.1 Intracellular targeting of BDNF transcripts affects the spatial distribution, number, and length of the overall dendritic arbor

To understand how development of the dendritic arbor is affected by the targeting of BDNF mRNA to different sites in the neuron, cultures were transfected at DIV 7 with the plasmids depicted in Figure 4-1 and fixed approximately 72 hr later at DIV 10. Representative images from each condition are shown in Figure 4-3A. Importantly, this time window matches the 72 hr treatment time used in our previous studies examining the effects of global application of BDNF (Kwon, Fernandez et al. 2011) and microbead delivery of BDNF (Chapter 3) on the dendritic arbor.

To determine how dendrite numbers are affected in a distance-dependent manner by overexpression and targeting of BDNF, we performed Sholl analysis for all orders of dendrites (Total Sholl), shown in Figure 4-3B, using the Inside-Out labeling scheme (O'Neill, Akum et al. 2015). To better illustrate the effects overexpression, the first 120 μm of the Total Sholl analysis is shown in Figure 4-3C. Importantly, dendrites

significantly increase regardless of which BDNF transcript is expressed. Additional details are provided in Figure 4-4 and Table 4-1.

Moreover, we investigated the effects of overexpression and targeting of BDNF transcripts on the total number of dendrites and the average length of dendrites. Neurons transfected with constructs for BDNF cds (BDNF) or BDNF cds with the short 3' UTR (Short) had significantly more dendrites than control neurons (pIRES), as shown in Figure 4-3D. Neurons transfected with constructs encoding the BDNF cds with the long 3' UTR (Long) had significantly shorter dendrites than control neurons, as shown in Figure 4-3E.

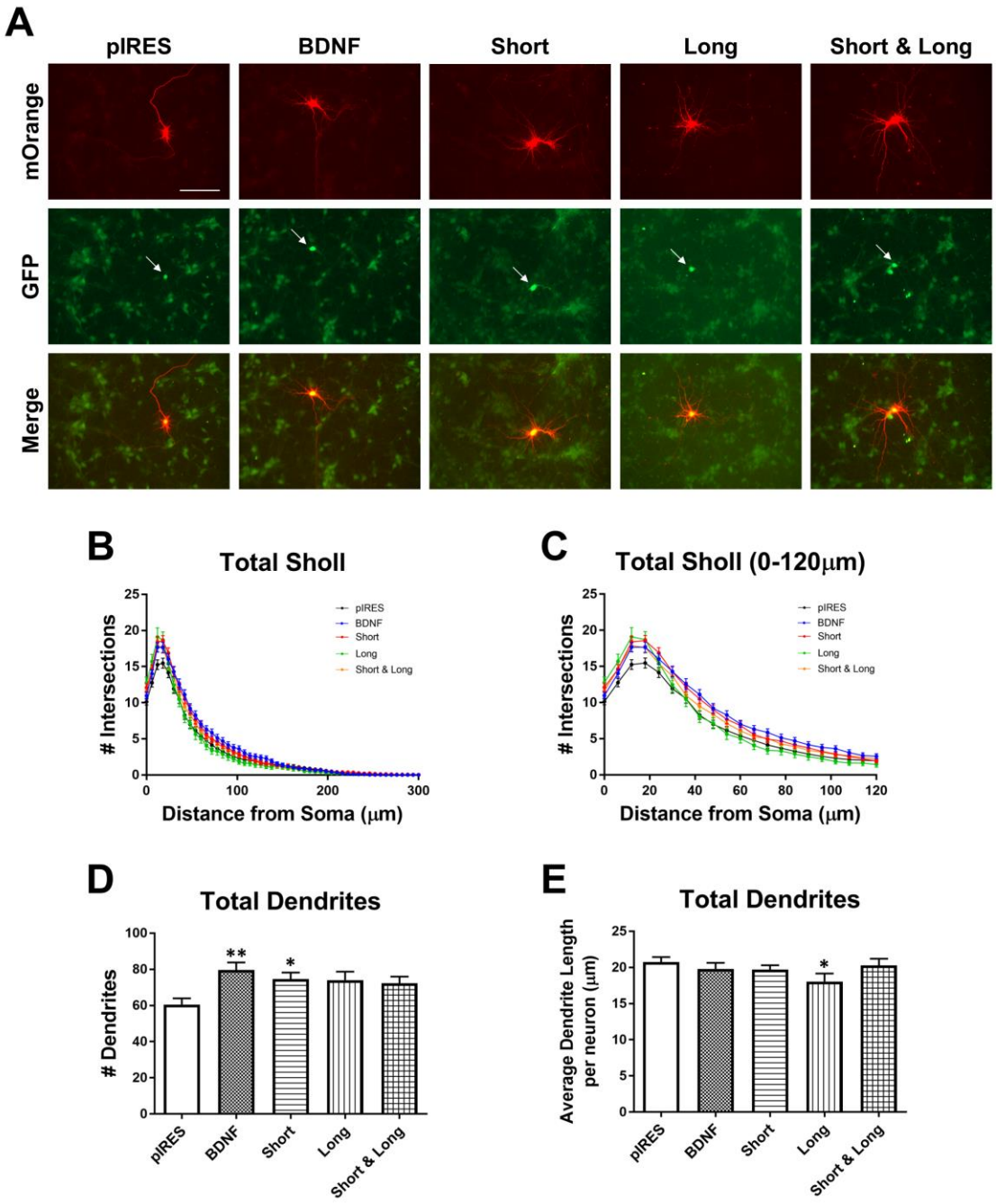

Figure 4-3: Overexpression of BDNF with and without the targeting UTRs results in changes to Sholl curves, total dendrite number, and average dendrite length.
A. Representative images are shown for each condition. Neurons co-expressing mOrange and GFP are indicated with white arrows. Scale bar = 100 μm. **B.** Total Sholl analysis for all conditions. **C.** The first 120 μm of Total Sholl analysis shown in B. **D.** Neurons expressing BDNF and Short have significantly more dendrites than control neurons. **E.** Neurons expressing Long have significantly shorter dendrites than control neurons. For D and E, *p<0.05 and **p<0.01 calculated using Kruskal-Wallis Test followed by Dunn's multiple comparisons test. All conditions were compared to neurons

transfected with pIRES (control) and to neurons expressing BDNF. n(pIRES)=68; n(BDNF)=74; n(Short)=76; n(Long)=33; n(Short&Long)=79.

To better visualize Total Sholl data from Figure 4-3B,C, the Sholl curves are graphed separately according to the comparisons. The plots show comparisons of all conditions to each other in Figure 4-4, and the statistics are summarized in Table 4-1.

All neurons transfected with constructs for BDNF cds have significantly more dendrites than control neurons whether or not 3' UTRs are present (Figure 4-4A-D). The effects on the dendritic arbor depend on where BDNF is targeted. Transfection of neurons with a construct for BDNF cds only (BDNF) results in significantly increased dendrites over the largest area (6-102 μm away from the soma; Figure 4-4A) when compared with control neurons. Transfection of neurons with a construct for BDNF cds with the short 3' UTR (Short), which preferentially targets the BDNF mRNA to the soma, also results in increased dendrites at 6-60 μm away from the soma (Figure 4-4B) when compared with control neurons. This increase occurs at fewer sites in the arbor than in neurons transfected with a construct for BDNF cds only (compare Figure 4-4A and Figure 4-4B). Transfection of neurons with a construct for BDNF cds with the long 3' UTR (Long), which targets the BDNF mRNA to both the soma and dendrites, results in increased dendrites at 0-18 μm away from the soma (Figure 4-4C) when compared with control neurons. Notably, this increase occurs at fewer sites in the arbor than in neurons transfected with constructs for BDNF cds only (BDNF) or for BDNF cds with the short 3' UTR (Short). Finally, transfection of neurons with a construct for BDNF cds with the short and long 3' UTR (Short & Long) also significantly increases dendrites at 0-30 μm and at 42-48 μm away from the soma (Figure 4-4D) compared with control neurons.

Significant changes to the arbor in neurons expressing BDNF cds with the short and long 3' UTR (Short & Long) occurs at distances intermediate of neurons expressing BDNF cds with the short 3' UTR (Short) and those expressing BDNF cds with the long 3' UTR (Long).

To understand how the targeting of BDNF affects the dendritic arbor when BDNF is overexpressed, we compared neurons transfected with constructs for BDNF cds only (BDNF) to those transfected with constructs for BDNF cds with one of the 3' UTRs (Figure 4-4E-G). Neurons expressing BDNF cds only (BDNF) and neurons expressing BDNF cds with the short 3' UTR (Short) exhibit similar Sholl curves (Figure 4-4E), with neurons expressing Short showing increased dendrites at the soma. Neurons expressing BDNF cds with the long 3' UTR (Long) exhibit distinct Sholl curves from neurons expressing BDNF cds only (BDNF). As shown in Figure 4-4F, neurons expressing Long show significantly more dendrites proximal to the soma (0-12 μm away from the soma), but neurons expressing BDNF show significantly more dendrites distal to the soma (30-108 μm away from the soma). Neurons expressing BDNF cds with the short and long 3' UTR (Short & Long) show significantly fewer dendrites at 36 μm, 42 μm, and 54 μm away from the soma when compared with neurons expressing BDNF cds only (BDNF), as seen in Figure 4-4G.

Finally, we compared the effects of targeting BDNF mRNA to the soma with targeting BDNF mRNA to both the soma and dendrites (Figure 4-4H-J). Neurons expressing BDNF cds with the short 3' UTR (Short) show significantly more dendrites than neurons expressing BDNF cds with the long 3' UTR (Long) at 24-72 μm away from the soma (Figure 4-4H). Neurons expressing BDNF cds with the short 3' UTR (Short)

also show significantly more dendrites than neurons expressing BDNF cds with the short and long 3' UTR (Short & Long), but only at two locations (24 μm and 36 μm away from the soma; Figure 4-4I). Finally, neurons expressing BDNF cds with the long 3' UTR (Long) show significantly fewer dendrites than neurons expressing BDNF cds with the short and long 3' UTR (Short & Long) at 42 μm, 54 μm, and 72 μm away from the soma (Figure 4-4J).

These comparisons illustrate that targeting BDNF mRNA with the short 3' UTR and the long 3' UTR have distinct effects on the overall dendritic arbor and that expression of mRNA containing the two UTRs together result in an averaging of the effects seen when mRNA with either UTR alone is expressed.

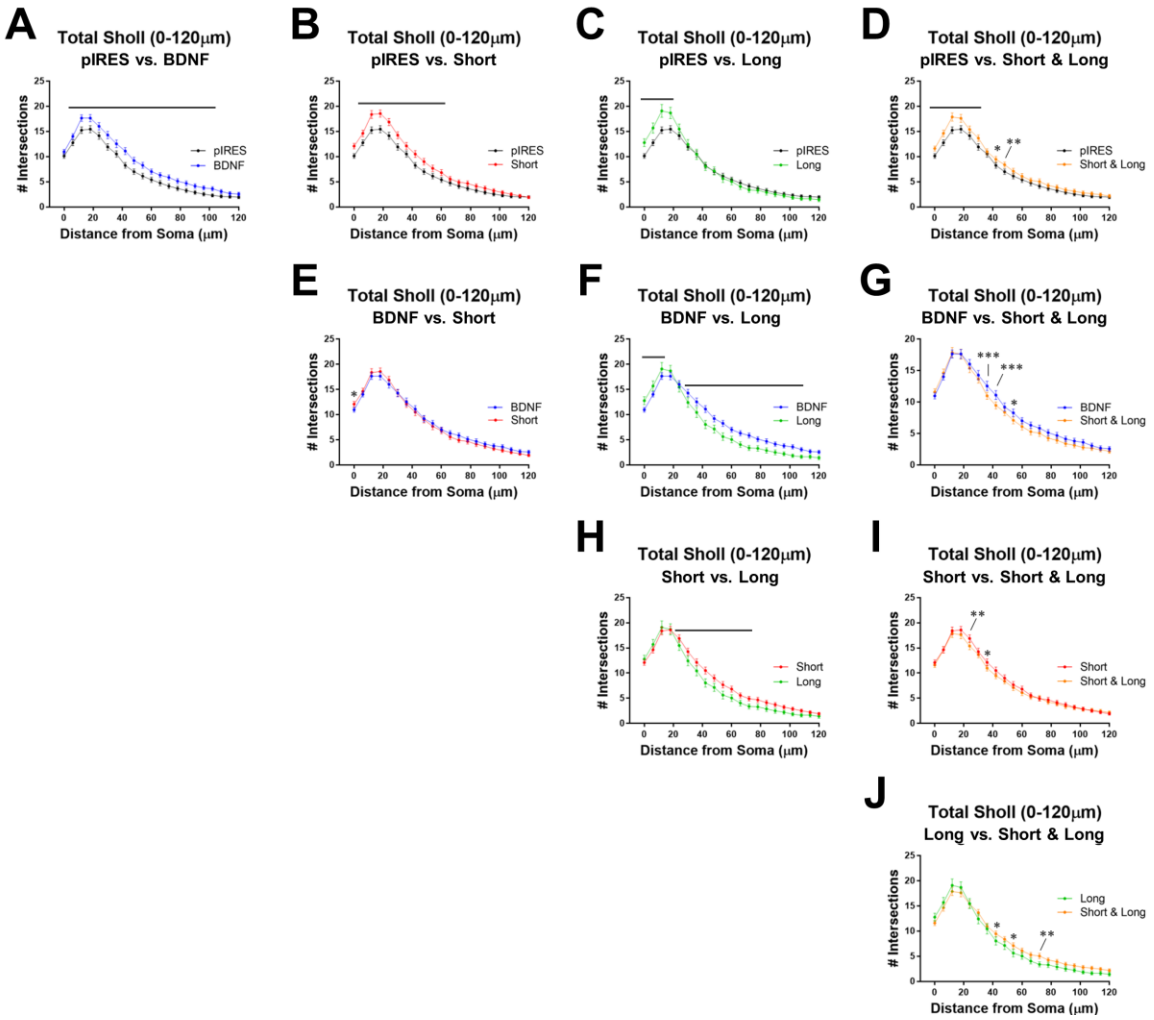

Figure 4-4: Total Sholl analysis showing comparisons between all conditions. Stars indicate exact level of significance, and bars indicate significance of at least *p<0.05. **A.** Neurons that express BDNF show significantly more dendrites than control neurons transfected with pIRES at 6-102 μm away from the soma. **B.** Neurons expressing Short show significantly more dendrites than control neurons at 6-60 μm away from the soma. **C.** Neurons expressing Long show significantly more dendrites than control neurons at 0-18 μm away from the soma. **D.** Neurons expressing Short & Long show significantly more dendrites than control neurons at 0-30 μm and at 42-48 μm away from the soma. **E.** Neurons expressing Short show significantly more dendrites than neurons expressing BDNF at the soma. **F.** Compared with neurons expressing BDNF, neurons expressing Long show significantly more dendrites at 0-12 μm and significantly fewer dendrites at 30-108 μm away from the soma. **G.** Neurons expressing Short & Long show significantly fewer dendrites than neurons expressing BDNF at 36-42 μm and at 54 μm away from the soma. **H.** Neurons expressing Long show significantly fewer dendrites than neurons expressing Short at 24-72 μm away from the soma. **I.** Neurons expressing Short & Long show significantly fewer dendrites than neurons expressing Short at 24 μm and at 36 μm away from the soma. **J.** Neurons expressing Short & Long show

significantly more dendrites than neurons expressing Long at 42 μm, 54 μm, and 72 μm away from the soma. Statistics calculated by two-way ANOVA followed by Bonferroni's multiple comparisons test (*p<0.05, **p<0.01, ***p<0.001, ****p<0.0001).

Total Sholl	Locations of significance	Level	Effect
pIRES vs. BDNF	6-102 μm	* - ****	+
pIRES vs. Short	6-60 μm	** - ****	+
pIRES vs. Long	0-18 μm	****	+
pIRES vs. Short & Long	0-30, 42-48 μm	* - ****, * - **	+, +
BDNF vs. Short	0 μm	*	+
BDNF vs. Long	0-12, 30-108 μm	* - ****	+, -
BDNF vs. Short & Long	36-42, 54 μm	***, *	-
Short vs. Long	24-72 μm	* - ****	-
Short vs. Short & Long	24, 36 μm	**, *	-, -
Long vs. Short & Long	42, 54, 72 μm	*, *, **	+, +, +

Table 4-1: Statistical details of comparisons between conditions for Total Sholl analysis.
The table shows sites of significant differences in dendrites (in μm away from the soma), the level of significance, and the effect of significance (whether there was an increase or decrease in dendrites). For example, a positive ("+") effect for pIRES vs. BDNF means that neurons expressing BDNF show significantly more dendrites than control neurons expressing pIRES at the indicated distances from the soma. Statistics calculated by two-way ANOVA followed by Bonferroni's multiple comparisons test (*p<0.05, **p<0.01, ***p<0.001, ****p<0.0001).

4.3.2 Intracellular targeting of BDNF transcripts affects the spatial distribution of specific orders of dendrites

In addition to conventional Sholl analysis (Total Sholl), we employed order-specific Sholl analysis to understand how overexpression and targeting of BDNF affects the spatial organization of specific orders of dendrites. A summary of the effects on primary, secondary, and tertiary and higher order dendrites, according to the Inside-Out labeling scheme, is shown in Figure 4-5. Plots of comparisons between all conditions for all orders of dendrites are shown in Figures 4-6 through 4-8, and the statistics are summarized in Tables 4-2 through 4-4.

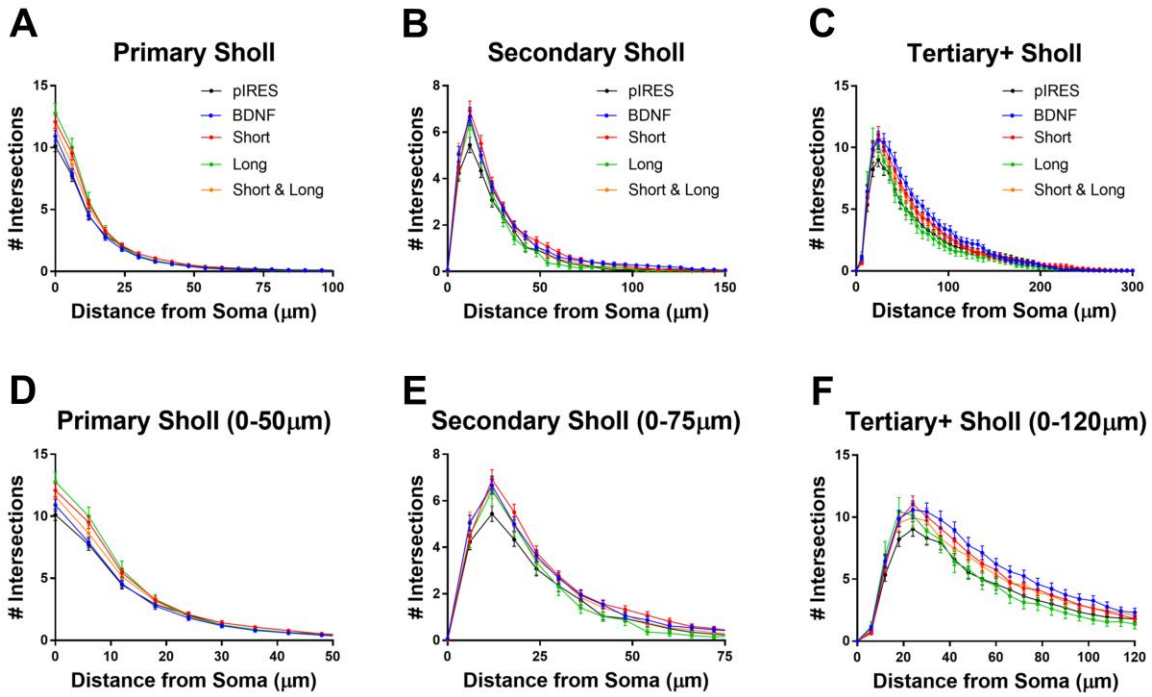

Figure 4-5: Order-specific Sholl analysis reveals how overexpression of BDNF affects the spatial organization of different orders of dendrites.
A. Sholl analysis of primary dendrites (Primary Sholl) for all conditions. **B.** Sholl analysis of secondary dendrites (Secondary Sholl) for all conditions. **C.** Sholl analysis of tertiary and higher order dendrites (Tertiary+ Sholl) for all conditions. **D.** Primary Sholl analysis shown for the first 50 μm. **E.** Secondary Sholl analysis shown for the first 75 μm. **F.** Tertiary+ Sholl analysis shown for the first 120 μm. Comparisons and significant changes are shown in Figures 4-6 through 4-8.

The plots of Sholl curves comparing primary dendrites for all conditions are shown in Figure 4-6, and the statistics are summarized in Table 4-2.

Neurons expressing BDNF cds show significantly more primary dendrites than control neurons (pIRES), whether or not 3' UTRs are present (Figure 4-6A-D). Transfection of neurons with a construct for BDNF cds only (BDNF) results in significantly increased primary dendrites at the soma (Figure 4-6A) when compared with control neurons. Transfection of neurons with a construct for BDNF cds with the short 3' UTR (Short) significantly increases primary dendrites at 0-18 μm away from the

soma (Figure 4-6B) when compared with control neurons. Transfection of neurons with a construct for BDNF cds with the long 3' UTR (Long) significantly increases primary dendrites at 0-12 μm away from the soma (Figure 4-6C) when compared with control neurons. Transfection of neurons with a construct for BDNF cds with the short and long 3' UTR (Short & Long) significantly increases primary dendrites at 0-12 μm away from the soma (Figure 4-6D) when compared with control neurons. Interestingly, targeting of BDNF transcripts to specific regions of the neuron significantly increases primary dendrites at more locations within the dendritic arbor than when BDNF is overexpressed from a transcript lacking a 3'UTR that would otherwise restrict BDNF expression.

To understand how the targeting of BDNF transcripts affects primary dendrites, we compared neurons transfected with a construct for BDNF cds only (BDNF) to those transfected with constructs for BDNF cds with one of the 3' UTRs (Figure 4-6E-G). Primary dendrites increase in neurons in all conditions in which BDNF is overexpressed and targeted (Short, Long, and Short & Long) compared with neurons that overexpress BDNF from a transcript lacking 3'UTRs (BDNF). The dendritic arbor changed at 0-18 μm away from the soma, and this change is independent of where BDNF transcripts are targeted. Specific comparisons between neuron expressing BDNF cds with the short 3' UTR (Short), BDNF cds with the long 3' UTR (Long), or BDNF cds with the short and long 3' UTR (Short & Long) and neurons expressing BDNF cds only (BDNF) are shown in Figure 4-6E, Figure 4-6F, and Figure 4-6G, respectively.

Finally, we compared the effects on primary dendrites of targeting BDNF to the soma with targeting BDNF to both the soma and dendrites (Figure 4-6H-J). Neurons expressing BDNF cds with the short 3' UTR (Short) show significantly fewer primary

dendrites than neurons expressing BDNF cds with the long 3' UTR (Long) at 0-6 μm away from the soma (Figure 4-6H). Neurons expressing BDNF cds with the short 3' UTR (Short) show significantly more primary dendrites than neurons expressing BDNF cds with the short and long 3' UTR (Short & Long) at 0-6 μm away from the soma (Figure 4-6I). Neurons expressing BDNF cds with the long 3' UTR (Long) show significantly more primary dendrites than neurons expressing BDNF cds with the long 3' UTR (Long) at 0-12 μm away from the soma (Figure 4-6H).

These comparisons illustrate that targeting BDNF transcripts with the short 3' UTR and the long 3' UTR result in similar effects on the spatial organization of primary dendrites.

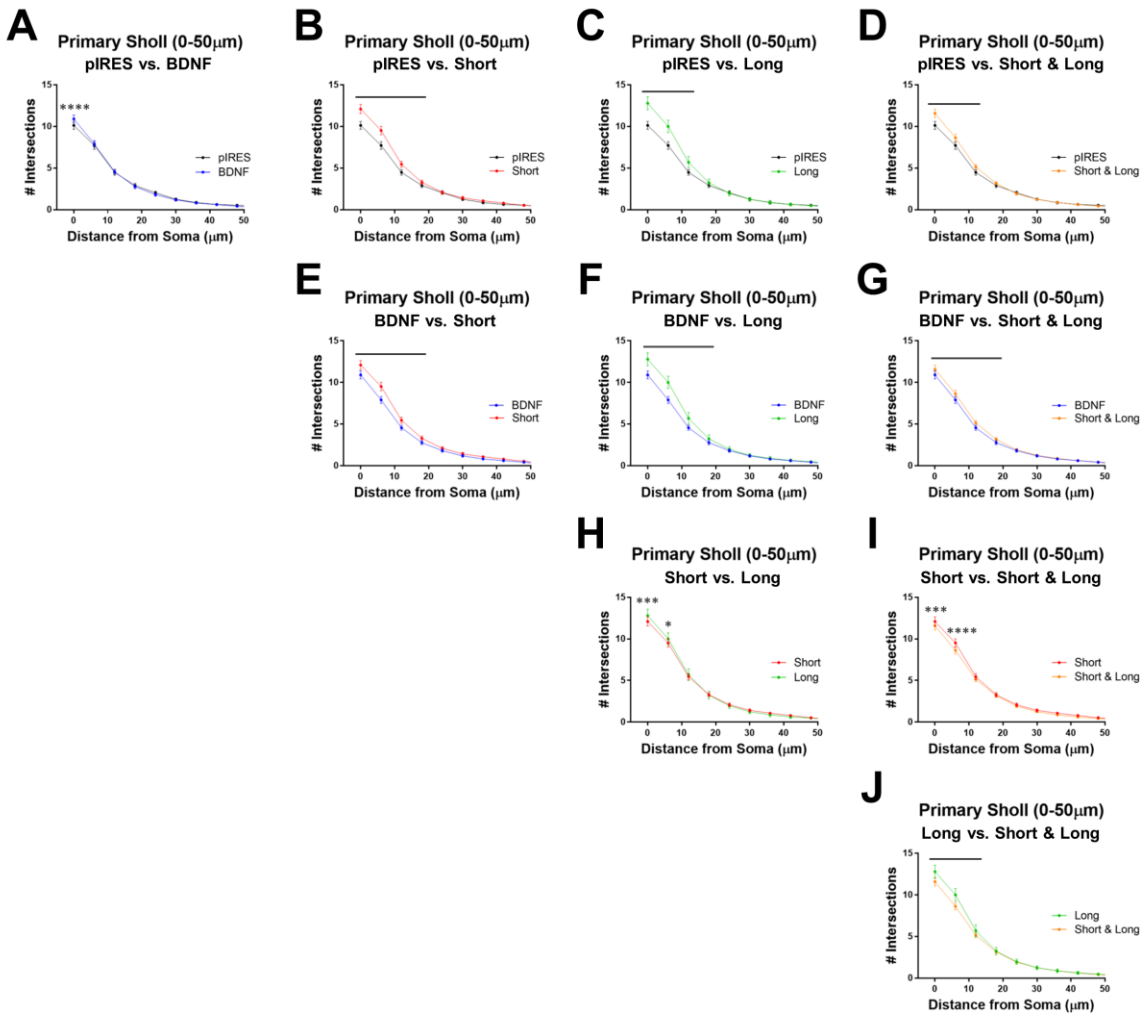

Figure 4-6: Sholl analysis of primary dendrites showing comparisons between all conditions.

Stars indicate exact level of significance, and bars indicate significance of at least *p<0.05. **A.** Neurons expressing BDNF show significantly more primary dendrites than control neurons (pIRES) at the soma (0 μm). **B.** Neurons expressing Short show significantly more primary dendrites than control neurons at 0-18 μm away from the soma. **C.** Neurons expressing Long show significantly more primary dendrites than control neurons at 0-12 μm away from the soma. **D.** Neurons expressing Short & Long show significantly more primary dendrites than control neurons at 0-12 μm away from the soma. **E.** Neurons expressing Short show significantly more primary dendrites than neurons expressing BDNF at 0-18 μm away from the soma. **F.** Neurons expressing Long show significantly more primary dendrites than neurons expressing BDNF at 0-18 μm away from the soma. **G.** Neurons expressing Short & Long show significantly more primary dendrites than neurons expressing BDNF at 0-18 μm away from the soma. **H.** Neurons expressing Long show significantly more primary dendrites than neurons expressing Short at 0-6 μm away from the soma. **I.** Neurons expressing Short & Long show significantly fewer primary dendrites than neurons expressing Short at 0-6 μm

away from the soma. **J.** Neurons expressing Short & Long show significantly fewer primary dendrites than neurons expressing Long at 0-12 μm away from the soma. Statistics calculated by two-way ANOVA followed by Bonferroni's multiple comparisons test (*p<0.05, **p<0.01, ***p<0.001, ****p<0.0001).

Primary Sholl	Locations of significance	Level	Effect
pIRES vs. BDNF	0 μm	****	+
pIRES vs. Short	0-18 μm	* - ****	+
pIRES vs. Long	0-12 μm	****	+
pIRES vs. Short & Long	0-12 μm	****	+
BDNF vs. Short	0-18 μm	*** - ****	+
BDNF vs. Long	0-18 μm	* - ****	+
BDNF vs. Short & Long	0-18 μm	* - ****	+
Short vs. Long	0-6 μm	***, *	+, +
Short vs. Short & Long	0-6 μm	***, ****	-, -
Long vs. Short & Long	0-12 μm	** - ****	-

Table 4-2: Statistical details of comparisons between conditions for Primary Sholl analysis.
The table shows sites of significant differences in dendrites (in μm away from the soma), the level of significance, and the effect of significance (whether there was an increase or decrease in dendrites). For example, a positive ("+") effect for pIRES vs. BDNF means that neurons expressing BDNF show significantly more dendrites than control neurons expressing pIRES at the indicated distances from the soma. Statistics calculated by two-way ANOVA followed by Bonferroni's multiple comparisons test (*p<0.05, **p<0.01, ***p<0.001, ****p<0.0001).

We also examined the Sholl curves of secondary dendrites. The plots of Sholl curves comparing secondary dendrites for all conditions are shown in Figure 4-7, and the statistics are summarized in Table 4-3.

All neurons that were transfected with a construct for BDNF cds show significantly more secondary dendrites than control neurons (pIRES), whether or not the 3' UTRs are present (Figure 4-7A-D). Transfection of neurons with a construct for BDNF cds (BDNF) significantly increases secondary dendrites at 6-24 μm and at 42 μm away from the soma (Figure 4-7A) when compared with control neurons. Transfection of neurons with a construct for BDNF cds with the short 3' UTR (Short) significantly

increases secondary dendrites at 12-30 μm and at 42-48 μm away from the soma (Figure 4-7B) when compared with control neurons. Transfection of neurons with a construct for BDNF cds with the long 3' UTR (Long) significantly increases secondary dendrites at 12-18 μm away from the soma (Figure 4-7C) when compared with control neurons. Transfection of neurons with a construct for BDNF cds with the short and long 3' UTR (Short & Long) significantly increases secondary dendrites at 6-30 μm and at 42 μm away from the soma (Figure 4-7D) when compared with control neurons. Several of the conditions (BDNF, Short, and Short & Long) had similar sites of increased secondary dendrites when compared with the control.

To understand how the targeting of BDNF affects secondary dendrites when BDNF is overexpressed, we compared neurons transfected with a construct for BDNF cds only (BDNF) to those transfected with a construct for BDNF cds with one of the 3' UTRs (Figure 4-7E-G). Neurons expressing BDNF cds with the short 3' UTR (Short) show significantly fewer secondary dendrites at 6 μm away from the soma and significantly more secondary dendrites at 18 μm away from the soma (Figure 4-7E) compared with neurons expressing BDNF cds only (BDNF). Neurons expressing BDNF cds with the long 3' UTR (Long) show significantly fewer secondary dendrites at 6 μm, 36-42 μm, and 54 μm away from the soma (Figure 4-7F) compared with neurons expressing BDNF cds only (BDNF). As seen in Figure 4-7G, there were no significant differences in the Sholl curves of secondary dendrites when comparing neurons expressing BDNF cds with the short and long 3' UTR (Short & Long) and neurons expressing BDNF cds only (BDNF).

Finally, we compared the effects on secondary dendrites of targeting BDNF to the soma with targeting BDNF to both the soma and dendrites (Figure 4-7H-J). Neurons expressing BDNF cds with the short 3' UTR (Short) show significantly more secondary dendrites than neurons expressing BDNF cds with the long 3' UTR (Long) at several sites in the dendritic arbor (12-18 μm, 30-42 μm, and 54-60 μm away from the soma; Figure 4-7H). Neurons expressing BDNF cds with the short 3' UTR (Short) show significantly fewer secondary dendrites at 6 μm away from the soma and significantly more secondary dendrites at 12-18 μm away from the soma compared with neurons expressing BDNF cds with the short and long 3' UTR (Short & Long), as seen in Figure 4-7I. Neurons expressing BDNF cds with the long 3' UTR (Long) show significantly fewer secondary dendrites at only one dendritic site (6 μm away from the soma) compared with neurons expressing BDNF cds with the short and long 3' UTR (Short & Long), as seen in Figure 4-7J.

These comparisons illustrate the differences that targeting BDNF mRNA with the short or the long 3' UTR exerts on the spatial organization of secondary dendrites. In this case, targeting of BDNF mRNA with the long 3' UTR exerts the smallest effects when compared with control neurons, significantly increasing secondary dendrites at two locations. Overexpression of BDNF mRNA without a 3' UTR, with the short 3' UTR, or both the short and long 3' UTR (BDNF, Short, and Short & Long conditions, respectively) results in similar effects on the distribution of secondary dendrites.

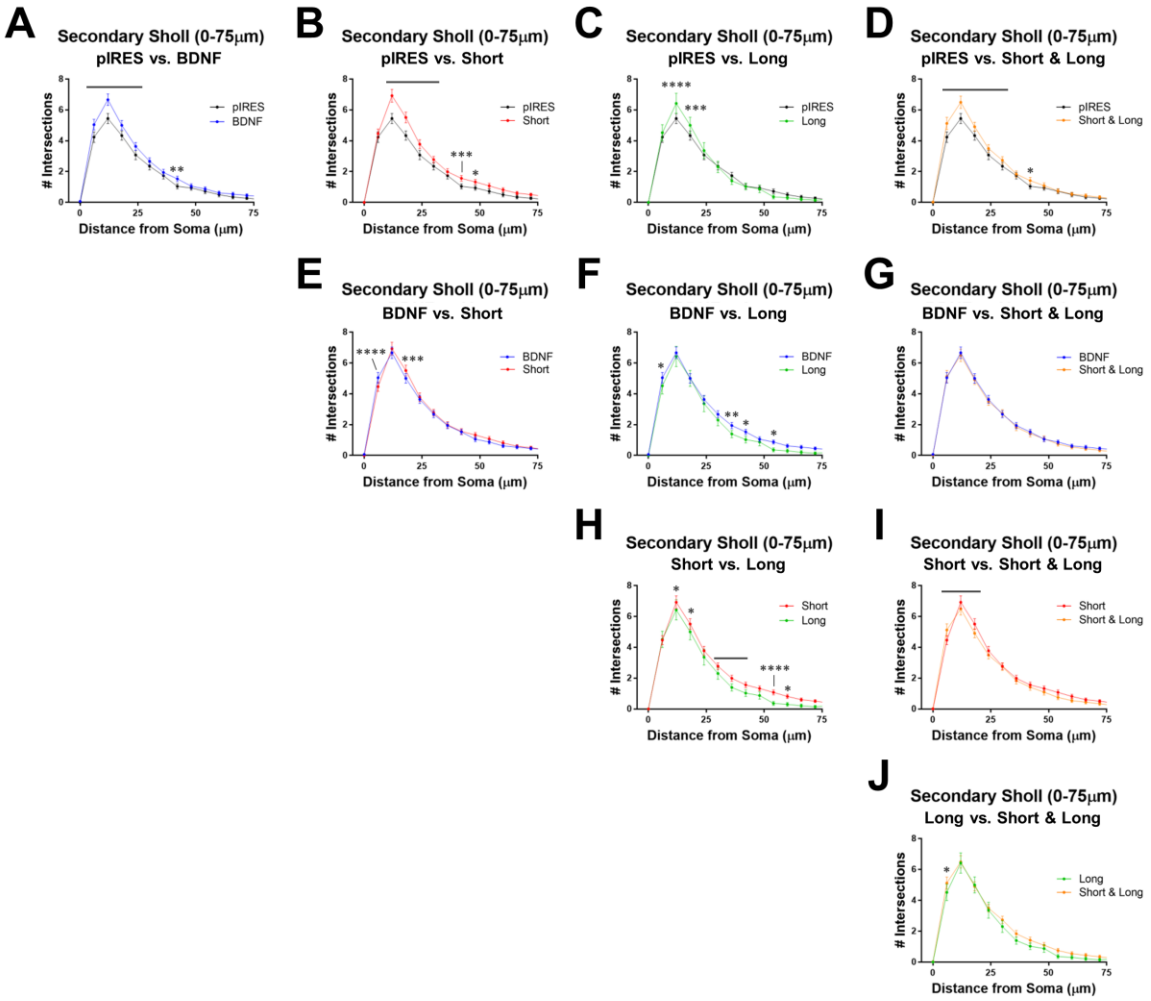

Figure 4-7: Sholl analysis of secondary dendrites showing comparisons between all conditions.

Stars indicate exact level of significance, and bars indicate significance of at least *p<0.05. **A.** Neurons expressing BDNF show significantly more secondary dendrites than control neurons (pIRES) at 6-24 μm and at 42 μm away from the soma. **B.** Neurons expressing Short show significantly more secondary dendrites than control neurons at 12-30 μm and at 42-48 μm away from the soma. **C.** Neurons expressing Long show significantly more secondary dendrites than control neurons at 12-18 μm away from the soma. **D.** Neurons expressing Short & Long show significantly more secondary dendrites than control neurons at 6-30 μm and at 42 μm away from the soma. **E.** Compared to neurons expressing BDNF, neurons expressing Short show significantly fewer secondary dendrites at 6 μm and significantly more dendrites at 18 μm away from the soma. **F.** Neurons expressing Long show significantly fewer secondary dendrites than neurons expressing BDNF at 6 μm, 36-42 μm, and 54 μm away from the soma. **G.** Neurons expressing Short & Long show similar secondary arbors compared to neurons expressing BDNF. **H.** Neurons expressing Long show significantly fewer dendrites than neurons expressing Short at 12-18 μm, 30-42 μm, and 54-60 μm away from the soma. **I.** Compared with neurons expressing Short, neurons expressing

Short & Long show significantly more dendrites at 6 μm and significantly fewer dendrites at 12-18 μm away from the soma. **J.** Neurons expressing Short & Long show significantly more dendrites than neurons expressing Long at 6 μm away from the soma. Statistics calculated by two-way ANOVA followed by Bonferroni's multiple comparisons test (*p<0.05, **p<0.01, ***p<0.001, ****p<0.0001).

Secondary Sholl	Locations of significance	Level	Effect
pIRES vs. BDNF	6-24, 42 μm	*** - ****, **	+, +
pIRES vs. Short	12-30, 42-48 μm	* - ****	+, +
pIRES vs. Long	12-18 μm	****, ***	+, +
pIRES vs. Short & Long	6-30, 42 μm	* - ****, *	+, +
BDNF vs. Short	6, 18 μm	****, ***	-, +
BDNF vs. Long	6, 36-42, 54 μm	*, * - **, *	-, -, -
BDNF vs. Short & Long	None	N/A	N/A
Short vs. Long	12-18, 30-42, 54-60 μm	* - ****	-, -, -
Short vs. Short & Long	6-18 μm	** - ****	+, -, -
Long vs. Short & Long	6 μm	**	+

Table 4-3: Statistical details of comparisons between conditions for Secondary Sholl analysis.
The table shows sites of significant differences in dendrites (in μm away from the soma), the level of significance, and the effect of significance (whether there was an increase or decrease in dendrites). For example, a positive ("+") effect for pIRES vs. BDNF means that neurons expressing BDNF show significantly more dendrites than control neurons expressing pIRES at the indicated distances from the soma. Statistics calculated by two-way ANOVA followed by Bonferroni's multiple comparisons test (*p<0.05, **p<0.01, ***p<0.001, ****p<0.0001).

We also examined the Sholl curves of tertiary and higher order dendrites. The plots of Sholl curves comparing tertiary and higher order dendrites for all conditions are shown in Figure 4-8, and the statistics are summarized in Table 4-4.

All neurons that were transfected with a construct for BDNF cds show significantly more tertiary and higher order dendrites than control neurons (pIRES), whether or not 3' UTRs are present (Figure 4-8A-D). Transfection of neurons with a construct for BDNF cds (BDNF) significantly increases tertiary and higher order dendrites at 12-102 μm away from the soma (Figure 4-8A) when compared with control neurons. Transfection of neurons with a construct for BDNF cds with the short

3’ UTR (Short) significantly increases tertiary and higher order dendrites at 18-60 μm away from the soma (Figure 4-8B) when compared with control neurons. Transfection of neurons with a construct for BDNF cds with the long 3’ UTR (Long) significantly increases tertiary and higher order dendrites at 12-18 μm away from the soma (Figure 4-8C) when compared with control neurons. Transfection of neurons with a construct for BDNF cds with the short and long 3’ UTR (Short & Long) significantly increases tertiary and higher order dendrites at 18 μm, 30 μm, and 48-54 μm away from the soma (Figure 4-8D) when compared with control neurons. The differences among the conditions are similar to those seen in Total Sholl analysis in Figure 4-4: neurons expressing BDNF show increased dendrites at the most locations within the arbor; neurons expressing Short show increased dendrites at many locations within the arbor; neurons expressing Long show increased dendrites at the fewest locations; and neurons expressing Short & Long condition show an average of dendrites observed in neurons expressing Short and Long separately.

To understand how the targeting of BDNF affects tertiary and higher order dendrites when BDNF is overexpressed, we compared neurons expressing BDNF cds only (BDNF) to those expressing BDNF cds with one of the 3’ UTRs (Figure 4-8E-G). Neurons expressing BDNF cds with the short 3’ UTR (Short) show significantly fewer tertiary and higher order dendrites at 72 μm away from the soma (Figure 4-8E) compared with neurons expressing BDNF cds only (BDNF). Neurons expressing BDNF cds with the long 3’ UTR (Long) show significantly fewer tertiary and higher order dendrites at 30-102 μm away from the soma (Figure 4-8F) compared with neurons expressing BDNF cds only (BDNF). Neurons expressing BDNF cds with the short and long

3’ UTR (Short & Long) show significantly fewer tertiary and higher order dendrites at 36-42 μm and at 54 μm away from the soma (Figure 4-8G) compared with neurons expressing BDNF cds only (BDNF).

Finally, we compared the effects of targeting BDNF to the soma with targeting of BDNF to both the soma and dendrites on tertiary and higher order dendrites (Figure 4-8H-J). Neurons expressing BDNF cds with the short 3’ UTR (Short) show significantly more tertiary and higher order dendrites than neurons expressing BDNF cds with the long 3’ UTR (Long) at 42-60 μm away from the soma (Figure 4-8H). Neurons expressing BDNF cds with the short 3’ UTR (Short) show significantly more tertiary and higher order dendrites at 24 μm away from the soma compared with neurons expressing BDNF cds with the short and long 3’ UTR (Short & Long), as seen in Figure 4-8I. Neurons expressing BDNF cds with the long 3’ UTR (Long) show significantly fewer tertiary and higher order dendrites at 72 μm away from the soma compared with neurons expressing BDNF cds with the short and long 3’ UTR (Short & Long), as seen in Figure 4-8J.

These comparisons illustrate the differences that targeting BDNF with the short or the long 3’ UTR causes regarding the spatial organization of tertiary and higher order dendrites. Changes to tertiary and higher order dendrites in Tertiary+ Sholl analysis are similar to those seen in Total Sholl analysis (compare Figure 4-4 and Figure 4-8).

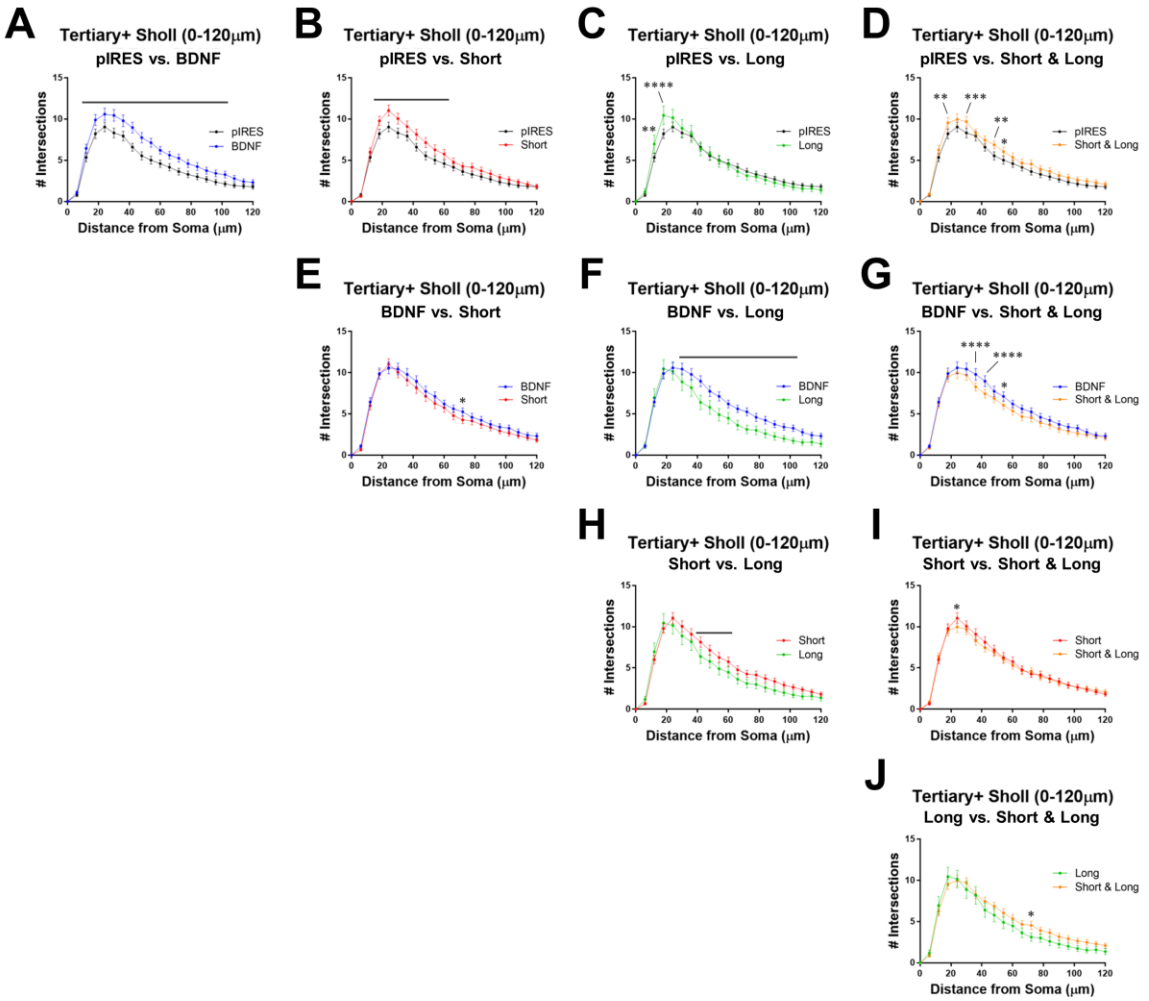

Figure 4-8: Sholl analysis of tertiary and higher order dendrites showing comparisons between all conditions.

Stars indicate exact level of significance, and bars indicate significance of at least *p<0.05. **A.** Neurons expressing BDNF show significantly more tertiary and higher order dendrites than control neurons (pIRES) at 12-102 μm away from the soma. **B.** Neurons expressing Short show significantly more tertiary and higher order dendrites than control neurons at 18-60 μm away from the soma. **C.** Neurons expressing Long show significantly more tertiary and higher order dendrites than control neurons at 12-18 μm away from the soma. **D.** Neurons expressing Short & Long show significantly more tertiary and higher order dendrites than control neurons at 18 μm, 30 μm, and 48-54 μm away from the soma. **E.** Neurons expressing Short show significantly fewer tertiary and higher order dendrites than neurons expressing BDNF at 72 μm away from the soma. **F.** Neurons expressing Long show significantly fewer tertiary and higher order dendrites than neurons expressing BDNF at 30-102 μm away from the soma. **G.** Neurons expressing Short & Long show significantly fewer tertiary and higher order dendrites than neurons expressing BDNF at 36-42 μm and at 54 μm away from the soma. **H.** Neurons expressing Long show significantly fewer tertiary and higher order dendrites than neurons expressing Short at 42-60 μm away from the soma. **I.** Neurons expressing

Short & Long show significantly fewer tertiary and higher order dendrites than neurons expressing Short at 24 μm away from the soma. **J.** Neurons expressing Short & Long show significantly more tertiary and higher order dendrites than neurons expressing Long at 72 μm away from the soma. Statistics calculated by two-way ANOVA followed by Bonferroni's multiple comparisons test (*p<0.05, **p<0.01, ***p<0.001, ****p<0.0001).

Tertiary+ Sholl	Locations of significance	Level	Effect
pIRES vs. BDNF	12-102 μm	* - ****	+
pIRES vs. Short	18-60 μm	* - ****	+
pIRES vs. Long	12-18 μm	**, ****	+, +
pIRES vs. Short & Long	18, 30, 48-54 μm	* - ***	+, +, +
BDNF vs. Short	72 μm	*	-
BDNF vs. Long	30-102 μm	* - ****	-
BDNF vs. Short & Long	36-42, 54 μm	****, *	-, -
Short vs. Long	42-60 μm	* - ***	-
Short vs. Short & Long	24 μm	*	-
Long vs. Short & Long	72 μm	*	+

Table 4-4: Statistical details of comparisons between conditions for Tertiary+ Sholl analysis.
The table shows sites of significant differences in dendrites (in μm away from the soma), the level of significance, and the effect of significance (whether there was an increase or decrease in dendrites). For example, a positive ("+") effect for pIRES vs. BDNF means that neurons expressing BDNF show significantly more dendrites than control neurons expressing pIRES at the indicated distances from the soma. Statistics calculated by two-way ANOVA followed by Bonferroni's multiple comparisons test (*p<0.05, **p<0.01, ***p<0.001, ****p<0.0001).

4.3.3 Intracellular targeting of BDNF transcripts affects the number and length of specific orders of dendrites

In addition to order-specific Sholl analysis, we investigated whether overexpression of BDNF with or without the targeting UTRs affects the number and length of specific orders of dendrites. Neurons expressing BDNF cds with the long 3' UTR (Long) show significantly more primary dendrites (*p<0.05) than control neurons (pIRES; Figure 4-9A). Neurons expressing BDNF cds only (BDNF) or BDNF cds with the short 3' UTR (Short) show significantly more secondary dendrites

(both *p<0.05) than control neurons (Figure 4-9B). Neurons expressing BDNF cds only (BDNF) show significantly more tertiary and higher order dendrites (*p<0.05) than control neurons (Figure 4-9C). In addition, neurons expressing BDNF cds with the long 3' UTR (Long) show significantly shorter tertiary and higher order dendrites (*p<0.05) than control neurons (Figure 4-10C).

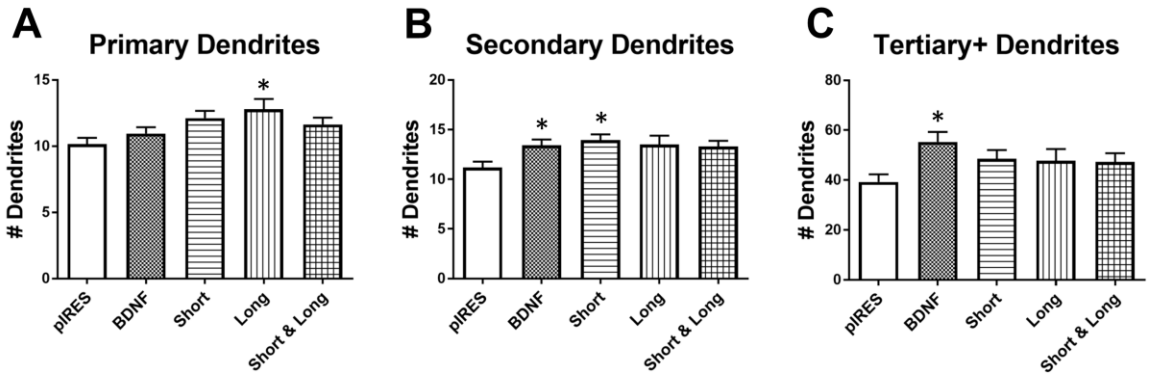

Figure 4-9: Targeting BDNF mRNA to different parts of the cell has distinct effects on specific orders of dendrites.
A. Neurons expressing Long show significantly more primary dendrites than control neurons (pIRES; *p<0.05). **B.** Neurons expressing BDNF and Short show significantly more secondary dendrites than control neurons (both *p<0.05). **C.** Neurons expressing BDNF show significantly more tertiary and higher order dendrites than control neurons (*p<0.05). Statistics were calculated using the Kruskal-Wallis Test followed by Dunn's multiple comparisons test. All conditions were compared to control (pIRES) and to BDNF.

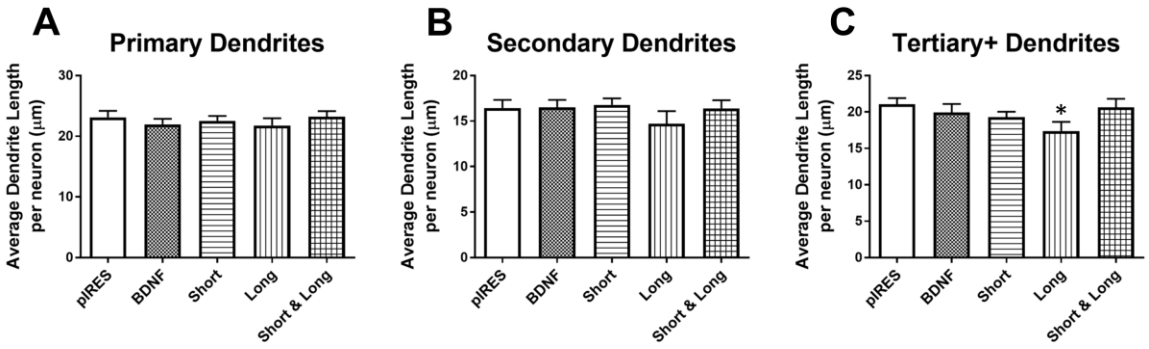

Figure 4-10: Targeting BDNF mRNA with the long 3' UTR affects tertiary and higher order dendrite length.

A. Overexpression of BDNF mRNA with or without the 3' UTRs does not affect average primary dendrite length. **B.** Overexpression of BDNF mRNA with or without the 3' UTRs does not affect average secondary dendrite length. Four outliers were eliminated from the BDNF condition using the ROUT method with Q=1%. **C.** Neurons expressing Long show significantly shorter tertiary and higher order dendrites than control neurons (pIRES; $p<0.05$). Statistics were calculated using the Kruskal-Wallis Test followed by Dunn's multiple comparisons test. All conditions were compared to control (pIRES) and to BDNF.

4.4 Discussion

Previous work from our laboratory examined the mechanism by which extracellular application of BDNF modulates the development of the dendritic arbor, either via bath application (Kwon, Fernandez et al. 2011) or via delivery on microbeads (Chapter 3). The work presented in this chapter represents the first time our laboratory has sought to understand how overexpression and intracellular targeting of BDNF mRNA, and hence protein, affects the dendritic arbor. We initially hypothesized that overexpression of BDNF would increase dendrite branching and that targeting of BDNF to the soma and to dendrites via mRNA containing the long 3' UTR would increase branching over a greater range of dendritic distances from the cell body than would targeting of BDNF to only the soma with mRNA containing the short 3' UTR. Surprisingly, our results suggest the opposite: targeting of BDNF mRNA with the short 3' UTR increases dendrite branching over a wider range of distances from the cell body (compare Figure 4-4B and Figure 4-4C). Moreover, we hypothesized that targeting of BDNF mRNA to the dendrites with the long 3' UTR would result in greater increases to dendrites distally than those promoted by expression of BDNF mRNA containing the short 3' UTR; however, we found the opposite to be true. Increases in branching caused by overexpression of BDNF transcript containing the long 3' UTR occur close to the soma (Figure 4-4C), and the

increase observed conventional Sholl curves is most likely due to significant increases observed in primary dendrite numbers (Figure 4-9A). Furthermore, since primary dendrites increase, the significant decrease in the length of tertiary and higher order dendrites promoted by overexpression of BDNF transcript containing the long 3' UTR may be due to a limiting reagent needed for dendrite extension, such as tubulin (Figure 4-10C). Interestingly, overexpression of BDNF mRNA containing only the coding sequence, without any of the targeting UTRs, results in increases in dendrite branching over the widest range of distances from the soma, as observed in conventional Sholl curves (Figure 4-4A). Moreover, overexpression of transcripts containing the BDNF coding sequence alone results in the greatest change to dendrite numbers, significantly increasing both secondary and tertiary and higher order dendrites (Figure 4-9B,C). A schematic summary of the results is shown in Figure 4-11.

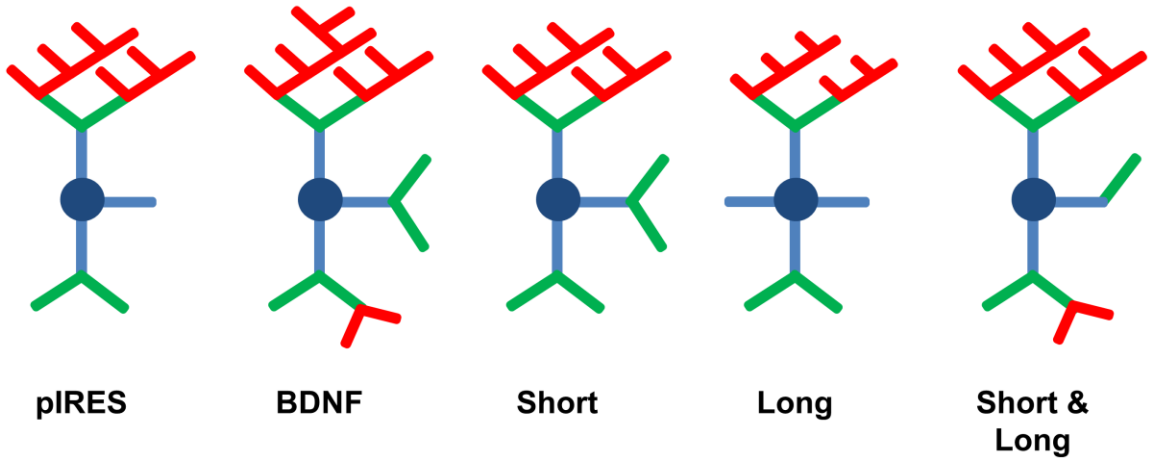

Figure 4-11: Schematic depicting changes caused by overexpression of BDNF with and without 3' UTRs.
Primary dendrites are shown in blue, secondary dendrites in green, and tertiary and higher order dendrites in red. Overexpression of BDNF mRNA without targeting UTRs (BDNF) results in neurons showing increased secondary and tertiary and higher order dendrites compared to control neurons (pIRES). Overexpression of BDNF mRNA with the short 3' UTR (Short) results in increased secondary dendrites. Overexpression of

BDNF mRNA with the long 3' UTR (Long) results in increased primary dendrites and significantly shorter tertiary and higher order dendrites. Overexpression of BDNF mRNA with both the short and long 3' UTR (Short & Long) results in increased dendrites, but these increases are not order-specific.

How do the effects observed in this study compare to our laboratory's previously published work? We have shown that BDNF significantly increases primary and secondary dendrites proximal to the soma when BDNF is bath administered for 72 hours to cultures of hippocampal neurons (Kwon, Fernandez et al. 2011). In the current work, we found that overexpression of BDNF mRNA containing only the coding sequence in hippocampal neurons increases primary and secondary dendrites, similar to results of bath application. Neurons overexpressing BDNF mRNA containing the long 3' UTR show increased primary dendrites (Figure 4-9A); neurons overexpressing BDNF mRNA either without a targeting UTR or containing the short 3' UTR show increased secondary dendrites (Figure 4-9B). Bath application of BDNF does not affect tertiary and higher order dendrites, whereas overexpression of the mRNA containing the BDNF coding sequence alone significantly increases tertiary and higher order dendrites (Figure 4-9C). Moreover, increases in the dendritic arbor resulting from BDNF mRNA overexpression not only overlapped with those resulting from bath application of BDNF but were also present in more distal regions of the arbor.

Targeting of BDNF mRNA influences local translation of the BDNF protein. Dendritically localized BDNF and TrkB mRNAs are not translated unless that portion of the dendrite is stimulated, thus restricting BDNF and TrkB synthesis to synaptically active sites (Bramham and Wells 2007, Baj, Pinhero et al. 2016). Moreover, it has been proposed by that upon stimulation, BDNF is translated and secreted as pro-BDNF, after

which it is cleaved by the tissue plasminogen activator (tPa)/plasmin system in the extracellular space to form mature BDNF (Waterhouse and Xu 2009). The newly processed mature BDNF then activates, in an autocrine manner, the TrkB receptors at that same synapse (Horch, Kruttgen et al. 1999, Waterhouse and Xu 2009, Harward, Hedrick et al. 2016). It is likely that some or all of the observed effects on dendrite branching caused by overexpression of BDNF mRNA are activity dependent, and future studies will include determining which type of activity, excitatory or inhibitory, is responsible for the changes.

The neuron itself may also serve as a determinant of localized production and release of BDNF. The RNA-binding protein HuD binds to a region in the long 3' UTR in BDNF mRNA, regulating expression from this mRNA but not the mRNA containing the short 3 'UTR (Vanevski and Xu 2015). Furthermore, the rodent BDNF gene consists of eight alternative 5' UTRs, resulting in different developmental profiles of expression of these BDNF transcripts (Aid, Kazantseva et al. 2007). Trafficking of the BDNF 5' UTR splice variant resulting from exon 6 is impaired in mice expressing the BDNF human variant Val66Met (Mallei, Baj et al. 2015), having implications for BDNF action on the dendritic arbor. Thus, expression of specific mRNAs for BDNF by the neuron may indeed act in an autocrine manner to regulate dendritogenesis.

How does BDNF increase dendrite branching when it is overexpressed, and why does targeting of the BDNF mRNA with the short or long 3' UTR result in different changes to the dendritic arbor? It is possible that the differences lie in the fact that the short 3' UTR mediates translation when the neuron is at rest, whereas the long 3' UTR enhances activity-dependent translation (Lau, Irier et al. 2010). It is possible that

increased dendritic branching mediated by the transcript containing the long 3'UTR occurs in active regions near the soma where the long 3' UTR promotes translation and dendritogenesis of primary dendrites (Harward, Hedrick et al. 2016). It is also possible that enhancement of at-rest translation by mRNA containing the short 3' UTR (Lau, Irier et al. 2010) has wider-ranging effects on the dendritic arbor since promotion of translation is not limited to active dendrites.

Our results suggest that targeting BDNF mRNA to specific sites in neurons results in distinct changes to the dendritic arbor. The observed results *in vitro* point to the physiological significance of alternative splicing of mRNAs *in vivo*. Future studies are ongoing to understand the role of TrkB in the observed changes to dendrite branching by specifically targeted BDNF mRNAs. It is of interest to examine the number and morphology of spines and to determine the synaptic pathways (excitatory or inhibitory) that are responsible for the observed changes in the dendritic arbor.

4.5 Acknowledgements

I would like to acknowledge Katherine Donohue for help provided with imaging and analysis of the data presented in this chapter.

CHAPTER 5: THE ROLE OF BRAIN-DERIVED NEUROTROPHIC FACTOR IN REGULATING NEURONAL NETWORK DEVELOPMENT AND DYNAMICS

5.1 Introduction

BDNF plays important roles in the maturation of neurons (Huang, Kirkwood et al. 1999, Ward and Hagg 2000, Waterhouse, An et al. 2012) by regulating dendritic outgrowth (McAllister, Lo et al. 1995, Jin, Hu et al. 2003) and synapse development (He, Gong et al. 2005, Lang, Stein et al. 2007, Gottmann, Mittmann et al. 2009, Waterhouse and Xu 2009, Yoshii and Constantine-Paton 2010). Changes to the morphology of dendrites or structure of synapses can affect the activity of a neuron and, therefore, its contribution to the larger network into which it is integrated. For example, BDNF affects dendrite and synapse number, is known to have consequences at the network level *in vivo* (Egan, Kojima et al. 2003), and is implicated in neurodegenerative diseases (Liu, Walther et al. 2005).

BDNF is an important player in mediating neuronal activity and synaptic plasticity. In CA1 hippocampal neurons, the BDNF high affinity receptor, TrkB, is present at postsynaptic spines of dendrites in organotypic slice cultures from postnatal rats, indicating the role of BDNF in synaptic modulation. External application of BDNF increases the total number of synapses and the number of docked vesicles in presynaptic terminals of excitatory synapses onto CA1 pyramidal neurons of the hippocampus (Tyler and Pozzo-Miller 2001). BDNF also modulates synaptic activity differently depending on the timing of its application. A rapid increase in extracellular BDNF transiently activates

TrkB and strongly enhances basal synaptic transmission. A slow increase in extracellular BDNF, on the other hand, results in sustained TrkB activation and an increased magnitude of long-term potentiation (LTP) (Ji, Lu et al. 2010). BDNF regulates the expression of vesicular glutamate receptors 1 and 2 (VGLUT1 and VGLUT2), perhaps contributing to the increase seen in LTP under certain conditions (Melo, Mele et al. 2013). Moreover, local translation and posttranslational modifications of many synaptic proteins are induced by exogenous application of BDNF (Waterhouse and Xu 2009). For example, bath application of BDNF rapidly phosphorylates NMDA receptor subunit 1 (NR1) (Suen, Wu et al. 1997) and NMDA receptor subunit 2B (NR2B) in postsynaptic densities (Lin, Wu et al. 1999).

The effects of BDNF on the activity of single neurons *in vitro* has been widely investigated (Pang, Teng et al. 2004, He, Gong et al. 2005, Gottmann, Mittmann et al. 2009, Melo, Mele et al. 2013, Montalbano, Baj et al. 2013), but it is not yet understood how BDNF affects the development and activity of neuronal networks *in vitro*. The advent of microelectrode array (MEA) technology over the past three decades has permitted monitoring of the development of *in vitro* neuronal network activity (Gross, Rieske et al. 1977, Pine 1980). MEA recordings are noninvasive, thus allowing for multiple recordings of the same neuronal culture, and have been used to extensively characterize the development of dissociated hippocampal and cortical neuronal network activity (Segev and Ben-Jacob 2001, Opitz, De Lima et al. 2002, Wagenaar, Pine et al. 2006, Raichman and Ben-Jacob 2008). Our previous results examining the role of BDNF in modulating the dendritic arbor during the active branching period (Kwon, Fernandez et al. 2011) suggest an additional role for BDNF in regulating the development of neuronal

networks. In this chapter, we ask how BDNF regulates neuronal network development by applying BDNF for 72 hr to dissociated hippocampal neurons cultured on MEAs. We performed recordings of spontaneous activity and quantified the short- and long-term effects of BDNF application on neuronal network dynamics. We examined parameters describing the overall activity and the synchronization of these networks.

5.2 Materials and Methods

5.2.1 Preparation of microelectrode arrays (MEAs) and cell culture

Standard 60-electrode MEAs (59 electrodes plus 1 reference electrode) were used for all experiments. Electrodes had diameters of 10 μm and an inter-electrode spacing of 200 μm (60MEA200/10iR-Ti-gr; Multi Channel Systems, Germany), as shown in Figure 5-1A,B. MEAs were prepared for cell culture as previously described (Kutzing, Luo et al. 2011, Kutzing, Luo et al. 2012). MEAs were washed for at least 48 hours in 1% Tergazyme solution (in dH_2O) prior to the day of dissection. On the day of dissection, MEAs were autoclaved, rinsed once with sterile water, and left to dry in a sterile cell culture hood. MEAs were then coated with 0.5 mg/mL poly-D-lysine (PDL; Sigma) and allowed to incubate at 37 ºC for at least 1 hr. MEAs were then washed three times with sterile water and allowed to dry in a sterile cell culture hood. Immediately prior to plating of cells, MEAs were coated with 10 μg/ml laminin for 30 min at 37 ºC.

Neuronal cultures were prepared from the hippocampi of rat embryos at 18 days of gestation (E18) as described previously (Firestein, Brenman et al. 1999). The hippocampi were dissociated using manual trituration, and cells were plated onto PDL and laminin-coated MEAs at a density of $1x10^6$ cells per MEA. Cultures were kept in a

humidified 37 ºC incubator with 5% CO_2 and maintained in NbActiv4 medium (Brain Bits), which contains Neurobasal medium, B27, glutamine, creatine, estrogen, and cholesterol (Brewer, Boehler et al. 2008). Additionally, 1% penicillin-streptomycin (Life Technologies) was added to culture mediums to prevent contamination. Half of the culture medium was changed every other day. All studies were performed in accordance with the Institutional Animal Care and Use Committee (IACUC) standards.

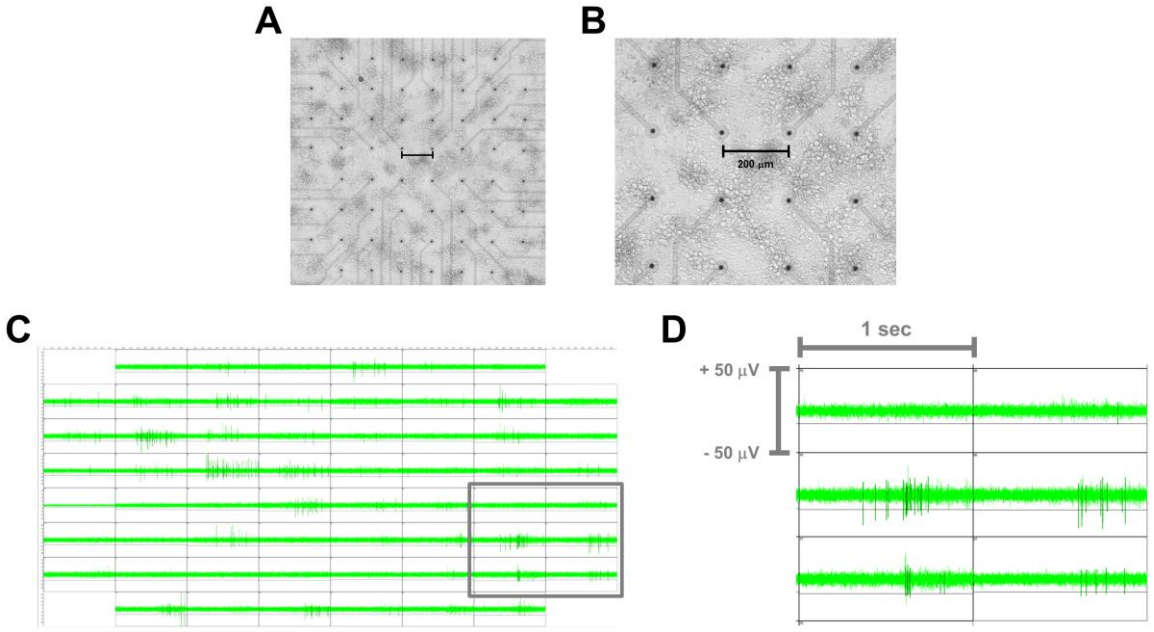

Figure 5-1: Dense cultures of hippocampal neurons on MEAs exhibit spontaneous spiking and bursting activity.
A. Recording area of hippocampal neurons cultured for 14 DIV on an MEA with clear electrodes. **B.** Zoomed in area from A, showing hippocampal neurons near electrodes. Scale bar = 200 µm. **C.** Screen shot from MCRack showing network-wide bursting during recording. **D.** Zoomed in area from C. Each box represents the activity on an electrode over the course of 1 sec. The *y*-axis represents the filtered signal with a range of -50 µV to +50 µV. For visualization purposes, the threshold for activity is set at the beginning of the recording to be 5 times the standard deviation of the noise. Spikes are in dark green, and background noise is in bright green.

5.2.2 Microelectrode array recordings

The spontaneous activity of hippocampal networks on MEAs was recorded at DIV 7, 10, and 17 using the data acquisition software MCRack (Multi Channel Systems, Germany; Figure 5-1C and D). Recordings were performed at 37 ˚C on a heat-controlled stage at room atmosphere as previously described (Kutzing, Luo et al. 2011, Kutzing, Luo et al. 2012). Data were acquired at a sampling rate of 20 kHz using an MEA1060-Inv-BC amplifier (Multi Channel Systems, Germany). A recording solution containing the following components was used to regularize bursting behavior: NaCl (144mM), KCl (10mM), $MgCl_2$ (1mM), $CaCl_2$ (2mM), HEPES (10mM), Na-pyruvate (2mM), and glucose (10mM) at physiological pH (pH 7.4). During recording, MEAs were covered with semi-permeable lids (ALA MEA-MEM, Multi Channel Systems) that selectively allow gases to diffuse through but that prevent airborne pathogens from contaminating the cultures. Prior to recording, cultures were allowed to equilibrate in recording solution for 5-10 min. Spontaneous activity was then recorded for 5 min. Afterwards, cultures were washed once with growth medium, and then treatment was applied or conditioned medium was returned, as described below.

5.2.3 Experimental setup: BDNF treatment and recording schedule

Cultures of hippocampal neurons were maintained for 7 DIV prior to treatments and recordings. The schedule used for all experiments in this chapter is shown in Figure 5-2A. Shorthand abbreviations used in plots are shown in Figure 5-2B.

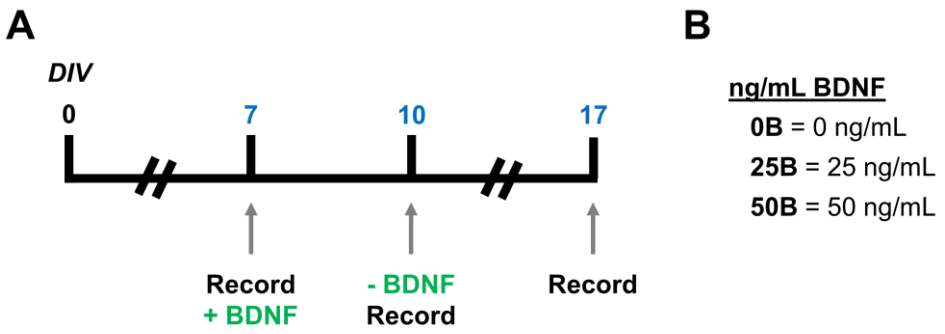

Figure 5-2: Recording and treatment schedule for BDNF dose response experiments.
A. Recording and treatment schedule for all data generated in this chapter. Cultures were maintained for 7 DIV prior to beginning experiments. **B.** Shorthand abbreviations used in data plots. 0B indicates control networks that received no treatment (0 ng/ml BDNF). 25B indicates networks treated with 25 ng/ml BDNF. 50B indicates networks treated with 50 ng/ml BDNF.

Baseline recordings were performed at DIV 7 using MCRack software. Immediately after recording, an activity check was performed. Cultures having less than 2000 spikes (a spike rate of less than 6.7 Hz) were not used for further experimentation. Remaining cultures that did pass the activity threshold were randomly assigned to one of three treatment groups: control (0 ng/ml BDNF), 25 ng/ml BDNF, or 50 ng/ml BDNF. BDNF or vehicle (sterile water) was added to conditioned media, which was then applied to cultures for 72 hr. We used the additional treatment concentration of 50 ng/ml because MEA cultures are plated 3.5 times more densely than cultures used for dendrite branching experiments. At DIV 10, after 72 hr of BDNF or vehicle treatment, an additional recording was performed, and treatment medium was replaced with regular culture medium. Importantly, this treatment window corresponds to that of our previous work, in which BDNF was applied at 25 ng/ml to cultures of hippocampal neurons for 72 hr, resulting in increases in proximal branching (Kwon, Fernandez et al. 2011). This is also the same treatment window used in Chapter 3 (via microbead application) and

Chapter 4 (via targeting of BDNF transcripts). A final recording was performed at DIV 17 (one week post-treatment) to determine whether BDNF exerts any long-term effects on network dynamics.

5.2.4 Signal processing

All methods of MATLAB data analysis used in this chapter and in Chapter 6 are based on previous work (Kutzing, Luo et al. 2011, Kutzing, Luo et al. 2012) but have been redeveloped specifically for the analysis of hippocampal neuron network activity. During recordings, electrodes showing excessive noise were noted and excluded from later analysis. Raw data were imported into MATLAB (MathWorks, Inc.) using MEAtools, an open source toolbox. Signals were filtered in 10 sec chunks (300 sec = 30 chunks total) through a 4^{th} order Butterworth bandpass filter (20-2,000 Hz) and a 60 Hz notch filter to remove electrical noise. Importantly, both filters were infinite impulse response (IIR) filters and were implemented using the built-in MATLAB function *filtfilt()*, which is a zero-phase forward and reverse digital IIR filter. This type of filter does not introduce a time delay, unlike traditional finite impulse response (FIR) filters (corresponding MATLAB function is *filter()*, a standard one-dimensional digital FIR filter).

5.2.5 Spike detection and related parameters

Spikes are defined as a single event in which the voltage surpasses a positive or negative threshold and are detected using an adaptive thresholding method. Spike thresholds were defined as 4.5 times the standard deviation of the background noise (Wagenaar, DeMarse et al. 2005) and were calculated for each 10 sec period of filtered signal. Importantly, the threshold is recalculated for each subsequent period and

calculated separately for each electrode. The background noise can change over the course of the recording period, and electrodes tend to have slightly different background noise levels. Spikes are detected at maximum absolute value (positive or negative), and to ensure that the same spike is not counted twice, a condition was introduced that required the interspike interval (ISI) to be at least 2 msec. Spike detection is demonstrated in Figure 5-3, in which the spikes are indicated by pink circles.

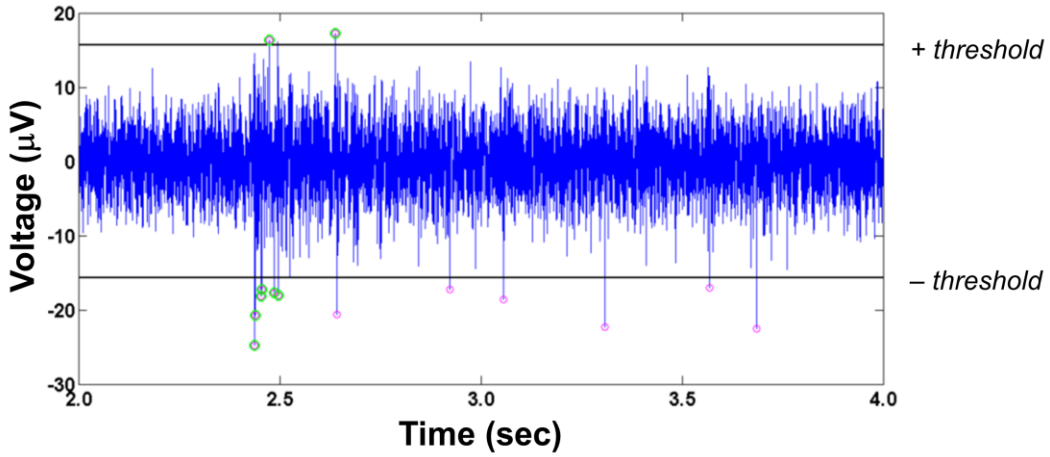

Figure 5-3: Diagram demonstrating spike and burstlet detection.
Two seconds of filtered signal from one electrode is displayed in blue. The adaptive threshold (*4.5*SD(noise)*), both positive and negative values, is displayed as a black line. Spikes are indicated with pink circles, and spikes that are part of a burstlet are indicated by green circles.

Other parameters derived from spike numbers and timing are the following: average spike voltage, overall interspike interval (*Total ISI*), average interspike interval per electrode (*Avg. ISI per E*), coefficient of variation of the Total ISI (*CV(Total ISI)*), and the Fano factor of the spike count. The ISI is the length of time between two spikes (Softky and Koch 1993). The overall ISI is the average of all ISIs, regardless from which electrode they originate. For the average ISI per electrode, the ISIs are separated

based on the electrode from which they originate. Subsequently, the average ISI for each electrode is calculated, and those values are averaged. Furthermore, the ratio of the Spike rate to the Fano Factor (*S.R./F.F.*) was calculated to determine how the degree of spiking activity is related to the timing of spikes.

The Coefficient of Variation (CV) is a metric for determining the dispersion of data. We calculated the Coefficient of Variation of all ISIs (*CV(Total ISI)*) to determine the variability of our ISIs, which is standard in the field (Vogel, Hennig et al. 2005). The CV is the relationship of the standard deviation to the mean (Softky and Koch 1993):

$$CV(Total\ ISI) = \sigma/\mu$$

For networks that exhibit regular firing, and therefore similar ISI values, the CV is close to 0. A higher CV value corresponds to higher ISI variability. Networks that exhibit irregular firing, such as those described in this work, have CVs greater than 1 (Softky and Koch 1993).

The Fano factor measures the variability of the spike count within a specific window of time *w*, which was determined to be 1 sec for our networks. For 300 sec recordings, we calculated the number of spikes that occurred in 1 sec bins (from seconds 0-1, seconds 1-2, *etc.*), giving us 300 spike count values. The Fano factor is calculated as the ratio of the variance to the mean of these spike counts (Eden and Kramer 2010):

$$FF = \sigma_w^2(spike\ count)/\mu_w(spike\ count)$$

Similar to CV, the Fano factor tends to 0 for networks with regularly-spaced spikes (Churchland, Yu et al. 2010, Litwin-Kumar and Doiron 2012). When the spike rate is random and follows a Poisson distribution, the Fano factor is theoretically equal to 1 (Eden and Kramer 2010, Gambazzi, Gokce et al. 2010). Higher Fano factor

values are indicative of irregular firing, which is observed in our hippocampal neuron networks (Churchland, Yu et al. 2010, Litwin-Kumar and Doiron 2012).

5.2.6 Burstlet detection and related parameters

Spikes occurring in rapid succession on an electrode are referred to as an individual burst, or burstlet. After all spikes were detected, it was determined whether spikes were part of a burstlet. Burstlets are composed of a core group of very closely spaced spikes with a peripheral group of spikes surrounding the core. To implement these criteria for detection of burstlets, our detection algorithm searched for groups of at least 4 spikes that had ISIs of 100 msec or 4 times the firing rate of that electrode, whichever was smaller. Upon finding the core groups the spikes, the algorithm searched for peripheral spikes that had ISIs of 200 msec or 3 times the firing rate of that electrode, whichever was smaller (Wagenaar, DeMarse et al. 2005). After all burstlets in each 10 sec period were detected, the algorithm checked whether, on any electrode_i, a burstlet at the end of period_j overlapped with a burstlet at the beginning of period_{j+1}. If so, these burstlets were combined into one. Burstlet detection is demonstrated in Figure 5-3, in which spikes that are part of a burstlet are indicated by green circles.

Additional parameters derived from burstlet numbers and timing are the following: average burstlet width, number of spikes per burst, and average interburst interval (IBI) per electrode (*Avg. IBI per E*). The IBI is calculated by determining the length of time between successive burstlets on each electrode. If an electrode has no burstlets, that value is not included in the average IBI. Additionally, the average ratio of burstlet rate to spike rate (*B.R./S.R.*) was calculated to understand the relationship between bursting and spiking.

Since all other parameters are derived from the number or timing of spikes and burstlets, we employ an adaptive threshold to eliminate user bias from our data analysis. The number of detected spikes and burstlets are improved by adaptive thresholding over manual thresholding (Figure 5-4).

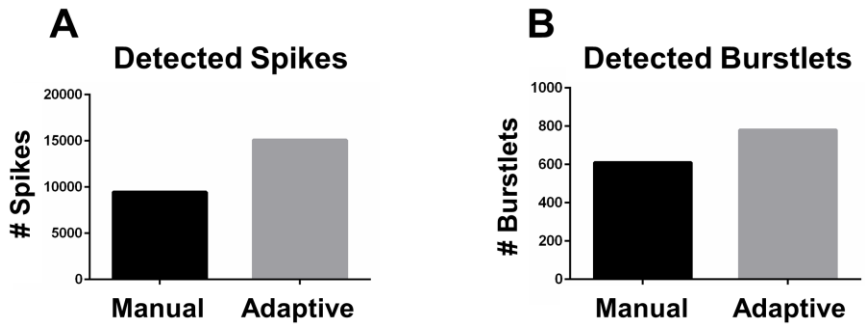

Figure 5-4: Adaptive thresholding improves the number of spikes and burstlets detected during recording compared with manual thresholding.
These data compare the results of employing a manual threshold, in which the same threshold is applied to all electrodes, versus using an adaptive threshold, which updates every 10 seconds and is different for each electrode. **A.** Number of spikes detected during a 5 min recording when using a manual or adaptive threshold. Using an adaptive threshold improves spike detection by 50%. **B.** Number of burstlets detected during a 5 min recording when using a manual or adaptive threshold. Because adaptive thresholding increases the number of spikes detected, it necessarily increases the number of burstlets detected. Burstlet detection is increased by 33%.

5.2.7 Global burst detection and related parameters

Dissociated neurons cultured on MEAs not only exhibit random spiking and bursting activity on individual electrodes, but often they will also display network-wide bursts, known as synchronized bursting events (Segev and Ben-Jacob 2001), which occur when multiple electrodes record burstlets at the same time (Figure 5-1C,D). Physiologically, synchronized bursting events represent the synchronous activity that is necessary for many brain functions (Chiappalone, Vato et al. 2007, Fuchs, Ayali et al. 2007) and, thus, are an important measure of culture activity. Here, we refer to these

network-wide bursts as global bursts, and they are detected as at least three overlapping burstlets on different electrodes (Wagenaar, DeMarse et al. 2005).

Additional parameters calculated from the number and timing of global bursts are the following: average width of global bursts, global IBI, and number of burstlets per global burst. The global IBI is calculated by determining the length of time between successive global bursts. Additionally, the ratio of the average global burst width to the average burstlet width (*Avg GB Width/B Width*) was calculated to understand the relationship between burstlet width and global burst width.

5.2.8 Synchronization calculation

Synchronization between electrodes is based on the overlapping of individual burstlets on different electrodes and is referred to as Synchrony of Firing (*SF*). This type of synchronization measure indicates how correlated the bursting of one electrode is with other electrodes. SF is calculated by taking the ratio of the number of times electrodes *x* and *y* burst together ($B_{x\&y}$) versus the maximum number of times either electrode bursts on its own ($B_{x|y}$) (Kutzing, Luo et al. 2011):

$$SF = B_{x\&y}/B_{x|y}$$

To assess changes in synchronization, we average all SF values across each MEA to give an average synchronization value. Additionally, we examined the changes that occur to electrodes possessing specific baseline levels of synchronization. We categorized electrodes into the following initial synchronization bins: 0-0.2, 0.2-0.4, 0.4-0.6, 0.6-0.8, and 0.8-1.0. These bins differ from the categories used in our previous work with cortical neurons (Kutzing, Luo et al. 2011, Kutzing, Luo et al. 2012) because of the inherently different nature of hippocampal versus cortical network activity.

5.2.9 Data representation and statistics

Unless otherwise noted, all data are represented as fold change, normalized to the baseline value of that parameter for that MEA (Kutzing, Luo et al. 2011, Kutzing, Luo et al. 2012).

Occasionally, networks will exhibit activity that results in no burstlets or no global bursts, which poses a potential issue for calculating the parameters that depend on burstlets or global bursts. To remain consistent in our data analysis, we adhered to the following rules: 1) quantities that are counted can be represented as 0 and included in the average, and 2) quantities that are measured should not be included in the average. For example, if a culture has 0 burstlets, the average number of spikes per burst would be 0 and would be included in the average because it can be counted. However, the average burstlet width would not be included since it cannot be measured.

All data are plotted using Graphpad Prism and are shown as mean ± standard error of the mean (SEM) with *n* indicating the number of MEAs in that particular condition, unless otherwise noted. One-way ANOVAs and *t*-tests were calculated using Instat (Graphpad), and two-way ANOVAs were calculated using Graphpad Prism. Outliers were eliminated in Graphpad Prism using the ROUT method with Q=1% for synchronization and Q=0.5% for all other parameters.

5.3 Results

To investigate the effects of BDNF treatment on the network dynamics of developing hippocampal neurons, we recorded the spontaneous activity of networks at DIV 7 and then treated with 0 (vehicle), 25, or 50 ng/ml BDNF for 72 hr. At DIV 10,

BDNF- or vehicle-containing medium was removed and replaced with regular medium, and an additional recording was performed to assess the short-term consequences of BDNF treatment. A final recording was performed at DIV 17 to assess the long-term consequences of BDNF treatment. Our laboratory and others have reported that DIV 7-12 is a period of active dendrite branching whereas DIV 12-17 is dominated by pruning of dendrites (Wu, Zou et al. 1999, Cline 2001, Charych, Akum et al. 2006). Our recording timepoints correspond to these periods and will illuminate how BDNF treatment affects neuronal network development during periods of changes to dendritic morphology. Seven experiments were completed for all data shown, but the data from one DIV 17 recording session are not included since the control conditions were not sufficiently active, indicating impending contamination or unhealthy cultures.

5.3.1 BDNF treatment affects spike rate and variability

Analyses of spike rate and timing are commonly employed methods for describing the overall activity of a network (Brewer, Boehler et al. 2009, Biffi, Ragalia et al. 2013). First, we examined how the spike rate, magnitude, and variability changes during network development and as a result of BDNF treatment. Networks treated with 25 ng/ml BDNF exhibit significantly decreased spike rate at DIV 17 compared with the same treatment condition at DIV 10 and with untreated networks at DIV 10 (Figure 5-5A). The average magnitude of spiking, however, does not change over time or with BDNF treatment (Figure 5-5B). The Fano factor, which describes the variability of the spike rate, significantly increases at DIV 17 for networks treated with 50 ng/ml BDNF compared to the same treatment DIV 10 (Figure 5-5C). Moreover, the ratio of the spike rate to the Fano factor (S.R./F.F.) significantly decreases at DIV 17 for

networks treated with either 25 or 50 ng/ml BDNF compared to the same treatment conditions, respectively, at DIV 10 (Figure 5-5D). The significant decreases over time in the S.R./F.F. ratio reflects the changes seen in spike rate (Figure 5-5A) and the Fano factor (Figure 5-5C) for networks treated with 25 and 50 ng/ml BDNF, respectively.

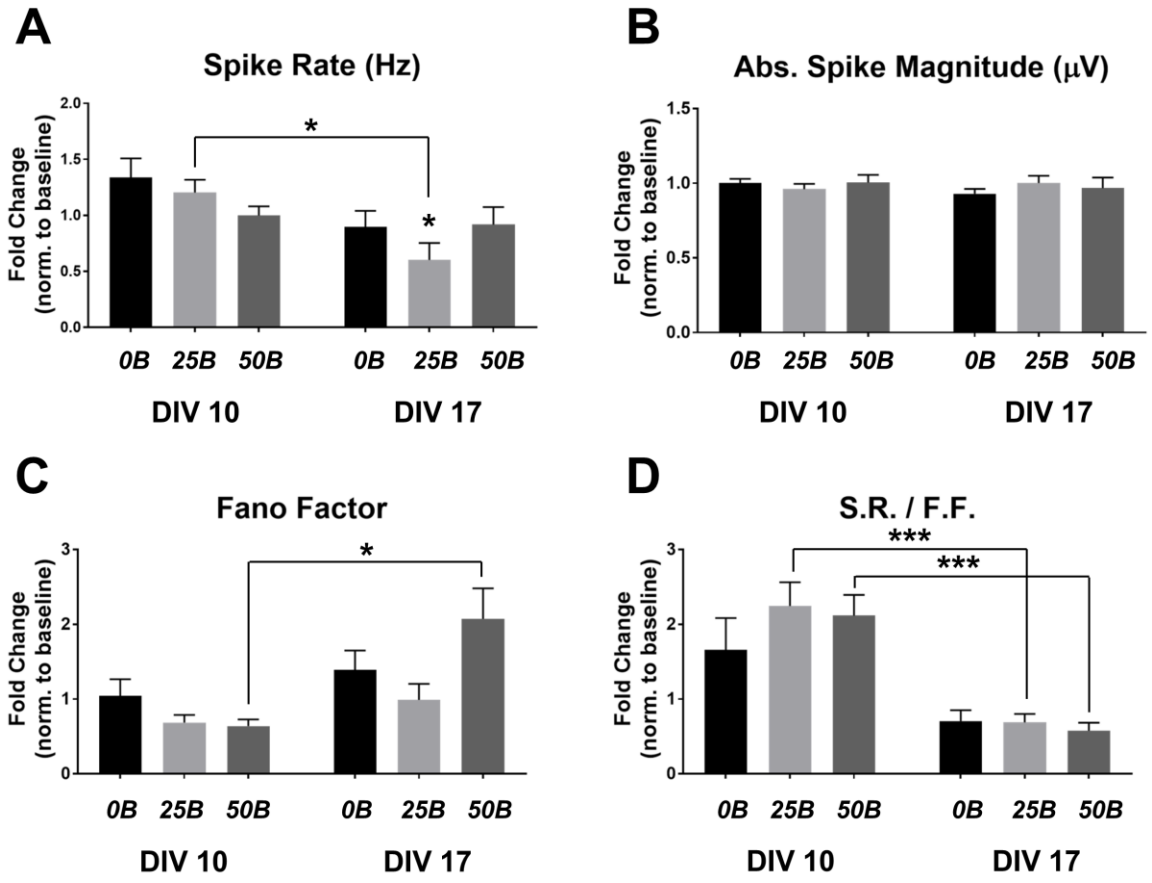

Figure 5-5: Spike rate and variability are affected by BDNF treatment.
Asterisks indicate significance with respect to the control (0B DIV10), and lines indicate significance between connected bars. **A.** Spike rate significantly decreases when comparing 25B on DIV17 to the control and to 25B on DIV10. **B.** The magnitude of spiking does not change over time or with BDNF treatment. **C.** The Fano factor significantly increase when comparing DIV17 to DIV10 for 50B. **D.** The ratio of Spike Rate to the Fano Factor (S.R./F.F.) significantly decreases for 25B when comparing DIV10 and DIV17 and for 50B when comparing DIV10 and DIV17. *$p<0.05$ and ***$p<0.001$ calculated by Kruskal-Wallis test followed by Dunn's multiple comparisons test. Comparisons are between all conditions and the control (0B DIV10), between the treatment conditions within each timepoint, and between timepoints with matching

treatments. Outliers eliminated using ROUT method with Q=0.5%. n = 12-17 for all conditions. Error bars indicate SEM.

In addition to examining changes in spike rate and variability, we examined how BDNF treatment affects the average interspike interval (ISI) length and variability. Although the higher average magnitude of the Total ISI at DIV 17 reflects decreases in spike rate at DIV 17 seen in Figure 5-5A, no significant differences are observed in Total ISI between any of the conditions (Figure 5-6A). Moreover, although there were significant differences in spike rate variability at DIV 17 for networks treated with 50 ng/ml BDNF compared to the same treatment at DIV 10, as represented by the Fano Factor (Figure 5-5C), no significant differences occur in variability of the Total ISI, as represented by CV (Figure 5-6B). Additionally, no significant differences are observed when comparing the average ISI per electrode (Figure 5-6C).

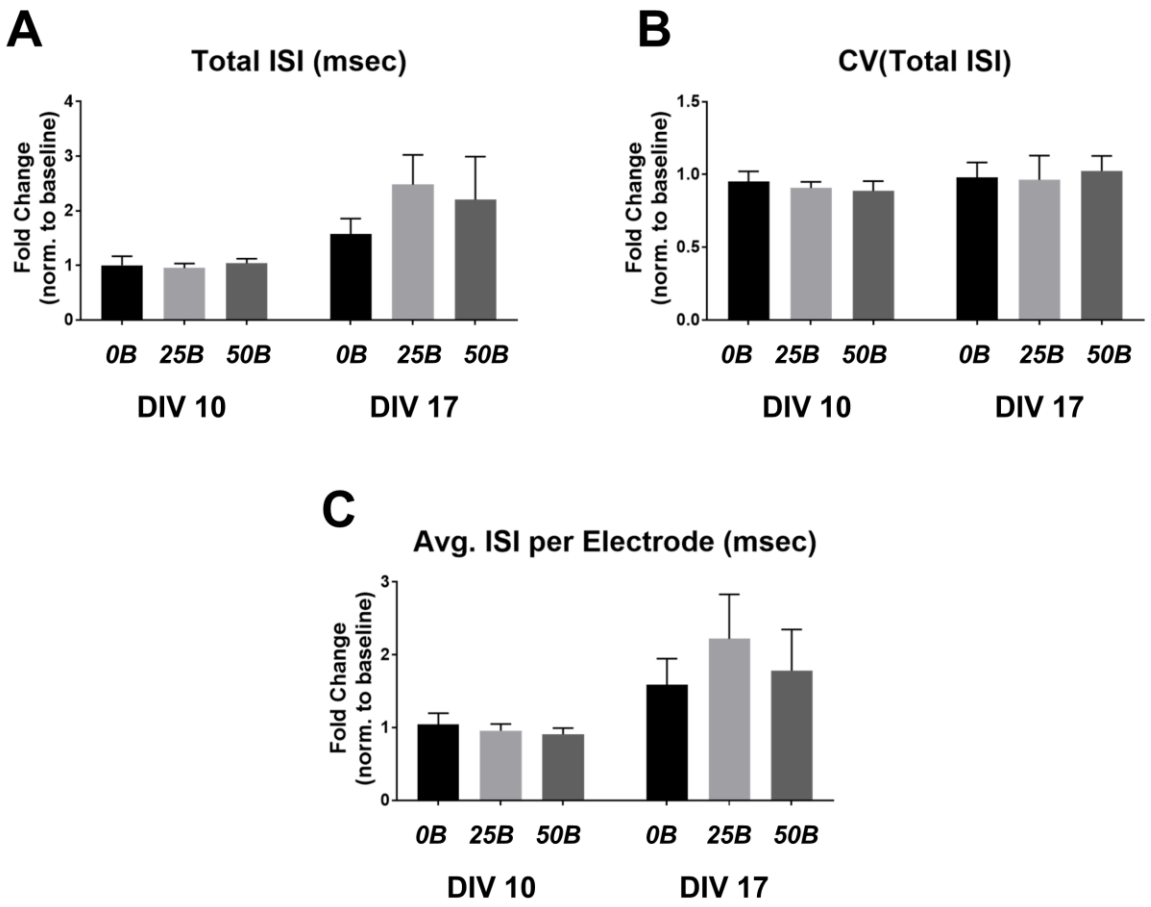

Figure 5-6: BDNF treatment does not affect the ISI length or variability.
A. The Total ISI does not significantly change over time or with BDNF treatment. **B.** The CV of the Total ISI does not significantly change over time or with BDNF treatment. **C.** The average ISI per electrode does not significantly change over time or with BDNF treatment. Statistics calculated by Kruskal-Wallis test followed by Dunn's multiple comparisons test. Comparisons are between all conditions and the control (0B DIV10), between the treatment conditions within each timepoint, and between timepoints with matching treatments. No outliers were eliminated. n = 12-17 for all conditions. Error bars indicate SEM.

Including analysis of both spike rate and spike variability reveals differing roles for BDNF, depending on its concentration, in the modulation of spiking activity in developing neuronal networks.

5.3.2 BDNF treatment modulates certain aspects of bursting activity

In addition to examining how spiking activity is modulated by BDNF treatment, we investigated how bursting activity is affected by BDNF treatment. As described in the Methods section of this chapter, burstlets are groups of closely-spaced spikes (Wagenaar, DeMarse et al. 2005), and analysis of burst rate is another commonly employed method for assessing changes in network activity (Wagenaar, Pine et al. 2006, Kapucu, Tanskanen et al. 2012). First, we examined how burstlet rate and composition are altered by BDNF treatment. Burstlet rate and average burstlet width do not significantly change over time or as a result of BDNF treatment (Figure 5-7A and B, respectively). Despite no observed change in average burstlet width, the number of spikes per burstlet significantly increases at DIV 17 for networks treated with 50 ng/ml BDNF compared to the same treatment at DIV 10 (Figure 5-7C). The average ratio of the burstlet rate to spike rate (B.R./S.R.) does not significantly change over time or with BDNF treatment (Figure 5-7D).

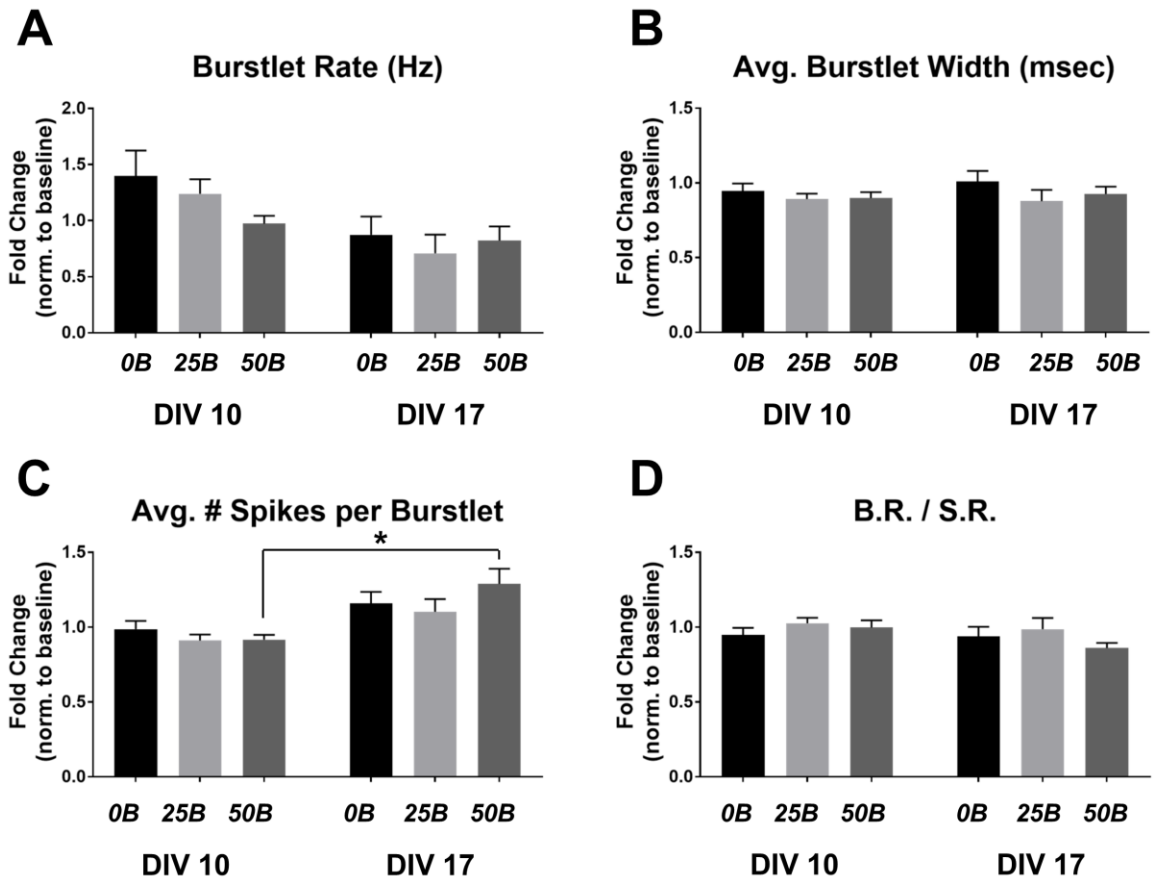

Figure 5-7: BDNF treatment alters the number of spikes per burstlet without altering burstlet rate or the average burstlet width.
Asterisks indicate significance with respect to the control (0B DIV10), and lines indicate significance between connected bars. **A.** The burstlet rate does not significantly change with BDNF treatment or over time. **B.** The average burstlet width does not significantly change with BDNF treatment or over time. **C.** The number of spikes per burstlet significantly increases for 50B when comparing DIV10 to DIV17. **D.** The average ratio of the burst rate (B.R.) to the spike rate (S.R.) does not significantly change with BDNF treatment or over time. *$p<0.05$; For A and C, statistics calculated using the Kruskal-Wallis test followed by Dunn's multiple comparisons test. Comparisons are between all conditions and the control (0B DIV10), between the treatment conditions within each timepoint, and between timepoints with matching treatments. For B and D, statistics calculated using Tukey's multiple comparisons test (comparisons between all conditions). Outliers eliminated using ROUT method with Q=0.5%. n = 12-17 for all conditions. Error bars indicate SEM.

Next, we examined how global bursting rate, composition, and timing changes over time and with BDNF treatment. As described in the Methods section of this chapter,

global bursts are composed of at least three overlapping burstlets on different electrodes (Wagenaar, DeMarse et al. 2005) and are indicative of network-wide synchronized activity. The number of global bursts significantly decreases at DIV 17 for networks treated with 25 and 50 ng/ml BDNF when compared with untreated networks at DIV 10, and global bursts significantly decrease at DIV 17 for networks treated with 25 ng/ml BDNF when compared with the same treatment at DIV 10. The average width of global bursts and the average number of burstlets per global burst do not change over time or with BDNF treatment (Figure 5-8B and C, respectively). The ratio of average global burst width to average burstlet width significantly decreases for untreated networks at DIV 17 compared to DIV 10, but BDNF treatment with either concentration does not result in any significant changes to this ratio (Figure 5-8D).

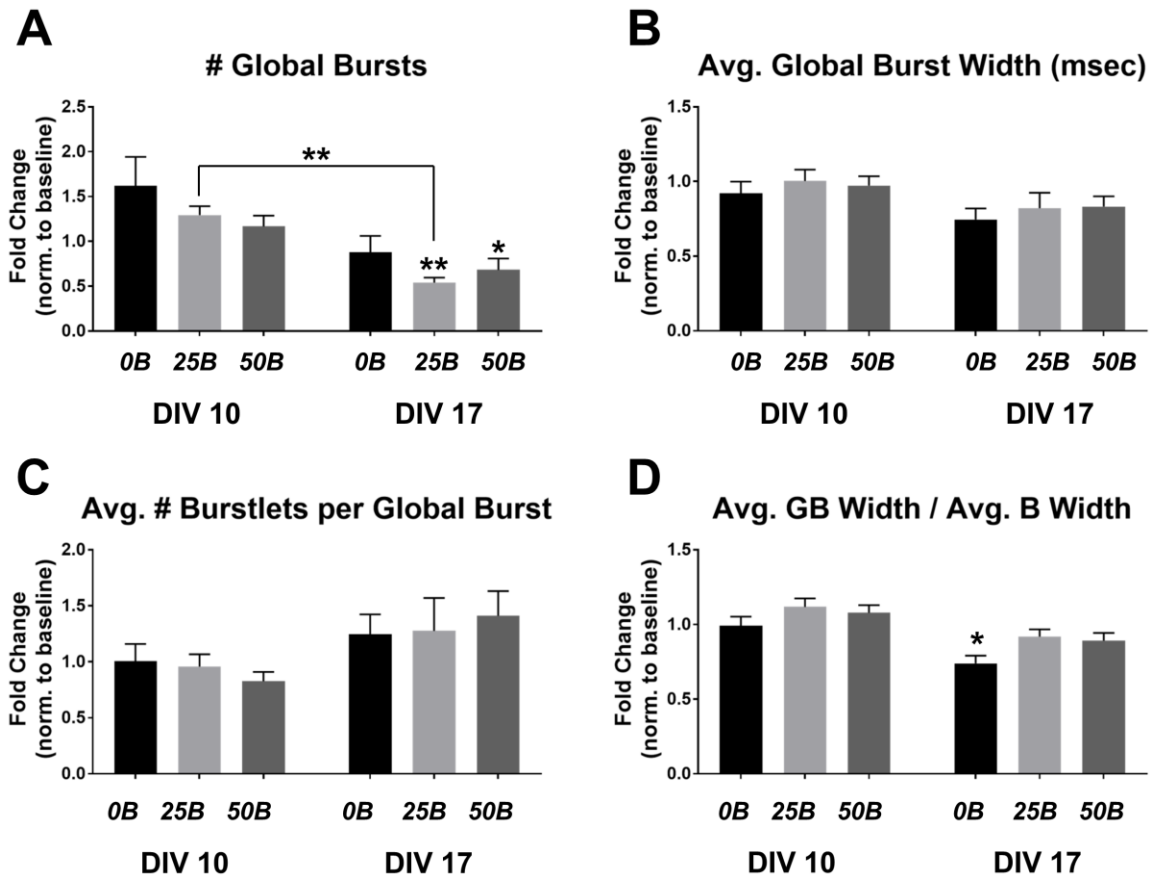

Figure 5-8: BDNF treatment alters global burst number without altering other parameters.

Asterisks indicate significance with respect to the control (0B DIV10), and lines indicate significance between connected bars. **A.** The number of global bursts significantly decreases at DIV17 for both 25B and 50B when compared with the control. The number of global bursts also significantly decreases for 25B when comparing DIV10 and DIV17. **B.** The average width of global bursts does not significantly change over time or with BDNF treatment. **C.** The average number of burstlets per global burst does not significantly change over time or with BDNF treatment. **D.** The ratio of average global burst width to average burstlet width significantly decreases at DIV 17 for untreated networks compared with DIV 10. *$p<0.05$ and **$p<0.01$; For A, B, and C, statistics calculated using the Kruskal-Wallis test followed by Dunn's multiple comparisons test. Comparisons are between all conditions and the control (0B DIV10), between the treatment conditions within each timepoint, and between timepoints with matching treatments. For D, statistics calculated using one-way ANOVA followed by Tukey's multiple comparisons test (comparing all conditions to each other). Outliers eliminated using ROUT method with Q=0.5%. n = 12-17 for all conditions. Error bars indicate SEM.

Finally, we examined how the interburst interval (IBI) changes for global bursts and individual burstlets. The global IBI significantly increases at DIV 17 for networks treated with 25 ng/ml when compared to the same treatment condition at DIV 10 (Figure 5-9A). On the other hand, the average IBI per electrode significantly increases at DIV 17 for networks treated with 50 ng/ml when compared to the same treatment condition at DIV 10 (Figure 5-9B).

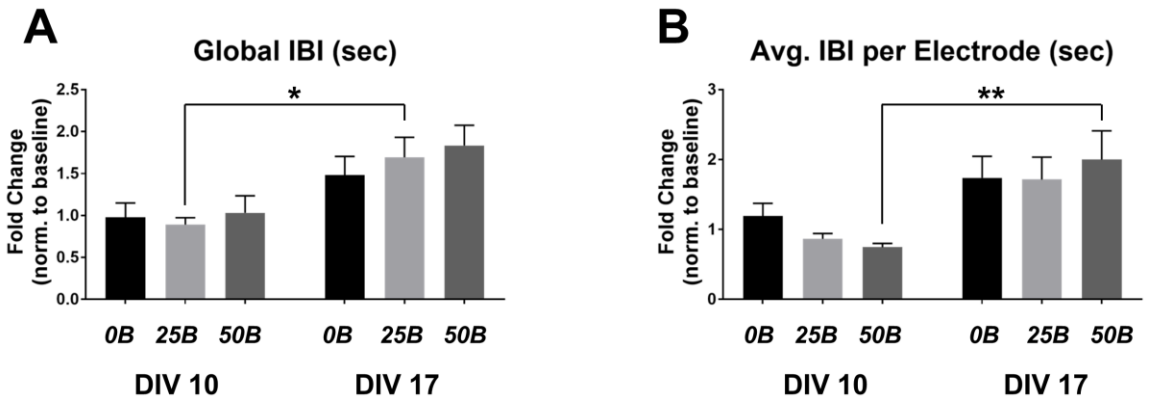

Figure 5-9: BDNF treatment affects the average interburst interval of global bursts and individual burstlets, depending on BDNF concentration.
Asterisks indicate significance with respect to the control (0B DIV10), and lines indicate significance between connected bars. **A.** The average IBI between global bursts significantly increases for 25B when comparing DIV10 and DIV17. **B.** The average IBI between burstlets on individual electrodes significantly increases for 50B when comparing DIV10 and DIV17. *$p<0.05$ and **$p<0.01$ calculated using the Kruskal-Wallis test followed by Dunn's multiple comparisons test. Comparisons are between all conditions and the control (0B DIV10), between the treatment conditions within each timepoint, and between timepoints with matching treatments. No outliers were eliminated. n = 12-17 for all conditions. Error bars indicate SEM.

Taken together, our data suggest that BDNF affects the bursting activity of hippocampal neuron networks differently depending on the concentration at which it is applied. Moreover, a general trend of decreasing synchronized activity over time is present, although significant decreases are not observed for every comparison. The lower

burstlet rate (Figure 5-7A) and global burst rate (Figure 5-8A) observed at the DIV 17 timepoint is consistent with observations from our laboratory (Rodriguez et al., 2017, unpublished data) and others (Tau and Peterson 2010, Litwin-Kumar and Doiron 2012, Biffi, Ragalia et al. 2013) in that activity decreases over time as networks mature.

5.3.3 BDNF modulates the synchronization of hippocampal networks over time

In addition to examining the spiking and bursting activity, we investigated how the synchronization of networks changes over time and as a result of BDNF treatment. As described in the Methods section of this chapter, we calculated the Synchrony of Firing (SF) for each electrode, which is derived from measuring the frequency that burstlets on different electrodes overlap (Kutzing, Luo et al. 2011, Kutzing, Luo et al. 2012). To obtain a measure of average synchronization, all SF values are averaged for each MEA, and this average synchronization value is compared to the baseline. The average synchronization significantly increases at DIV 17 for networks treated with 50 ng/ml BDNF compared to the same treatment condition at DIV 10. This change is not significant when compared with the control at DIV 10 or at DIV 17 (Figure 5-10).

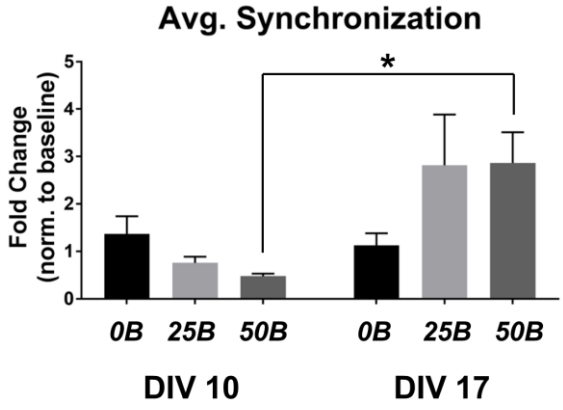

Figure 5-10: Treatment with 50 ng/ml BDNF significantly increases long-term synchronization.

Asterisks indicate significance with respect to the control (0B DIV10), and lines indicate significance between connected bars. Average synchrony of firing is averaged for each electrode to yield the average synchronization per MEA. Average synchronization is significantly increased for 50B when comparing DIV10 and DIV17. There is no significant difference between any of the other conditions. *$p<0.05$ calculated using the Kruskal-Wallis test followed by Dunn's multiple comparisons test. Comparisons are between all conditions and the control (0B DIV10), between the treatment conditions within each timepoint, and between timepoints with matching treatments. Outliers eliminated using ROUT method with Q=1%. n(0B DIV10)=14; n(25B DIV10)=15; n(50B DIV10)=12; n(0B DIV17)=10; n(25B DIV17)=13; n(50B DIV17)=13. Error bars indicate SEM.

To better understand how synchronization changes over time and as a result of BDNF treatment, we separated connections between electrodes based on initial SF into five categories: initial SF value ($SF_{initial}$) of 0-0.2, 0.2-0.4, 0.4-0.6, 0.6-0.8, and 0.8-1.0. The fold change in SF was tracked for each connection in each category except for the weakest category (0-0.2), and an average fold change was calculated for each category on a per MEA basis (Kutzing, Luo et al. 2011, Kutzing, Luo et al. 2012). No significant changes are observed in any of the categories when comparing the treatments at DIV 10 (Figure 5-11B) or at DIV 17 (Figure 5-11C). There is also no significant change to the fold change in SF over time for untreated networks (Figure 5-11D) or for networks treated with 50 ng/ml BDNF (Figure 5-11F). For networks treated with 25 ng/ml BDNF, a significant decrease in synchronization is observed for connections with $SF_{initial}$=0.2-0.4 at DIV 17 compared to DIV 10 (Figure 5-11E).

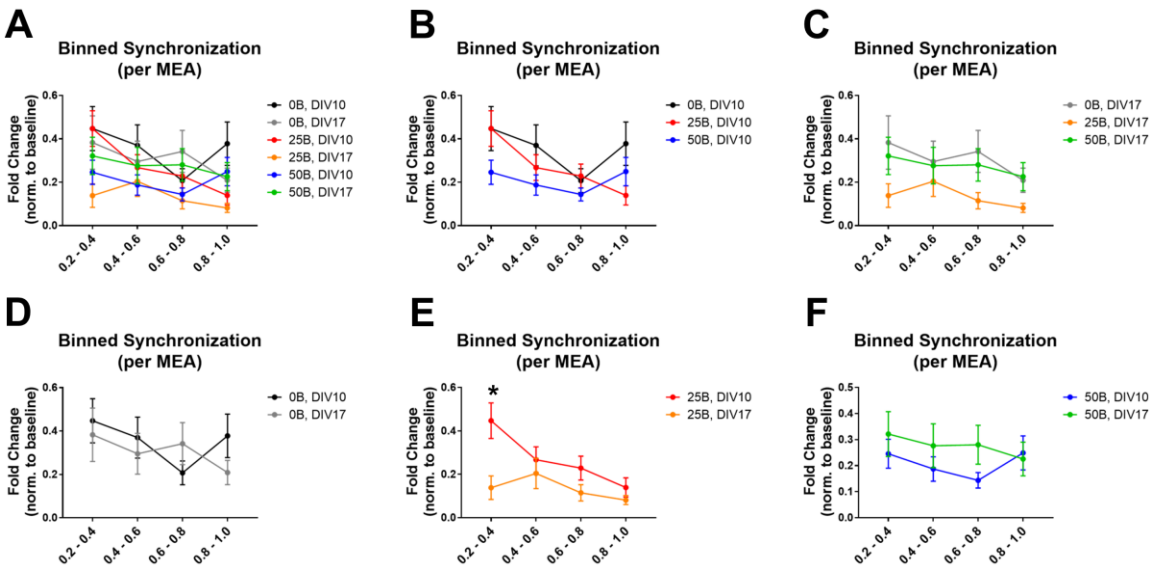

Figure 5-11: BDNF modulates the synchronization of electrodes (averaged per MEA) with different initial synchronizations.
Binned synchronization changes for electrodes with different initial synchronizations averaged per MEA. **A.** Overlaid synchronization changes over time and with different BDNF treatments. **B.** Binned synchronization changes comparing the different BDNF treatments at DIV10. **C.** Binned synchronization changes comparing the different BDNF treatments at DIV17. **D.** Binned synchronization changes comparing the 0B conditions at both timepoints. **E.** Binned synchronization changes comparing the 25B conditions at both timepoints. Binned synchronization at DIV17 significantly decreases compared to binned synchronization at DIV10 for $SF_{initial}$=0.2-0.4. For 0.2-0.4 binning, 25B DIV17 networks also significantly decrease compared with the control (0B DIV10; $p<0.05$; not shown). **F.** Binned synchronization changes comparing the 50B conditions at both timepoints. *$p<0.05$ calculated by two-way ANOVA followed by Tukey's multiple comparisons test (comparing all conditions). Outliers eliminated using ROUT method with Q=1%. For 0.2-0.4: n(0B DIV10)=14; n(25B DIV10)=17; n(50B DIV10)=14; n(0B DIV17)=12; n(25B DIV17)=12; n(50B DIV17)=13. For 0.4-0.6, n(0B DIV10)=14; n(25B DIV10)=14; n(50B DIV10)=13; n(0B DIV17)=14; n(25B DIV17)=14; n(50B DIV17)=13. For 0.6-0.8, n(0B DIV10)=12; n(25B DIV10)=15; n(50B DIV10)=14; n(0B DIV17)=13; n(25B DIV17)=14; n(50B DIV17)=13. For 0.8-1.0, n(0B DIV10)=13; n(25B DIV10)=12; n(50B DIV10)=13; n(0B DIV17)=14; n(25B DIV17)=13; n(50B DIV17)=13. n indicates the number of MEAs. Error bars indicate SEM.

We also examined the changes that occur when the synchronization of all connections is averaged, as this allows equal contribution from each connection on an electrode. The changes in SF were tracked for each category, and an average for each category was obtained.

Treatment with BDNF significantly affects the synchronization of connections between electrodes at DIV 10 (Figure 5-12B). Treatment with 25 ng/ml BDNF significantly increases synchronization of connections with $SF_{initial}$=0.8-1.0 compared to the untreated condition at this timepoint. In contrast, treatment with 50 ng/ml BDNF significantly decreases the synchronization of connections with $SF_{initial}$=0.2-0.4 and 0.6-0.8 compared to the untreated condition at this timepoint, but this same treatment significantly increases synchronization of the strongest category ($SF_{initial}$=0.8-1.0) compared to the untreated condition at this timepoint. Moreover, treatment with 25 ng/ml BDNF significantly increases synchronization of two categories of connections ($SF_{initial}$=0.2-0.4 and 0.4-0.6) when compared to treatment with 50 ng/ml BDNF.

Treatment with BDNF also significantly affects the synchronization of connections at DIV 17 (Figure 5-12C). Treatment with both concentrations of BDNF significantly decreases the synchronization of connections with $SF_{initial}$=0.2-0.4 when compared to the untreated condition at that timepoint. Treatment with 25 ng/ml BDNF significantly decreases the synchronization of connections with $SF_{initial}$=0.6-0.8 compared to the untreated condition at that timepoint.

Treatment with 50 ng/ml BDNF significantly decreases the synchronization of connections with $SF_{initial}$=0.4-0.6 but significantly increases the synchronization of connections with $SF_{initial}$=0.8-1.0 compared to the untreated condition at that timepoint. In addition, treatment with 50 ng/ml BDNF significantly increases the synchronization of connections with $SF_{initial}$=0.6-0.8 and 0.8-1.0 compared to treatment with 25 ng/ml BDNF.

Significant differences are observed when comparing treatment over time. Untreated networks show significant increases in the synchronization of connections with $SF_{initial}$=0.2-0.4 over time (Figure 5-12D). Treatment with 25 ng/ml BDNF results in a significant decrease in synchronization over time for connections in three categories ($SF_{initial}$=0.2-0.4, 0.6-0.8, and 0.8-1.0; Figure 5-12E). Similar to the untreated conditions, treatment with 50 ng/ml BDNF results in a significant increase over time in the synchronization of connections with $SF_{initial}$=0.2-0.4 (Figure 5-12F) .

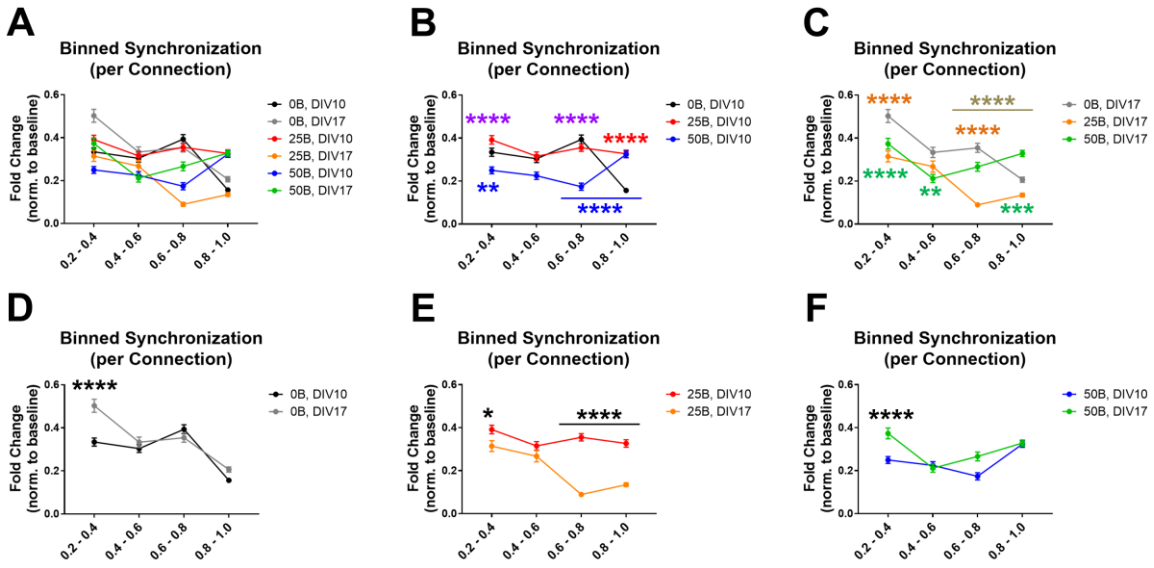

Figure 5-12: BDNF modulates the synchronization of electrodes with different initial synchronizations.
Binned synchronization changes for connections with different initial synchronizations. **A.** Overlaid synchronization changes over time and with different BDNF treatments. **B.** Binned synchronization comparisons between the different BDNF treatments at DIV10. Red stars indicate significance between the 25B and 0B conditions. Blue stars indicate significance between the 50B and 0B conditions. Purple stars indicate significance between the 25B and 50B conditions. **C.** Binned synchronization comparisons between the different BDNF treatments at DIV17. Orange stars indicate significance between the 25B and 0B conditions. Green stars indicate significance between the 50B and 0B conditions. Brown stars indicate significance between the 25B and 50B conditions. **D.** Binned synchronization comparisons between the 0B condition (control) at the different timepoints. **E.** Binned synchronization comparisons between the 25B conditions at the different timepoints.

F. Binned synchronization comparisons between the 50B conditions at the different timepoints. *p<0.05, **p<0.01, ***p<0.001, and ****p<0.0001 calculated by two-way ANOVA followed by Tukey's multiple comparisons test (comparing all conditions). No outliers were eliminated. For 0.2-0.4: n(0B DIV10)=1704; n(25B DIV10)=1384; n(50B DIV10)=1428; n(0B DIV17)=1098; n(25B DIV17)=1084; n(50B DIV17)=1246. For 0.4-0.6, n(0B DIV10)=930; n(25B DIV10)=726; n(50B DIV10)=634; n(0B DIV17)=562; n(25B DIV17)=510; n(50B DIV17)=620. For 0.6-0.8, n(0B DIV10)=580; n(25B DIV10)=694; n(50B DIV10)=392; n(0B DIV17)=532; n(25B DIV17)=750; n(50B DIV17)=406. For 0.8-1.0, n(0B DIV10)=1872; n(25B DIV10)=506; n(50B DIV10)=732; n(0B DIV17)=824; n(25B DIV17)=1080; n(50B DIV17)=784. n indicates the number of connections. Error bars indicate SEM.

Overall, treatment with 50 ng/ml BDNF significantly increases the average synchronization of networks over time. When examining changes in synchronization of specific strengths on a per MEA basis, many changes are masked by averaging. Additional insight into the action of BDNF is uncovered when all connections are weighted equally in the average synchronization of specific categories. When examining the changes that occur to individual connections with specific initial synchronizations, it is clear that both concentrations of BDNF distinctly modulate the synchronization of connections between electrodes over time. Although there is a significant increase in average overall synchronization over time, it should be noted that all categories of synchronization significantly decrease over time (compare Figure 5-10 to Figure 5-11 and Figure 5-12). It is possible that connections starting with very weak synchronization ($SF_{initial}$=0-0.2) contribute to the increase in average overall synchronization, but they were not included in the analysis that separates synchronization by category for normalization reasons.

5.4 Discussion

In this chapter, we employed MEA technology to understand how external application of BDNF during the active dendrite branching period affects hippocampal network development. Previous experiments in our laboratory recorded spontaneous activity from hippocampal neurons starting at either DIV 10 (Rodriguez et al., 2017, unpublished data) or DIV 14 (Kutzing, Luo et al. 2011, Kutzing, Luo et al. 2012). Thus, this work represents the first recordings from hippocampal neurons during an early period of network development. We found that hippocampal networks exhibit robust spiking and bursting as early as DIV 7 and that this activity tends to decrease by DIV 10 and DIV 17, regardless of whether or not BDNF treatment has been applied. This overall decrease in activity mirrors the pruning that occurs to the dendritic arbor. Younger networks display greater bursting activity as synaptic connections are established. As the networks mature, stable synaptic connections develop, and the unnecessary connections are eliminated, resulting in a mature circuit (Tau and Peterson 2010, Litwin-Kumar and Doiron 2012, Biffi, Ragalia et al. 2013).

The motivation for the work in this chapter was based on previous work in our laboratory, which illustrated that extracellular application of BDNF for 72 hr modulates the development of the dendritic arbor, specifically by increasing primary and secondary dendrites (Kwon, Fernandez et al. 2011). We initially hypothesized that application of BDNF to hippocampal networks cultured on MEAs would result in increased synaptic connections due to increases in dendrites close to the soma, thereby increasing both overall activity and synchronization immediately after BDNF treatment. While treatment with 50 ng/ml BDNF increases the average synchronization of networks by DIV 17,

hippocampal networks are surprisingly resistant to BDNF-promoted changes at DIV 10. No significant differences are observed at DIV 10 for networks treated with 25 or 50 ng/ml BDNF compared to the control (no treatment at DIV 10) for any parameter. These data suggest that there are homeostatic mechanisms that prevent networks from changing during the treatment period of DIV 7-10. Despite the structural changes that may occur to the dendritic arbor or to synapses during the treatment period of DIV 7-10, there are no detectable differences in network dynamics at DIV 10. Moreover, instead of increased network activity, spike rate significantly decreases at DIV 17 for networks treated with 25 ng/ml BDNF when compared with the same treatment at DIV 10 and to untreated networks at DIV 10. In general, treatment with 50 ng/ml BDNF promotes changes to a greater number of parameters by DIV 17 compared with treatment with 25 ng/ml BDNF. A summary of significant changes is included in Table 5-1.

	0B		25B		50B	
	DIV 10	DIV 17	DIV 10	DIV 17	DIV 10	DIV 17
Spike Rate		X	X	↓	X	X
Fano Factor		X	X	X	X	↑
Avg. # Spikes per Burstlet		X	X	X	X	↑
# Global Bursts		X	X	↓	X	↓
Global IBI		X	X	↑	X	X
Avg. IBI per Electrode		X	X	X	X	↑
Avg. Synch.		X	X	X	X	↑

Table 5-1: Summary of significant changes to the network dynamics of hippocampal neurons over time and as a result of BDNF treatment.

How does external application of BDNF alter network dynamics? BDNF has been shown to act at both pre- and post-synaptic sites (Yoshii and Constantine-Paton 2010, Edelmann, Leßmann et al. 2014) and to be involved in the regulation of synchronized network activity, which is thought to influence gene expression (Buonanno and Fields 1999, O'Donovan 1999). BDNF modulates correlated network activity in the immature hippocampus by activating MAPK/ERK pathways in the postsynaptic neuron (Mohajerani, Sivakumaran et al. 2007). Similarly, we previously reported that external application of BDNF increases cypin mRNA and protein expression via activation of the MAPK pathway (Kwon, Fernandez et al. 2011), suggesting a potential role for cypin in the development of neuronal networks.

Overexpression of BDNF has been shown to increase synaptogenesis in developing neuronal networks, increasing GABAergic synapses three-fold and non-GABAergic synapses by 50% (Aguado, Carmona et al. 2003). An increase in inhibitory synapses via a TrkB-dependent mechanism would explain decreased spiking activity at DIV 17 observed after treatment with 25 ng/ml BDNF. This concentration of BDNF primarily reflects action at the TrkB receptor, suggesting that TrkB mediates these changes. In contrast, treatment with 50 ng/ml BDNF activates both the TrkB receptor and non-specifically activates other Trk receptors (Barbacid 1994, Chao 2003, Segal 2003). Activation of multiple Trk receptors with 50 ng/ml BDNF treatment could explain why an increase in synchronization is observed for networks treated with this concentration but not for networks treated with the lower concentration of BDNF. Moreover, the relative expression of TrkB and the other Trk receptors changes over time in the developing nervous system (Fryer, Kaplan et al. 1996, Ohira, Shimizu et al. 1999, Ohira

and Hayashi 2003). It is possible that BDNF treatment alters the normal course of developmental expression of TrkB in hippocampal networks, and changes to the amount of TrkB and/or the other Trk receptors are responsible for the observed differences in network dynamics. Indeed, it has been shown that application of BDNF increases both TrkB and BDNF mRNAs in the dendrites, thus also influencing protein expression (Tongiorgi, Righi et al. 1997, Righi, Tongiorgi et al. 2000). Future work will use Western Blotting to determine whether changes in TrkB receptor content change over time or as a result of BDNF treatment.

In addition to altering network dynamics differently, the two BDNF treatments exert distinct effects on connections with different initial synchronizations. Treatment with either concentration of BDNF results in significantly increased synchronization of connections with initial synchronization of 0.8-1.0 compared with the untreated condition at DIV 10; however, only treatment with the higher concentration of BDNF significantly increases the synchronization of this category at DIV 17, indicating that the higher concentration of BDNF exerts greater long-term effects on this category of synchronization. Thus, BDNF may mediate distinct effects on the neural network, depending on its concentration, and thus, the receptors it activates.

Despite promoting synaptogenesis, BDNF significantly decreases the number of global bursts by DIV 17, and this decrease is independent of BDNF concentration. It is well established that mature networks exhibit decreased activity as unnecessary connections are pruned (Tau and Peterson 2010, Biffi, Ragalia et al. 2013), and perhaps BDNF treatment accelerates this process by promoting clustering of connections, and, thus, decreased activity (Litwin-Kumar and Doiron 2012). Future work will employ

clustering analysis (Patel, Ventre et al. 2012, Patel, Ventre et al. 2013, Kang, Cao et al. 2015) to determine whether changes to network structure have occurred that are not revealed with more traditional parameters.

Finally, it is important to note that while dissociated hippocampal networks replicate some important features of *in vivo* network activity, such as connectivity, plasticity, and repeating activity motifs (Wagenaar, Pine et al. 2006, Chiappalone, Massobrio et al. 2008, Raichman and Ben-Jacob 2008), the experimental system used for the work in this chapter possesses limitations. The most prominent difference between dissociated *in vitro* networks and *in vivo* networks is the lack of oligodendrocytes and mature astroglial cells. Due to the culture medium used – NbActiv4 (Brewer, Boehler et al. 2008), which is similar to Neurobasal medium (Brewer, Torricelli et al. 1993) – glial cells, mainly astroglia, are immature and do not express glutamate transporters as part of our cultured *in vitro* networks. Furthermore, these cultures lack oligodendrocytes (Swiatkowski and Firestein 2017, unpublished data). Glial cells have many important functions; in particular, the tri-partite synapse theory suggests that they modulate synaptic neuronal communication (reviewed in (Eroglu and Barres 2010)). Therefore, the networks used in this study lack an important component of *in vivo* networks. Other methods of culturing neurons, such as acute slices or organotypic slices, may offer a closer approximation to *in vivo* networks since the native architecture of the hippocampus is not disrupted. Thus, the work in this chapter offers insight into how BDNF treatment affects the development of primarily cultured dissociated networks, and these changes may differ in the actual hippocampus.

5.5 Acknowledgements

I would like to acknowledge Ana Rodriguez for determining the techniques necessary for successfully maintaining dissociated hippocampal cultures on MEAs.

CHAPTER 6: THE ROLE OF BRAIN-DERIVED NEUROTROPHIC FACTOR IN NEUROPROTECTION FROM GLUTAMATE-INDUCED EXCITOTOXICITY

6.1 Introduction

In addition to being used for studying the development of *in vitro* networks of neurons, microelectrode array (MEA) technology has been employed to investigate the effects of toxicity (Morefield, Keefer et al. 2000, Keefer, Gramowski et al. 2001, Gopal 2003, Parviz and Gross 2007) or injury (Srinivas, Jain et al. 2007, Kutzing, Luo et al. 2011, Kutzing, Luo et al. 2012) and the effects of gene overexpression or knockdown (Gullo, Manfredi et al. 2014) on network activity. MEAs have the potential to serve as drug- or compound-screening platforms (Johnstone, Gross et al. 2010, Frega, Pasquale et al. 2012) because neuronal cultures respond to the same concentration ranges of compounds that cause functional changes *in vivo* (Xia, Gopal et al. 2003, Xia and Gross 2003). Previously, our laboratory used MEAs to investigate the effects of glutamate-induced excitotoxicity on cortical neuron networks (Kutzing, Luo et al. 2011) and whether memantine could be neuroprotective (Kutzing, Luo et al. 2012). In this chapter, we extend this line of work to hippocampal neurons to investigate whether BDNF can be neuroprotective for this distinct type of network.

Multiple groups have reported that BDNF acts as a pro-survival factor (Lindholm, Dechant et al. 1993, Ghosh, Carnahan et al. 1994, Walton and Druganow 2000) and confers neuroprotection to cells injured by both physical (Sendtner, Holtmann et al. 1992, Giehl and Tetzlaff 1996, Hofer and Bardet 1998) and chemical trauma (Lindholm,

Dechant et al. 1993, Mattson, Lovell et al. 1995, Kiprianova, Freiman et al. 1999). For example, BDNF is overexpressed in neurons that survive ischemic injury (Ikonomidou and Turski 2002) and selectively protects excitatory synapses through the mitogen-activated protein kinase (MAPK) and phosphatidylinositol-4,5-bisphosphate 3-kinase (PI3K) pathways (Almeida, Manadas et al. 2005, Melo, Okumoto et al. 2013). Furthermore, neuroprotection by NMDA from subsequent exposure to higher concentrations of NMDA acts via a BDNF-dependent mechanism. After NMDA stimulation, BDNF is released within minutes and triggers the cascade of TrkB phosphorylation and activation, autocrine binding of BDNF to TrkB, and transcription of BDNF mRNA (Jiang, Tian et al. 2005).

Motivation for using BDNF as a neuroprotective agent is derived from the fact that promising drugs have been tested in clinical trials as a treatment for glutamate-induced excitotoxicity, and they have failed. These drugs are NMDA receptor (NMDAR) antagonists and bind competitively or allosterically to NMDARs without inducing normal function. One hypothesis for their failure is that glutamate is necessary at a physiological concentration, and thus, blocking receptor function completely results in undesirable side effects (Ikonomidou and Turski 2002). Indeed, there are reports that blocking NMDARs is detrimental to neuronal survival due to nonspecific action of the drugs being used (Ikonomidou, Bosch et al. 1999, Pohl, Bittigau et al. 1999, Young, Lawlor et al. 1999, Hansen, Briem et al. 2004). Moreover, it has been shown that differentially located NMDARs play specific roles in regulating cell death pathways. Extrasynaptic NMDARs, such as ones activated by excess glutamate, block cAMP response element binding protein (CREB) function, which regulates expression of BDNF and other pro-survival

genes. On the other hand, calcium influx through synaptic NMDARs upregulates the function of CREB, and therefore, the expression of BDNF (Hardingham, Fukunaga et al. 2002). Thus, it is the activity of extrasynaptic rather than synaptic NMDARs that should be attenuated to prevent glutamate excitotoxicity. Specific neurons in the hippocampus can better survive hypoxic and ischemic conditions due to higher CREB activity and BDNF expression. Additionally, it has been suggested that there is a positive feedback loop between CREB and BDNF (Walton and Druganow 2000, Ikonomidou and Turski 2002).

In this chapter, we examined whether BDNF can be neuroprotective to hippocampal neurons following excitotoxic injury. First, we determined optimal concentrations of glutamate that induce mild and moderate injury to cultures of hippocampal neurons. We applied BDNF to cultures of hippocampal neurons that received no injury, mild injury, or moderate injury, and we performed recordings of spontaneous activity and quantified the changes to the network that occur at 24 hr and 72 hr post-injury. We examined parameters describing the overall activity and the synchronization of these networks.

6.2 Materials and Methods

6.2.1 Preparation of microelectrode arrays (MEAs) and cell culture

Standard 60-electrode MEAs (59 electrodes plus 1 reference electrode) were used for all experiments. Electrodes had diameters of 10 μm and an inter-electrode spacing of 200 μm (60MEA200/10iR-Ti-gr; Multi Channel Systems, Germany), as shown in Figure 5-1A,B. MEAs were prepared for cell culture as previously described (Kutzing,

Luo et al. 2011, Kutzing, Luo et al. 2012). MEAs were washed for at least 48 hours in 1% Tergazyne solution (in dH_2O) prior to the day of dissection. On the day of dissection, MEAs were autoclaved, rinsed once with sterile water, and left to dry in a sterile cell culture hood. MEAs were then coated with 0.5 mg/mL poly-D-lysine (PDL; Sigma) and allowed to incubate at 37 ºC for at least 1 hr. MEAs were then washed three times with sterile water and allowed to dry in a sterile cell culture hood. Immediately prior to plating of cells, MEAs were coated with 10 μg/ml laminin for 30 min at 37 ºC.

Neuronal cultures were prepared from the hippocampi of rat embryos at 18 days of gestation (E18) as described previously (Firestein, Brenman et al. 1999). The hippocampi were dissociated using manual trituration, and cells were plated onto PDL and laminin-coated MEAs at a density of $1x10^6$ cells per MEA. Cultures were kept in a humidified 37 ºC incubator with 5% CO_2 and maintained in NbActiv4 medium (Brain Bits), which contains Neurobasal medium, B27, glutamine, creatine, estrogen, and cholesterol (Brewer, Boehler et al. 2008). Additionally, 1% penicillin-streptomycin (Life Technologies) was added to culture mediums to prevent contamination. Half of the culture medium was changed every other day. All studies were performed in accordance with the Institutional Animal Care and Use Committee (IACUC) standards.

6.2.2 Microelectrode array recordings

The spontaneous activity of hippocampal networks on MEAs was recorded at DIV 14, 15, and 17 using the data acquisition software MCRack (Multi Channel Systems, Germany; Figure 5-1C and D). Recordings were performed at 37 ˚C on a heat-controlled stage at room atmosphere as previously described (Kutzing, Luo et al. 2011, Kutzing,

Luo et al. 2012). Data were acquired at a sampling rate of 20 kHz using an MEA1060-Inv-BC amplifier (Multi Channel Systems, Germany). A recording solution containing the following components was used to regularize bursting behavior: NaCl (144mM), KCl (10mM), $MgCl_2$ (1mM), $CaCl_2$ (2mM), HEPES (10mM), Na-pyruvate (2mM), and glucose (10mM) at physiological pH (pH 7.4). During recording, MEAs were covered with semi-permeable lids (ALA MEA-MEM, Multi Channel Systems) that selectively allow gases to diffuse through but that prevent airborne pathogens from contaminating the cultures. Prior to recording, cultures were allowed to equilibrate in recording solution for 5-10 min. Spontaneous activity was then recorded for 5 min. Afterwards, cultures were washed once with growth medium, and then injury with or without treatment was induced or conditioned medium was returned, as described below.

6.2.3 Determination of glutamate concentrations that result in mild and moderate injury of hippocampal neurons

To determine which concentrations of glutamate result in mild and moderate injury of hippocampal neurons cultured on MEAs, cultures were maintained for 14 DIV prior to treatment and recording. The schedule used for these experiments is shown in Figure 6-1A. Shorthand abbreviations used in plots are shown in Figure 6-1B.

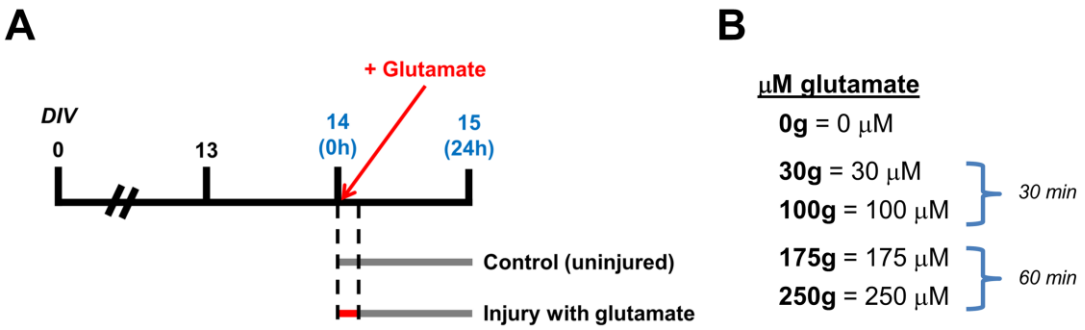

Figure 6-1: Recording and treatment schedule used for determining the appropriate concentrations of glutamate for injuring hippocampal cultures.
A. Recording and treatment schedule for injury data generated in this chapter. Cultures were maintained for 14 DIV prior to beginning experiments. **B.** Shorthand abbreviations used in data plots. 0g indicates control networks (no injury, 0 μM glutamate). 30g indicates networks injured with 30 μM glutamate for 30 min. 100g indicates networks injured with 100 μM glutamate for 30 min. 175g indicates networks injured with 175 μM glutamate for 1hr. 250g indicates networks injured with 250 μM glutamate for 1 hr.

Baseline recordings were performed at DIV 14 using MCRack software. Immediately after recording, an activity check was performed. Cultures having less than 2000 spikes (a spike rate of less than 6.7 Hz) were not used for further experimentation. Remaining cultures that did pass the activity threshold were randomly assigned to one of five injury groups: no injury (0 μM glutamate), 30 μM glutamate, 100 μM glutamate, 175 μM glutamate, or 250 μM glutamate. Glutamate or vehicle (sterile water) was added to conditioned medium, which was then applied to cultures for the indicated time. Injury with higher levels of glutamate (175 and 250 μM) was induced for 1 hr (Kutzing, Luo et al. 2011) while injury with lower levels of glutamate (30 and 100 μM) was induced for 30 min. After injury, glutamate-containing medium was replaced with conditioned medium.

6.2.4 Experimental setup: Injury with glutamate, BDNF recovery treatment, and recording schedule

After determining which concentrations of glutamate result in sublethal injury to cultures of hippocampal neurons (30 and 60 μM injury for 30 min), cultures were maintained for 14 DIV prior to treatments and recordings. The schedule used for these experiments is shown in Figure 6-2A. Shorthand abbreviations used in plots are shown in Figure 6-2B.

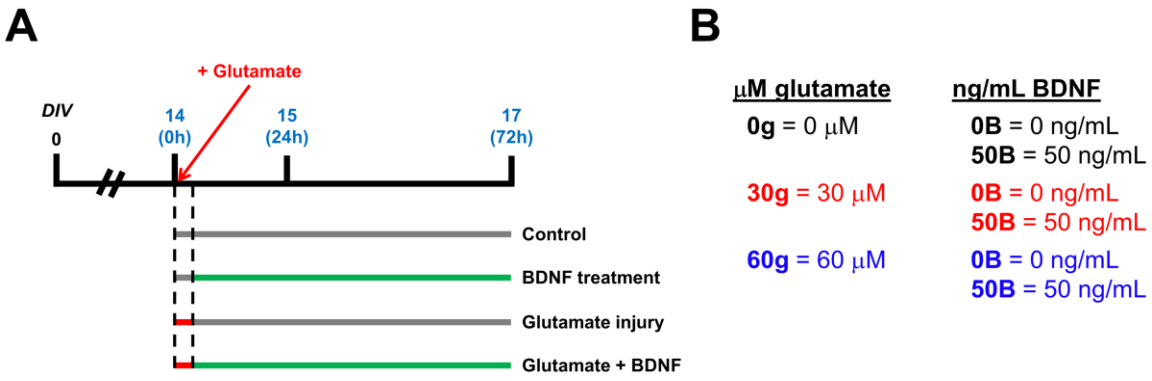

Figure 6-2: Recording and treatment schedule used for glutamate injury and BDNF recovery experiments.
A. Recording and treatment schedule for injury and recovery data generated in this chapter. Cultures were maintained for 14 DIV prior to beginning experiments. **B.** Shorthand abbreviations used in data plots. 0g indicates control networks (no injury, 0 μM glutamate). 30g indicates networks injured with 30 μM glutamate for 30 min. 60g indicates networks injured with 60 μM glutamate for 30 min. 0B and 50B indicate networks treated with 0 and 50 ng/mL BDNF, respectively, during the recovery period.

Baseline recordings were performed at DIV 14 using MCRack software. Immediately after recording, an activity check was performed. Cultures having less than 2000 spikes (a spike rate of less than 6.7 Hz) were not used for further experimentation. Remaining cultures that did pass the activity threshold were randomly assigned to one of three injury groups: no injury (0 μM glutamate), 30 μM glutamate, or 60 μM glutamate.

Glutamate or vehicle (sterile water) was added to conditioned medium, which was then applied to cultures for 30 min. After injury, cultures were randomly assigned to one of two treatment groups: no treatment (0 ng/mL BDNF) or treatment with 50 ng/mL BDNF. Cultures were maintained in treatment medium with or without BDNF until the 24 hr-post injury recording on DIV 15. After this recording, the treatment medium with or without BDNF was reapplied, and cultures were maintained in this medium until the 72 hr-post injury recording on DIV 17.

6.2.5 Signal processing and parameter calculation

Processing of raw data and calculation of parameters were performed as described in Chapter 5.

6.2.6 Data representation and statistics

Unless otherwise noted, all data are represented as fold change, normalized to the baseline value of that parameter for that MEA (Kutzing, Luo et al. 2011, Kutzing, Luo et al. 2012). In cases where there are no burstlets or global bursts, related parameters are represented as discussed in Chapter 5.

All data are plotted in Graphpad Prism and are shown as mean ± standard error of the mean (SEM) with *n* indicating the number of MEAs in that particular condition, unless otherwise noted. Two-way ANOVAS were calculated using Graphpad Prism. Outliers were eliminated in Graphpad Prism using the ROUT method with Q=1% for synchronization and number of global bursts and Q=0.5% for all other parameters

6.3 Results

6.3.1 Hippocampal neuron networks are more sensitive to glutamate-induced injury than are cortical neuron networks

To understand how hippocampal neurons cultured on MEAs respond to injury from excess glutamate, we treated the networks with several concentrations of glutamate and assessed electrical activity. First, networks were injured with 175 μM and 250 μM glutamate for 1 hr since these concentrations were used in previous work and resulted in mild and moderate injury, respectively, of cortical neurons (Kutzing, Luo et al. 2011). Upon visual inspection of the recordings performed at 24 hr after injury, it was clear that networks injured with 175 μM and 250 μM glutamate show almost no spiking or bursting activity. These qualitative observations were confirmed quantitatively. Likely, these higher concentrations of glutamate cause lethal injury to the hippocampal neuron networks. Therefore, lower concentrations of glutamate (30 μM and 100 μM) and a shorter injury time (30 min) were used in an attempt to cause sublethal injury to hippocampal networks. Four experiments were completed for all data shown, but one experiment was eliminated because the control conditions were not sufficiently active at the 24 hr timepoint, indicating impending contamination or unhealthy cultures. Thus, several parameters do not show significance due to low *n*; experiments are ongoing to rectify this.

The rate and magnitude of spiking in hippocampal networks are affected by injury. The spike rate trends towards decreasing in all injury conditions, with the 100 μM, 175 μM, and 250 μM injury conditions showing similar values (Figure 6-3A) although this decrease is only statistically significant for the 175 μM injury condition is

significantly decreased when compared with the control. The lack of significance for the 100 μM and 250 μM injury conditions is most likely due to the high variability in spike rate in control networks. The average spike voltage significantly decreases for networks injured with 100 μM, 175 μM, and 250 μM glutamate (Figure 6-3B), indicating less robust spiking, but not for networks injured with 30 μM glutamate.

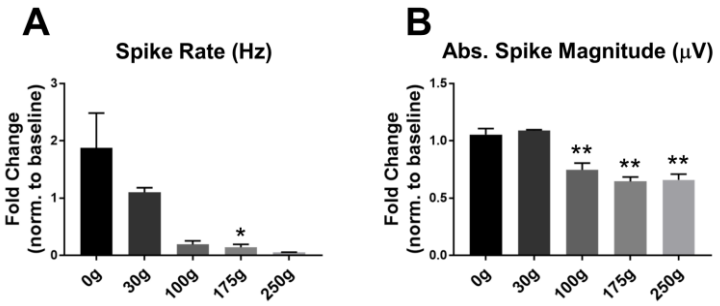

Figure 6-3: The spike rate and average spike magnitude decrease with injury.
A. Average spike rate trends towards decreasing for all injury conditions, though the decrease is only significant for the 175g condition. The lack of significance in the 100g and 250g conditions may be due to low number of repeats and high variability in the control condition. **B.** Average spike voltage significantly decreases for injury induced with concentrations of glutamate greater than 100 μM (100g, 175, and 250g conditions). *$p<0.05$ and **$p<0.01$ calculated by one-way ANOVA followed by Dunnett's multiple comparisons test, which compared all conditions to the control (0g). n(0g)=4, n(30g)=2, n(100g)=2, n(175g)=3, n(250g)=2. Error bars indicate SEM.

The bursting activity of hippocampal networks is affected by injury. The burstlet rate is almost abolished in injury induced with concentrations of glutamate greater than 100 μM (Figure 6-4A), although statistical tests did not reveal significance due to low *n*. The average number of spikes per burst varies across conditions and is not significantly changed by injury (Figure 6-4B). The average ratio of burstlet rate to spike rate (B.R./S.R.) reveals the relationship of bursting activity to spiking activity, and it significantly decreases in injury induced with concentrations of glutamate greater than

100 μM (Figure 6-4C). These data confirm the observation that while spiking activity decreases in networks injured with concentrations of glutamate greater than 100 μM glutamate or more, bursting activity in these networks is virtually abolished.

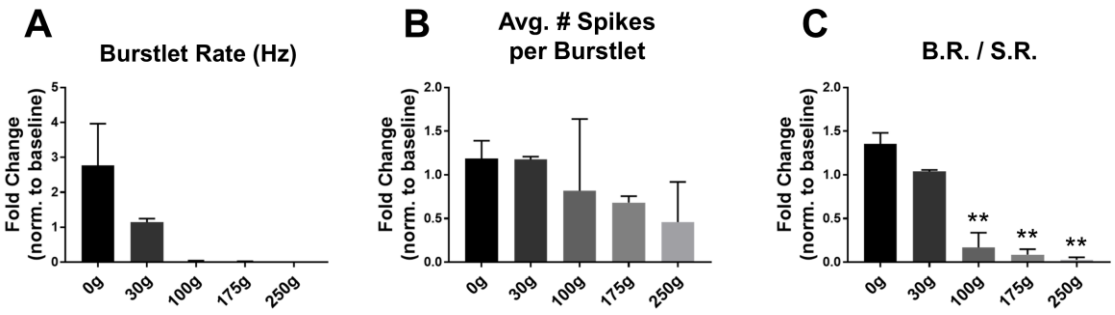

Figure 6-4: Bursting parameters are affected by injury.
A. Burstlet rate decreases for all injury conditions and is close to 0 for injuries over 100 μM. The 100g, 175, and 250g conditions do not show significance due to lack of repeats. **B.** Average number of spikes per burstlet does not significantly change with injury. **C.** Ratio of burstlet rate (B.R.) to spike rate (S.R.) significantly decreases in injury induced with concentrations of glutamate greater than 100 μM (100g, 175, and 250g conditions). **p<0.01 calculated by one-way ANOVA followed by Dunnett's multiple comparisons test, which compared all conditions to the control (0g). n(0g)=4, n(30g)=2, n(100g)=2, n(175g)=3, n(250g)=2. Error bars indicate SEM.

The number of global bursts and average synchronization of hippocampal networks are also affected by injury. The number of global bursts significantly decreases in injury induced with concentrations of glutamate greater than 100 μM (Figure 6-5A). The global IBI increases for networks injured with 100 μM glutamate compared with the control and with networks injured with 30 μM glutamate, although the increase is not significant due to low *n*. The global IBI is nonexistent for the 175 μM and 250 μM glutamate-induced injury conditions since those conditions do not show any global bursts (Figure 6-5B). The average synchronization significantly decreases in networks injured with concentrations of glutamate greater than 100 μM (Figure 6-5C).

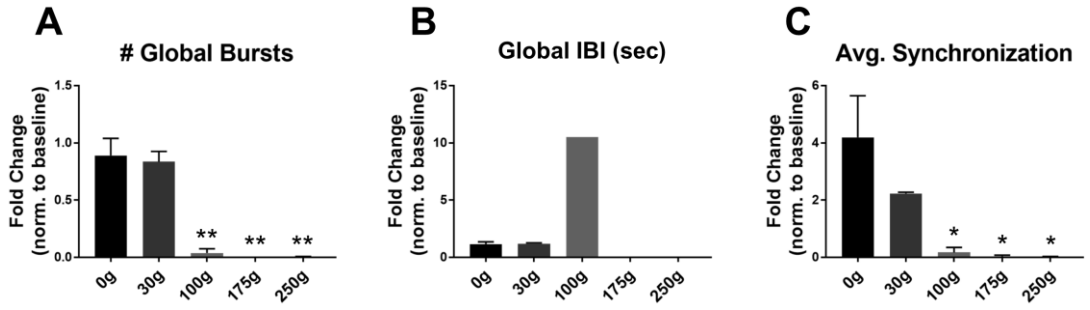

Figure 6-5: Number of global bursts and average synchronization decrease as a result of injury.
A. Global bursts significantly decrease in injury induced with concentrations of glutamate greater than 100 μM (100g, 175, and 250g conditions). One data point for 0g was not included because the network started with 0 global bursts, and thus, the data could not be normalized. n(0g)=3, n(30g)=2, n(100g)=2, n(175g)=3, n(250g)=2. **B.** Global inter-burst interval increases for the 100g condition, although not significantly due to n=1 for 100g. The 175g and 250g conditions do not have global bursts, and thus, global IBI could not be calculated. n(0g)=4, n(30g)=2, n(100g)=1, n(175g)=0, n(250g)=0. **C.** Average synchronization significantly decreases in injury induced with concentrations of glutamate greater than 100 μM (100g, 175, and 250g conditions). One outlier was removed for the 0g condition using the ROUT method and Q=1%. n(0g)=3, n(30g)=2, n(100g)=2, n(175g)=3, n(250g)=2. For A and C, *$p<0.05$ and **$p<0.01$ calculated by one-way ANOVA followed by Dunnett's multiple comparisons test, which compared all conditions to the control (0g). For B, statistics calculated using an unpaired two-tailed *t*-test between the 0g and 30g conditions ($p=0.9149$). Error bars indicate SEM.

Hippocampal networks injured with concentrations equal to or greater than 100 μM glutamate demonstrate the greatest changes in network dynamics. Injury with 30 μM glutamate does not significantly change any measure of network activity. Thus, in future experiments, 30 μM and 60 μM glutamate will be used to induce mild and moderate injuries, respectively, to hippocampal networks.

6.3.2 Spiking dynamics are affected by mild and moderate injury with glutamate and BDNF treatment

To investigate the whether BDNF can exert neuroprotective effects on hippocampal neuron networks that receive mild and moderate excitotoxic injury, we recorded the spontaneous activity of networks at DIV 14 and then injured networks with 0, 30, or 60 μM glutamate for 30 min. Immediately after injury, glutamate-containing medium was replaced with recovery medium containing 0 or 50 ng/ml BDNF. A recording was performed at DIV 15, approximately 24 hr post-injury, to assess whether BDNF promotes short-term neuroprotection. A final recording was performed at DIV 17, approximately 72 hr post-injury, to determine whether BDNF promotes longer-term neuroprotection. Seven experiments were completed for all data shown.

We first examined how the spike rate, magnitude, and variability are affected by injury with glutamate and recovery with or without BDNF treatment. At 24 hr post-injury, spike rate significantly decreases for moderately injured networks, regardless of whether they received BDNF treatment, compared with uninjured networks, regardless of whether they received BDNF treatment. Spike rate also decreases for mildly injured networks treated with BDNF compared with uninjured networks treated with BDNF. Moreover, there are marginally significant differences between mildly injured networks treated with BDNF and the control ($p=0.0546$) and between mildly injured networks compared with uninjured networks treated with BDNF ($p=0.0708$). At 72 hr post-injury, the spike rate of both mildly injured and moderately injured networks significantly decreases compared with the control, regardless of whether networks were treated with BDNF (Figure 6-6A). The average magnitude of spiking (Figure 6-6B) and the Fano

factor (Figure 6-6C) do not change after injury or BDNF treatment at either timepoint, indicating that the robustness and variability of spiking are not altered. However, at 24 hr post-injury, the decrease in spike magnitude approaches marginal significance for moderately injured networks compared with the control ($p=0.0727$). At 72 hr post-injury, the ratio of the spike rate to the Fano factor (S.R./F.F.) significantly decreases for mildly injured networks treated with BDNF, moderately injured networks, and moderately injured networks treated with BDNF compared with uninjured networks that were treated with BDNF. The S.R./F.F. ratio also significantly decreases for moderately injured networks, whether or not they were treated with BDNF, compared with mildly injured networks receiving no treatment (significance not shown; Figure 6-6D). The rate, magnitude, and variability of spiking indicate that BDNF treatment does not prevent any of the observed changes in spiking after mild or moderate injury.

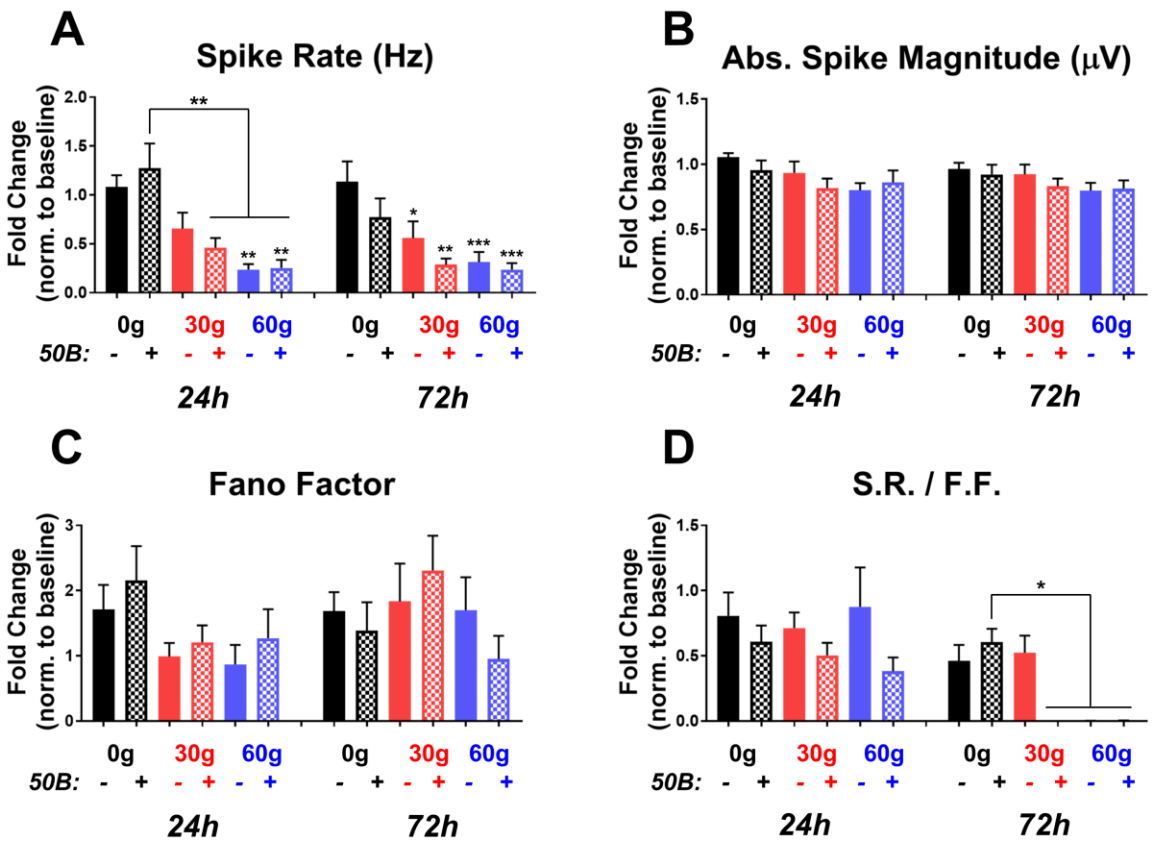

Figure 6-6: Glutamate-induced injury and BDNF treatment affect spike rate. Asterisks indicate significance with respect to the control (0g 0B) within that timepoint, and lines indicate significance between connected bars. **A.** At 24h post-injury, spike rate significantly decreases for moderately injured networks (60g 0B and 60g 50B) compared with uninjured networks (0g 0B and 0g 50B). At 72h post-injury, spike rate significantly decreases for all injury conditions (30g 0B, 30g 50B, 60g 0B, and 60g 50B) compared with the control. **B.** The average magnitude of spiking does not significantly change after injury or BDNF treatment for either timepoint. **C.** The Fano factor does not significantly change after injury or BDNF treatment for either timepoint. **D.** At 24h post-injury, the ratio of spike rate to the Fano factor (S.R./F.F.) does not significantly change after injury or BDNF treatment. At 72h post-injury, the ratio of spike rate to the Fano factor significantly decreases for 30g 50B, 60g 0B, and 60g 50B when compared with 0g 50B. The S.R./F.F. ratio also significantly decreases for moderately injured networks (60g 0B and 60g 50B) when compared with 30g 0B ($p<0.05$; not shown). *$p<0.05$, **$p<0.01$, and ***$p<0.001$ calculated by two-way ANOVA followed by Tukey's multiple comparisons test (comparing all conditions). Outliers eliminated using ROUT method with Q=0.5%. n = 7-13 for all conditions. Error bars indicate SEM.

In addition to examining changes in spike rate and variability, we examined how injury and BDNF treatment affect the average interspike interval (ISI) length and

variability. At 72 hr, the Total ISI significantly increases for moderately injured networks compared with uninjured networks with and without BDNF treatment. A marginally significant increase ($p=0.0521$) is also observed for moderately injured networks treated with BDNF compared with the control (Figure 6-7A). At 24 hr post-injury, the CV of the Total ISI significantly decreases for moderately injured networks, with and without BDNF treatment, compared with uninjured networks treated with BDNF. There is also a marginally significant decrease in CV for moderately injured networks compared with the control ($p=0.0785$; Figure 6-7B). At 24 hr post-injury, the average ISI per electrode is not significantly increased for moderately injured networks with and without BDNF treatment compared with the control ($p=0.1460$ and $p=0.1387$, respectively). At 72 hr post-injury, the average ISI per electrode significantly increases for moderately injured networks compared to both uninjured and mildly injured networks, regardless of whether they were treated with BDNF (Figure 6-7C). For both Total ISI and average ISI per electrode at 72 hr post-injury, there are no significant differences between moderately injured networks treated with BDNF and any other condition, indicating that BDNF may play a role in modulating the ISI after moderate injury.

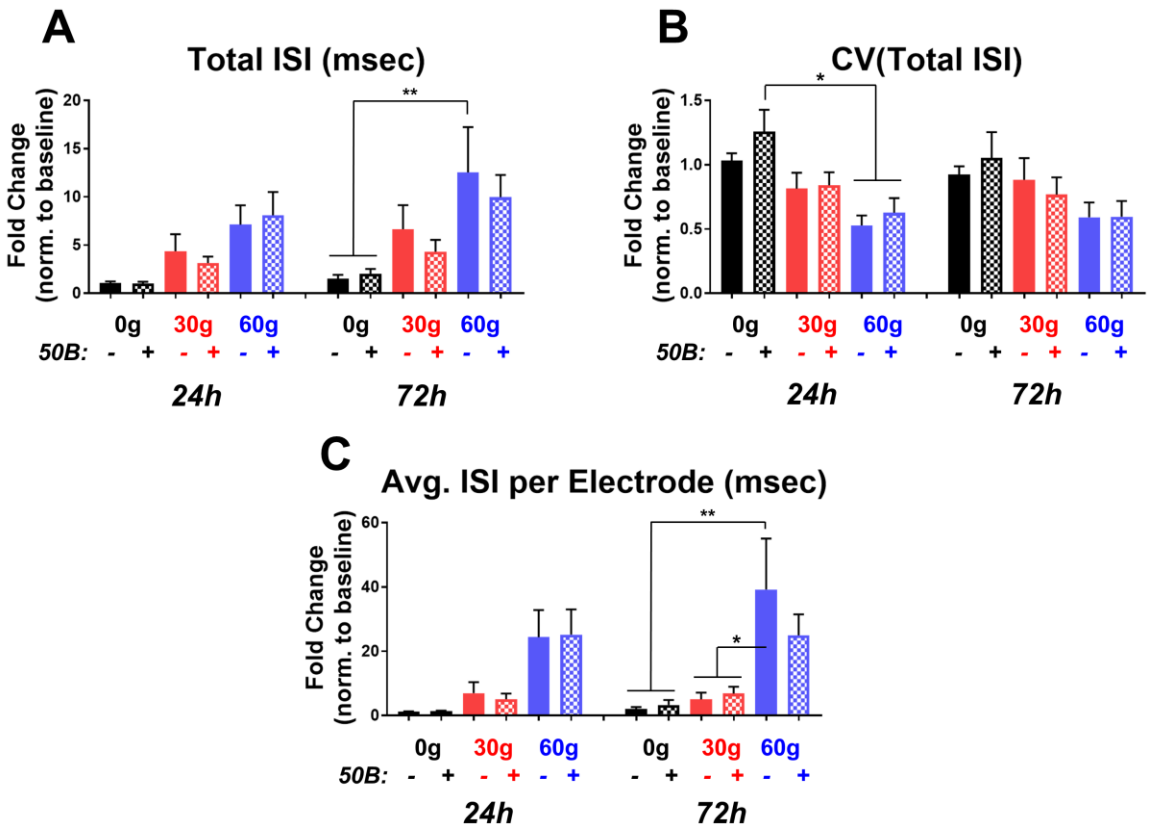

Figure 6-7: The length and variability of the ISI are affected by injury and BDNF treatment.

Asterisks indicate significance with respect to the control (0g 0B) within that timepoint, and lines indicate significance between connected bars. **A.** At 24h post-injury, Total ISI does not significantly change. At 72h post-injury, the Total ISI significantly increases for 60g 0B when compared with uninjured conditions (0g 0B and 0g 50B). **B.** At 24h post-injury, the CV(Total ISI) significantly decreases for moderately injured networks (60g 0B and 60g 50B) compared with 0g 50B. At 72h post-injury, CV(Total ISI) does not significantly change. **C.** At 24h post-injury, the average ISI per electrode does not significantly change. At 72h post-injury, the average ISI per electrode significantly increases for 60g 0B compared with uninjured networks (0g 0B and 0g 50B) and with mildly injured networks (30g 0B and 30g 50B). *p<0.05 and **p<0.01 calculated by two-way ANOVA followed by Tukey's multiple comparisons test (comparing all conditions). For B, outliers eliminated using ROUT method with Q=0.5%. n = 8-13 for all conditions. Error bars indicate SEM.

6.3.3 Bursting dynamics are affected by mild and moderate injury with glutamate and BDNF treatment

In addition to examining how spiking activity changes after injury and with BDNF treatment, we evaluated how the bursting dynamics of hippocampal neuron networks are altered. Burstlet rate significantly decreases at both 24 hr and 72 hr after injury for moderately injured networks, whether or not networks were treated with BDNF, compared with the control. At 72 hr, the burstlet rate of mildly injured networks significantly decreases, whether or not networks were treated with BDNF, but at 24 hr, only the burstlet rate of mildly injured networks treated with BDNF significantly decreases compared with the control. Additionally, the burstlet rate for uninjured networks treated with BDNF significantly decreases compared with the control at 72 hr post-injury (Figure 6-8A). The average burstlet width (Figure 6-8B) and average number of spikes per burstlet (Figure 6-8C) do not significantly change after injury or with BDNF treatment. The ratio of burstlet rate to spike rate (B.R./S.R.) significantly decreases for moderately injured networks, whether or not networks were treated with BDNF, at both 24 hr and 72 hr post-injury compared with the control. Additionally, at 24 hr post-injury, the B.R./S.R. ratio of mildly injured networks treated with BDNF significantly decreases when compared with uninjured networks that were or were not treated with BDNF. Finally, at 72 hr post-injury, the B.R./S.R. ratio of moderately injured networks treated with BDNF significantly decreases compared with uninjured networks treated with BDNF (Figure 6-8D).

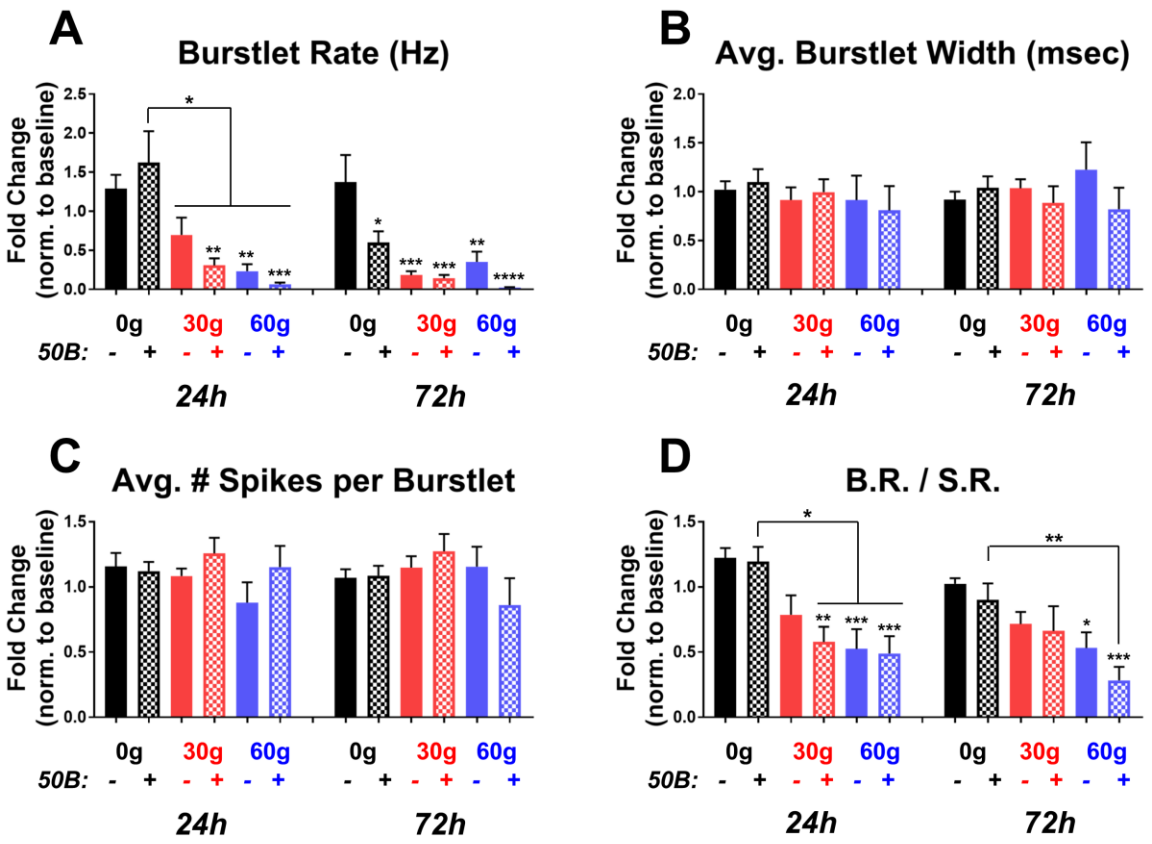

Figure 6-8: Bursting activity is modulated by injury and BDNF treatment. Asterisks indicate significance with respect to the control (0g 0B) within that timepoint, and lines indicate significance between connected bars. **A.** At 24h post-injury, burstlet rate significantly decreases for moderately injured networks (60g 0B and 60g 50B) and for 30g 50B compared with both the control and 0g 50B. There is also statistically significant decrease for 30g 0B when compared with 0g 50B. At 72h post-injury, burstlet rate significantly decreases for 0g 50B and for all injury conditions (30g 0B, 30g 50B, 60g 0B, and 60g 50B) compared with the control. **B.** Average burstlet width does not significantly change after injury or BDNF treatment for either timepoint. **C.** Average number of spikes per burst does not significantly change after injury or BDNF treatment for either timepoint. **D.** At 24h post-injury, the ratio of burst rate to spike rate (B.R./S.R.) significantly decreases for 30g 50B, 60g 0B, and 60g 50B compared with both the control and with 0g 50B. At 72h post-injury, B.R./S.R. significantly decreases for moderately injured networks (60g 0B and 60g 50B) compared with the control. The B.R./S.R. ratio also significantly decreases for 60g 50B when compared with 0g 50B. *p<0.05, **p<0.01, ***p<0.001, and ****p<0.0001 calculated by two-way ANOVA followed by Tukey's multiple comparisons test (comparing all conditions). Outliers eliminated using ROUT method with Q=0.5%. n = 7-13 for all conditions. Error bars indicate SEM.

We also investigated the number, timing, and composition of global bursts, which are composed of several overlapping burstlets (Wagenaar, DeMarse et al. 2005). At 24 hr post-injury, the significant differences observed for the number of global bursts (Figure 6-9A) mirror those seen for burstlet rate (Figure 6-8A). At 24 hr post-injury, the number of global bursts significantly decreases for moderately injured networks, with and without BDNF treatment, when compared with uninjured networks that were or were not treated with BDNF. The number of global bursts also significantly decreases for mildly injured networks treated with BDNF when compared with the control. The decrease in global burst number for mildly injured networks is not significant compared with the control ($p=0.2750$). Additionally, the number of global bursts significantly decreases for mildly injured networks with and without BDNF treatment compared with uninjured networks treated with BDNF. At 72hr post-injury, global burst number significantly decreases for moderately injured networks treated with BDNF when compared with the control. The decrease in global burst number for moderately injured networks is marginally significant compared with the control ($p=0.0593$; Figure 6-9A). The average width of global bursts does not significantly change after injury or with BDNF treatment (Figure 6-9B). Additionally, the ratio of the average global burst width to average burstlet width does not significantly change after injury or with BDNF treatment, mirroring the lack of change of either parameter individually (Figure 6-9D). The average number of burstlets per global bursts significantly decreases at 24 hr post-injury for moderately injured networks (Figure 6-9C). Thus, while BDNF treatment does not alleviate the decreases in global bursts for moderately injured networks at 24 hr, it does prevent a decrease in the

average number of burstlets per global burst, indicating that the number of electrodes recruited for global bursting does not change for moderately injured networks that were treated with BDNF.

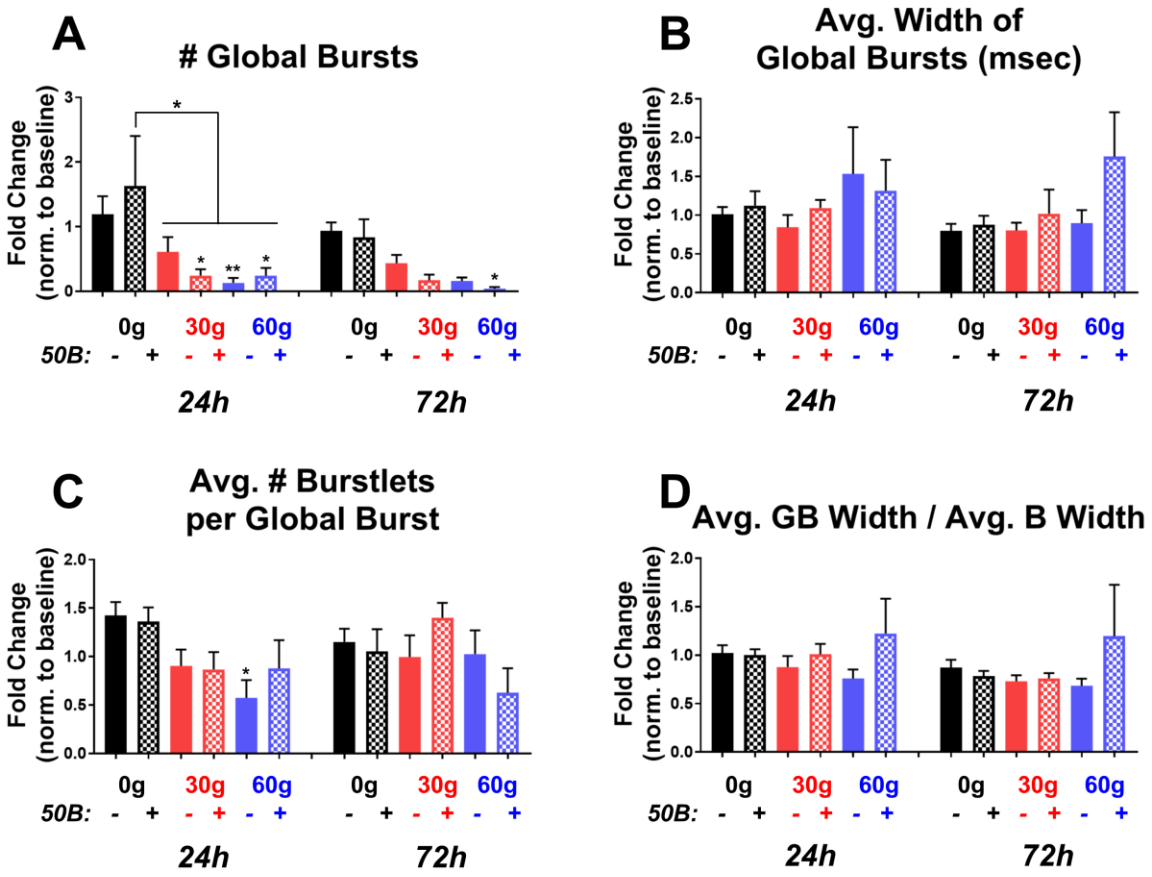

Figure 6-9: Global burst number and composition are altered by injury and BDNF treatment.
Asterisks indicate significance with respect to the control (0g 0B) within that timepoint, and lines indicate significance between connected bars. **A.** At 24h post-injury, global burst number significantly decreases for 30g 50B, 60g 0B, and 60g 50B when compared with both the control and with 0g 50B. Global burst number also significantly decreases for 30 0B when compared with 0g 50B. At 72h post-injury, global burst number significantly decreases for 60g 50B compared with the control. **B.** The average width of global bursts does not significantly change after injury or with BDNF treatment for either timepoint. **C.** At 24h post-injury, the average number of burstlets per global burst significantly decreases for 60g 0B compared with the control. At 72h post-injury, the average number of burstlets per global burst does not change. **D.** The ratio of the average global burst width to average burstlet width does not significantly change after injury or with BDNF treatment for either timepoint. *p<0.05 and **p<0.01 calculated by two-way

ANOVA followed by Tukey's multiple comparisons test (comparing all conditions). Outliers eliminated using ROUT method with Q=1% for global burst number and Q=0.5% for all other parameters. n = 5-12 for all conditions. Error bars indicate SEM.

In addition to examining the number of timing of individual burstlets and global bursts, we investigated the timing between burstlets and between global bursts. At 24 hr post-injury, global IBI significantly increases for moderately injured networks that were treated with BDNF compared with uninjured networks with and without BDNF treatment. At 72 hr post-injury, global IBI significantly increases for mildly injured networks treated with BDNF compared with the control (Figure 6-10A). The average IBI per electrode significantly increases for moderately injured networks treated with BDNF compared with all other conditions (Figure 6-10B). Both injury and BDNF treatment clearly play roles in modulating both types of IBIs, but it is unclear if the role of BDNF is neuroprotective.

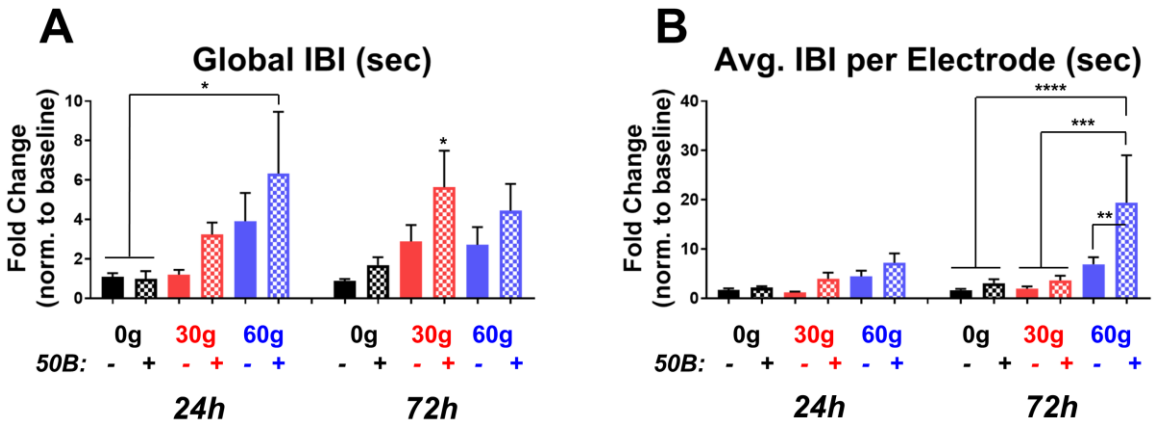

Figure 6-10: Interburst interval is affected by injury and BDNF treatment. Asterisks indicate significance with respect to the control (0g 0B) within that timepoint, and lines indicate significance between connected bars. **A.** At 24h post-injury, the average global IBI significantly increases for 60g 50B compared with uninjured networks (0g 0B and 0g 50B). At 72h post-injury, the average global IBI significantly increases for 30g 50B compared with the control. **B.** At 24 post-injury, the average IBI per electrode does not change. At 72h post-injury, the average IBI per electrode

significantly increases for 60g 50B compared with all other conditions. *p<0.05, **p<0.01, ***p<0.001, and ****p<0.0001 calculated by two-way ANOVA followed by Tukey's multiple comparisons test (comparing all conditions). No outliers were eliminated. n = 5-13 for all conditions. Error bars indicate SEM.

6.3.4 Synchronization of specific categories of connections is affected by mild and moderate injury with glutamate and BDNF treatment

To better understand how injury and BDNF treatment affect hippocampal networks, we investigated changes in overall synchronization. We calculated the Synchrony of Firing (SF) for each electrode and averaged all SF values for each MEA. The average synchronizations at 24 hr and 72 hr post-injury were then compared to the baseline synchronization. At 24 hr post-injury, average synchronization does not change for any of the injury conditions when compared with the control due to high variability in the control. However, the average synchronization of uninjured networks treated with BDNF significantly increases when compared with the control and with all injury conditions. At 72 hr post-injury, average synchronization does not significantly change between any of the conditions (Figure 6-11A). Even though BDNF treatment does not affect the synchronization of injured networks, the significant synchronization increase observed at 24 h post injury for uninjured networks treated with BDNF suggests that pre-treatment with BDNF may be help networks recover from injury.

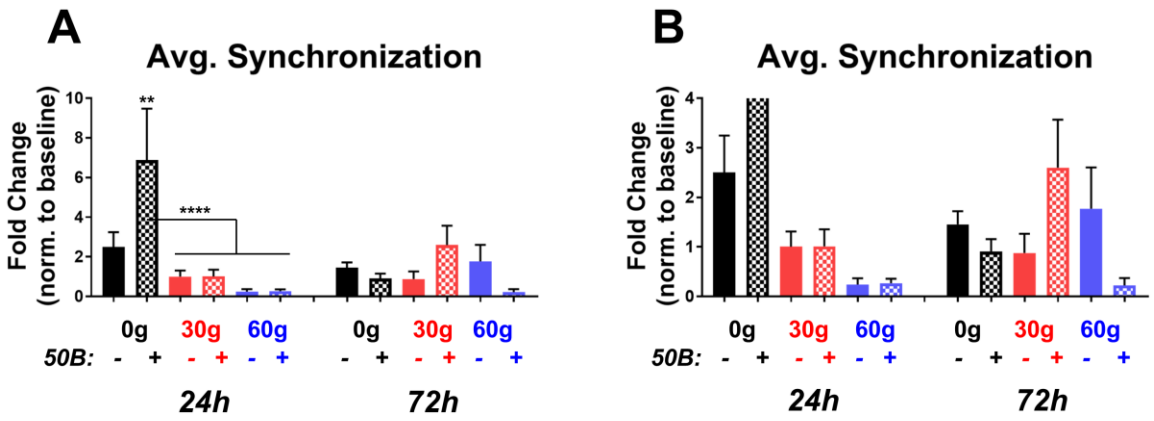

Figure 6-11: Average synchronization of networks is affected by injury and BDNF treatment.
Asterisks indicate significance with respect to the control (0g 0B) within that timepoint, and lines indicate significance between connected bars. **A.** At 24h post-injury, the average synchronization of 0g 50B significantly increases compared with the control and all injury conditions (30g 0B, 30g 50B, 60g 0B, 60g 50B). At 72h post-injury, the average synchronization does not significantly change. **B.** A zoomed-in view from A. **p<0.01, and ****p<0.0001 calculated by two-way ANOVA followed by Tukey's multiple comparisons test (comparing all conditions). Outliers eliminated using ROUT method with Q=1%. n = 7-11 for all conditions. Error bars indicate SEM.

In addition to examining changes in overall synchronization, we investigated how connections with specific initial synchronizations ($SF_{initial}$) changed after injury and BDNF treatment. Connections were categorized according to whether $SF_{initial}$ = 0-0.2, 0.2-0.4, 0.4-0.6, 0.6-0.8, or 0.8-1.0, and the average change for each category was calculated per MEA. When averaged on a per MEA basis, two changes are observed at 24 hr post-injury: 1) the synchronization of connections with $SF_{initial}$=0.4-0.6 significantly increases for uninjured networks treated with BDNF compared with moderately injured networks treated with BDNF, and 2) the synchronization of connections with $SF_{initial}$=0.6-0.8 significantly increases for uninjured networks treated with BDNF compared with moderately injured networks (significance not shown; Figure 6-12F).

Binned synchronization does not change after injury or with BDNF treatment at 72 hr post-injury (Figure 6-12G-J).

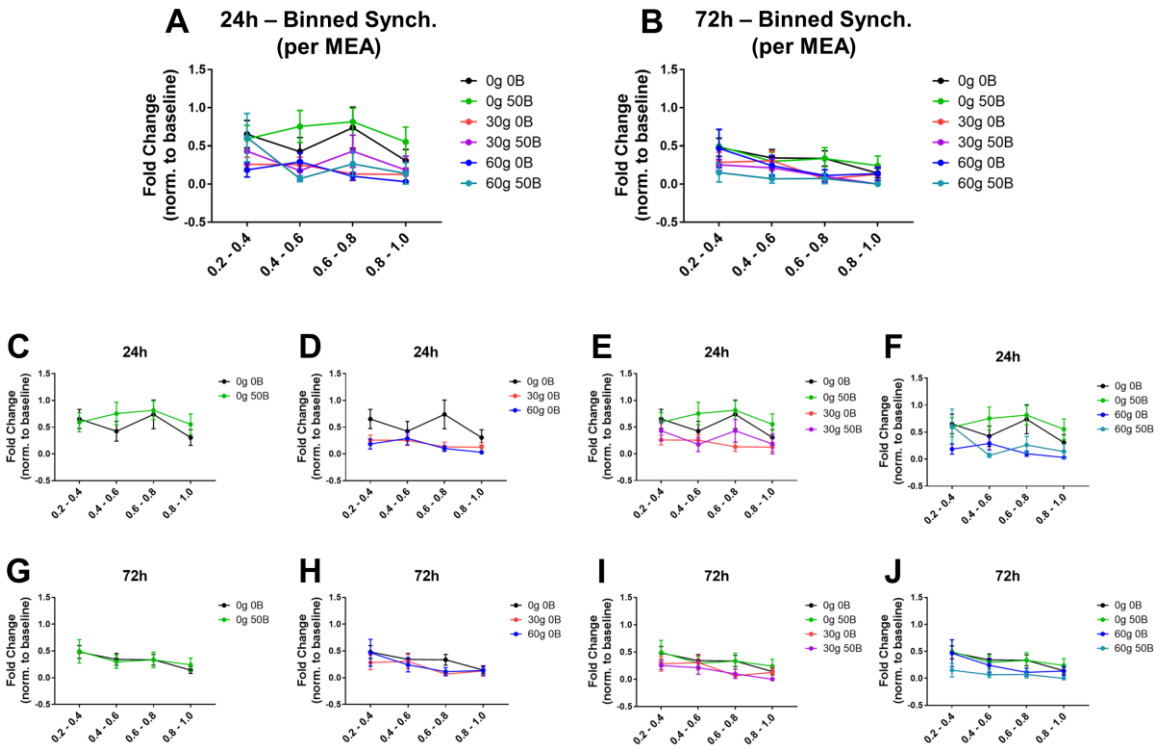

Figure 6-12: Neither injury with excess glutamate nor BDNF treatment modulates the synchronization of connections (averaged per MEA) with different baseline values.

Binned synchronization changes for electrodes with different initial synchronizations averaged per MEA. **A.** Overlaid synchronization changes at 24h post-injury. **B.** Overlaid synchronization changes at 72h post-injury. **C-F.** Binned synchronization changes at 24h post-injury. **G-J.** Binned synchronization changes at 72h post-injury. **C,G.** Binned synchronization comparisons between uninjured networks that either did or did not receive BDNF treatment at 24 and 72h post-injury, respectively. **D,H.** Binned synchronization comparisons between mildly and moderately injured networks compared with the control at 24 and 72h post-injury, respectively. **E,I.** Binned synchronization comparisons between uninjured networks and mildly injured networks at 24 and 72h post-injury, respectively. **F,J** Binned synchronization comparisons between uninjured networks and moderately injured networks at 24 and 72h post-injury, respectively. Statistics calculated by two-way ANOVA followed by Tukey's multiple comparisons test (comparing all conditions). No outliers were eliminated. For 0g 0B: n=3-8 at 24h and n=9-13 at 72h. For 0g 50B: n=3-5 at 24h and n=7-10 at 72h. For 30g 0B: n=5-9 at 24h and n=8-12 at 72h. For 30g 50B: n=5-9 at 24h and n=4-8 at 72h.

For 60g 0B: n=7-10 at 24h and n=11-13 at 72h. For 60g 50B: n=6-7 at 24h and n=6-10 at 72h. n indicates the number of MEAs. Error bars indicate SEM

We also examined the changes that occur when the synchronization of all connections is averaged, as this allows equal contribution from each connection on an electrode. The changes in SF were tracked for each category, and an average for each category was obtained.

Treatment with BDNF significantly affects the synchronization of connections between electrodes at 24 and 72 hr post-injury. At 24 hr post-injury, treatment of uninjured networks with BDNF significantly increases synchronization of all categories except $SF_{initial}$=0.6-0.8 compared with the control (Figure 6-13C). At 72 hr post-injury, treatment of uninjured networks with BDNF significantly increases synchronization of all categories except $SF_{initial}$=0.4-0.6 compared with the control (Figure 6-13G).

Injury with excess glutamate also affects the synchronization of connections at both the 24 hr and 72 hr timepoints. When comparing the effects of mild and moderate injury at the 24 hr timepoint, mild injury significantly decreases synchronization of all categories compared with the control, whereas moderate injury significantly decreases all categories of synchronization except $SF_{initial}$=0.2-0.4. Moreover, this same category significantly decreases for mildly injured networks compared with moderately injured networks (Figure 6-13D). At 72 hr post-injury, the synchronization of all categories significantly decreases for both mildly and moderately injured networks, and there is no significant difference for any category between the two injury levels (Figure 6-13H).

BDNF treatment protects distinct categories of connections after mild injury in a time-dependent manner. At 24 hr post-injury, mild injury significantly decreases

synchronization of all categories compared with the control, but when mildly injured networks are treated with BDNF, these same decreases are not present. Indeed, the synchronization significantly increases for mildly injured networks treated with BDNF for all categories of synchronization when compared with mildly injured networks (Figure 6-13E), indicating that BDNF plays a role in the protection of all connections from changes at 24 hr post-injury, regardless of baseline synchronization. At 72 hr post-injury, mild injury significantly decreases synchronization of all categories compared with the control, whether or not networks were treated with BDNF. However, synchronization significantly increases for $SF_{initial}$=0.2-0.4 and 0.4-0.6 for mildly injured networks that were treated with BDNF compared with mildly injured networks (Figure 6-13I), suggesting that BDNF only protects connections with lower baseline synchronization of mildly injured networks at 72 hr post-injury.

BDNF treatment does not protect synchronization after moderate injury. At 24 hr post-injury, moderate injury significantly decreases synchronization of three categories ($SF_{initial}$=0.4-0.6, 0.6-0.8, and 0.8-1.0) compared with the control, and when networks were treated with BDNF, synchronization significantly decreases across all categories. Additionally, synchronization significantly decreases for $SF_{initial}$=0.2-0.4 and 0.4-0.6 for moderately injured networks treated with BDNF compared with moderately injured networks (Figure 6-13F). At 72 hr post-injury, moderate injury significantly decreases synchronization of all categories, regardless of whether networks were treated with BDNF. Additionally, synchronization significantly decreases for $SF_{initial}$=0.4-0.6 for moderately injured networks treated with BDNF compared with moderately injured

networks (Figure 6-13H). These data suggest that BDNF is not neuroprotective for moderately injured networks and may actually exacerbate injury.

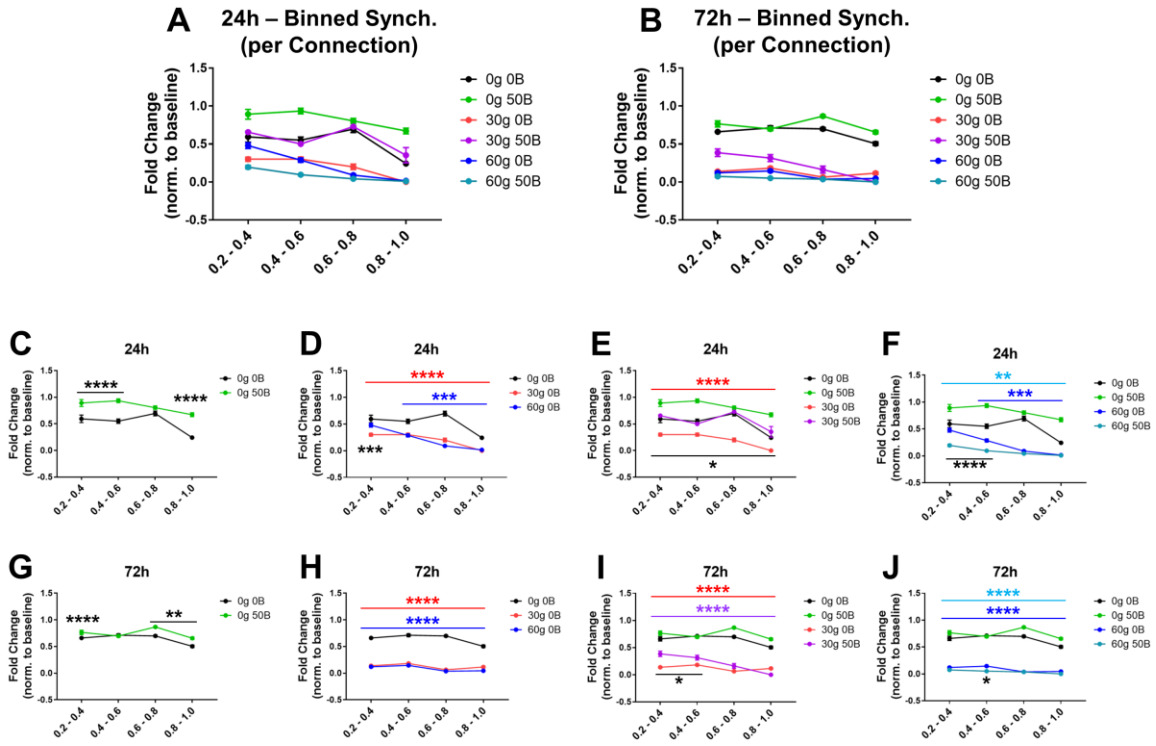

Figure 6-13: BDNF aids in the recovery of mildly injured networks with specific initial synchronizations.
Binned synchronization changes for connections with different initial synchronizations. **A.** Overlaid synchronization changes at 24h post-injury. **B.** Overlaid synchronization changes at 72h post-injury. **C-F.** Binned synchronization changes at 24h post-injury. **G-J.** Binned synchronization changes at 72h post-injury. **C,G.** Binned synchronization comparisons between uninjured networks that either did or did not receive BDNF treatment at 24 and 72h post-injury, respectively. **D,H.** Binned synchronization comparisons between mildly and moderately injured networks compared with the control at 24 and 72h post-injury, respectively. **E,I.** Binned synchronization comparisons between uninjured networks and mildly injured networks at 24 and 72h post-injury, respectively. **F,J.** Binned synchronization comparisons between uninjured networks and moderately injured networks at 24 and 72h post-injury, respectively. For C and G, black stars indicate significance between 0g 50B and the control. For D, black stars indicate significance between 30g 0B and 60g 0B. For E and I, black stars indicate significance between 30g 0B and 30g 50B. For F and J, light blue stars indicate significance between 60g 50B and the control, and black stars indicate significance between 60g 0B and 60g 50B. For D, E, H, and I, red stars indicate significance between 30g 0B and the control. For I, purple stars indicate significance between 30g 50B and the control. For D,

H, F, and J, dark blue stars indicate significance between 60g 0B and the control. *p<0.05, **p<0.01, ***p<0.001, and ****p<0.0001 calculated by two-way ANOVA followed by Tukey's multiple comparisons test (comparing all conditions). No outliers were eliminated. For 0g 0B: n=134-236 at 24h and n=316-746 at 72h. For 0g 50B: n=142-280 at 24h and n=472-1164 at 72h. For 30g 0B: n=178-866 at 24h and n=262-1220 at 72h. For 30g 50B: n=26-470 at 24h and n=28-362 at 72h. For 60g 0B: n=324-688 at 24h and n=466-1146 at 72h. For 60g 50B: n=288-810 at 24h and n=406-1026 at 72h. n indicates the number of connections. Error bars indicate SEM.

Treatment with 50 ng/ml BDNF significantly increases the overall average synchronization of uninjured networks at 24 hr post-injury when compared with untreated networks. This increase is mirrored by that seen when the changes in specific categories of initial synchronization are examined. While the overall average synchronization of uninjured networks does not significantly change compared with the control at 72 hr post-injury, specific categories of synchronization significantly increase. When examining specific categories of synchronization, it also becomes clear that mild and moderate injury affect synchronization uniquely and respond to BDNF in distinct ways. Moderate injury does not cause a decrease for $SF_{initial}$=0.2-0.4 at 24 hr post injury, but mild injury does. Moreover, BDNF may be neuroprotective for mildly injured networks but not for moderately injured networks.

6.4 Discussion

In this chapter, we employed MEA technology to examine how glutamate-induced excitotoxicity alters the networks dynamics of hippocampal neurons and whether treatment with BDNF can be neuroprotective after this type of injury. We accomplished this goal by recording the spontaneous activity of hippocampal networks prior to injury at DIV 14 when synaptic connections are well established, inducing mild or moderate

injury, and then recording at 24 hr and 72 hr post injury. Importantly, this timeline matches that used in our previous work, which explored how cortical neurons are affected by glutamate-induced injury (Kutzing, Luo et al. 2011) and how memantine promotes recovery of specific connections (Kutzing, Luo et al. 2012). The work in this chapter extends previous work from our laboratory to understand how the network dynamics of hippocampal neurons are affected by injury.

How does glutamate-induced excitotoxicity affect hippocampal networks compared with cortical networks? First, we found hippocampal neurons are much more sensitive to glutamate-induced injury than are cortical neurons. Attempting to induce mild and moderate injury in hippocampal networks by using the same concentrations of glutamate (175 and 250 μM) that had been used for cortical neurons (Kutzing, Luo et al. 2011) resulted in abolishment of spiking activity, bursting activity, and, most importantly, average synchronization. We found that inducing injury with 30 and 60 μM glutamate is sufficient to induce mild and moderate injury, respectively, in hippocampal networks. Hippocampal neurons are likely more sensitive than cortical neurons due to differences in how the two types of neurons respond to input. Low frequency stimulation induces long-term depression in hippocampal neurons but long-term potentiation in cortical neurons (Komatsu, Fujii et al. 1988, Dudek and Bear 1992, Mulkey and Malenka 1992, Kirkwood, Dudek et al. 1993), suggesting that there exist inherently different firing rates in the cortex and hippocampus that contribute to the differing responses to glutamate-induced excitotoxicity.

Despite the need to use different concentrations of glutamate, both studies resulted in mild to moderate injury of neuronal networks, and specific parameters

describing network activity show similar trends in resulting changes. For example, the spike rate and burstlet rate significantly decrease for moderately injured networks of both hippocampal and cortical neurons. However, the average overall synchronization of cortical networks does not decrease after mild or moderate injury (Kutzing, Luo et al. 2011), whereas this parameter does significantly decrease for moderately injured hippocampal networks. Moreover, distinct categories of synchronization are altered differently in hippocampal and cortical networks. Mild injury to cortical networks significantly decreases the synchronization of weak and strong connections while sparing medium connections, but moderate injury significantly decreases all categories of synchronization (Kutzing, Luo et al. 2011). In contrast, at 24 hr post-injury, mild injury to hippocampal networks significantly decreases all categories of initial synchronization whereas moderate injury spares the weakest category. These differences in changes to synchronization may reflect the dissimilar vulnerability of hippocampal and cortical networks to glutamate-induced excitotoxicity, specifically of distinct categories of connections.

Our results suggest a role for BDNF in modulating the recovery of hippocampal networks that is dependent on both time and level of injury. BDNF is known to be a pro-survival factor (Merlio, Ernfors et al. 1993, Kiprianova, Freiman et al. 1999, Kiprianova, Sandkühler et al. 1999, Rostami, Krueger et al. 2014), but the effects of BDNF treatment on the network dynamics of injured hippocampal neurons are not clear. We initially hypothesized, based on our work in Chapter 5, that BDNF would promote the recovery of average overall synchronization at 72 hr after mild or moderate injury, since this would match the treatment length in our previous studies. Instead, we found that BDNF

treatment significantly increases the synchronization of uninjured cultures at 24 hr post-injury but has no effect on mildly or moderately injured networks. BDNF does not prevent decreases in any global measure of activity (spiking, bursting, or global bursting), yet it blocks changes to distinct connection types after mild injury. It is possible that BDNF is actually excitotoxic when applied externally during the acute phase of injury (Rudge, Mather et al. 1998, Blaha, Raghupathi et al. 2000). Furthermore, BDNF and TrkB are involved in the early excitotoxic response (Mudó, Persson et al. 1993, Goutan, Martí et al. 1998), and it is possible that we did not extend our study far enough into the recovery period to observe any neuroprotective effects exerted by BDNF. Indeed, our results from Chapter 5 suggest that BDNF exerts long-term effects on network dynamics, so it is possible that the neuroprotective effects of BDNF would be observed at one week post-injury or later. It is also possible that by decreasing global activity, BDNF exerts neuroprotective effects. BDNF prevents decreases in the interspike intervals and in the number of burstlets in global bursts, and these changes to spike timing may represent the underlying mechanism for protection of distinct categories of synchronization. Examining changes in network synchronization is crucial as synchronization is thought to be particularly important for network viability and is required for many aspects of brain function (Womelsdorf, Schoffelen et al. 2007). A summary of significant changes is included in Table 6-1.

	Injury effect (24h)	BDNF effect (24h)	Injury effect (72h)	BDNF effect (72h)
Spike Rate	↓ 60	X	↓ 30, 60	X
ISI (Total & Avg.)	X	X	↑ 60	✓
Burstlet Rate	↓ 60	X	↓ 30, 60	X
Global Bursts	↓ 60	X	X	X
# Burstlets per Global Burst	↓ 60	✓	X	X
Avg. Synch.	X	↑	X	X
Binned Synch.	↓ 30, 60	✓ 30 X 60	↓ 30, 60	✓ 30 X 60

Table 6-1: Summary of significant changes to the network dynamics of hippocampal neurons after injury with glutamate and recovery with BDNF treatment.

Similar to the work in Chapter 5, the work in this chapter possesses limitations caused by the experimental system employed. Dissociated neurons cultured in Neurobasal medium (Brewer, Torricelli et al. 1993), or similar culture medium such as NbActiv4 (Brewer, Boehler et al. 2008), possess very few mature astroglial cells and no oligodendrocytes (Swiatkowski and Firestein 2017, unpublished data), which is not representative of *in vivo* networks. In addition to being important regulators of neuronal communication and network development (Eroglu and Barres 2010), glial cells are also crucial to the injury response (Frisen, Verge et al. 1993, Kiprianova, Freiman et al. 1999). In particular, a subset of astrocytes express excitatory amino acid transporters 1 and 2 (EAAT1 and 2, respectively) and, thus, help to reduce the amount of excess glutamate after excitotoxic injury (Ross and Cleveland 2006, Van Landeghem, Weiss et al. 2006, Yi and Hazell 2006). A network without mature glia will respond very differently to injury than one with a substantial population of mature glia. It is possible that the hippocampal networks used in this chapter were more sensitive to glutamate-induced excitotoxicity

than the *in vivo* hippocampus would be due to a lack of mature glial cells. Thus, this work represents a study of the dissociated culture response to excitotoxicity in the absence of a mature glial population.

Additionally, the networks used in this study are derived from embryonic rats. While the networks are allowed to mature for 14 days *in vitro* prior to injury, they are still developing and are plastic. The injury response is different in mature networks cultured on MEAs for several months, but it would be technically challenging to ensure neuronal survival and prevent contamination for a longer timepoint in culture. Thus, the work in this chapter illuminates how developing networks respond to injury with excess glutamate and treatment with BDNF, but the findings might differ if mature networks were studied. Overall, the work in this chapter suggests that BDNF is involved in protection of developing networks from excitotoxic injury, but its role has not been made clear by the parameters that were examined. Future work is ongoing to induce long-term potentiation with bicuculline and record from the networks after injury, which would allow us to understand whether BDNF preserves induced synchronization in developing networks (Kang, Cao et al. 2015).

6.5 Acknowledgements

I would like to acknowledge Ana Rodriguez for determining the techniques necessary for successfully culturing dissociated hippocampal neurons on MEAs.

CHAPTER 7: SUMMARY AND FUTURE DIRECTIONS

Neuronal network function depends on correctly formed dendritic arbors and proper synaptic integration of neurons into the network. Dysregulation of dendritic morphology affects network function and results in cognitive deficits present in many diseases and neurodegenerative disorders (Zoghbi 2003, Tau and Peterson 2010, Kulkarni and Firestein 2012). In this dissertation, we explored the roles of BDNF in the regulation of dendrite morphology, modulation of hippocampal neuron network development, and neuroprotection of networks after glutamate-induced excitotoxicity. This work increases our understanding of how BDNF affects the structure of single hippocampal neurons and the activity of hippocampal neuronal networks.

In Chapter 2, we explored how using distinct methods of labeling dendrites improves conventional Sholl analysis. Our laboratory has previously shown that cypin increases dendrites (Akum, Chen et al. 2004, Chen, Lucas et al. 2005, Chen and Firestein 2007, Fernandez, Welsh et al. 2008), but we had not examined the spatial locations of order-specific increases. We overexpressed cypin in hippocampal neurons at two developmental time points (DIV 6-10 and DIV 10-12), and we employed three different methods of dendrite labeling: Inside-Out, RIT, and Tips-In. Using order-specific Sholl analyses, we learned the following: 1) when cypin is overexpressed from DIV 6-10, the increases in branching are mainly due to increased primary and terminal branches close to the soma, and 2) when cypin is overexpressed from DIV 10-12, the increases in branching are mainly due to increased primary and higher order dendrites (O'Neill, Akum et al. 2015). The work in Chapter 2 illustrates the importance of employing

multiple types of Sholl analysis to better understand the changes that occur to the dendritic arbor.

In Chapter 3, we examined how BDNF modulates the dendritic arbor when applied locally via microbeads at DIV 7 for treatment lengths of between 5 and 72 hours, and we compared these results with our previously published work. Bath application of BDNF increases proximal dendrite branching after 72 hours (Kwon, Fernandez et al. 2011), whereas bead application increases distal branching after 48 hours and both proximal and distal branching after 72 hours. We also found that cypin plays a role in BDNF-mediated increases after 24 hours of bead application but not for other treatment lengths. This finding differs from our previously published work, in which cypin knockdown prevents BDNF-mediated increases in dendrites after 72 hours (Kwon, Fernandez et al. 2011). Moreover, we found that application of BDNF-coupled beads attenuates the natural pruning process that occurs between DIV 7-10. The work in Chapter 3 reveals how BDNF regulates development of the dendritic arbor differently depending on the method of application. Future work will investigate the pathways and receptors that are responsible for changes to the dendritic arbor mediated by BDNF-coated bead application. Is the MAPK pathway involved, as it is when BDNF is administered as a bath application, or are other pathways responsible for the observed changes? We will also investigate how TrkB signaling affects changes caused by local administration of BDNF. Does local administration of BDNF stimulate both full length TrkB and truncated TrkB? If so, does this differ from bath application of BDNF? Future studies will probe the mechanisms behind changes that BDNF-coated bead application causes to the dendritic arbor.

In Chapter 4, we explored how overexpression of BDNF regulates arbor development and how changes to the arbor depend on the targeting of BDNF mRNA to specific intracellular locations. We overexpressed BDNF in hippocampal neurons from DIV 7-10 and observed how targeting of BDNF mRNA with the short, long, or both short & long 3' UTRs influences dendrite branching. While we initially hypothesized that overexpression of BDNF mRNA containing the long 3' UTR would exert the greatest effect on distal dendrites because it targets BDNF mRNA to both the soma and dendrites, surprisingly, we found that overexpression of mRNA containing the long 3' UTR significantly increases proximal dendrites. Interestingly, overexpression of BDNF mRNA lacking a 3' UTR increases dendrites over the greatest area of the arbor, and overexpression of BDNF mRNA containing the short 3' UTR increases dendrites more distally than does overexpression of mRNA containing the long 3' UTR. Furthermore, overexpression of BDNF mRNA containing both the short & long 3' UTR results in an average of the effects that overexpression of BDNF mRNA containing either the short or long 3' UTR exerts alone. These data suggest that mRNA containing the short and containing the long 3' UTRs play distinct roles in development of the dendritic arbor due to specific intracellular targeting of BDNF mRNA. Future work will investigate the role of TrkB signaling in changes to the dendritic arbor caused by the overexpression of distinct transcripts of BDNF mRNA. Is expression of one of the TrkB isoforms enhanced by overexpression of certain BDNF mRNAs, and if so, where in the cell do these changes in receptor content occur? Do these changes play a role in dendritic arbor development? Future work will answer these questions and will also attempt to determine the intracellular pathways responsible for changes to the arbor.

In Chapter 5, we studied neurons at the network level to understand how BDNF treatment affects hippocampal neuron network dynamics. We built on the work in the previous chapters that examined how BDNF affects the dendritic arbor by employing MEA technology to understand how BDNF modulates network development. In this chapter, networks were treated with BDNF in bath application at two concentrations from DIV 7-10, and we recorded the spontaneous activity of hippocampal networks. We initially hypothesized that BDNF treatment would promote dendritogenesis and synaptogenesis in individual neurons, thereby increasing both synchronization and overall activity in networks immediately after treatment ended. This hypothesis was partially correct. Higher concentrations of BDNF increase overall synchronization, but lower concentrations of BDNF decrease spiking activity. Moreover, BDNF treatment does not change any parameter immediately after treatment; significant changes are only observed one week after treatment ends. In addition to increasing synchronization, the higher concentration of BDNF increases spike variability, as measured by the Fano factor, and the number of spikes per burstlet. Higher Fano factor values suggest that connections among neurons are clustered as opposed to being uniformly distributed (Litwin-Kumar and Doiron 2012), and increased number of spikes per burstlet supports the notion that more neurons are firing together. This would indicate that morphological changes caused by treatment with the higher concentration of BDNF promote the formation of synchronized subnetworks within the larger hippocampal network. Future work will determine whether BDNF treatment changes the ratio of excitatory to inhibitory synapses and whether TrkB signaling is responsible for the observed increases in synchronization. We will attempt to directly correlate how

structural changes to individual neurons, whether at the dendrite level or synapse level, affect the network dynamics of hippocampal neurons.

In Chapter 6, we extended our MEA work to an *in vitro* model of TBI and explored whether BDNF is neuroprotective at higher concentrations. First, we compared how hippocampal networks undergo injury to how cortical neurons undergo injury (Kutzing, Luo et al. 2011). We found that hippocampal networks are more sensitive to glutamate-induced injury: the same concentrations of glutamate abolish spiking, bursting, and synchronization in hippocampal networks do not do so for cortical networks. Thus, we treated hippocampal networks with lower concentrations of glutamate for a shorter time than we did with cortical networks, and we studied whether BDNF is neuroprotective after mild and moderate injury of hippocampal networks. We hypothesized that the overall activity and synchronization of injured networks would decrease after injury and, based on how BDNF affects network development, that BDNF would restore synchronization to baseline levels. Spike rate and burstlet rate decrease at 24 hours after moderate injury and at 72 hours after mild or moderate injury. However, when examining conventional parameters, we found that BDNF only restores the interspike interval (both Total ISI and average ISI per electrode) and the number of burstlets per global burst of moderately injured networks to control levels. The neuroprotective effects of BDNF only become clear when examining how connections with specific initial synchronizations change after injury and BDNF treatment. Both mild and moderate injury cause decreases in binned synchronization at 24 and 72 hours post-injury, but BDNF blocks changes to all categories of synchronization at 24 hours after mild injury and partially blocks changes to weaker initial synchronizations at 72 hours

after mild injury. This work illustrates the importance of examining specific categories of connections in addition to global activity parameters. Future work will explore BDNF further as a neuroprotective agent. Does local administration of BDNF or overexpression of distinct BNDF mRNAs improve neuroprotection? If so, what are the mechanisms that bring about these changes? We will complement our MEA studies with imaging at the synaptic level to reveal changes that occur to networks during recovery. We will also extend our studies to one week-post injury to determine whether BDNF exerts long-term effects on network recovery that are not detected within 72 hours after injury.

The importance of proper targeting, packaging, and secretion of BDNF to the development of neuronal structure and network function cannot be overemphasized. Improper expression of BDNF has been linked to cognitive diseases, ranging from Alzheimer's Disease to schizophrenia (Szeszko, Lipsky et al. 2005). Additionally, several studies have linked polymorphisms in the BDNF gene to impairments in memory. Of interest is one particular single nucleotide polymorphism (SNP), known as Val66Met, that results in a Valine to Methionine mutation at codon 66 of the *BDNF* gene. This alteration in the *BDNF* gene affects intracellular trafficking and packaging of pro-BDNF, thereby affecting the secretion and extracellular abilities of mature BDNF. This SNP affects cognitive functioning in healthy individuals and in those who have experienced TBI, underscoring the importance of BDNF signaling to cognitive function (Egan, Kojima et al. 2003, Barbey, Colom et al. 2014). Thus, BDNF is crucial to both network development and network maintenance.

Taken together, this dissertation reveals roles for BDNF in the development of neuronal morphology, maturation of network activity, and neuroprotection after mild

excitotoxic injury. However, all studies in this dissertation were performed *in vitro* with relatively young networks that lack oligodendrocytes and a substantial mature astroglial population, as discussed in Chapters 5 and 6. This type of experimental setup limits the conclusions that can be made from the work in this dissertation, and *in vivo* studies should be performed to verify how BDNF affects neuronal structure, network function, and response to excitotoxic injury in the intact hippocampus. It would also be ideal to study how immature versus mature networks are affected by BDNF treatment and injury, as BDNF treatment may exert beneficial effects at one stage of development and harmful effects, or no effect, at another stage.

Finally, to fully understand how different sources of BDNF (bath application, local administration, and overexpression) affect neuronal structure and function, dendrite branching experiments should be combined with both single neuron electrophysiology and MEA experiments. Understanding how, for example, local administration of BDNF not only affects dendritic arborization but also single neuron activity and network activity would provide a more complete picture of how changes to the arbor affect neuronal function. Moreover, neuronal network modeling could be incorporated with adjustable parameters that take into account neuronal morphology (*i.e.* more proximal dendrites or fewer excitatory synapses). Thus, future work will attempt to directly correlate changes in single neuron morphology to changes in network dynamics, and ideally, these changes would be observed at the *in silico*, *in vitro*, and *in vivo* levels.

REFERENCES

Aguado, F., et al. (2003). "BDNF regulates spontaneous correlated activity at early developmental stages by increasing synaptogenesis and expression of the K+/Cl- co-transporter KCC2." Development **130**: 1267-1280.

Aid, T., et al. (2007). "Mouse and rat BDNF gene structure and expression revisited." Journal of Neuroscience Research **85**: 525-535.

Akum, B. F., et al. (2004). "Cypin regulates dendrite patterning in hippocampal neurons by promoting microtubule assembly." Nature Neuroscience **7**(2): 145-152.

Almeida, R. D., et al. (2005). "Neuroprotection by BDNF against glutamate-induced apoptotic cell death is mediated by ERK and PI3-kinase pathways." Cell Death and Differentiation **12**: 1329-1343.

An, J. J., et al. (2008). "Distinct role of long 3' UTR BDNF mRNA in spine morphology and synaptic plasticity in hippocampal neurons." Cell **134**(1): 175-187.

Armanini, M. P., et al. (1995). "Truncated and catalytic isoforms of trkB are co-expressed in neurons of rat and mouse CNS." Eur J Neurosci **7**(6): 1403-1409.

Arundine, M. and M. Tymianski (2004). "Molecular mechanisms of glutamate-dependent neurodegeneration in ischemia and traumatic brain injury." Cellular and Molecular Life Sciences **61**: 657-688.

Ascoli, G. A., et al. (2007). "NeuroMorpho.Org: a central resource for neuronal morphologies." J Neurosci **27**(35): 9247-9251.

Baj, G., et al. (2016). "Signaling pathways controlling activity-dependent local translation of BDNF and their localization in dendritic arbors." Journal of Cell Science **129**: 2852-2864.

Baker, R. E., et al. (1998). "Growth of pyramidal, but not non-pyramidal, dendrites in long-term organotypic explants of neonatal rat neocortex chronically exposed to neurotrophin-3." Eur J Neurosci **10**(3): 1037-1044.

Barbacid, M. (1994). "The Trk family of neurotrophin receptors." Journal of Neurobiology **25**(11): 1386-1403.

Barbey, A. K., et al. (2014). "Preservation of general intelligence following traumatic brain injury: Contributions of the Met66 Brain-Derived Neurotrophic Factor." PLoS ONE **9**(2): e88733.

Biffi, E., et al. (2013). "The influence of neuronal density and maturation on network activity of hippocampal cell cultures: a methodological study." PLoS ONE **8**(12): e83899.

Biffo, S., et al. (1995). "Selective binding and internalisation by truncated receptors restrict the availability of BDNF during development." Development **121**(8): 2461-2470.

Blaha, G. R., et al. (2000). "Brain-derived neurotrophic factor administration after traumatic brain injury in the rat does not protect against behavioral or histological deficits." Neuroscience **99**(3): 483-493.

Bramham, C. R. and D. G. Wells (2007). "Dendritic mRNA: transport, translation and function." Nature Reviews Neuroscience **8**: 776-789.

Branco, T. and M. Häusser (2010). "The single dendritic branch as a fundamental functional unit in the nervous system." Current Opinion in Neurobiology **20**(4): 494-502.

Brewer, G. J., et al. (2008). "NbActiv4 medium improvement to Neurobasal/B27 increases neuron synapse densities and network spike rates on multielectrode arrays." Journal of Neuroscience Methods **170**(2): 181-187.

Brewer, G. J., et al. (2009). "Neuron network activity scales exponentially with synapse density." Journal of Neural Engineering **6**(1): 014001.

Brewer, G. J., et al. (1993). "Optimized survival of hippocampal neurons in B27-supplemented Neurobasal, a new serum-free medium combination." Journal of Neuroscience Research **35**(5): 567-576.

Buonanno, A. and R. D. Fields (1999). "Gene regulation by patterned electrical activity during neural and skeletal muscle development." Current Opinion in Neurobiology **9**: 110-120.

Cannon, R. C., et al. (1998). "An on-line archive of reconstructed hippocampal neurons." Journal of Neuroscience Methods **84**: 49-54.

Caserta, F., et al. (1995). "Determination of fractal dimension of physiologically characterized neurons in two and three dimensions." J Neurosci Methods **56**(2): 133-144.

Chao, M. V. (2003). "Neurotrophins and their receptors: a convergence point for many signalling pathways." Nat Rev Neurosci **4**(4): 299-309.

Charych, E. I., et al. (2006). "Activity-independent regulation of dendrite patterning by postsynaptic density protein PSD-95." Journal of Neuroscience **26**(40): 10164-10176.

Chen, H. and B. L. Firestein (2007). "RhoA regulates dendrite branching in hippocampal neurons by decreasing cypin protein levels." Journal of Neuroscience **27**(31): 8378-8386.

Chen, M., et al. (2005). "A novel role for Snapin in dendrite patterning: Interaction with Cypin." Molecular Biology of the Cell **16**: 5103-5114.

Chiappalone, M., et al. (2008). "Network plasticity in cortical assemblies." European Journal of Neuroscience **28**: 221-237.

Chiappalone, M., et al. (2007). "Network dynamics and synchronous activity in cultured cortical neurons." International Journal of Neural Systems **17**(2): 87-103.

Churchland, M. M., et al. (2010). "Stimulus onset quenches neural variability: a widespread cortical phenomenon." Nature Neuroscience **13**(3): 369-378.

Cline, H. T. (2001). "Dendritic arbor development and synaptogenesis." Current Opinion in Neurobiology **11**: 118-126.

Coronado, V. G., et al. (2011). "Surveillance for Traumatic Brain Injury-Related Deaths: United States, 1997-2007." Surveillance Summaries **60**(SS05): 1-32.

Deinhardt, K. and M. V. Chao (2014). "Shaping neurons: Long and short range effects of mature and proBDNF signalling upon neuronal structure." Neuropharmacology **76**: 603-609.

Dijkhuizen, P. A. and A. Ghosh (2005). "BDNF regulates primary dendrite formation in cortical neurons via the PI3-kinase and MAP kinase signaling pathway." The Journal of Neurobiology **62**(2): 278-288.

Dotti, C. G., et al. (1988). "The establishment of polarity by hippocampal neurons in culture." Journal of Neuroscience **8**(4): 1454-1468.

Dudek, S. M. and M. F. Bear (1992). "Homosynaptic long-term depression in area CA1 of hippocampus and effects of N-methyl-D-aspartate receptor blockade." Proceedings of the National Academy of Sciences **89**(10): 4363-4367.

Edelmann, E., et al. (2014). "Pre- and postsynaptic twists in BDNF secretion and action in synaptic plasticity." Neuropharmacology **76**: 610-627.

Eden, U. T. and M. A. Kramer (2010). "Drawing inferences from Fano factor calculations." Journal of Neuroscience Methods **190**(1): 194-152.

Egan, M. F., et al. (2003). "The BDNF val66met polymorphism affects activity-dependent secretion of BDNF and human memory and hippocampal function." Cell **112**: 257-269.

Eroglu, C. and B. A. Barres (2010). "Regulation of synaptic connectivity by glia." Nature **468**: 223-231.

Fernandez, J. R., et al. (2008). "Structural characterization of the zinc binding domain in cytosolic PSD-95 interactor (cypin): Role of zinc binding in guanine deamination and dendrite branching." Proteins **70**(3): 873-881.

Firestein, B. L., et al. (1999). "Cypin: a cytosolic regulator of PSD-95 postsynaptic targeting." Neuron **24**(3): 659-672.

Frega, M., et al. (2012). "Cortical cultures coupled to Micro-Electrode Arrays: A novel approach to perform *in vitro* excitotoxicity testing." Neurotoxicology and teratology **34**(116-127).

Frisen, J., et al. (1993). "Characterization of glial trkB receptors: differential response to injury in the central and peripheral nervous systems." Proc Natl Acad Sci U S A **90**(11): 4971-4975.

Fryer, R. H., et al. (1996). "Developmental and mature expression of full-length and truncated TrkB receptors in the rat forebain." Journal of Compartaive Neurology **374**: 21-40.

Fuchs, E., et al. (2007). "Coemergence of regularity and complexity during neural network development." Developmental Neurobiology **67**(13): 1802-1814.

Fukuchi, M. and M. Tsuda (2010). "Involvement of the 3'-untranslated region of the brain-derived neurotrophic factor gene in activity-dependent mRNA stabilization." Journal of Neurochemistry **115**: 1222-1233.

Gambazzi, L., et al. (2010). "Diminished activity-dependent BDNF expression underlies cortical neuron microcircuit hypoconnectivity resulting from exposure to mutant huntingtin fragments." The Journal of Pharmacology and Experimental Therapeutics **335**(1): 13-22.

Gao, X., et al. (2011). "Moderate traumatic brain injury causes acute dendritic and synaptic degeneration in the hippocampal dentate gyrus " PLoS ONE **6**(9): e24566.

Ghosh, A., et al. (1994). "Requirement for BDNF in activity-dependent survival of cortical neurons." Science **263**: 1618-1623.

Giehl, K. M. and W. Tetzlaff (1996). "BDNF and NT-3, but not NGF, prevent axotomy-induced death of rat corticospinal neurons *in vivo*." European Journal of Neuroscience **8**: 1167-1175.

Gladding, C. M. and L. A. Raymond (2011). "Mechanisms underlying NMDA receptor synaptic/extrasynaptic distribution and function." Molecular and Cellular Neuroscience **48**: 208-320.

Gopal, K. V. (2003). "Neurotoxic effects of mercury on auditory cortex networks growing on microelectrode arrays: a preliminary analysis." Neurotoxicology and teratology **25**(1): 69-76.

Gottmann, K., et al. (2009). "BDNF signaling in the formation, maturation and plasticity of glutamatergic and GABAergic synapses." Experimental Brain Research **199**: 203-234.

Goutan, E., et al. (1998). "BDNF, and full length and truncated TrkB expression in the hippocampus of the rat following kainic acid excitotoxic damage. Evidence of complex time-dependent and cell-specific responses." Molecular Brain Research **59**(2): 151-164.

Gross, G. W., et al. (1977). "A new fixed-array multi-microelectrode system designed for long-term monitoring of extracellular single unit neuronal activity in vitro." Neuroscience Letters **6**: 101-105.

Gullo, F., et al. (2014). "Multi-electrode array study of neuronal cultures expressing nicotinic β2-V287L subunits, linked to autosomal dominant nocturnal frontal lobe epilepsy. An in vitro model of spontaneous epilepsy." Frontiers in Neural Circuits **8**: 87.

Hales, C. M., et al. (2010). "How to culture, record and stimulate neuronal networks on micro-electrode arrays (MEAs)." Journal of Visualized Experiments **39**(39).

Hansen, H. H., et al. (2004). "Mechanisms leading to disseminated apoptosis following NMDA receptor blockade in the developing ratbrain." Neurobiology of Disease **16**: 440-453.

Hao, J., et al. (2009). "An arithmetic rule for spatial summation of excitatory and inhibitory inputs in pyramidal neurons." Proceedings of the National Academy of Sciences **106**: 21906-21911.

Hardingham, G. E. and H. Bading (2010). "Synaptic versus extrasynaptic NMDA receptor signalling: implications for neurodegenerative disorders." Nature Reviews Neuroscience **11**: 682-696.

Hardingham, G. E., et al. (2002). "Extrasynaptic NMDARs oppose synaptic NMDARs by triggering CREB shut-off and cell death pathways." Nature Neuroscience **5**(5): 405-414.

Hartmann, M., et al. (2004). "Truncated TrkB receptor-induced outgrowth of dendritic filopodia involves the p75 neurotrophin receptor." Journal of Cell Science **117**: 5803-5814.

Harward, S. C., et al. (2016). "Autocrine BDNF–TrkB signalling within a single dendritic spine." Nature **538**(7623): 99-103.

He, J., et al. (2005). "BDNF acutely modulates synaptic transmission and calcium signalling in developing cortical neurons." Cellular Physiology and Biochemistry **16**(1-3): 69-76.

Hofer, M. M. and Y.-A. Bardet (1998). "Brain-derived neurotrophic factor prevents neuronal death in vivo." Nature **331**: 261-262.

Horch, H. W. and L. C. Katz (2002). "BDNF release from single cells elicits local dendritic growth in nearby neurons." Nature Neuroscience **5**(11): 1177-1184.

Horch, H. W., et al. (1999). "Destabilization of cortical dendrites and spines by BDNF." Neuron **23**: 353-364.

Huang, Z. J., et al. (1999). "BDNF regulates the maturation of inhibition and the critical period of plasticity in mouse visual cortex." Cell **98**: 739-755.

Ikonomidou, C., et al. (1999). "Blockade of NMDA receptors and apoptotic neurodegeneration in the developing brain." Science **283**(70).

Ikonomidou, C. and L. Turski (2002). "Why did NMDA receptor antagonists fail clinical trials for stroke and traumatic brain injury?" The Lancet Neurology **1**: 383-386.

Ivanov, A., et al. (2006). "Opposing role of synaptic and extrasynaptic NMDA receptors in regulation of the extracellular signal-regulated kinases (ERK) activity in cultured rat hippocampal neurons." The Journal of Physiology **572**(Pt 3): 789-798.

Ji, Y., et al. (2010). "Acute and gradual increases in BDNF concentration elicit distinct signaling and functions in neurons." Nature Neuroscience **13**(3): 302-310.

Jiang, X., et al. (2005). "The excitoprotective effect of N-methyl-D-aspartate receptors is mediated by a brain-derived neurotrophic factor autocrine loop in cultured hippocampal neurons." The Journal of Neurochemistry **94**: 713-722.

Jin, X., et al. (2003). "Brain-derived neurotrophic factor mediates activity-dependent dendritic growth in nonpyramidal neocortical interneurons in developing organotypic cultures." J Neurosci **23**(13): 5662-5673.

Johnstone, A. F. M., et al. (2010). "Microelectrode arrays: A physiologically based neurotoxicity testing platform for the 21st century." NeuroToxicology **31**: 331-350.

Kang, W. H., et al. (2015). "Alterations in hippocampal network activity after *in vitro* traumatic brain injury." Journal of Neurotrauma **32**: 1011-1019.

Kapucu, F. E., et al. (2012). "Burst analysis tool for developing neuronal networks exhibiting highly varying action potential dynamics." Frontiers in Computational Neuroscience **6**(38).

Kazanis, I. (2005). "CNS injury research; reviewing the last decade: Methodological errors and a proposal for a new strategy." Brain Research Reviews **50**: 377-386.

Keefer, E. W., et al. (2001). "Characterization of acute neurotoxic effects of trimethylolpropane phosphate via neuronal network biosensors." Biosensors and Bioelectronics **16**: 513-525.

Kiprianova, I., et al. (1999). "Brain-derived neurotrophic factor prevents neuronal death and glial activation after global ischemia in the rat." Journal of Neuroscience Research **56**: 21-27.

Kiprianova, I., et al. (1999). "Brain-Derived Neurotrophic Factor Improves Long-Term Potentiation and Cognitive Functions after Transient Forebrain Ischemia in the Rat." Experimental Neurology **159**: 511-519.

Kirkwood, A., et al. (1993). "Common forms of synaptic plasticity in the hippocampus and neocortex *in vitro*." Science **260**(5113): 1518-1521.

Koleske, A. J. (2013). "Molecular mechanisms of dendrite stability." Nature Reviews Neuroscience **14**: 536-550.

Komatsu, Y., et al. (1988). "Long-term potentiation of synaptic transmission in kitten visual cortex." Journal of Neurophysiology **59**(1): 124-141.

Kulkarni, V. A. and B. L. Firestein (2012). "The dendritic tree and brain disorders." Molecular and Cellular Neuroscience **50**(1): 10-20.

Kutzing, M. K., et al. (2010). "Automated Sholl analysis of digitized neuronal morphology at multiple scales." Journal of Visualized Experiments(45).

Kutzing, M. K., et al. (2011). "Measurements of synchronous activity by microelectrode arrays uncovers differential effects of sublethal and lethal glutamate concentrations on cortical neurons." Annals of Biomedical Engineering **39**(8): 2252–2262.

Kutzing, M. K., et al. (2012). "Protection from glutamate-induced excitotoxicity by memantine." Annals of Biomedical Engineering **40**(5): 1170–1181.

Kwon, M., et al. (2011). "BDNF-promoted increases in proximal dendrites occur via CREB-dependent transcriptional regulation of cypin." Journal of Neuroscience **31**(26): 9735-9745.

Lang, S. B., et al. (2007). "Endogenous brain-derived neurotrophic factor triggers fast calcium transients at synapses in developing dendrites." The Journal of Neuroscience **27**(5).

Langhammer, C. G., et al. (2010). "Automated Sholl analysis of digitized neuronal morphology at multiple scales: Whole cell Sholl analysis versus Sholl analysis of arbor subregions." Cytometry Part A **77A**(12): 1160-1168.

Larkum, M. E. and T. Nevian (2008). "Synaptic clustering by dendritic signalling mechanisms." Current Opinion in Neurobiology **18**: 321-331.

Lau, A. G., et al. (2010). "Distinct 3′UTRs differentially regulate activity-dependent translation of brain-derived neurotrophic factor (BDNF)." Proceedings of the National Academy of Sciences **107**(36): 15945–15950.

Leveille, F., et al. (2008). "Neuronal viability is controlled by a functional relation between synaptic and extrasynaptic NMDA receptors." The FASEB Journal **22**: 4258-4271.

Lin, S. Y., et al. (1999). "Brain-derived neurotrophic factor enhances association of protein tyrosine phosphatase PTP1D with the NMDA receptor subunit NR2B in the cortical postsynaptic density." Molecular Brain Research **70**(1): 18-25.

Lindholm, D., et al. (1993). "Brain-derived neurotrophic factor is a survival factor for cultured rat cerebellar granule neurons and protects them against glutamate-induced neurotoxicity." European Journal of Neuroscience **5**: 1455-1464.

Litwin-Kumar, A. and B. Doiron (2012). "Slow dynamics and high variability in balanced cortical networks with clustered connections." Nature Neuroscience **15**(11): 1498-1505.

Liu, G. (2004). "Local structural balance and functional interaction of excitatory and inhibitory synapses in hippocampal dendrites." Nature Neuroscience **7**(4): 373-379.

Liu, Q., et al. (2006). "Rodent BDNF genes, novel promoters, novel splice variants, and regulation by cocaine☆." Brain Research **1067**: 1-12.

Liu, Q., et al. (2005). "Human brain derived neurotrophic factor (BDNF) genes, splicing patterns, and assessments of associations with substance abuse and Parkinson's Disease." American Journal of Molecular Genetics **134B**(1): 93-103.

Lu, B., et al. (2013). "BDNF-based synaptic repair as a disease-modifying strategy for neurodegenerative diseases." Nature Reviews Neuroscience **14**: 401-416.

Mallei, A., et al. (2015). "Expression and dendritic trafficking of BDNF-6 splice variant are impaired in knock-in mice carrying human BDNF Val66Met polymorphism." International Journal of Neuropsychopharmacology: 1-10.

Martin, K. C. and A. Ephrussi (2009). "mRNA Localization: Gene Expression in the Spatial Dimension." Cell **136**(4): 719.

Mattson, M. P., et al. (1995). "Neurotrophic factors attenuate glutamate induced-accumulation of peroxides, elevation of intracellular Ca2+concentration, and neurotoxcity and increase antioxidant enzyme activities in hippocampal neurons." The Journal of Neurochemistry **65**: 1740-1751.

McAllister, A. K., et al. (1996). "Neurotrophin regulation of cortical dendritic growth requires activity." Neuron **17**: 1057–1064.

McAllister, A. K., et al. (1995). "Neurotrophins regulate dendritic growth in developing visual cortex." Neuron **15**: 791-803.

Meijering, E., et al. (2004). "Design and validation of a tool for neurite tracing and analysis in fluorescence microscopy images." Cytometry Part A **58A**(2): 167-176.

Melo, C. V., et al. (2013). "BDNF regulates the expression and distribution of vesicular glutamate transporters in cultured hippocampal neurons." PLoS ONE **8**(1): e53793.

Melo, C. V., et al. (2013). "Spatiotemporal resolution of BDNF neuroprotection against glutamate excitotoxicity in cultured hippocampal neurons." Neuroscience **237**: 66-86.

Merlio, J.-P., et al. (1993). "Increased production of the TrkB protein tyrosine kinase receptor after brain insults." Neuron **10**(2): 151-164.

Metsis, M., et al. (1993). "Differential usage of multiple brain-derived neurotrophic factor promoters in the rat brain following neuronal activation." 90(8802-8806).

Miller, J. P. and G. A. Jacobs (1984). "Relationships between neuronal structure and function." Journal of Experimental Biology **112**: 129-145.

Mitre, M., et al. (2017). "Neurotrophin signalling: novel insights into mechanisms and pathophysiology." Clinical Science **131**(1): 13-23.

Mohajerani, M. H., et al. (2007). "Correlated network activity enhances synaptic efficacy via BDNF and the ERK pathway at immature CA3–CA1 connections in the hippocampus." Proceedings of the National Academy of Sciences **104**(32): 13176-13181.

Montalbano, A., et al. (2013). "Blockade of BDNF signaling turns chemically-induced long-term potentiation into long-term depression." Hippocampus **23**: 879-889.

Morefield, S. I., et al. (2000). "Drug evaluations using neuronal networks cultured on microelectrode arrays." Biosensors & Bioelectronics **15**: 383-396.

Mudó, G., et al. (1993). "Increased expression of trkB and trkC messenger RNAS in the rat forebrain after focal mechanical injury." Neuroscience **57**(4): 901-912.

Mulkey, R. M. and R. C. Malenka (1992). "Mechanisms underlying induction of homosynaptic long-term depression in area CA1 of the hippocampus." Neuron **9**(5): 967-975.

Muragaki, Y., et al. (1995). "Expression of trk receptors in the developing and adult human central and peripheral nervous system." J Comp Neurol **356**(3): 387-397.

O'Donovan, M. J. (1999). "The origin of spontaneous activity in developing networks of the vertebrate nervous system." Current Opinion in Neurobiology **9**: 94-104.

O'Neill, K. M., et al. (2015). "Assessing effects on dendritic arborization using novel Sholl analyses." Frontiers in Cellular Neuroscience **9**: 285.

Oe, S. and Y. Yoneda (2010). "Cytoplasmic polyadenylation element-like sequences are involved in dendritic targeting of BDNF mRNA in hippocampal neurons." FEBS Letters **584**: 3424-3430.

Ohira, K. and M. Hayashi (2003). "Expression of TrkB subtypes in the adult monkey cerebellar cortex." Journal of Chemical Neuroanatomy **25**: 175-183.

Ohira, K., et al. (1999). "Change of expression of full-length and truncated TrkBs in the developing monkey central nervous system." Developmental Brain Research **112**: 21-29.

Opitz, T., et al. (2002). "Spontaneous development of synchronous oscillatory activity during maturation of cortical networks *in vitro*." Journal of Neurophysiology **88**(5): 2196-2206.

Pang, P. T., et al. (2004). "Cleavage of proBDNF by tPa/plasmin is essential for long-term hippocampal plasticity." Science **306**: 487-491.

Parviz, M. and G. W. Gross (2007). "Quantification of zinc toxicity using neuronal networks on microelectrode arrays." NeuroToxicology **28**(3): 520-531.

Patel, T. P., et al. (2013). "Single-neuron NMDA receptor phenotype influences neuronal rewiring and reintegration following traumatic injury." The Journal of Neuroscience **34**(12): 4200–4213.

Patel, T. P., et al. (2012). "Dynamic changes in neural circuit topology following mild mechanical injury in vitro." Annals of Biomedical Engineering **40**(1): 23-36.

Patterson, Z. R. and M. R. Holahan (2012). "Understanding the neuroinflammatory response following concussion to develop treatment strategies." Frontiers in Cellular Neuroscience **6**: 58.

Pine, J. (1980). "Recording action potentials from cultured neurons with extracellular microcircuit electrodes." Journal of Neuroscience Methods **2**(1): 19-31.

Pohl, D., et al. (1999). "N-Methyl-D-aspartate antagonists and apoptotic cell death triggered by head trauma in developing rat brain." Proceedings of the National Academy of Sciences **96**: 2508-2513.

Raichman, N. and E. Ben-Jacob (2008). "Identifying repeating motifs in the activation of synchronized bursts in cultured neuronal networks." The Journal of Neuroscience Methods **170**: 96-110.

Ray, S. K., et al. (2002). "Molecular mechanisms in the pathogenesis of traumatic brain injury." Histology and Histopathology: Cellular and Molecular Biology **17**: 1137-1152.

Righi, M., et al. (2000). "Brain-derived neurotrophic factor (BDNF) induces dendritic targeting of BDNF and tyrosine kinase B mRNAs in hippocampal neurons through a phosphatidylinositol-3 kinase-dependent pathway." Journal of Neuroscience **20**: 3165-3174.

Rodriguez, A. (2007). NeuronStudio Documentation.

Rodriguez, A., et al. (2006). "Rayburst sampling, an algorithm for automated three-dimensional shape analysis from laser scanning microscopy images." Nature Protocols **1**(14): 2152-2161.

Rodriguez, A. J., et al. (2008). "Mechanisms and cellular roles of local protein synthesis in mammalian cells." Current Opinion in Cell Biology **20**(2): 144-149.

Ross, C. A. and D. W. Cleveland (2006). "Intercellular miscommunication in polyglutamine pathogenesis." Nature Neuroscience **9**(10): 1205-1206.

Rostami, E., et al. (2014). "Alteration in BDNF and its receptors, full-length and truncated TrkB and p75NTR following penetrating traumatic brain injury." Brain Research **1542**: 195-205.

Rudge, J. S., et al. (1994). "Neurotrophic factor receptors and their signal transduction capabilities in rat astrocytes." Eur J Neurosci **6**(5): 693-705.

Rudge, J. S., et al. (1998). "Endogenous BDNF protein is increased in adult rat hippocampus after a kainic acid induced excitotoxic insult but exogenous BDNF is not neuroprotective." Experimental Neurology **149**(2): 398-410.

Segal, R. A. (2003). "Selectivity in neurotrophin signaling: theme and variations." Annu Rev Neurosci **26**: 299-330.

Segev, R. and E. Ben-Jacob (2001). "Spontaneous synchronized bursting in 2D neural networks." Physica A **302**(1-4): 64-69.

Sendtner, M., et al. (1992). "Brain-derived neurotrpphic factor prevents the death of motoneurons in newborn rats after nerve section." Nature **360**(24): 751.

Sholl, D. A. (1953). "Dendritic organization in the neurons of the visual and motor cortices of the cat." J Anat **87**(4): 387-406.

Shooter, E. M. (2001). "Early days of the nerve growth factor proteins." Annu Rev Neurosci **24**: 601-629.

Singh, K. K., et al. (2008). "Developmental axon pruning mediated by BDNF-p75nTR-dependent axon degeneration." Nature Neuroscience **11**(6): 649-658.

Softky, W. R. and C. Koch (1993). "The highly irregular firing of cortical cells is inconsistent with temporal integration and random EPSPs." The Journal of Neuroscience **13**(1): 334-350.

Soulé, J., et al. (2006). "Brain-derived neurotrophic factor and control of synaptic consolidation in the adult brain." Biochemical Society Transactions **34**(4): 600-604.

Srinivas, K. V., et al. (2007). "Small-world network topology of hippocampal neuronal network is lost, in an *in vitro* glutamate injury model of epilepsy." European Journal of Neuroscience **25**(11): 3276-3286.

Stenovec, M., et al. (2016). "Ketamine inhibits ATP-evoked exocytotic release of Brain-Derived Neurotrophic Factor from vesicles in cultured rat astrocytes." Molecular Neurobiology **53**(10): 6882-6896.

Steward, O. and E. M. Schuman (2001). "Protein synthesis at synaptic sites on dendrites." Annu Rev Neurosci **24**: 299-325.

Suen, P. C., et al. (1997). "Brain-derived neurotrophic factor rapidly enhances phosphorylation of the postsynaptic N-methyl-D-aspartate receptor subunit 1." Proceedings of the National Academy of Sciences **94**: 8191-8195.

Sweet, E. S., et al. (2011). "PSD-95 alters microtubule dynamics via an association with EB3." Journal of Neuroscience **31**(3): 1038-1047.

Sweet, E. S., et al. (2011). "To branch or not to branch: How PSD-95 regulates dendrites and spines." Bioarchitecture **1**(2): 69-73.

Szeszko, P. R., et al. (2005). "Brain-derived neurotrophic factor val66met polymorphism and volume of the hippocampal formation." Molecular Psychiatry **10**: 631-636.

Takei, N., et al. (2004). "Brain-derived neurotrophic factor induces mammalian target of rapamycin-dependent local activation of translation machinery and protein synthesis in neuronal dendrites." Journal of Neuroscience **24**(44): 9760-9769.

Takemoto, T., et al. (2015). "Neuroprotection elicited by nerve growth factor and brain-derived neurotrophic factor released from astrocytes in response to methylmercury." Environmental Toxicology and Pharmacology **40**: 199-205.

Tau, G. Z. and B. S. Peterson (2010). "Normal development of brain circuits." Neuropsychopharmacology Reviews **35**: 147-168.

Timmusk, T., et al. (1993). "Multiple promoters direct tissue-specific expression of the rat BDNF gene." Neuron **10**: 475-489.

Tongiorgi, E. (2009). "Activity-dependent expression of brain-derived neurotrophic factor in dendrites: facts and open questions." Neuroscience Research **61**(4): 335-346.

Tongiorgi, E., et al. (1997). "Activity-dependent dendritic targeting of BDNF and TrkB mRNAs in hippocampal neurons." The Journal of Neuroscience **17**(24): 9492-9505.

Torben-Nielsen, B. and K. M. Stiefel (2009). "Systematic mapping between dendritic function and structure." Network: Computation in Neural Systems **20**(2): 69-105.

Tyler, W. J. and L. D. Pozzo-Miller (2001). "BDNF enhances quantal neurotransmitter release and increases the number of docked vesicles at the active zones of hippocampal excitatory synapses." The Journal of Neuroscience **21**(12): 4249–4258.

Uylings, H. B. and J. Van Pelt (2002). "Measures for quantifying dendritic arborizations." Network: Computation in Neural Systems **13**(3): 397-414.

Van Landeghem, F. K. H., et al. (2006). "Decreased expression of glutamate transporters in astrocytes after human traumatic brain injury." The Journal of Neurotrauma **23**(10): 1518-1528.

Van Pelt, J. and R. W. Verwer (1985). "Growth models (including terminal and segmental branching) for topological binary trees." Bull Math Biol **47**(3): 323-336.

Van Pelt, J. and R. W. Verwer (1986). "Topological properties of binary trees grown with order-dependent branching probabilities." Bull Math Biol **48**(2): 197-211.

Vanevski, F. and B. Xu (2015). "HuD interacts with Bdnf mRNA and is essential for activity-induced BDNF synthesis in dendrites." PLoS ONE **10**(2): e0117264.

Verwer, R. W. and J. Van Pelt (1990). "Analysis of binary trees when occasional multifurcations can be considered as aggregates of bifurcations." Bull Math Biol **52**(5): 629-641.

Vetter, P., et al. (2001). "Propagation of action potentials in dendrites depends on dendritic morphology." The Journal of Neurophysiology **85**: 926-937.

Vicario, A., et al. (2015). "Dendritic targeting of short and long 3' UTR BDNF mRNA is regulated by BDNF or NT-3 and distinct sets of RNA-binding proteins." Frontiers in Molecular Neuroscience **8**: 62.

Vignoli, B., et al. (2016). "Peri-synaptic glia recycles Brain-Derived Neurotrophic Factor for LTP stabilization and memory retention." Neuron **92**: 873-887.

Vogel, A., et al. (2005). "Increase of neuronal response variability at higher processing levels as revealed by simultaneous recordings." The Journal of Neurophysiology **93**(6): 3548 –3559.

Wagenaar, D. A., et al. (2005). "MeaBench: A toolset for multi-electrode data acquisition and on-line analysis." Proceedings of the 2nd International IEEE EMBS.

Wagenaar, D. A., et al. (2006). "An extremely rich repertoire of bursting patterns during the development of cortical cultures." BMC Neuroscience **7**(11): 1-18.

Walton, M. R. and M. Druganow (2000). "Is CREB a key to neuronal survival?" Trends in Neuroscience **23**(2): 48-53.

Wang, M., et al. (2016). "Translation of BDNF-gene transcripts with short 3' UTR in hippocampal CA1 neurons improves memory formation and enhances synaptic plasticity-relevant signaling pathways." Neurobiology of Learning and Memory.

Ward, N. L. and T. Hagg (2000). "BDNF is needed for postnatal maturation of basal forebrain and neostriatum cholinergic neurons *in vivo*." Experimental Neurology **162**(2): 297-310.

Waterhouse, E. G., et al. (2012). "BDNF promotes differentiation and maturation of adult-born neurons through GABAergic transmission." The Journal of Neuroscience **32**(41): 14318-14330.

Waterhouse, E. G. and B. Xu (2009). "New insights into the role of brain-derived neurotrophic factor in synaptic plasticity." Molecular and Cellular Neuroscience **42**: 81–89.

Wetmore, C. and L. Olson (1995). "Neuronal and nonneuronal expression of neurotrophins and their receptors in sensory and sympathetic ganglia suggest new intercellular trophic interactions." J Comp Neurol **353**(1): 143-159.

Womelsdorf, T., et al. (2007). "Modulation of neuronal interactions through neuronal synchronization." Science **316**(1609-1612).

Wong, R. O. L. and A. Ghosh (2002). "Activity-dependent regulation of dendritic growth and patterning." Nature Reviews Neuroscience **3**: 803-812.

Wu, G. Y., et al. (1999). "Dendritic dynamics in vivo change during neuronal maturation." Journal of Neuroscience **19**(11): 4472-4483.

Xia, Y., et al. (2003). "Differential acute effects of fluoxetine on frontal and auditory cortex networks *in vitro*." Brain Research **973**(2): 151-160.

Xia, Y. and G. W. Gross (2003). "Histiotypic electrophysiological responses of cultured neuronal networks to ethanol." Alcohol **30**(3): 167-174.

Yacoubian, T. A. and D. C. Lo (2000). "Truncated and full-length TrkB receptors regulate distinct modes of dendritic growth." Nature Neuroscience **3**(4): 342-349.

Yi, J.-H. and A. S. Hazell (2006). "Excitotoxic mechanisms and the role of astrocytic glutamate transporters in traumatic brain injury." Neurochemistry International **48**: 394-403.

Yoshii, A. and M. Constantine-Paton (2010). "Postsynaptic BDNF-TrkB signaling in synapse maturation, plasticity, and disease." Developmental Neurobiology **70**: 304-322.

Young, D., et al. (1999). "Environmental enrichment inhibits spontaneous apoptosis, prevents seizures and is neuroprotective." Nature Medicine **5**: 448-453.

Yu, X. and R. C. Malenka (2004). "Multiple functions for the cadherin/catenin complex during neuronal development." Neuropharmacology **47**: 779-786.

Zoghbi, H. Y. (2003). "Postnatal neurodevelopmental disorders: meeting at the synapse?" Science **302**: 826-830.